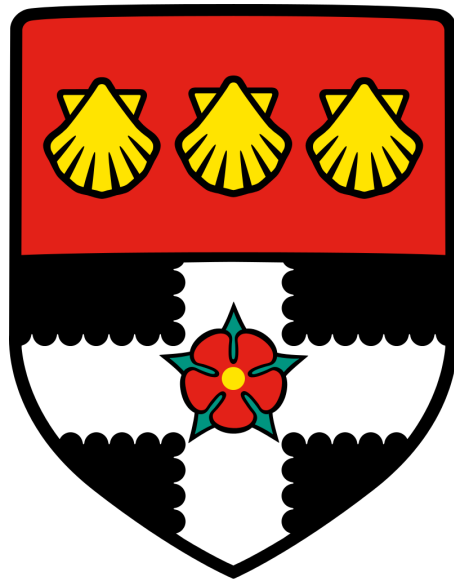


THE UNIVERSITY OF READING

Department of Meteorology



Understanding the Development of
Inter-monsoon Convective Storms over
the Western Peninsular Malaysia

Mohd Fadzil Firdzaus Bin Mohd Nor

A thesis submitted for the degree of Doctor of Philosophy

July 2016

Declaration

I confirm that this is my own work and the use of all material from other sources has been properly and fully acknowledge.

.....

Mohd Fadzil Firdzaus Bin Mohd Nor

.....

Date

Abstract

The western Peninsular Malaysia experiences biannual maxima in total rainfall. The first maximum is between October and December and the second is between March and May. During these periods, localised severe rainfall events are common. They are usually short, intense and sometime cause flash floods and landslides. Forecasting these local events is difficult, and continuous study to understand the mechanism of the rainfall events is important for the advancement of tropical weather forecasting in the future. This study focuses on inter-monsoons, which are April-May and September-October. Heavy rainfall days (daily total rainfall \geq the 90th percentile value) are determined by the average regional mean of three Peninsular Malaysia regions (northwest coast, west coast and inland). The analysis shows that a stronger easterly wind anomaly is common during these heavy rainfall days. Another common feature is a stronger ascending motion over the peninsula and also a high amount of moisture in the mid troposphere (around 700hPa pressure level) over the east side of the peninsula.

To investigate the mechanisms responsible for severe inter-monsoon convection in greater detail, two case studies were selected and simulated using the limited-area high-resolution UK MetOffice Unified Model. The Peninsular Malaysia and Sumatra Island influence the development of overnight rainfall over the Malacca Strait by constraining land-sea breezes and low-level flow. The Titiwangsa mountains over the Peninsular Malaysia then induce rainfall development at noon. The combination of these two events influences the development of severe convective storms of 2 May 2012 over the western Peninsular Malaysia. Sensitivity studies were carried out to investigate the influence of the local orography on this event. The flattened Peninsular Malaysia orography causes a lack of rainfall over the inland part of the Peninsular Malaysia and Sumatra Island yet still produces overnight rainfall over Malacca Strait but weaker. By removing Sumatra Island, it can be seen that the western and inland parts of the Peninsular Malaysia receive more rainfall, as it is influenced by the westerly wind and the Indian Ocean. The second case study of 24 September 2014 was inaccurately simulated thus further analysis on the mechanism of the convective storm development is rather impossible. However, the sensitivity experiments were still conducted and the results showed a significant difference in the rainfall pattern as the local orography was modified and Sumatra Island was removed. These results suggest the importance of the interaction between land masses, orography, low level flow and the diurnal cycle on the development of the severe rainfall events.

Acknowledgements



Firstly, I would like to thank the Department of Meteorology, University of Reading and staff for the opportunity and facility provided during my doctorate study, especially Dr Pete Inness for agreeing to be my supervisor and Dr Chris Holloway for being my co-supervisor. I am indebted to both of them for helping me with the scientific and modelling aspect of this work. PhD is a process of learning to do research and both of these individuals have taught and guided me enormously. I would also like to thank my monitoring committee, Prof. Geoff Wadge and Dr Andrew Turner for the insightful meeting every 6 month, helping me to get on track for the whole period of my PhD. I thank everyone in Tropical Group for their input, especially Stephanie Bush for her help in the sensitivity experiments.

I wish to express my sincere thanks to my sponsor, Majlis Amanah Rakyat (MARA) for their funding and the National Centre for Atmospheric Science (NCAS) in University of Reading for providing the UK MetOffice Unified Model facility that has proven to be an invaluable part of my research. This also goes to NCAS staff - Grenville Lister, William McGinty, Annette Osprey - for their support. A heartfelt gratitude to my colleagues at National Antarctic Research Center Malaysia (NARC) for their direct and indirect help and research ideas that led to the completion of this thesis and especially on my PhD application process. I express my thanks to the Malaysian Meteorological Department (MetMalaysia) and Department of Irrigation and Drainage Malaysia (DID) for providing me with observational data, such as rain gauges data and radar images. To my colleagues and friends in MetMalaysia whom I have directly contacted for questions and inquiry, I thank you. Special thanks to Bureau of Meteorology Australia for the Madden-Julian Oscillation data and phase diagram, Kochi University for the satellite images, Department of Atmospheric Science, the University of Wyoming for the sounding data and figures. Not to forget, I wish to thank Rezuan and Juhaida from Szakif Enterprise, Clare Sandford, Pn. Faizahani, Cik Sheikha, and Nick Byrne for proofreading my thesis.

Last but not least, thanks to my parents and siblings for being there for me and supporting me emotionally and mentally throughout my doctorate journey. Finally, my appreciation and thanks to my friends and colleagues in Malaysia and in the UK for the help and support. There are too many to mention here and I feel unfair if I mention just some. You know who you are.

Contents

1	Introduction	1
1.1	Introduction	1
1.1.1	General Climate of Malaysia	1
1.1.2	Motivation	2
1.1.3	Research Questions	5
1.1.4	Objectives	5
1.1.5	Dissertation Structure	5
2	The Climate and Weather of Malaysia	7
2.1	Monsoon and Inter-monsoon	7
2.2	Diurnal Cycle of Convection and Precipitation	14
2.3	Severe Convection over the Tropics	16
2.4	Processes Affecting Strong Convection over Peninsular Malaysia	24
3	Data and Methodology	28
3.1	Data	28
3.1.1	TRMM and APHRODITE Dataset	28
3.1.2	ERA-Interim Dataset	30
3.1.3	Rainfall Gauge Data	30
3.1.4	Radar, Satellite, and Sounding Data	32
3.2	Model Configuration	33
3.3	Methodology	34
3.3.1	Climatology	35
3.3.2	Severe Rainfall Events during Inter-monsoon	37
3.3.3	Case Studies	39
3.3.4	Sensitivity Experiments	40
3.4	Summary	42
4	Monsoon and Inter-monsoon Seasons	43
4.1	Introduction	43
4.1.1	Chapter Structure and Aim	43
4.2	Monthly Analysis on Rainfall and Wind	45

4.2.1	Analysis of Gridded Dataset	45
4.2.2	Analysis of Station Dataset	53
4.3	Seasonal Analysis on Rainfall and Wind	57
4.3.1	Analysis of Gridded Dataset	57
4.3.2	Analysis of Station Dataset	61
4.4	Analysis of Diurnal Cycle of Precipitation	63
4.5	Analysis of Air Temperature, Specific Humidity, and Sea Surface Temperature	66
4.6	Summary	67
5	Severe Convection over the Western Peninsular Malaysia	70
5.1	Introduction	70
5.1.1	Chapter Structure and Aim	70
5.2	Threshold and Monthly Mean	71
5.3	Inter-monsoon Outlook	76
5.4	Summary	84
6	Case Studies	87
6.1	Introduction	87
6.1.1	Chapter Structure and Aims	88
6.2	Case Study 1: First Inter-monsoon (April-May)	88
6.2.1	Introduction	88
6.2.2	Simulation : Control Run	95
6.2.3	Possible Mechanism	107
6.2.4	The Role of Local Orography and Sumatra Island	114
6.2.5	Summary	145
6.3	Case Study 2 : Second Inter-monsoon (Sept.-Oct.)	149
6.3.1	Introduction	149
6.3.2	Simulation: Control Run	154
6.3.3	The Role of Orography and Sumatra Island	159
6.3.4	Summary	164
7	Conclusion	166
7.1	Conclusion	166
7.1.1	Summary of Findings	166
7.1.2	Concluding remarks and future outlook	177
A	Appendix	182

Chapter 1

Introduction

1.1 Introduction

1.1.1 General Climate of Malaysia

In Köppen climate classification, the Maritime Continent is a tropical wet climate, which is hot and humid throughout the year. The Maritime Continent is affected by the monsoon and other types of climate variabilities such as Madden-Julian Oscillation and El Niño-Southern Oscillation. Malaysia consists of West Malaysia (Peninsular Malaysia) and East Malaysia (northwestern and northern part of Borneo). Malaysia is located in the north-west part of Maritime Continent, or south-east Asia. The geography of Peninsular Malaysia and the region is shown in Figure 1.1. Malaysia receives an abundant amount of rainfall and experiences convective storms throughout the year. In general, the average temperature of Malaysia is 26°C with an average of 2500 mm precipitation annually.

The weather in Malaysia is sometimes associated with severe events that cause floods and landslides. There are two distinct seasons, which are the wet season during boreal winter monsoon and a dry season during boreal summer monsoon (locally known as northeast monsoon and south-west monsoon, respectively). Malaysia is located near to the equator and experiences equatorial climate which is warm and wet all year around. The weather is mainly influenced by monsoon rain and the annual movement of the Intertropical Convergence Zone (ITCZ). For Malaysia, the winter monsoon starts in November and ends by March (Chang et al., 2006). The summer monsoon usually start by June and ends by September (Met-Malaysia, 2016a). The periods in between monsoons are called inter-monsoon and it occurs roughly between March-May and September-November. During the winter monsoon, the prevailing wind is northeasterly and during the summer monsoon, the prevailing wind is southwesterly. Due to the complex terrain and the different sizes of the islands, rainfall distribution varies over large and medium landmass due to the orography and rain shadow effects (Chan and Li, 2001). Generally, Malaysia

is mostly affected by the boreal winter monsoon where the rainfall can last more than 24 hours over the east coast of the Peninsular Malaysia and Sarawak (north-west Borneo), causing flooding and landslide events. However, during the monsoon transition (inter-monsoon) periods, the west coast of Peninsular Malaysia receives more rainfall compared to other seasons, as analysed using the Tropical Rainfall Measuring Mission (TRMM) rainfall dataset (Varikoden et al., 2010). The ITCZ passes through the equator (thus also Malaysia) during inter-monsoon periods.

The ITCZ is associated with the seasonal maximum temperature related to maximum solar heating over the Earth's surface (Barry and Chorley, 2009). The ITCZ is a low-pressure area where the trade wind from the northern hemisphere and southern hemisphere meet (Barry and Chorley, 2009) and usually identified as a belt of convective clouds over the tropics from satellite images (Waliser and Gautier, 1993). The area of the ITCZ is characterised by a rapid ascending motion of warm and moist air. The ITCZ passes the equator twice a year from the northern to southern of the hemispheres (around March to May) and vice versa (September-November). The ITCZ is associated with frequent convective rainfall and thunderstorms, and as for Peninsular Malaysia, depending on the region, the weather is influenced by the ITCZ, with additional monsoon flows on the east coast.

1.1.2 Motivation

Western Peninsular Malaysia is the most densely populated area of Peninsular Malaysia, and Strait of Malacca is one of the busiest sea traffic lanes in the world. According to the Department of Statistics Malaysia, an estimate of at least 65% of the total Malaysian population lives on the western and southern Peninsular Malaysia where the major cities and seaports are located. Flash floods, landslides, and strong windstorms are the main meteorological threats affecting the socio-economic aspect of the people in this region. Thus, a clear understanding of the local weather is important, especially for weather-related risk management.

The inter-monsoons are the transition periods between boreal winter monsoon (November to March) and boreal summer monsoon (June until Aug), which are around April-May and September-October. The inter-monsoon has received less attention, unlike boreal winter monsoon that caused major flooding events especially over the east coast and southern peninsula. There are a handful of case studies looking at inter-monsoon events, mainly to study localised rainfall events over the western Peninsular Malaysia and the Strait of Malacca, such as in Joseph et al. (2008) and Fujita et al. (2010) respectively. There are also other studies on the seasonal cycle of rainfall in Malaysia and surrounding areas such as in Yang and Slingo (2001), Tangang and Juneng (2004), Wang and Chang (2008), and Varikoden et al. (2010, 2011). However, these studies were more general as they did not focus

on specific seasons and locations. The development of the convective storms during the inter-monsoon period is usually associated with locally driven circulation, as there is no significant large-scale synoptic influence (monsoon) and it is the time when the maximum solar radiation at the equator which frequently causes unstable atmospheric condition over the Maritime Continent (Nieuwolt, 1986; Joseph et al., 2008). The afternoon convective storms during the inter-monsoon seasons are usually related to land mass heating which drives the land-sea breezes and later enhanced by the mountain-valley breezes, lee waves from terrain as well as sea breeze collision (Joseph et al., 2008; Lima and Wilson, 2008; Sow et al., 2011). These mechanisms are known to be the main possible mechanisms to induce local convective activity over this region, but there are more mechanisms to be explored. Most of these convective storms occur in the afternoon, but sometimes it could occur in the morning, evening or even at night.

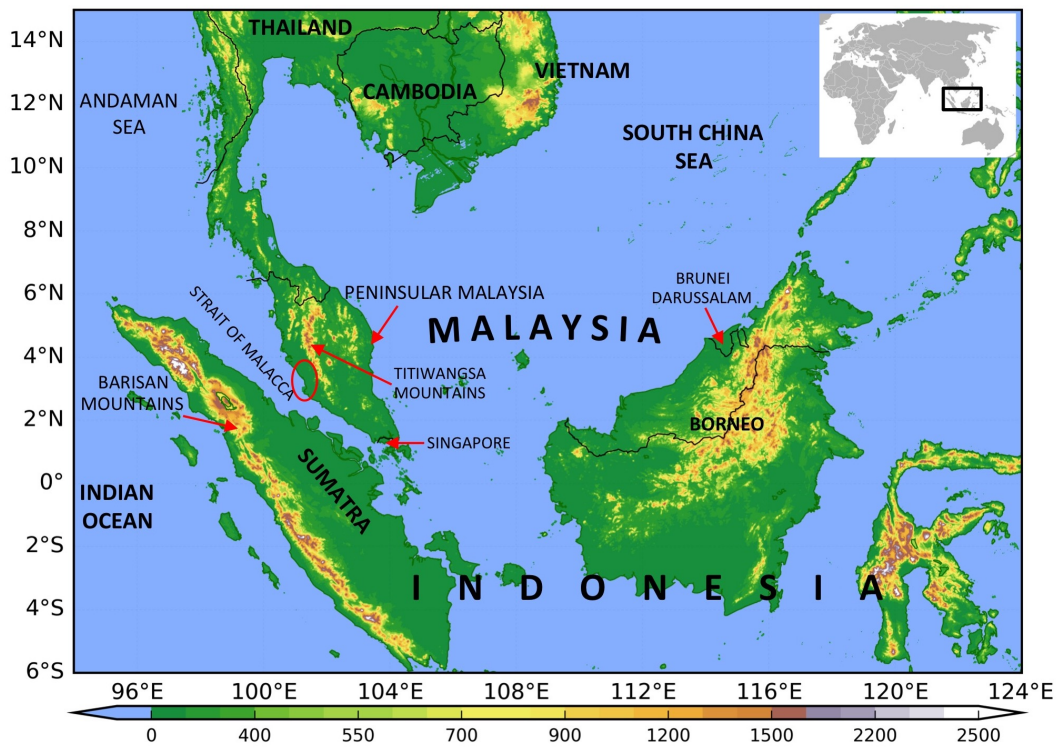


Figure 1.1: The geography of Peninsular Malaysia and part of Sumatra. The peaks of the Barisan Mountains in Sumatra are more than 2500 m above the mean sea level and the highest peak over the Titiwangsa mountains in Peninsular Malaysia are around 2000 m above the mean sea level. The red circle is the Klang Valley area, where one of the case studies is located. Orography data is the global orography dataset from National Center for Environmental Information of National Oceanic and Atmospheric Administration (NOAA). The shades represent the height in meter, above sea level.

Rainfall simulation over the tropics is not always easy but improving. For example, the simulations done by Love et al. (2011) using UKMO Unified Model version 7.1 over the Maritime Continent on the diurnal cycle of precipitation over the tropical region showed that the simulated precipitation was weak over the ocean and stronger over land. The models used were a regional 40km and 12km models

with the convective parameterisation switched on. The error is associated with the physical processes depicted in the model, specifically in the way the model calculated the heating process (solar radiation to the surface) at coarser resolution (in this case 40km model). The convective parameterisation in the 40km model did not respond realistically to gravity waves which caused too little rain over the ocean. Even though the heating profile was realistic, the convection promoted by the gravity waves resulted from the change of heat from convective form to stratiform component propagating at a slower phase speed than it should. This shows that the correct representation of heating profile and gravity wave propagation is important to get a realistic representation of precipitation over the tropical region (Love et al., 2011). In studies by Yang and Slingo (2001) and Neale and Slingo (2003), the maximum precipitation occurred too early in the day, around the time of maximum solar heating. Since most tropical weather involves small-scale physical process, the coarse resolution model simulations were believed to ignore the local orographic features by taking the mean values (for example, convective rainfall) instead of the exact (realistic) values of the process involved in each grid box. A realistic representation of the physical process in the model is important for a realistic representation of the development of the convection and precipitation. Yang and Slingo (2001) also stated that the error in the phase of the diurnal cycle of convection in the model simulation was closely related to fundamental errors in physical processes of the model, such as the technical implementation of radiation scheme. In some other cases, the simulation of the diurnal cycle of precipitation over the Maritime Continent showed a dry bias in precipitation (Neale and Slingo, 2003). The maximum precipitation occurred too early and the life cycle of convection in the model was too short. Early maximum precipitation affected the solar radiation to the surface by cutting the surface heating early thus creating a subsequent error in land-sea pressure gradients, sea-breeze and thus affecting the succeeding processes (Neale and Slingo, 2003).

As complicated as it is to simulate rainfall events over the tropics, it is also difficult to forecast (Sobel, 2012). A continuous study of the tropical weather is important especially in advancing the future weather forecasting, especially in the tropics. This research will explore the weather and severe rainfall events during inter-monsoon and analyse their characteristics. By using 1.5km limited area UK Met Office Unified Model (Met-UM), this research will look at the role of local orography and Sumatra Island on the development of severe rainfall events based on two case studies.

1.1.3 Research Questions

There are a few major questions that motivate this research. They are:

1. How different is the rainfall amount over the western Peninsular Malaysia during inter-monsoon periods compared to the monsoon seasons?
2. What are the common conditions during heavy rainfall events over this region during the AM and SO inter-monsoon?
3. How well are heavy rainfall events simulated by the Met-UM?
4. What are the mechanism involved in the development of the rainfall event based on case studies?
5. How important was the orography over both the Peninsular Malaysia and Sumatra Island in the development of the rainfall event over this region, based on these case studies?
6. How important is Sumatra Island in the development of severe rainfall events over the western Peninsular Malaysia, based on these case studies?

1.1.4 Objectives

This research has several main objectives:

1. To investigate the characteristics of the severe rainfall events over the Peninsular Malaysia during inter-monsoon.
2. To investigate the development of severe convection over the western Peninsular Malaysia during inter-monsoon.
3. To simulate the severe rainfall events over the western Peninsular Malaysia.
4. To understand the formation of severe rainfall events over the region based on case studies, for May and September cases.
5. To investigate the role of the orography of the Peninsular Malaysia and Sumatra Island on the development of severe convection over the western Peninsular Malaysia.

1.1.5 Dissertation Structure

The structure of this dissertation is as follows:

1. Chapter 2 presents the background study for this research, beginning with the general weather of Malaysia during monsoon and inter-monsoon. Then the discussion is continued with the discussion of the diurnal cycle of convection over the Maritime Continent in general, and Malaysia specifically.
2. Chapter 3 presents the data and methodology used in this research.
3. Chapter 4 presents the climatology study, where the analysis was done using currently available reanalysis dataset and some station data.
4. Chapter 5 presents severe convection studies. This study analysed the days that recorded daily total rainfall higher than the 90th percentile from TRMM

dataset. The study focused on the general characteristics of severe rainfall events over the western Peninsular Malaysia.

5. Chapter 6 presents the case studies on severe rainfall events on 12 May 2012 and 24 September 2014. Both rainfall events occurred during inter-monsoon periods. This chapter investigates the mechanisms involved in the development of the severe rainfall events using Met-UM. Further, during the analysis, a series of sensitivity experiments were done to investigate the role of orography and Sumatra Island in the development of these severe rainfall events.
6. Chapter 7 concludes this research and thesis.

Chapter 2

The Climate and Weather of Malaysia

2.1 Monsoon and Inter-monsoon

Located near the equator, Malaysia experiences an equatorial climate, where it is hot and wet throughout the year. As mentioned in Chapter 1, the main influence on the weather over this region is the Intertropical Convergence Zone (ITCZ) and monsoon flow, as well as other large-scale weather phenomena such as Madden-Julian Oscillation (MJO) and El Niño - Southern Oscillation (ENSO). The ITCZ is a low atmospheric pressure belt located over the tropical region across the globe, which moves northward (toward the Tropic of Cancer) and southward (toward the Tropic of Capricorn) following the seasonal movement of the solar zenith point. The low pressure is essentially caused by the maximum heating due to the above-mentioned solar zenith point. The exact location of the ITCZ varies based on the properties of the Earth's surface (land or ocean). The ITCZ also corresponds to the ascending region of a Hadley Cell, thus the low atmospheric pressure. In boreal summer, the solar zenith is near the Tropic of Cancer. Thus, the low atmospheric pressure area is located near the Tropic of Cancer. In boreal winter, the solar zenith is closer to the Tropic of Capricorn and so is the low atmospheric pressure, the ITCZ. These low atmospheric pressure regions are unstable and bring thunderstorms and severe weather. The low atmospheric pressure belt is also the main area where the trade winds from the northern hemisphere and southern hemisphere meet, which is well observed over the ocean.

The monsoon (from Arabic: *mausim*, Dutch: *monssoen*, and Portuguese: *monção*, which mean 'season'), can be explained as a large-scale land-sea breezes mechanism. During the boreal winter, the Asian continent receives less solar radiation thus the air cools and a higher pressure region builds up. This area is known as Siberian High. At the same time, the southern hemisphere is in its summer season and receives more solar radiation. This creates low atmospheric pressure area

over the southern hemisphere in general. At this point, the ITCZ is to the south of the equator, and specifically over the Maritime Continent, the monsoon trough resides. The monsoon trough is also a part of the ITCZ. Specifically, over the eastern hemisphere, the pressure difference in between continental Asia and the low pressure over the southern hemisphere induces surface-level air movement from the high-pressure area (continental Asia) to the low-pressure area (the ITCZ over the south of equator and australis summer region). This air movement is completing the Hadley circulation of the northern hemisphere section, as the monsoon trough becomes the ascending region of the air and the cold Asian landmass becomes the descending region. The cold air from the land moves towards the lower pressure areas and this cold air then combines with the moist easterly air from the tropical Pacific over the tropical region (South China Sea) and brings precipitation over the South China Sea and surrounding lands. The wind moving south from continental Asia is affected by the Coriolis force of the earth and becoming northeasterly when it is closer to the equator and turned to northwesterly as it crosses the equator. The surges continue to cross the equator towards the monsoon trough and bring precipitation along the way to the central and southern Maritime Continent. This annual cycle occurs during boreal winter and is known as Asian winter monsoon (or East Asian winter monsoon). An opposite condition occurs during boreal summer when the Asia landmass receives more solar radiation since the day is longer in summer. The landmass is also heated faster due to the low heat capacity of the land surface, which results in low pressure, and so the pressure over the nearer oceans (in this case, Indian Ocean) is relatively higher than the nearest land mass. The main low-pressure areas are over the south and central Asia, thus, the monsoon action is centred mostly over the South Asian region. Moist air from the Indian Ocean moves towards the land and brings precipitation over the low-pressure area over South Asia.

In general, the Asian winter monsoon regime dominates the south of equator, and the Asian summer monsoon regime dominates the north of equator and mixed regimes dominate the equator (Maritime Continent, between 5°N and 5°S) which is manifested through the spatial distribution of the rainfall and convection (Chang et al., 2004). Winter monsoon regime includes the area between 5°N and 10°S , while summer monsoon regime mostly affects the area north of 10°N . The larger area affected by the boreal winter monsoon is believed to be caused by the onshore northeasterly winter monsoon winds from north-west Pacific and the South China Sea (Chang et al., 2004). Over the southern South China Sea and north-west Borneo, the maximum convection is caused by the Borneo Vortices, which are caused by the land heating of the island and can develop any time of the year. During boreal winter monsoon, the combination of periodic northeast cold surge winds and low-level cyclonic shear vorticity off the north-west Borneo enhances the Borneo Vortices

and brings heavy rainfall to surrounding shores off the southern South China Sea (Johnson and Houze, 1987). Thus, over the Maritime Continent, boreal winter monsoon is associated with a wet season with prevailing easterly winds and boreal summer monsoon associated with a dry season with prevailing westerly winds.

The Maritime Continent is considered to be in winter monsoon regime because the maximum convection occurs during boreal winter monsoon and the extension of the effect of the boreal winter extends far northward of the equator, unlike the boreal summer regime that is only restricted to Indochina (Ramage, 1968; Chang et al., 2004). The extension includes northeast Peninsular Malaysia, northern Sumatra, north-eastern and north-western Borneo, eastern Philippines and eastern Vietnam. The maximum precipitation over these regions is mostly a result of the onshore northeasterly winter monsoon winds from north-western Pacific and the South China Sea. The local variation in precipitation distribution is highly associated with complex orographic interaction with onshore winds. Some regions (e.g. Borneo and New Guinea) experience high rainfall throughout the year. The east coast of Peninsular Malaysia experiences maximum rainfall during boreal winter monsoon. The average rainfall during the season can reach 1000 mm per month over the east coast of Peninsular Malaysia. Depending on the region, the rainy days can be continuous up to 30 days. Boreal summer monsoon is considered the driest season with a total rainfall amount ranging from 4 mm to 400 mm per month (MMD, monthly report 2013/14).

Inter-monsoon is a period between the two monsoon seasons during spring and autumn, depending on which hemisphere is referred to. This transition period is also associated with the crossing of the sun over the equator, marking the seasonal changing of the monsoon where the sun moves from the northern hemisphere (summer monsoon) towards the southern hemisphere (winter monsoon), and vice versa (from the southern hemisphere to northern hemisphere). Although the two inter-monsoon periods are associated with the position of the sun over the equator, each monsoon transition behaves differently. In boreal spring, the maximum convection centre mostly stays south of 5°N until they suddenly jump north over the South Asian region when the summer monsoon starts. The inter-monsoon regimes in the Maritime Continent are different in many ways. Boreal autumn inter-monsoon brings rainfall mostly over the north of the equator and particularly on the west part of the Maritime Continent and boreal spring inter-monsoon brings rainfall mostly over the south part of the equator and particularly over the east of the Maritime Continent. The regimes can be divided into two regions; the west side of 140°E is under the boreal autumn inter-monsoon regime and the east side of 140°E is under the boreal spring regime, both in the area between 10°N to 10°S . There are exceptions, namely over the South China Sea and the northern Philippines, although they are located north of 10°N (Chang et al., 2004).

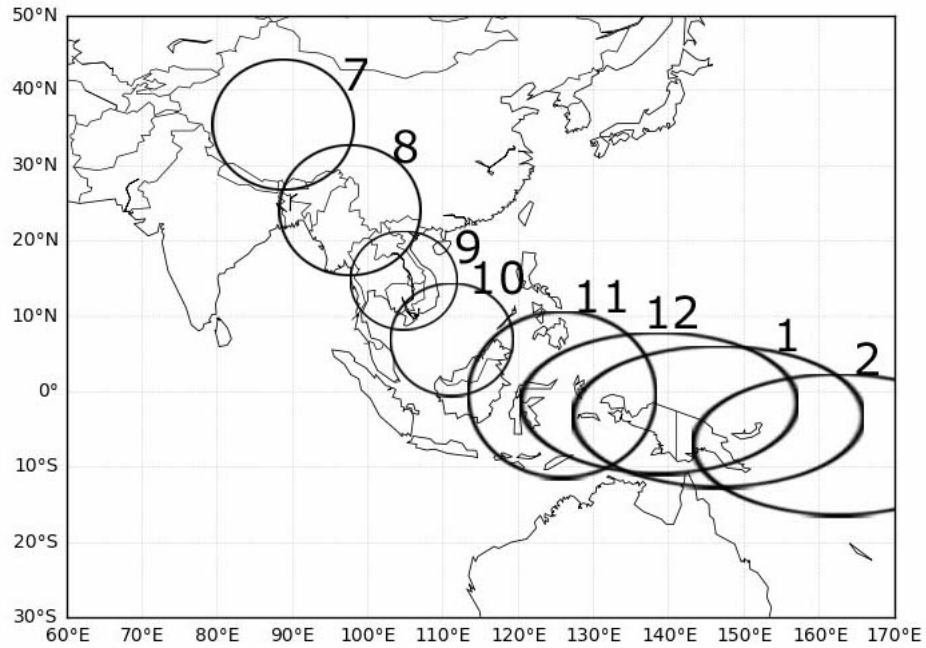


Figure 2.1: Monsoon diabatic heat sources migration during July to February (numerals represent respective months, e.g., 7 is July, and so on). The extent of the diabatic heat sources is determined from the area with $OLR < 225 \text{ Wm}^2$ from monthly OLR climatology (adapted from Lau and Chan (1983), pg. 2764).

The maximum convection in Asia can be explained by the movement of the maximum diabatic heating (convection) from summer monsoon regime in South Asia, moving south-easterly to the South East Asia and Maritime Continent during boreal autumn and towards the Australian landmass during boreal winter monsoon, as shown in Figure 2.1. However, the reverse movement (convection movement from winter monsoon regime towards the summer monsoon regime) is not as well defined as the southward movement. This asymmetric monsoon transition is influenced by several factors. First, Matsumoto and Murakami (2000) state that the cold surges from Asian continent during boreal autumn are stronger than the one from Australia during boreal spring. Later studies revealed that the asymmetric transition associated with the sea level pressure (SLP) difference between ocean and land is influenced by the geography of Asia-Australia, with a larger landmass and higher elevation over Asia and smaller and lower elevation over Australasia. These differences lead to asymmetric wind-terrain interaction, thus affecting the convergence and divergence activities over the Maritime Continent where convergence is stronger in boreal fall than in boreal spring (Chang et al., 2005b). A large SLP difference over East Asia leads to strong northeasterly winds over the northern South China Sea and northwestern Pacific. The SLP gradient favours cyclonic flow in the southern South China Sea, therefore, there will be deep convection during boreal autumn inter-monsoon. Then, the convection is enhanced by the interaction of the wind and the terrain over western Sumatra and western Borneo (Chang et al., 2005b). The east-west pressure gradient across the equatorial Indian Ocean also contributes

to the development of equatorial westerly winds that lead to more convection where the onshore flow causes convergence along the west coast of Sumatra and Peninsular Malaysia. Aside from modulating the SLP difference between regions, orography also plays an important role in this asymmetric behaviour. The maximum rainfall is usually located on the windward side of high terrains, which essentially produces a significant seasonal preferential zone of convergence and divergence (Chang et al., 2005b).

The SLP difference associated with asymmetric monsoon transition behaviour can also be explained by the thermal memory of the ocean. The ocean releases previously stored heat later than the land or the atmosphere, thus the lag of the sea surface temperature (SST) change is about one to two months compared to the landmass. Thus, local autumn will be warmer than local spring due to the heat stored in the ocean from the previous local summer. The SST relation is also explained in Chang et al. (2005b) which associates the lag in SST change to the mean SLP difference that drives the Walker circulation over the Pacific and Indian Oceans during boreal autumn and boreal spring. The equatorial Pacific is affected by the eastern Pacific cold tongue and it is intense during boreal autumn. The intense cold tongue results in a higher SST gradient and favours convection over the Maritime Continent. The western equatorial Indian Ocean is warmest in boreal spring and favours convection over the eastern Africa thus reducing the tendency of convective activity over the Maritime Continent. This was explained by Wang and Chang (2008) when they investigated the maximum convection march from South Asia to Maritime Continent during September-November season and the sudden jump from Maritime Continent to continental Asia in March-May season (Figure 2.1). Using ECHAM4.0 model developed by European Center for Medium-Range Weather Forecast (ECMWF), two experiments were done by using climatological SST and adjusted SST (in which the SST during March-May and September-November are the same). The latter experiment showed a gradual maximum convection movement from south to north in MAM but less gradual for the north to south movement in SON. Overall, the experiment shows that the annual cycle is symmetrical. This experiment shows a clear conclusion that the SST during MAM and SON need to be different to reproduce the asymmetric maximum rainfall over the Maritime Continent.

Other than SST, another possible factor is the different behaviour of the Walker circulation over the Maritime Continent during spring and autumn, which is driven by zonal SST gradients over both the equatorial Pacific and Indian Oceans. The Pacific Walker cell may favour convection over the Maritime Continent in boreal autumn rather than in boreal spring because the cold tongue over the South China Sea is stronger during boreal autumn than in boreal spring (Chang et al., 2005a). The asymmetric monsoon transition is also related to the asymmetric equatorial

flow or wave response to heating. A strong Kelvin-type mean flow over western equatorial Pacific during boreal autumn allows the convection to move southward and the flow weakens during boreal spring (Hung et al., 2004; Matsumoto and Murakami, 2002). The absence of the northward movement of the maximum convection is also associated with the blocked northward Inter-tropical Convergence Zone (ITCZ) movement caused by the subsidence over the ocean to the west of the heat source (India, Indochina and Philippines) as a result of the Rossby wave response to the monsoon-desert mechanism suggested by Rodwell and Hoskins (1996). The asymmetry is also attributed to an internal atmospheric dynamics mechanism by which equatorial oceanic convection tends to propagate eastward due to the production of a boundary layer convergence to the east of the deep convection (Hung et al., 2004).

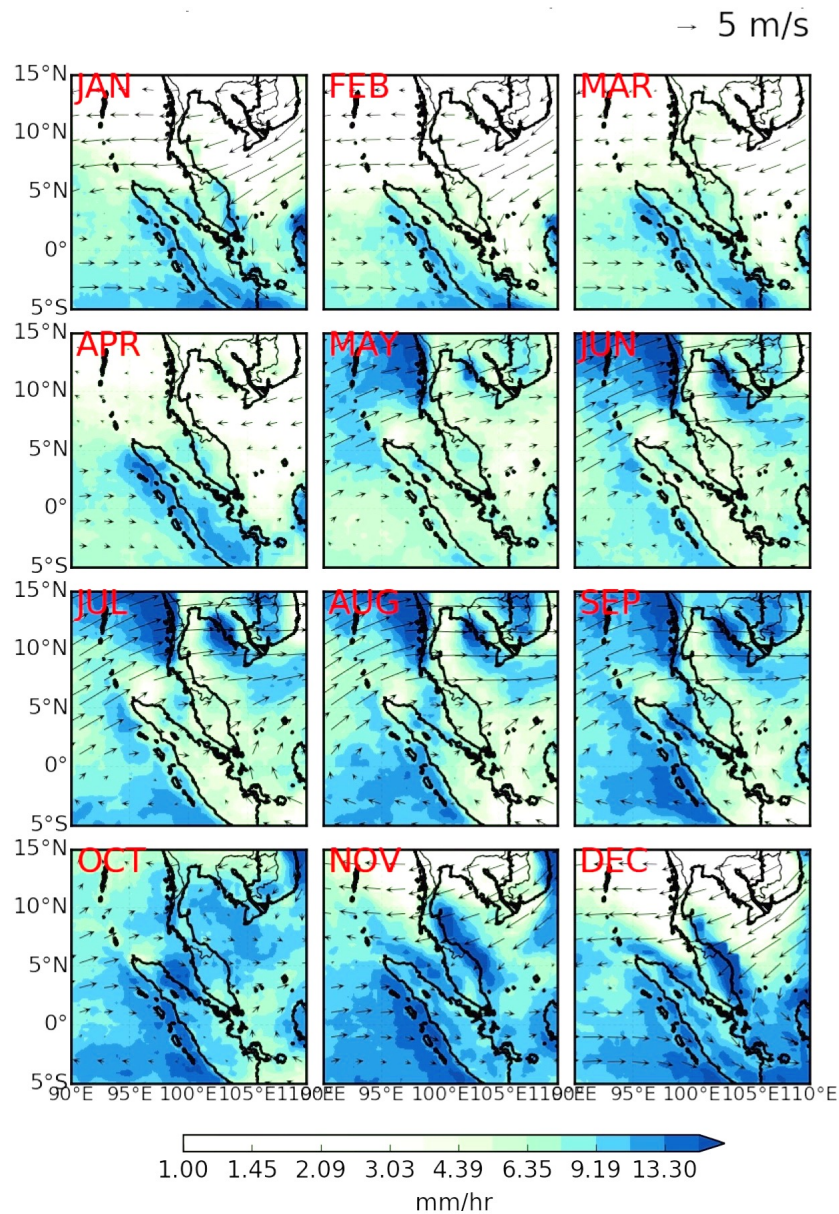


Figure 2.2: Monthly mean of 850 hPa winds (from ERA-Interim dataset) and rainfall (from TRMM dataset) from 1998 to 2013.

In the Peninsular Malaysia, the wettest period is during the Asian winter monsoon in boreal winter. Based on Chang et al. (2006), Asian winter monsoon starts in November and ends in March. Thus, this definition is also used in Malaysia. As seen in Figure 2.2, during Asian winter monsoon, the wind is mostly northeasterly from the South China Sea and easterly after crossing the Peninsular Malaysia, with the cross-equatorial westerlies in the south. During this season, the east coast of Peninsula Malaysia receives the most rainfall, due to the monsoon surge from the northeast. The relatively driest season is during the summer monsoon, which is from June until August. This is similar to the period of Asian Summer Monsoon. The wind is mostly westerly over the vicinity of Peninsular Malaysia (see Jun-Aug, Figure 2.2). Inter-monsoon is the time when the winds are changing from either southwesterly to northeasterly and vice versa. Monthly wind over the Peninsular Malaysia as shown in Figure 2.2 (Apr and May) shows that the first period of changing winds is observed between April and May (AM), where the winds change from easterly to southwesterly. The second period for the changing of the wind direction is in between October and November, but because most of the onset dates are in the first two weeks of November (MetMalaysia, 2016a), September and October (SO) is considered as the second inter-monsoon. Monsoon onset here is defined by Met-Malaysia as the 850 hPa wind steadiness (a magnitude and mean vector wind over a period of time) at Kota Bharu station, in the east coast of the Peninsular Malaysia. The monsoon is defined to commence when this index exceeds 0.6, and at the same time at least one of the east coast principal meteorological stations accumulates rainfall of at least 3 inches (76.2 mm) rain. This measurement starts from the 1st of October (Cheang, 1980; Moten et al., 2014). Unlike the first inter-monsoon, the winds are mainly westerly in SO (Figure 2.2; Sep and Oct).

On average, the Peninsular Malaysia receives more rainfall during winter monsoon, followed by second inter-monsoon (SON) with the rainfall rate as much as 14 mm day^{-1} over the east coast and the high rainfall covers the area in between 1.5°N and 6.25°N . This high rainfall is due to the cold surges during winter monsoon (Varikoden et al., 2010). During the inter-monsoon (April-May and September-October), Peninsular Malaysia receives a relatively higher rainfall than the annual mean, with an exception to the east coast region. The high rainfall rate during SON is concentrated over the west Peninsular Malaysia between 4°N and 6°N , while during MAM, the high rainfall is observed over the western coastal region of the peninsula (Varikoden et al., 2010). Based on recorded data available, the west and central peninsula receive higher rainfall during boreal autumn than during boreal spring (Wang and Chang, 2008). The local differences over the region are related to the interaction between local topography and the low-level winds and rain shadow effect (Chang et al., 2004; Lau and Chan, 1983).

2.2 Diurnal Cycle of Convection and Precipitation

The diurnal cycle of precipitation and convection over the Maritime Continent are highly influenced by the local effects such as topography and local air circulation, and it is important in shaping the tropical weather (Yang and Slingo, 2001; Johnson, 2011; Love et al., 2011). The land-sea breezes, mountain-valley circulation, and orography affect the precipitation pattern. Generally, landmass is heated by insolation, reaching a maximum in the afternoon, one to two hours after the maximum solar heating (which usually occurs at midday). The heating induces atmospheric convection, thus the rate of convection over land is usually maximum during the afternoon (Yang and Slingo, 2001). This circulation is of course modulated by orographic effects and synoptic influence. At night, the maximum convection occurs over the adjacent sea. Land breeze and offshore gravity wave propagation play an important role in the in the diurnal cycle of precipitation over the ocean.

These studies suggest several mechanisms in the diurnal cycle of convection (and diurnal cycle of precipitation) over this region. Some of the known mechanisms are the combination of land-sea breezes, mountain-valley breezes, and orography on the development of the diurnal convection as well as the precipitation pattern (Johnson, 2011). Previous studies analysed the diurnal cycle of precipitation over the tropical region by using data such as rain gauges, TRMM (Tropical Rainfall Measuring Mission) and GPCP (Global Precipitation Climatology Project). Several other studies (for example, Yang and Slingo (2001) and Peatman et al. (2014)) looked at the blackbody temperature data (equivalent to brightness temperature data from cold-cloud coverage data) to analyse precipitation.

Land breeze and the propagation of gravity waves from land to the adjacent sea at the night time play an important role in the diurnal cycle of precipitation over the ocean in most of the tropical region, especially over the Maritime Continent (Yang and Slingo, 2001; Love et al., 2011). Land breeze, as opposed to the sea breeze, is the opposite circulation as a response to the pressure difference between the landmass (a relatively higher atmospheric pressure area at night) and the adjacent ocean (a relatively lower atmospheric pressure area at night). The low pressure over the ocean also promotes convection over the adjacent ocean (Barry and Chorley, 2009). The daytime heating over the landmass heats the troposphere and changes the vertical profile later in the afternoon. Later in the afternoon, the heating in the upper troposphere and the cooling in the mid-troposphere over the landmass generate gravity waves that gradually propagate outward to the adjacent ocean. This gravity wave has positive temperature anomalies and stabilises the atmosphere and the convection offshore is suppressed. By midnight, subsequent gravity waves after the earlier waves slowly propagate toward the ocean and because

the lower troposphere features a negative temperature anomaly, it destabilises the column and promotes convection over the coastal and adjacent ocean (Love et al., 2011).

The diurnal cycle of convection can be split into 2 categories, thermodynamic processes that affect stability and processes that affect boundary layer convergence (Wallace, 1975). The first category involves daytime solar heating near land surface and destabilising of the boundary layer which is commonly associated with the observed afternoon and early evening maximum precipitation over land. The same idea was also observed over the ocean but to a lesser degree (Chen and Houze, 1997; Johnson et al., 2001). The instability process includes cloud radiation effects, where during the daytime, the absorption of solar radiation near cloud top stabilises the atmosphere near cloud top and at night, the longwave cooling destabilises the cloud top (Kraus, 1963; Randall et al., 1991).

The second category involves other processes such as land-sea breezes over the coastal regions, mountain-valley breezes, and wind variation at the top of the boundary layer associated with the diurnal variation in static stability and changes in frictional drag (Johnson, 2011; Wallace, 1975). There are also other mechanisms such as semi-diurnal pressure wave (Brier and Simpson, 1969) and cloudy and cloud-free regions coupling (Gray and Jacobson, 1977). The cloudy and cloud-free mechanism can be explained by the circulation steered by the horizontal temperature gradient between the two regions at night, associated with the longwave cooling over the cloud-free regions which enhance the low-level convergence over the cloudy region and results in the peak in rainfall in the late night-early morning hours.

In terms of precipitation, the general time for maximum precipitation over land is during the late afternoon and early evening, which is associated with the maximum heating during the early afternoon (Johnson, 2011). Thunderstorms are more frequently observed in the late afternoon than other time of the day in all seasons and are associated with the maximum convective available potential energy (CAPE) and minimum convective inhibition (CIN) due to insolation (Dai, 2001b). Interesting enough, Qian (2008) observed that the different island size has a different maximum precipitation peak, where a small or narrow island such as Java has a maximum precipitation peak at around 1300-1900LT, a medium-sized island such as Sumatra has the maximum precipitation peak at around 1600-2100LT and a larger island such as Borneo has a maximum precipitation peak at around 1900-0100LT. The island size has an impact on the propagation of the moisture inland and convergence of opposite sea breezes fronts, but, size may not be the only reason determining the occurrence time of maximum peak.

The diurnal cycle of convective precipitation, as concluded by Dai (2001b) can be summarised by these main points:

1. Convective precipitation over land is more frequent in the afternoon. While

over the open ocean and coastal, the maximum is usually during late night and early morning. Convection is more effective and intense over the land than over the ocean. The intense heating on the landmass by solar radiation destabilises the boundary layer which promotes convection. The process is intensified by local orography, such as sea breeze, mountain breeze as well as sea breeze collision. The solar insolation also occurs over the ocean but to a lesser degree, due to the high heat capacity of the water.

2. There are exceptions over a larger continental area (such as in the United States and Tibet), where the summer precipitation is higher during the night to early morning. Over the ocean, Bay of Bengal and part of South China Sea record maximum precipitation in the afternoon. One of the mechanisms for the late precipitation over land is associated with the propagation of convection which originates from the mountainous region (in the case of the USA). The afternoon maximum over the ocean is associated with the gravity waves originating from the land in the afternoon and slowly propagating further over the ocean.

3. Precipitation frequency has larger diurnal variation than the intensity. It means, the weaker the diurnal cycle, the more variable it is, and vice versa. For example, the Dai et al. (1999) study of US rainfall in summer suggested that rainfall can occur any time of the day, thus the frequency has large variability. The rainfall is the most intense (in this case, summer rainfall in the US) in the afternoon, and this is true for the stations over the east of the Rocky Mountains.

4. In some tropical stations, there is secondary semidiurnal (12-hour cycle) peak in precipitation. The secondary peak is weaker and the peak is around 0300 LST for a case of the tropical region, and around 0600 LST for a case of the mid-latitude region. There are theories on why the secondary peak exists over the tropics. For example, one of the reasons is, some areas are affected by the monsoon where the early morning rainfall is the result of the convergence between the monsoon flow and the local breeze (Oki and Musiaka, 1994).

2.3 Severe Convection over the Tropics

Severe convection over the tropics is common, especially in the equatorial region. Generally, maximum weather activity over the tropics is associated with the migration of the annual cycle of insolation (the ITCZ as well as the diabatic heat source migration as discussed in Figure 2.1), and the convective activity and rains do lag the insolation maximum by several weeks (Barnes, 2001). The maximum convective activity over the equatorial tropic (including Malaysia) is when the ITCZ is located over the equator when the solar zenith point is over the equator, thus the ITCZ is over the equatorial tropic following the maximum solar heating. The ITCZ brings

unstable atmosphere over the equatorial tropic promoting thunderstorms and severe rainfall to occur. However, extreme instability does not always produce severe convection storms, but slow movement of a storm system due to the wind condition and a deep layer of moist air can result in heavy rainfall and most of the time flash floods.

The effect of convective clouds are sometimes unpredictable, even convective clouds of modest size can cause flash floods. Deep convective clouds associated with the thunderstorm is common over the tropics, but not all resulting in severe weather events. Other than that, local orography plays an important role in guiding the water flow and causing a stream and the river to overflow and causing floods (Nor and Rakhecha, 2008). Severe weather events related to convective storms over the tropics sometimes produce tornadoes, hail with a diameter greater than 20 mm and winds exceeding 26 m s^{-1} . Deep convection size can reach a diameter of 3-5 km and as high as 10 km and can last 15-30 minutes, or maybe longer in the case of clustering storms (Barnes, 2001). Large hail requires a formation of hail embryo about 5 mm in diameter, accompanied by a strong and wide updraft. A severe convective storm in the tropics can produce strong straight winds, hails and on rare occasions, tornadoes. Strong straight-line winds rely on the evaporation of rain into the dry air below cloud base. The pre-monsoon season is known as the period where instability and the vertical shear of the horizontal winds can reach extreme magnitude to produce severe convection storms. A region with warm, moist air over the lower troposphere and cooler and dry air aloft, often produce severe convection storms. Lightning and thunder need a vigorous updraft (updraft movement greater than 10 m s^{-1}) to produce a volume above 5.5 km (freezing level in the tropics) that contains water in both liquid and ice form. Severe thunderstorm requires warm and moist air in the lower troposphere and cold and dry air aloft, including different wind direction and speed with height (wind shear) to produce severe weather. The deep convective clouds observed through satellite imagery usually produce thunderstorm and torrential rain events but do not always produce severe weather such as flash floods and tornadoes (Barnes, 2001).

High frequency of rainfall is observed over the near tropical convergence zone in the Pacific and Atlantic, and spatially larger over the Indian Ocean, Maritime Continent and the western Pacific. Results from observation datasets from around 15000 stations globally in Dai (2001a) shows that the mean rainfall rate over the tropics is around 1.5 to 3 m hr^{-1} . The intensity of the rain varies seasonally over the tropical land mass, which is associated with the seasonal maximum of solar heating. During boreal summer, thunderstorms frequently occur over South Asia, Indo-China, central America and the western part of the equatorial Africa. In austral summer, more thunderstorms occur south of equatorial Africa and central South America. During MAM and SON, 20%-50% of the days experience wet thunder-

storms over equatorial Africa and 20%-30% in southeastern Asia and central South America. Large precipitation amount over the tropics is mostly from frequently-occurring events rather than the intensity of the convective activity itself (Dai, 2001a).

From a study using TRMM dataset, Hamada et al. (2014) introduce three types of extreme rainfall categories; intense and extensive (IE), intense but less extensive (ILE), and extensive but less intense (ELI). IE is common over the oceans and near coasts and is associated with tropical cyclone and monsoon, ILE is widely over land and Maritime Continent and is related to afternoon convection and mesoscale convective system. ELI is commonly over the ocean, associated with well organised Mesoscale Convective System and the extratropical cyclone. Most of the severe storms over the tropics are convective related. Several regions experience squall line types of storms. Ariff et al. (2012), using a rain gauge dataset, also found that convective storm intensity is dependent on the geographical location, where an area prone to monsoon flows has a different intensity and type of storm compared to the regions that are less affected by the monsoon.

The most common mechanism of the development of severe weather event over the tropics is convection due to insolation. Then, the local orographic feature, as well as the large-scale weather, will influence the local weather circulation and pattern. Land-sea breeze, valley-mountain breeze, sea breeze collisions and orographic lifting are common over the tropics in the development of convective activity and sometimes become severe. The combination of these mechanisms is normal over the equatorial tropics to produce convection, but to produce severe convection, the right condition should be met.

For the convective cloud to occur, a lifting mechanism is required to lift up the moist air in the surface vertically to form clouds. Under the most condition, cooler and moist air is heavier than warm and dry air. The cooler moist air at the surface could not rise on its own, such lifting mechanisms are required. In an air parcel theory, when solar radiation heats up the moist and unsaturated air parcel on the surface of the Earth, the air parcel will be lifted upwards as it is warmer and less dense. To continue moving upward, the parcel needs to overcome its negative buoyancy to reach the lifted condensation level and form clouds. The negative buoyancy here known as Convective Inhibition (CIN), suppressed the air from ascending. As the air rises and reaches the lifted condensation level (LCL) it condensed, and then rises due to its own positive buoyancy to the LNB. The energy released by the parcel as it moves from the level of free convection (LFC) to the level of neutral buoyancy (LNB) is the CAPE (Ambaum, 2010). To continue rising, the air must continue to be warmer than its surrounding. As the moist air cools more slowly than dry air (due to the higher heat capacity of water), the ascending air will be warmer and continue rising until it reaches the parcel temperature equal

to the environment temperature (LNB, or also known as the equilibrium level, EL) (Trier, 2003).

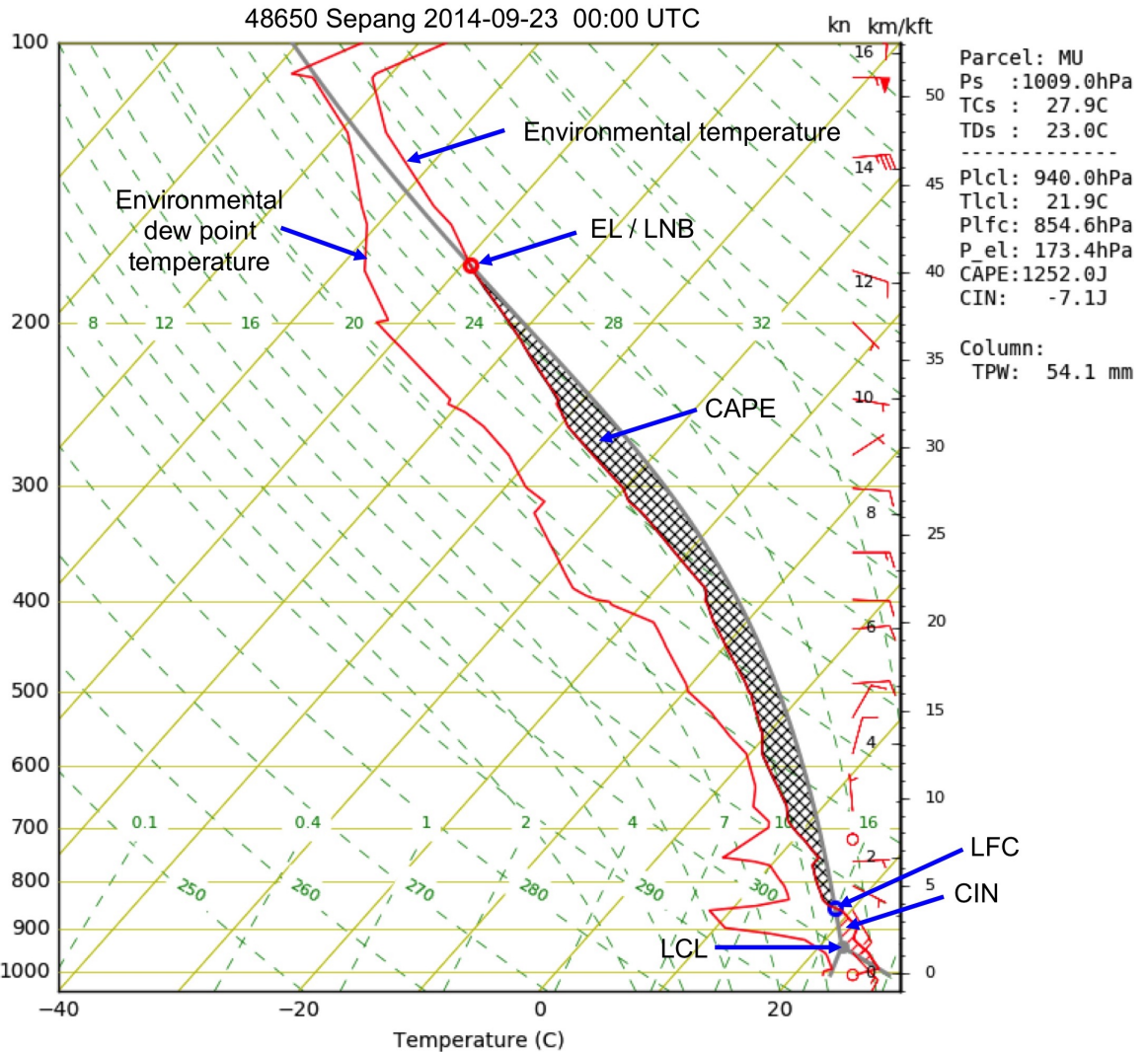


Figure 2.3: An example of a Skew-T diagram at one of the west coast station of the Peninsular Malaysia. Black cross-hatched representing the amount of CAPE, the red hatched represents CIN. The lifted condensation level (LCL), level of free convection (LFC), and equilibrium level or level of neutral buoyancy (EL or LNB) are pointed in the figure above. The image was created using a skew-t module of the Python language. Data was taken from the Sounding website of the University of Wyoming.

In observing the potential of a development of severe convective rainfall or storm, the CAPE and CIN are used to assess the atmospheric instability a particular profile of an area and determines the potential of the development of convective storm (Ambaum, 2010). In a Skew-T plot (see example in Figure 2.3), CAPE is represented by the area between the theoretical parcel air temperature and the actual temperature (environmental temperature) where the parcel temperature is greater than the actual temperature (Roff and Yano, 2002). CAPE (in J kg^{-1}) determines how strong updrafts will be and is calculated as the amount of energy available for convection. CIN is the area where the negative value of the theoretical parcel temperature is colder than the environment (Roff and Yano, 2002). As

mentioned previously, CIN is the energy needed for the parcel to overcome negative buoyancy to reach the level of free convection, and the unit is in J kg^{-1} . If a parcel of air rises in this region it will sink back down, thus there will be no convection to develop to a convective cloud (Roff and Yano, 2002). Skew-T or Tephigram plots are usually used to determine atmospheric instability and if there is a potential for a storm to grow. When the CAPE of a certain region is large enough and the CIN is small enough relative to the available lifting energy, the atmosphere is considered unstable and favours the development of the severe convective storm.

Other than solar heating, factors such as land-sea breeze, orographic lifting and circulation around the orography can also trigger a convective storm, by assisting moist air to move upward to its condensation level. For example, in sea breeze circulation, as the different rate of heating between land and the adjacent sea, the pressure gradient between land (heats faster, creates low-pressure zone) and the adjacent sea (heats slower, becomes a relatively high-pressure zone) creates airflow moving toward the land mass. As the heated air below lifted, it is replaced by the inflow from the sea bringing moisture. The ascending motion in land and descending motion over the sea creates a sea breeze circulation. As the heating continues, the continuous circulation will be able to overcome the CIN to ascend beyond the LCL and LFC. This will trigger the development of convective clouds and then possibly a convective storm (Birch et al., 2015). When heating is not available, convective clouds could also be a result of a flow of a moist air mass over a mountainous region is lifted up to its LCL. The mountains assist the lifting of the moist air against the CIN toward the LCL and triggering the development of convective cloud. Further, the lifting mechanism allows the air parcel to be able to rise to the LFC and could trigger the development of the convective storm (Houze, 2012). Other than that, lee and gravity waves created over the lee side of the mountains when an airflow crossing over will create disturbance and form clouds over the lee side of the mountains. If the instability is strong enough to overcome the CIN level and extended through the LFC, the resulting convective clouds could develop into a severe storm (Houze, 2012). Additional discussion of these mechanisms will be presented at the end of Section 2.4.

Forecasting and simulating precipitation over the tropics is not an easy task. In mid-latitudes, the weather is mostly dominated by the movement of frontal system influenced by cyclonic and anticyclonic atmospheric flow. The gradual movement of this weather system made the forecast of the weather in mid-latitude often reliable. Unlike in the mid-latitudes, the weather in the tropics is not largely dominated by a predicted weather system except during the Tropical Cyclone seasons, and monsoon flows. Most of the weather events are predominantly affected by the diurnal circulation (for example land-sea breeze). Thus, to forecast using a weather model the exact *when* and *where* the rain will occur in the tropic is slightly com-

plicated. Forecasting rainfall during inter-monsoon is one of the examples. During inter-monsoon, other than MJO and occasional tropical cyclones, most of the rainfall events are locally formed. Although the timing of the rain is likely to happen mostly after the maximum temperature is reached, it also depends on other factors such as moisture, wind and the interaction of both moisture and wind flow with the local orography (Sobel, 2012). Higher resolution simulations may produce storms which are located in a different location. Using Coupled Ocean/Atmosphere Mesoscale Prediction System (COAMPS), Joseph et al. (2008) found that the simulation (of the 2 km resolution model) has a good agreement with the observation of the relative humidity and surface winds. On simulating Hector thunderstorm over Tiwi Island using an earlier version of UKMO mesoscale model, Golding (1993) suggested a higher vertical resolution with better vertical profile input (sounding data) in the initial condition should be able to improvise the model performance. Even though both horizontal and vertical resolution is now improving in many simulation and forecasting models, the subject of accuracy is still open for improvement.

Climate models tend to underestimate the rainfall over the Maritime Continent due to the complex terrains over the region (Pope et al., 2000; Love et al., 2011), but Yang and Slingo (2001) argued that the model (atmosphere only Hadley Climate Model, HadAM3) produced an acceptable simulation of results of tropical precipitation and circulation, and the dissimilarity produced are due to systematic errors in the basic physics of the climate model (Pope et al., 2000), and small sample sizes in relation to Yang and Slingo (2001) experiment on the comparison between a dataset from Cloud Archive User Service (CLAUS) project and HadAM3 model simulation (limited to one year comparison, 1991-1992). Furthermore, a study by Schiemann et al. (2013) on the sensitivity of tropical circulation over Maritime Continent using Hadley Centre General Environment Model (HadGEM1) found that a higher resolution climate model enhances the representation of Walker circulation and increases moisture convergence thus correcting the dry bias over the Maritime Continent. Higher resolution in climate models reduces the tropical precipitation bias over the Maritime Continent, the western Pacific Ocean and the western Indian Ocean. Dry bias over the Maritime Continent was reduced by 33% and shows an improvement in the precipitation results over the western Pacific and Indian Oceans (Schiemann et al., 2013). As the resolution increased, the specification of surface boundary condition is better resolved. Increased resolution also improved the representation of complex and heterogeneous regions such as Maritime Continent and reduced the need of parameterisation of the coastal region, thus increasing the representation of the latent heat flux. Higher resolution models are expensive but reduce systematic error (Qian, 2008).

Even though models tend to have a precipitation bias over the tropics, most

models are able to capture the mechanisms of the development of deep convection. A higher horizontal and vertical resolution model (for example a 4km convection-permitting model) is also proven to be able to capture the mechanism of the thunderstorm development over the tropics. For example, Saito et al. (2001) simulation study on Tiwi Island using Meteorological Research Institute non-hydrostatic model (MRI NHM) shows that the model managed to reproduce the cloud merger process and squall line formation. In another example, Golding (1993), the 3-km UKMO model is able to capture the topographically forced thunderstorm genesis and the internal structure of the thunderstorm including the trade level inversion and mid-level rotation very well. Gravity waves were also well represented by the higher resolution model as in the 4km UKMO Unified Model run in Love et al. (2011) when representing the propagation of convection over the Sumatra region. This gravity wave is considered important because the error in lower resolution model (as in 40km run in the Love et al. (2011) study) may have been caused by the insensitivity of the convective parameterisation to the gravity wave structure.

There are a few suggestions regarding the model error. Firstly, Yang and Slingo (2001) suggest that the discrepancy in the phase of the diurnal cycle of convection in the UM is related to the implementation of the radiation scheme. In their simulation study, the UM updates the radiation every 3 hours and this opens a chance for an error as the radiation may change drastically in reality. Due to the imbalance of solar heating and longwave cooling, the diurnal cycle of temperature was out of phase as the maximum temperature is before noon, thus affecting the convection phasing (earlier than observed). These premature occurrences are also hypothesised to be caused by the systematic error in the interaction between the diurnal cycle of shortwave heating with the surface, the planetary boundary layer and its interaction with the surface, and the convective scheme and its interaction with the near-surface buoyancy (Yang and Slingo, 2001).

Secondly, the parameterised convection scheme which is usually used in lower resolution models produced dry bias over the Maritime Continent and more rain over the land and too little rain over the ocean. In the parameterisation scheme used in the model, errors in the surface scheme (for example soil moisture) are also thought to be a factor of the error in the phasing of the diurnal cycle of precipitation. The diurnal cycle of precipitation is too strong and peaks too early in the morning over land and too weakly over the ocean (Love et al., 2011). The explicit convection scheme which is usually used in higher resolution simulates the rainfall much better, where the diurnal cycle phase is better represented and similar to the observation. Error in the parameterised convection scheme may be due to the way the parameterised scheme hinders the interaction between the rainfall and the surrounding circulation by consuming CAPE and reaching radiative-convective equilibrium too quickly. Both parameterised and explicit convection schemes used in the models

produced a similar change in heating profile, where the mid-troposphere heating occurred in the early afternoon to the stratiform component, upper troposphere heating and mid-tropospheric cooling (Holloway et al., 2012). The coarse vertical resolution may also cause a weaker rainfall intensity as it fails to represent the real physical process of cloud turbulence. Joseph et al. (2008) claimed the models tend to underestimate the temperature in between 0700 to 1900 LT. The maximum temperatures depicted by the simulated results are around 1500 LT (± 1 hour). There are also some other issues such as less accuracy on the storm movements and local wind perturbation due to the failure in the interaction between convection and the mean flow (Crook, 2001).

Finally, as the tropical convective storm is sensitive to temperature, humidity, and winds, Zhu et al. (2012) claimed that the European Centre for Medium-Range Weather Forecasts (ECMWF) operational analysis system is not able to capture these variables in detail without additional observation data (as in scientific campaigns) assimilated into it. Especially when the ECMWF data is only a 6-hourly dataset and $0.5^\circ \times 0.5^\circ$ spatial resolution. Thus, using ECMWF data as the initial boundary condition, the model simulated the thunderstorm unrealistically, where the storm location is not the same as in the observation. This discrepancy can also be caused by the fixed SST when analyses are forced by fixed SST rather than incorporating the SST diurnal cycle over the region of interest. When the model used fixed SST and no diurnal variability, the model (Unified Model, based on the Chen and Houze (1997)) did not produce the diurnal phasing of the maximum temperature properly resulting in an error in convection initiation. Sea skin temperature variability is important, and as observed in the Weller and Anderson (1996) study of The Tropical Ocean Global Atmosphere Coupled Ocean-Atmosphere Response Experiment (TOGA COARE), near sea temperature is changing around one degree Celsius diurnally half of the time. A change of one degree Kelvin can induce light winds to trigger convection, thus the diurnal variability in skin temperature is important for the model to induce convection. Therefore, accurate model initialisation and lateral boundary conditions are important to better represent the simulation of the convection and need to be improved.

Few suggestions on how to produce more accurate simulations have been issued but they are not suitable for operational forecast due to limited resources. Upper air sounding data is probably useful to reproduce a storm. Using Weather Research and Forecasting (WRF) model, Zhu et al. (2012) simulated 4 tropical convective storm Hector cases where 3 of the cases incorporated observed data such as radiosonde and aircraft data. The simulation produced storms that are less intense and smaller in size. The observed data incorporated in the simulation process improves the simulation results. Moreover, a better representation of the boundary condition (with more improvement in data assimilation process) is vital

to improving the model output.

2.4 Processes Affecting Strong Convection over Peninsular Malaysia

Over the Peninsular Malaysia and Strait of Malacca area, little research has been done to study the thunderstorm development outside of the monsoon seasons. The storm development has a close relationship with the orography of the area. As discovered by Qian (2008), when a big tropical island is flattened to 1.5m orography, the rainfall starts and ends earlier than observed (3 hours earlier) due to a weaker land breeze and smooth penetration of sea breeze inland due to no orographic blocking. Water vapour merged inland and most of the convection is inland. Flattened orography also produces less rainfall inland, but more rainfall over the coastal region. The precipitation is underestimated when the orography is underestimated. Orography is important on the spatial distribution of the precipitation (Qian, 2008; Sow et al., 2011).

Sumatra Island is known to have an influence on the nocturnal precipitation over the Strait of Malacca by adjusting the timing and position of the convection. Air flow convergence coming from both lands is the key to the convective activity over the strait, where the cold front from the cold outflow of the land breeze is caused by evaporation cooling over the Sumatra and the Malay Peninsula, which is induced by the afternoon precipitation. Normally, the cold outflow which usually is the result of the previous evening precipitation will converge over the Strait of Malacca at around 10 hours after it is initiated. For example, when the cold outflow started at 1900 LT, the convergence happened in the middle of the strait at around 0500 LT when the condition is suitable for strong convection, with 5-6 m s⁻¹ of flow speed. Diurnal circulation over the straits was also clearly represented, where there is a clear downward motion around 1800 LT, an upward motion in 0300 LT and there is precipitation following the strong upward motion around 0500 LT (Fujita et al., 2010). This flow is well simulated by the WRF model version 3 in Fujita et al. (2010).

To look at the role of the local orography on the nocturnal precipitation over the strait, Fujita et al. (2010) did a few experiments by adjusting the width of the mountain peaks in Sumatra (Barisan mountains) and Peninsula Malaysia (Titiwangsa mountains). Sensitivity experiments (wider strait experiments) showed a significant difference where the maximum precipitation over the Strait of Malacca was observed to be around three hours late for every 100km. The first experiment was done by widening the two mountains range over the Sumatra and Peninsular Malaysia to 100km. In this experiment, with the same speed of the cold flow propagation as in the control run (5 to 7 m s⁻¹) from Sumatra and the peninsula,

the average peak time of maximum precipitation was around 0700 LT. The vertical motion was also weaker. The second experiment (200km wide experiment), shows the peak time of maximum precipitation is around 1000 LT, with also a weaker upward motion over the strait. The third experiment (300km wide experiment) shows the peak time was 1300 LT and a weaker upward motion over the strait. In both the 200km and 300 km experiments, two squall lines exist over the strait, before merging at the centre of the strait. Because of the slow speed of the cold flows (5 to 6 m s⁻¹), the merging of the cold flows (thus yielding maximum precipitation) was delayed. Thus, the two cold outflows from Sumatra and the peninsula did not manage to converge before daytime.

The air moisture plays an important role in the simulation model. As in the study conducted by Crook (2001) over Tiwi Island, Australia, a sensitivity experiment comparing the dry and moist condition showed that the moist atmosphere simulated a similar result as observed in terms of the storm intensity, and the convection intensity is directly proportional to the wind speed. This holds true until a certain threshold of 4 m s⁻¹ when the rainfall decrease and the wind speed increase. Heat and moisture fluxes are important in determining the convection strength because when the fluxes were increased, the convection strength is increased, making the heat flux become more important than the moisture flux, as the heat drives the sea breeze and convergence to generate convection. The environment must be moist to produce a deep convection. Dry run simulations produced a weaker convection, with a weak outflow of air from the lands, and weak vertical motion (Crook, 2001).

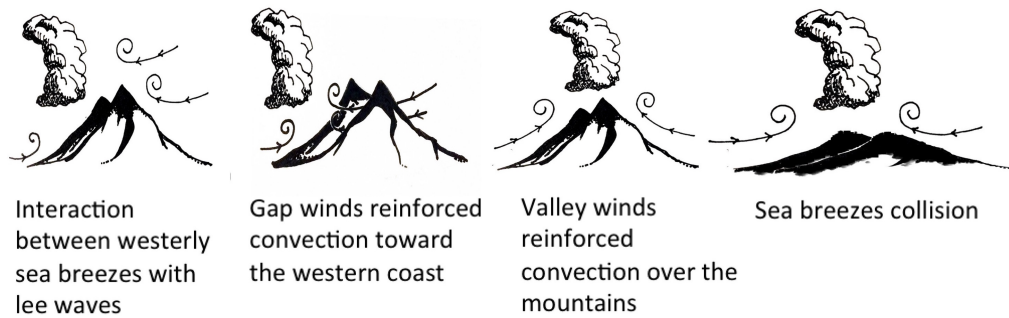
Some studies managed to get an approximately similar location and spatial distribution, as well in terms of convection development and evolution. Specifically, over the western Peninsular Malaysia, a few studies show some similarities and discrepancies between model and observation in terms of rainfall, winds, humidity and near-surface temperature. In a study by Sow et al. (2011) on late afternoon thunderstorms over the central western Peninsular Malaysia, the accumulated rainfall yielded from the model (MM5) output, was overestimated compared to actual observation. However, the location and spatial distribution were generally in agreement with the observation. Other than rainfall, the simulation is also in agreement with the observation of the winds and relative humidity. In another study by Joseph et al. (2008) on the simulation of sea breeze over the western Peninsula Malaysia on 23 April 2002, it was found that the model (COAMPS) has a reasonable agreement with the observation of winds and humidity, but tends to underestimate the daytime temperature around 0700 to 1900 LT, for about 1 to 2 °C colder than observation. The model, however, managed to simulate the convective clouds similarly to the observation. They, however, did not discuss the rainfall, but only the development of the deep convective cloud. The importance of representing small islands especially in the climate model is crucial to creating a realistic result. In

this case, a simple misrepresentation of islands to ocean contributes to the errors in the climate models as compared to the observation. Not representing small islands affects the diurnal cycle of convection and precipitation over the region (for example as explained by Neale and Slingo (2003) and Qian (2008)) this can indirectly affect the global circulation in Global Climate Models. Thus, small islands should not be ignored (and replaced by sea) in order to get better representation, especially in a coarse resolution model.

Some studies explained several mechanisms that are common in the development of severe convective storms particularly over the west Peninsular Malaysia, as summarised in Figure 2.4, namely the interaction between the advancing westerly sea breeze front with the gravity waves produced by the orography which then initiates severe convection events. The orography also sometimes produces lee waves as a result of an advancing easterly sea breeze. The lee waves converge with the westerly sea breeze and enhance convection which sometimes produces severe weather events (Joseph et al., 2008). The collision of east and west sea breezes in the front inland are common over the southern peninsula, where there is low orography and no breeze blocking (Joseph et al., 2008; Qian, 2008; Sow et al., 2011).

Orography also plays an important role in the development of inland convection. The mountain surface (slope) heats faster than the valley area at the beginning of the day. The air over the mountain slope is heated, rises and creates a low-pressure region. The low-pressure region attracts air over the valley to move to the upper altitude region. This air movement is known as valley breeze and induces earlier convection over the mountainous region to produce convective cloud (Qian, 2008). The interaction between the westerly sea breeze and the gap winds from the easterly sea breeze passing through the mountainous region is also one of the mechanisms that affected the development of severe convection over the central west coast specifically, and the strong easterly gap winds push the deep convection further west over the Klang Valley (central west coast) region. This mechanism is proved by Sow et al. (2011) with an experiment by adjusting the easterly wind to a uniform flow. At this point, the geographical characteristic of the region is believed to play an important role in the extreme rainfall development. The existence of Titiwangsa Mountains over the peninsula which blocks prevailing winds (be it northeasterly in boreal winter or southwesterly in boreal summer) could be the reason of the rainfall pattern over the west of Peninsular Malaysia (Jamaludin et al., 2010).

Atmospheric convection plays a major role in the development of convection (and also the transformation to deep or severe convection) over the tropics, and other large-scale influences such as monsoon flow enhance the convection to develop to be severe. Based on the study of Sow et al. (2011) using the Pennsylvania State University - National Center for Atmospheric Research fifth-generation



(Joseph et.al.(2008), Qian J. H. (2008), Sow et. al. (2011))

Figure 2.4: Theories on the severe convection development over the west coast of Peninsular Malaysia adapted from Joseph et al. (2008), Qian (2008), Sow et al. (2011), and Houze (2012). Figures were illustrated by the author based on the figures in Houze (2012)

Mesoscale Model (MM5), the afternoon convection activities over the western Peninsular Malaysia may have been developed by the combination of these mechanisms:

1. Thermal convection by surface heating, as the land heats due to solar insolation;
2. Sea breeze interaction, as the land heats faster than the sea because water has high heat capacity, leading to a difference in atmospheric pressure between land and sea. This circulation also enhances convection over land as well as supplying extra moisture from the sea;
3. Mountain breeze, as the higher altitude surface heats air quickly, the convection over the higher altitude produces low pressure that attracts air over the valley to move to the upper altitude region;
4. Dynamic convection by orographic lifting, where the existence of mountains in the path of the air movement can cause the air to be lifted to the higher altitude, reaching the condensation level and creates clouds; and
5. Lee side enhancement of convection, as the winds move inland and across the mountains, the wind is forced to cross to the lee side and causes a disturbance. The interaction between the sea breeze over the lee side of the mountain and this disturbance creates atmospheric instability over the lee side of the mountain.

Chapter 3

Data and Methodology

3.1 Data

The first part of this research utilises and compares gridded dataset from three sources: the Tropical Rainfall Monitoring Mission (TRMM), The European Centre for Medium-Range Weather Forecasts (ECMWF) as well as data from Asian Precipitation - Highly-Resolved Observational Data Integration Towards Evaluation of Water Resources (APHRODITE). The case studies used the ECMWF Operational datasets, retrieved through the Department of Meteorology, University of Reading.

3.1.1 TRMM and APHRODITE Dataset

The TRMM dataset is a joint mission between National Aeronautics and Space Administration (NASA) and Japan Aerospace Exploration Agency (JAXA) launched in 1997 and ended in 2015. The dataset obtained was on rainfall rate measurement from TRMM satellite as well as other satellites data. The 3B-42 algorithm was used to produce the adjusted rainfall rate which combined other precipitation estimates from TRMM Microwave Imager (TMI), Special Sensor Microwave Imager (SSM/I), Advanced Microwave Scanning Radiometer for Earth Observing System (AMSR-E), Special Sensor Microwave Imager/Sounder (SSMIS), Microwave Humidity Sounder (MHS), Advanced Microwave Sounding Unit (AMSU), and microwave-adjusted merged geo-infrared (IR) (Huffman et al., 2007). This dataset consisted of 3-hourly (3B42 Version 7), daily (3B42 version 7) and monthly (3B43 Version 7) datasets ranging from January 1998 until December 2013, with the spatial resolution of $0.25^\circ \times 0.25^\circ$ where all values are in mm hr^{-1} . It is available from 50°S to 50°N latitude and 0° to 360° longitude and at link

http://disc.gsfc.nasa.gov/datacollection/TRMM_3B42_V7.shtml.

The TRMM 3B42 dataset is considered more realistic in representing precipitation than any Global Climate Model dataset (Iida et al., 2010). However, Bowman et al. (2003) argued that the dataset from a satellite is susceptible to ran-

dom and systematic error, and is more accurate over the ocean than land due to the variation in surface emissivity. The error may also be associated with the difficulty in detecting shallow rainfall by the TRMM Microwave Imager (TMI) especially in the early stage of the rainfall system due to little or no ice scattering. This brings us to other issues such as the rainfall detected by satellite may not be captured in rain gauge due to the little surface rainfall and evaporation near the surface or the tilt of the storm system (Furuzawa and Nakamura, 2005). Even though TRMM 3B42 tends to overestimate the rainfall of over Malaysia (Semire et al., 2012), a good correlation coefficient between the TRMM and gauge dataset as shown in Semire et al. (2012) and Varikoden et al. (2010) studies give confidence that the dataset is able to represent precipitation over this region.

Meanwhile, the APHRODITE dataset (version V1101) is collected from a rain-gauge-observation network, a project initiated by the Research Institute for Humanity and Nature (RIHN) and the Meteorological Research Institute of Japan Meteorological Agency (MRI/JMA). The gauge data was then interpolated to produce the gridded data. The data was only available on landmass but not on the ocean (Yatagai et al., 2009, 2012). The dataset consists of daily data available from 1950 to 2007, but for the purpose of this study, the recent dataset from January 1978 until December 2007 was used (30 years). The data available is in $0.5^\circ \times 0.5^\circ$ and $0.25^\circ \times 0.25^\circ$, but for the purpose of this study, the latter spatial resolution was used (higher resolution). The data covers an area of $60.0^\circ\text{E} - 150.0^\circ\text{E}$ and $15.0^\circ\text{S} - 55.0^\circ\text{N}$. The rain gauge collected from Malaysia specifically, was collected from MetMalaysia rain gauge network. Depending on the year, the number of rain gauge stations used in this project is in between 10 to 25 stations over the Peninsular Malaysia alone (see Figure 3.1). For example, 25 stations data were used (or available) for the year 2000 but only 10 rain gauge stations were used (or available) for the year 2004. The data collected by APHRODITE project were collected from Malaysian Meteorological Department and one station from a "Global Summary of the day" (GTS) dataset. The rain gauge stations used for this project are shown in the following Figure 3.1 (Yatagai et al., 2009) and available at <http://www.chikyu.ac.jp/precip/english/products.html>.

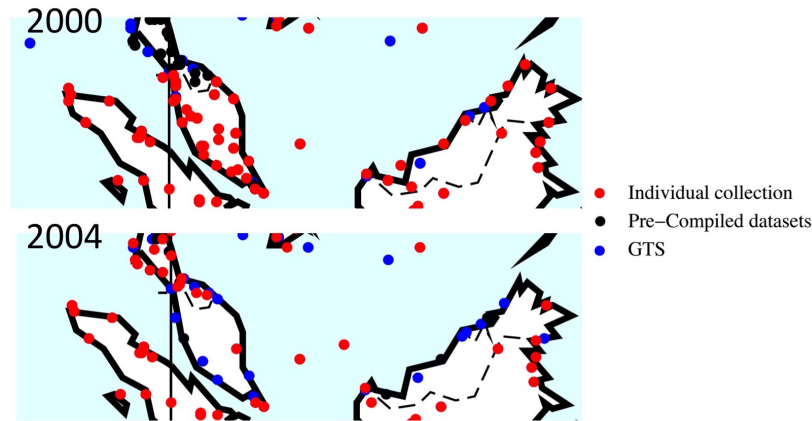


Figure 3.1: The location of the gauge stations used in APHRODITE project for the year 2000 and 2004 as an example of the rain gauge network density. The stations available for the project is in between 10 to 25 gauge stations. Individual collection (red dots) is the stations where the data is collected from the national meteorological service (Malaysian Meteorological Department), Pre-Compiled dataset (black dots) are data compiled from other project or organisation, and the GTS (blue dots) is Global Summary of the day - based dataset. (Yatagai et al., 2009).

3.1.2 ERA-Interim Dataset

The ERA-Interim dataset is a global reanalysis dataset available from 1979 until the present, provided by ECMWF (Dee et al., 2011). Data such as temperatures, zonal (U) and meridional (V) winds, relative and specific humidity were taken into account in this study. The study used data from 1980 to 2010 as a climatology reference and additional data of the subsequent years for case studies and TRMM-comparison analysis (since TRMM dataset used in this research was from 1998-2013 only). The dataset spatial resolution is approximately 79 km spacing on a reduced Gaussian grid and 60 vertical levels, with 6-hourly and monthly temporal resolution. The 6-hourly dataset is the instantaneous values while the monthly datasets used are monthly mean.

3.1.3 Rainfall Gauge Data

Dataset of several stations from Malaysian Meteorological Department (Met-Malaysia) and the Department of Irrigation and Drainage (DID) were retrieved and analysed. These datasets are dependent on their availability where 10-year rain gauge datasets from MetMalaysia and 16-year datasets were obtained from DID except Dengkil station (13 years) and Bota station (15 years). The difference in the availability of the data is due to the difference in the two stations starting operational date. The location of these stations is shown in Figure 3.2. Observational data from MetMalaysia and DID were also retrieved for comparison. Each station representing northeast coast (NWC), west coast (WC), inland (IL), south-west peninsula (SP), south-east (SE) and east coast (EC) regions. The list of data

3.1. DATA

and stations are as listed in Table 3.1. The location of the stations is shown in Figure 3.2.

MetMalaysia	Location	Daily data range	Hourly data range
1. Alor Setar 1 (NWC)	6.2° N, 100.4° E	Jan-Dec, 2005-2014	Sep-Oct 2014
2. Ipoh (WC/IL)	4.57° N, 101.1° E	Jan-Dec, 2005-2014	-
3. Sepang (WC)	2.73° N, 101.7° E	Jan-Dec, 2005-2014	-
4. Cameron Highlands 1 (IL)	4.47° N, 101.37° E	Jan-Dec, 2005-2014	-
5. Batu Pahat 1 (SP)	1.87° N, 102.98° E	Jan-Dec, 2005-2014	-
6. Petaling Jaya (WC)	3.1° N, 101.65° E	-	Jan-Dec 2012
DID	Location	Daily data range	Hourly data range
1. Alor Setar 2, (NWC)	6.11° N, 100.39° E	Jan-Dec, 1998-2013	Jan-Dec, 1998-2013
2. Bota, (WC)	4.37° N, 100.90° E	Jan-Dec, 1998-2012	Jan-Dec, 1998-2012
3. Cameron Highlands 2, (IL)	4.52° N, 101.38° E	Jan-Dec, 1998-2013	Jan-Dec, 1998-2013
4. Dengkil (WC)	2.86° N, 101.68°E	Jan-Dec, 2002-2014	Jan-Dec, 2002-2014
5. Batu Pahat 2 (SP)	1.88° N, 103.05° E	Jan-Dec, 1998-2013	Jan-Dec, 1998-2013
6. Mersing (SE)	2.47°N, 103.81° E	Jan-Dec, 1998-2013	Jan-Dec, 1998-2013
7. Kota Bharu (EC)	6.02°N, 102.29° E	Jan-Dec, 1998-2013	Jan-Dec, 1998-2013

Table 3.1: List of the rainfall gauge dataset from Malaysian Meteorological Department (MetMalaysia) and Malaysian Department of Irrigation and Drainage (DID).

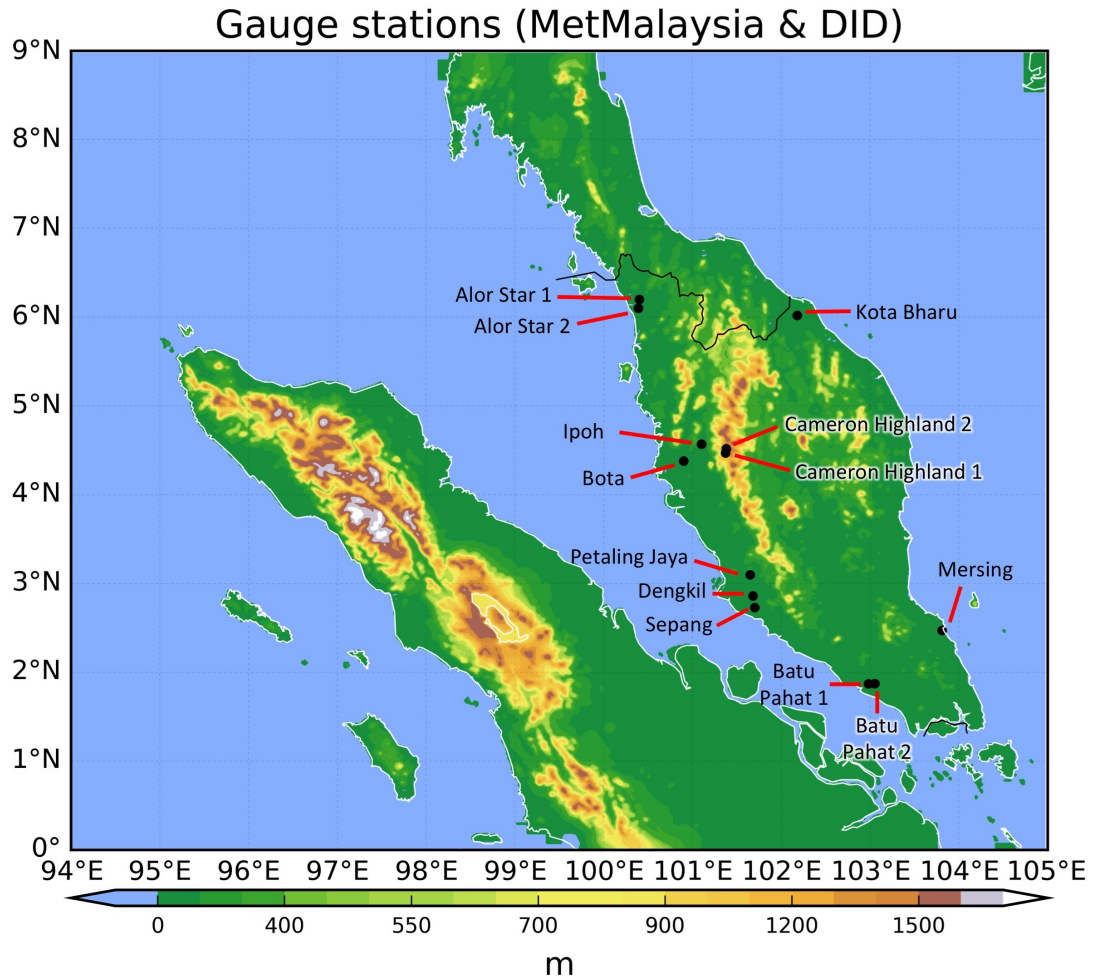


Figure 3.2: Locations of the different gauge stations used in this study. Alor Setar 1, Ipoh, Cameron Highlands 1, Sepang and Batu Pahat 1 are MetMalaysia stations. Alor Setar 2, Bota, Cameron Highlands 2, Dengkil, Batu Pahat 2, Mersing and Kota Bharu are DID stations.

3.1.4 Radar, Satellite, and Sounding Data

Other observational data such as radar images were also retrieved from Met-Malaysia to be used in the case studies. The first case study used radar images from 0000 LT 2 May 2012 - 2000 LT 2 May 2012 that were retrieved from MetMalaysia website whilst images from 0400 LT 24 September 2014 - 2000 LT September 2014 were for the second case study. Based on a study by MetMalaysia, (Kamaruzaman et al., 2012), the radar data used by MetMalaysia is optimised by using radar reflectivity factor (Z)-rainfall rate (R) relationship (Z-R relationship method) as suggested in Battan (1973) and this was used to compare to the rain gauge. The method is essentially converting the radar reflectivity values (Z) in $\text{mm}^6 \text{m}^{-3}$ to rainfall rate in mm hr^{-1} . However, there are issues to be considered as potential errors. As mentioned in Sebastianelli et al. (2010), the elevation angle of the radar may capture different rain rate values than the rain gauge catchment on the surface. When the radar is pointed too high in altitude, there is a potential that the radar reflects the raindrop as weaker than the rain gauge catchment measured if the coalescence process occurred before the raindrops reached the surface. On the other hand, there is also a potential error where the rainfall evaporates before reaching the ground and in this case, the radar may have returned higher reflectivity values (rain rate values) than the actual rain gauge values.

The satellite images for this study were retrieved from Kochi University Weather website and are free to be used for research and educational purposes. They are therefore used for the comparison with other product (namely TRMM) for the development of the convective cloud for both case studies. The satellite images were from the Himawari 7 (MTSAT-2) satellite (infrared image IR1 (10.3-11.3 μm)) and are available at <http://weather.is.kochi-u.ac.jp/archive-e.html>. Meanwhile, the upper air data for the case studies were retrieved from University of Wyoming's Atmospheric Sounding Weather Website which is available at <http://weather.uwyo.edu/upperair/sounding.html>.

The sounding images were only be used as a reference for the severe convective rainfall (or thunderstorm) development for the case studies.

3.2 Model Configuration

One of the main works in this study used the UK-Met Office Unified Model (Met-UM) to simulate two case studies on understanding the development of severe convection or severe rainfall events. This project used Met-UM version 7.5 which is semi-implicit semi-Lagrangian and non-hydrostatic Euler equation called New Dynamics dynamical core (Davies et al., 2005). This study used a limited area model, utilising lateral boundary condition by ECMWF operational analyses dataset with subscribed SST (fixed SST at the initial value) from the ECMWF analyses. Two domains, the 12km resolution for the outer domain (12km \times 12km grid resolution) and 1.5km resolution for the inner domain (1.5km \times 1.5km grid resolution) were used and the area of the domains can be viewed in Figure 3.3. The 12km model (154 \times 172 grid) used $0.11^\circ \times 0.11^\circ$ resolution while the 1.5km model (666 \times 814 grid) used $0.0135^\circ \times 0.0135^\circ$ resolution. The grid in both models is not rotated, with the poles being the same as in the real Earth. There are 38 vertical levels in the 12km resolution model with the maximum of 37km hybrid height and 10 hPa pressure level. The 1.5km model has the maximum height of 40km in hybrid height and 50hPa in pressure level. The hybrid height is the terrain-following level heights.

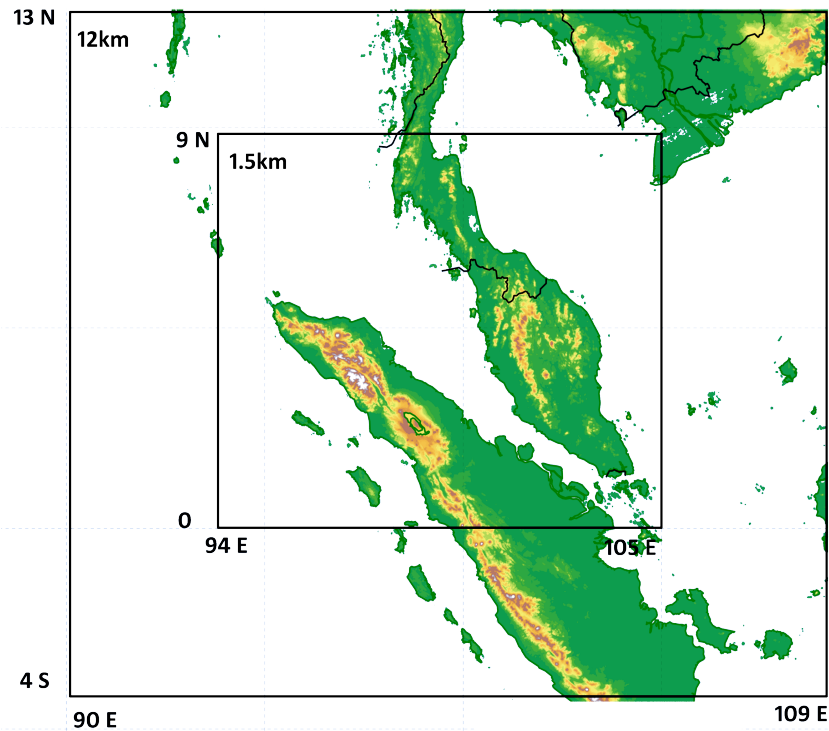


Figure 3.3: Domains for the simulation studies. The 12km model simulation used the outer domain and ECMWF operational dataset as the lateral boundary condition whilst the 1.5km model simulation used the inner domain and the output from the 12km model was used as the lateral boundary condition in the 1.5km model.

The 12km *param* model used a parameterised convection scheme and the lateral boundary condition was updated from ECMWF analyses every 6 hours through

an 8 model grid rim width around the domain. This model has a physics setting where it uses a Gregory-Rowntree convective parameterisation with a 30-minute convective available potential energy (CAPE) relaxation time scale (Gregory and Rowntree, 1990) and a 1D boundary layer turbulence scheme. On the other hand, in the 1.5km *3Dsmag* resolution model, resolved the convection entirely with the actual grid-scale dynamics and "large-scale" rain scheme, meaning the convection is resolved explicitly within the grid point without much use of the convective parameterisation. This model uses Smagorinsky mixing in all three dimensions. The lateral boundary condition was updated from the 12km model output for every 30 minutes through a 10 model grid rim width. The rim is where the prognostic fields blended linearly between the outer analyses data and inner model domain (Gregory and Rowntree, 1990). Since the 1.5km model is a high-resolution model (spatially) and is able to resolve convection on the model grid point, no convective parameterisation scheme was used thus, the convection is resolved explicitly. This model run is a one-way nested. Both 12km and 1.5km models run with the "QTidy" moisture conservation on.

3.3 Methodology

Figure 3.4 shows the research plan of the study in which the first part analysed variables such as precipitation, winds, temperature and humidity over the Peninsular Malaysia and the surrounding areas using reanalysis dataset to understand the annual, seasonal and monthly variations. This part of the study intended to analyse the rainfall, winds, temperature, and humidity pattern. For the analysis of the precipitation, TRMM, as well as APHRODITE data, were used the before comparing them to the observational rainfall data from various stations gauges, provided by MetMalaysia and DID. The rainfall gauge station dataset was also used to analyse the annual and seasonal rainfall and the diurnal mean patterns. Meanwhile, the winds, temperature and humidity climatology in the seasonal and monthly pattern were analysed using the ERA-Interim dataset. This is vital in determining the rainfall, winds, temperature and humidity pattern over west Peninsular Malaysia seasonally.

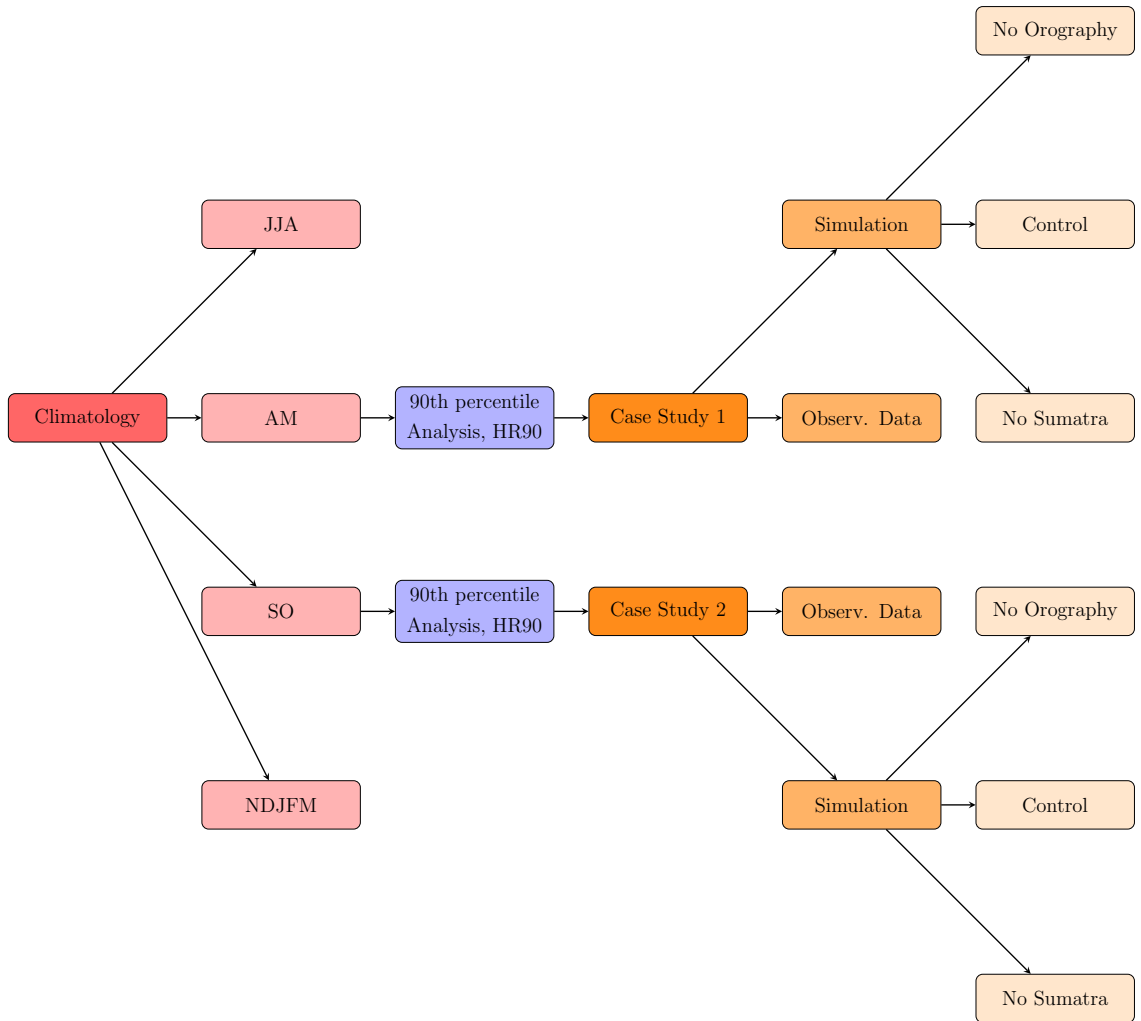


Figure 3.4: Research Plan for this study. The first part represents the climatology analysis, followed by ‘heavy rainfall days’ analysis and finally the two case studies including sensitivity experiments.

3.3.1 Climatology

Chang et al. (2006) argued that the East Asian winter monsoon happens between November and March (NDJFM), thus, this study will adopt Chang’s argument in considering the suggested months as winter monsoon. Summer monsoon is usually dry and is from June through August (JJA). There is no definite definition of the inter-monsoon period. However, in this study, the inter-monsoon will be defined by the time where the monthly mean wind direction changes direction (refer Figure 3.5), in this case, from northeasterly to southwesterly (April-May, AM) and the special case of September-October (SO). In SO case, the mean wind direction changes between October and November, but November is considered as the beginning of winter monsoon. Based on MetMalaysia reports, the monsoon onset always starts in November (MetMalaysia, 2016a).

To analyse the regional rainfall pattern for TRMM and APHRODITE dataset, the peninsula was divided into 5 regions where the rainfall average of each area (NWC, WC, IL, SP and EC) were calculated (Figure 3.6). This area division is

3.3. METHODOLOGY

a modified version of the one used in Suhaila and Jemain (2009) and is based on geographical division. Since the available TRMM dataset is until 2014 and APHRODITE data is only available until 2007, the TRMM data was thus used for the second part of this study.

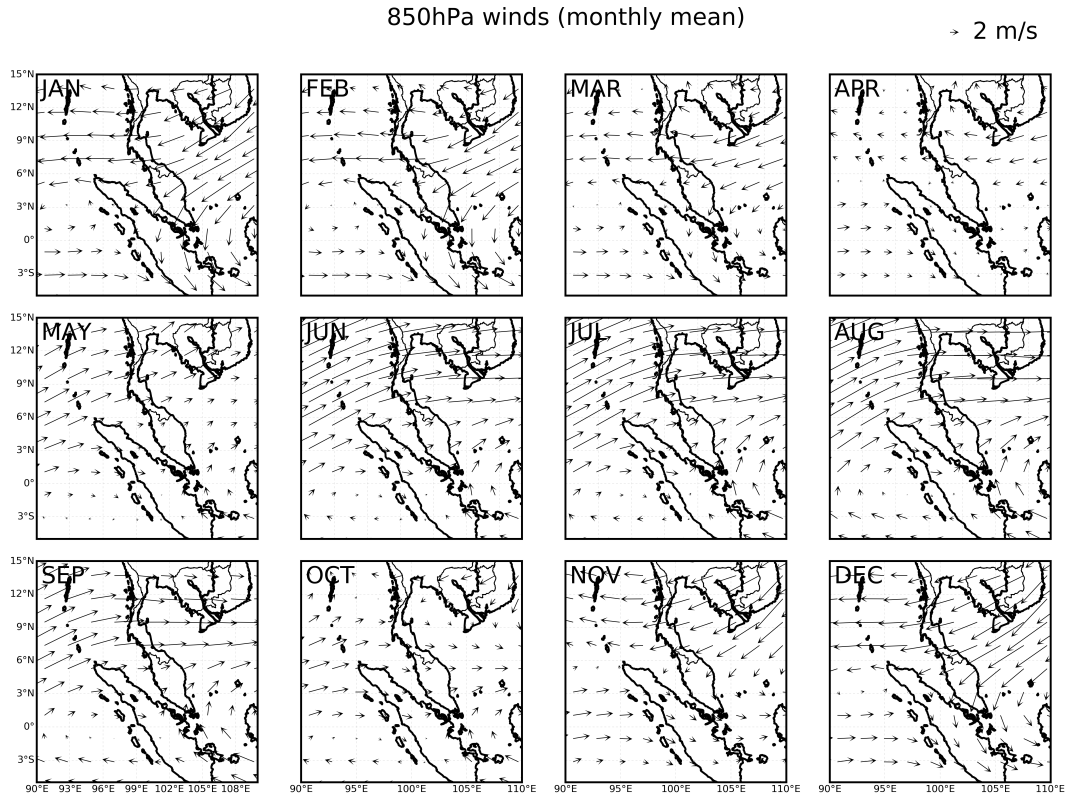


Figure 3.5: Monthly mean of 850hPa winds from ERA-Interim for the year 1981 until 2010. The first inter-monsoon (April-May, AM) is the time when the northeasterly winds over Peninsular Malaysia, South China Sea and the Andaman Sea changes to southwest-westerly. Meanwhile, the second inter-monsoon is when the wind direction changes between southwesterly to northeasterly. As for the second inter-monsoon, September-October months (SO) were chosen instead of October-November because November is usually the onset month of winter monsoon over Malaysia.

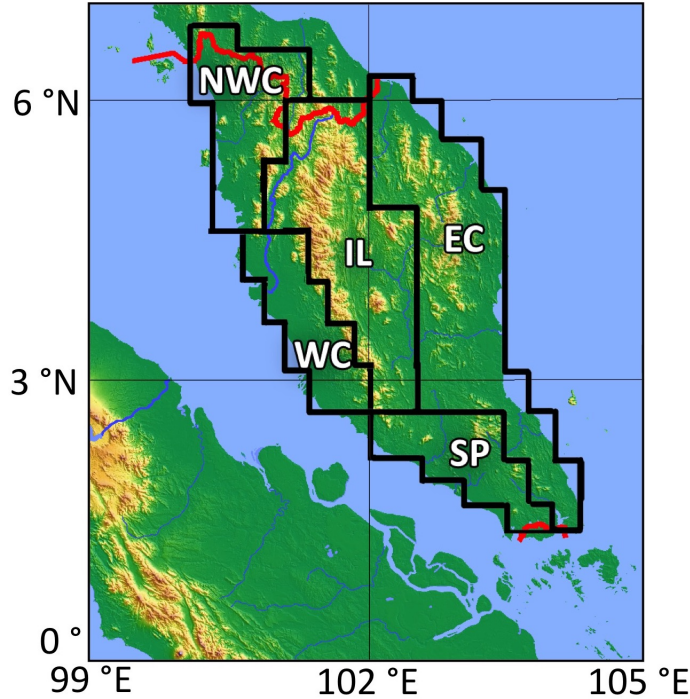


Figure 3.6: Regions are divided into 5 over the peninsula: NWC: north-west coast; WC: west coast; IL: inland; SP: south peninsula; and EC: east coast. The division is based on the geography and is modified from Suhaila and Jemain (2009). Only NWC, WC and IL will be focused in this study.

3.3.2 Severe Rainfall Events during Inter-monsoon

The second part of the study looks at the heavy rainfall (defined as days with above 90th percentile, or the top 10% of daily rainfall total). An analysis using TRMM was conducted using rainy day frequency where the daily rate is above the 90th percentile and daily rain rate from 1st January 1998 until 31st December 2013. The rainy days here is defined as days with greater or equal to 1 mm per day. Thus, the calculation of the 90th percentile for each region (for gridded dataset) and station (rain gauge data) was based on the list of days with daily rainfall total above 1 mm per day. The same process was also done for APHRODITE dataset on the daily rainfall rate from 1970-2007. The values of the 90th percentile were then determined and using these values, the days that recorded more than or equal to the 90th percentile were selected.

From the new list, the days associated with the active phase of Madden-Julian Oscillation (MJO, phase 3, 4 and 5 in Real-time Multivariate (RMM) index as in Wheeler and Hendon (2004), refer Figure 3.8) were eliminated and the remaining days were considered as *Heavy Rainfall Days (HR90)*. As suggested by Wheeler and Hendon (2004), the calculation of Real-time Multivariate MJO was done using Empirical Orthogonal Function (EOF) analysis of the combination between Outgoing Longwave Radiation (OLR), 850hPa zonal wind, and 200hPa zonal wind to determine the MJO phases. The first and second leading EOFs from this analysis

are known as RMM MJO phase 1 (RMM1) and phase 2 (RMM2). To determine the MJO phases, the amplitude (daily value) of the MJO was calculated and plotted onto the Wheeler-Hendon phase diagram. Meanwhile, the list of these RMM indexes was taken from the MJO monitoring web page of Bureau of Meteorology Australia website (<http://www.bom.gov.au/climate/mjo/graphics/rmm.74toRealttime.txt>) When the value (of a certain date) falls in the inside circle, the MJO is considered not to be in an active phase. In different circumstances, if the date falls into one of the regions outside of the circle, it is thus regarded as an active phase of MJO. Depending on the values, the date may fall in one of the 8 regions, signifying which region experiences an active (or suppressed) MJO phase.

The above step is important to make sure all the selected events were not associated with any large-scale phenomena. For example, MJO is common throughout the year including during inter-monsoon. This is important because this study only focuses on the rainfall events that were developed locally. With that restriction, we can study the severe rainfall event that was developed mostly by local weather circulation. The whole selection process is simplified in Figure 3.7. Other than MJO, other large-scale phenomena such as El Niño-Southern Oscillation (ENSO) and Indian Ocean Dipole (IOD) may also have an influence on the severe convection during inter-monsoon over the peninsula. La Niña event (positive phase of ENSO) and negative IOD phase are associated with the more convection activity thus indicating a wetter condition over the Maritime Continent. However, for the purpose of this study, only MJO will be considered.

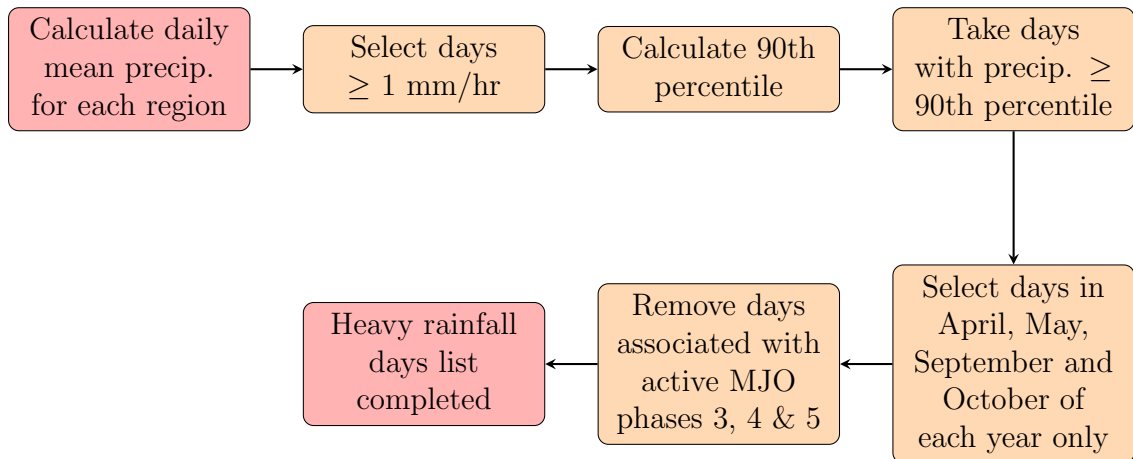


Figure 3.7: A flow chart showing the process using the list of Heavy Rainfall Days (**HR90**) in part two of this study.

The composite of precipitation, winds, temperature and relative humidity on these dates were analysed to observe the spatial pattern of the considerably heavy rainfall days, especially the rainfall distribution as well as the winds and temperature mean and anomalies. This part of the study determines the average pattern of the rainfall and winds during the heavy rainfall days. The list is also used as a guide on selecting the case studies for the third part of this study.

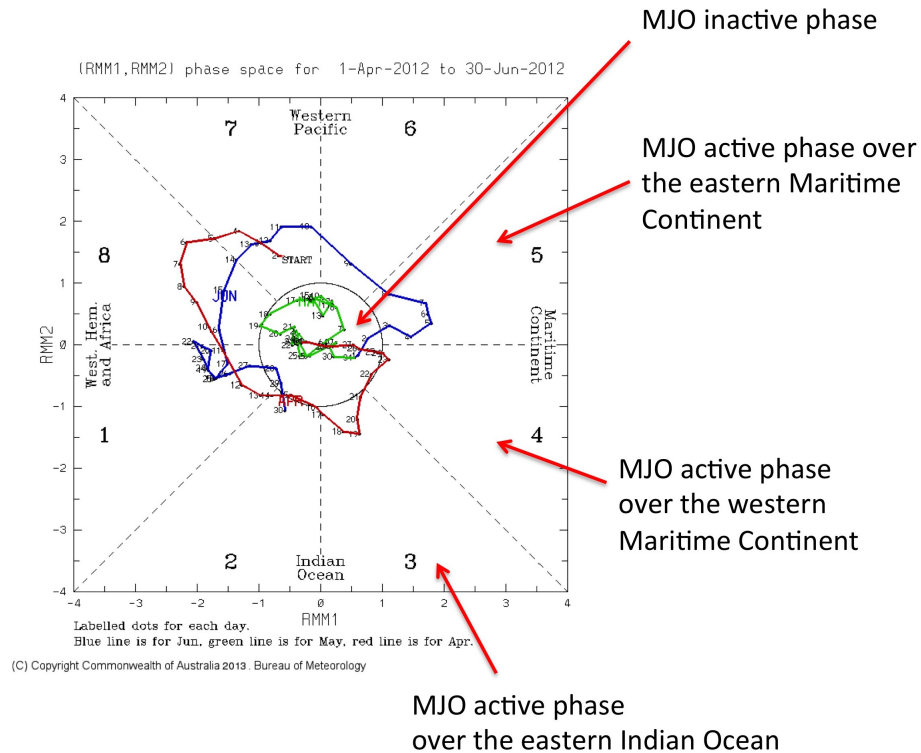


Figure 3.8: An example of MJO phase diagram from Wheeler and Hendon (2004) showing the evolution of the MJO from Phase 1 (western Africa) to Phase 8 (western hemisphere) for the month of April until June 2012. The amplitude of RMM1 and RMM2 determine the strength of the MJO for each day. Depending on the values, the day is plotted on the diagram. When the daily value falls inside the circle, the MJO is in a suppressed (inactive) phase. However, if the daily value falls into one of the regions outside of the circle, the region is considered experiencing an active MJO phase on that day. Original figure retrieved from Bureau of Meteorology Australia and used with permission.

3.3.3 Case Studies

The final part of this study is a model simulation. Two case studies from each inter-monsoon periods (April-May and September-October) were selected and also compared with the *Heavy Rainfall Days* list to make sure the events are listed. Using the Met-UM, the two case studies were simulated using the high-resolution model and the output is used to study how the severe rainfall events developed. This simulation is important to investigate in detail the mechanism which was not captured or available in the reanalysis dataset such as rainfall for every 15 minutes and hourly wind flows.

The first run (control, CTR) was done for 5 model-days, from 0000 UTC on 30 April 2012 and ended at 0000 UTC on 5th May 2012 (the output excluding 0000 UTC of 5th May 2012). The 6-hourly ECMWF analysis from 0000 UTC on 30 April 2012 until 1800 UTC on 4th May 2012 were reconfigured to Met-UM data for the Lateral Boundary Condition (LBC) file. The LBC file was used as the boundary condition for the 12km model run for five model days at once and updates the lateral boundary condition for every 6 hours. The 12km model was run for the five

model-days at once. A start dump from ECMWF reanalysis (0000 UTC 30 April 2012 with subscribed climatological SST) was used as the start file (start dump) for the 12km model run which in turn produced an LBC file for the 1.5km model. This LBC file was used to update the boundary condition in the 1.5km model for every 30 minutes. The start dump for the 1.5km run was reconfigured from the start dump provided by the 12km model run (for 0000 UTC 30 April 2012) and the 1.5km model ran one model day at a time. This used the start dump created by the 12km model run.

As for the remaining four model-days (model-day two until five), it used the start dump which was produced from the previous run. As mentioned in the previous section, the model run is a one-way nested run. Meanwhile, for the second case study, the same setup was used and the model was run for the 5 model-days, starting from 0000 UTC 22 September 2014 until 0000 UTC 27 September 2014. The 1.5km model output was compared to the observation and then analysed. The output of this simulation was used in the investigation, where the mechanism of the severe rainfall event development was studied qualitatively and quantitatively.

3.3.4 Sensitivity Experiments

Sensitivity experiments were conducted to investigate the role of orography and Sumatra Island in the development of the severe rainfall event. The same model reconfiguration as in the control run was used, except for the orography and land-sea mask fields which were modified according to the objective of the experiment. As the experiment was only run on the 1.5km model, the same 12km model LBC file and start dump from the control run were used as the boundary condition and input file respectively. No new run for the 12km model was done in each experiment. The experiments were run on the same model-day period, from 0000 UTC on 30 April 2012 and end at 0000 UTC on 5th May 2012 (the output excluding 0000 UTC of 5th May 2012), which was the same as the control run and the rest of the experiment. The modification in each experiment can be visualised in Figure 3.9. The experiments only modified the orography and land-sea mask as follows:

1. The first sensitivity experiment is flattened Peninsular Malaysia (**flatPM**). The orography of the peninsula was flattened to the sea level.
2. The second sensitivity experiment is the flattened Sumatra Island (**flatSI**). The orography file was adjusted by flattening the orography of the Sumatra Island and the surrounding small islands to the sea level.
3. The third sensitivity experiment is the flattened Sumatra Island and Peninsular Malaysia (**flatALL**). The orography file was adjusted by flattening the orography of the Peninsular Malaysia, Sumatra Island and the surrounding small islands to the sea level.
4. The fourth sensitivity experiment is the No Sumatra Island (**noSI**), where

the Sumatra Island was removed. The orography of the Sumatra Island was initially flattened to the sea level and the land-sea mask file was adjusted by removing the land mask of the Sumatra Island as well as the surrounding small islands. This adjustment replaced the island with an ocean.

No other fields in the ancillary file were changed, for example, the vegetation and land used remained the same. The results of these experiments were then analysed and compared to the control run. As for the sensitivity experiments, the values of other fields (temperature, surface pressure, etc) were not manually added when the orography was flattened (temperature, surface pressure, etc) or the Sumatra Island was removed (SST, surface pressure, etc). Instead, the model interpolates the values from the initial condition and surrounding values. This will affect at least the first 12 hours of the run. Thus the first 24 hours of the model run is considered as the spin-up period.

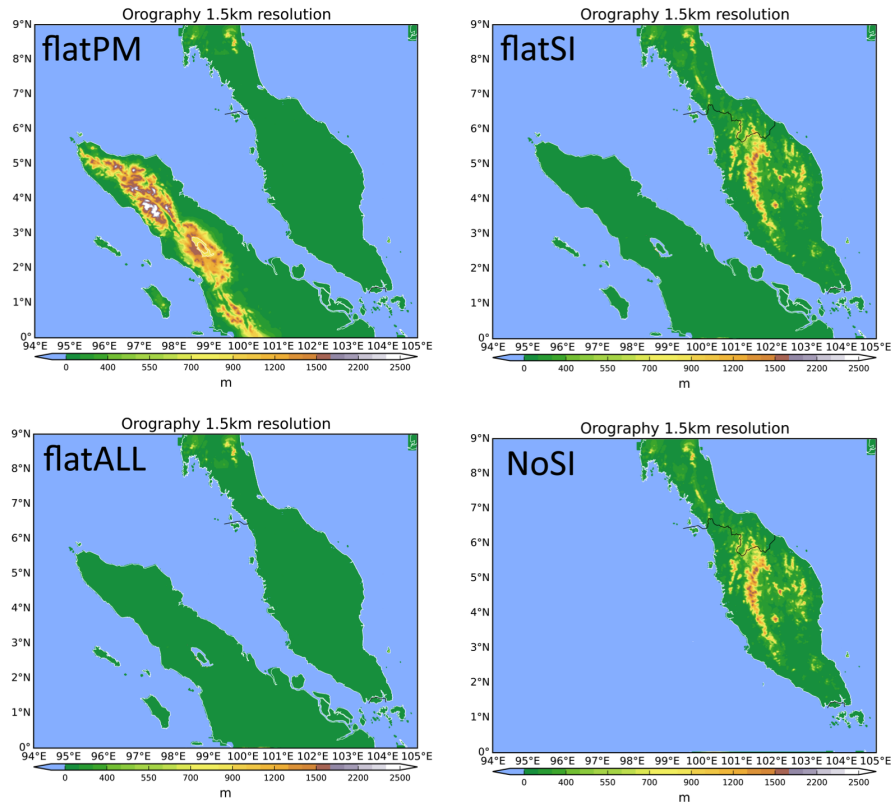


Figure 3.9: The four sensitivity experiments conducted. Flat Peninsular Malaysia orography (**flatPM**), flat Sumatra Island orography (**flatSI**), flat both Peninsular Malaysia and Sumatra Island orography (**flatALL**), and the Sumatra Island was removed (**noSI**). The flatten experiments were done by flattening the orography to the sea level in the 1.5km model. Sumatra Island was removed by first flattening the orography and then removing the Sumatra in land-sea mask file in the 1.5km model.

3.4 Summary

This study uses a relatively recent dataset for the climatological analysis. The rainfall gauge dataset from MetMalaysia and DID were also useful in comparing the gauge and TRMM (as well as APHRODITE) data to confirm the reliability of the TRMM dataset to be used in this study. The severe rainfall events analysis on the TRMM is a simple but significant analysis in looking at the common patterns in terms of wind circulation and rainfall distribution during heavy rainfall days. Excluding events that were influenced by any synoptic events (in this study, active MJO phases), these severe rainfall events were believed to be local events, with no influence from large-scale weather phenomena. They are highly dependent on the local weather and topography in modulating the daily weather pattern. However, these reanalysis datasets were not enough to investigate the process involved in the development of the rainfall events in greater details.

To study in greater details, a high-resolution model is needed. The Met-UM was selected to realise this objective. As discussed in Figure 3.2, the Met-UM is capable of running and producing high-resolution data and this is important to investigate the process involved in the development of the severe rainfall event over this region. However, the process to simulate all severe rainfall events is time-consuming and expensive. Thus, only two severe rainfall events were selected in this research as its case studies. Two case studies are definitely not enough to generalise the process, but this can be an additional information or knowledge to be added to the previous studies (such as in Joseph et al. (2008) and Sow et al. (2011)).

Since this study believed that orography and Sumatra Island play important roles in the development of severe rainfall event over western Peninsular Malaysia, four sensitivity experiments related to the orography were done. The four experiments are flatten Peninsular Malaysia (**flatPM**), flatten Sumatra Island (**flatSI**), flatten Sumatra and Peninsular Malaysia (**flatALL**) and without Sumatra Island (**noSI**). As the names suggest, the flat experiments were run with a flattened orography of the Peninsular Malaysia (or Sumatra or both) to the sea level. The no Sumatra experiment was run with no Sumatra Island and replaced by an ocean. These experiments were conducted to look at the role of each orography of each region in the development of the severe rainfall events. Although flattened orography experiments were done in a number of previous studies (for example, Sow et al. (2011)), an experiment with the Sumatra Island removed has never been published, at least using Met-UM on the severe rainfall events. These experiments will provide information on the role of the orography and Sumatra Island on the development of severe rainfall events over western Peninsular Malaysia.

Chapter 4

Monsoon and Inter-monsoon Seasons

4.1 Introduction

As discussed in Chapter 2, Peninsular Malaysia receives most of its total annual rainfall from the northeast monsoon. However, gauge-based data shows that different areas show a different annual maximum rainfall pattern throughout the peninsula. This study is focusing on the western peninsula. Figure 4.1 is retrieved from MetMalaysia shows the monthly mean rainfall measured at each station. As seen in the figure, the west and northwest part of Peninsular Malaysia experiences a biannual peak of maximum rainfall annually (for example, Bayan Lepas, Ipoh, Subang, and Cameron Highlands stations). The east coast of Peninsular Malaysia is influenced by the winter monsoon, where the maximum rainfall peaks in November or December (for example, Kota Bharu, Kuala Terengganu and Kuantan stations, as shown in Figure 4.1). The figure also shows that the west coast of Peninsular Malaysia receives more rainfall during inter-monsoon compared to in other monsoon seasons, climatologically. Thus, this study will further analyse the inter-monsoon rainfall, in the subsequent chapters.

4.1.1 Chapter Structure and Aim

This chapter presents the climatological observations of the regions by analysing the annual, seasonal and monthly means, focusing on rainfall and winds circulation, as well as a brief explanation on air temperature, humidity and Sea Surface Temperature. The first part of the chapter analyses the monthly pattern of rainfall and 850 hPa winds of the gridded dataset (TRMM, APHRODITE, and ERA-Interim, see Section 3.1). Then followed by the monthly analysis of rainfall based on the gauges dataset from MetMalaysia (sometimes referred as MMD in a few images) and the Department of Irrigation and Drainage (DID). The second part of this

chapter analyses the seasonal cycle of rainfall from the same gridded datasets and followed by the same rain gauge stations dataset. The third part will be looking at the diurnal cycle of rainfall from the rain gauge stations. The fourth part briefly discusses 2-meter air temperature, humidity and sea surface temperature (SST) over the Peninsular Malaysia and the region from ERA-Interim dataset (gridded dataset).

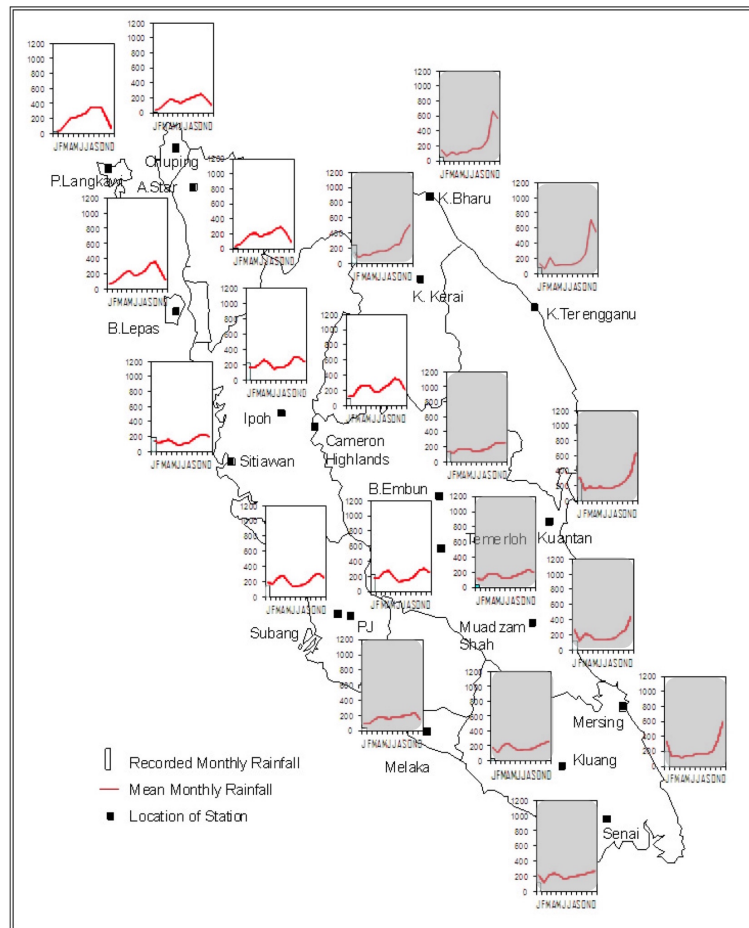


Figure 4.1: Rainfall climatology of the selected gauge stations from the Malaysian Meteorological Department (MetMalaysia), retrieved from www.met.gov.my webpage. This figure prompted interests for studying the severe rainfall events during inter-monsoon over western Peninsular Malaysia. Most of the western and inland stations (white boxes) showing biannual maximum peaks which coincide with one of the inter-monsoon months, namely April and October. Meanwhile, grey boxes are the east coast and southern peninsula stations which are excluded from the area of the study. Used with permission.

4.2 Monthly Analysis on Rainfall and Wind

4.2.1 Analysis of Gridded Dataset

The annual mean and monthly rainfall are shown in Figure 4.2. Based on gridded dataset such as TRMM, Peninsular Malaysia receives an average of 9 mm day⁻¹ rainfall annually, most of it over the east of the peninsula (Figure 4.2(a)). Besides that, more rainfall was recorded over the central Strait of Malacca than the land. Monthly mean for the rainfall is shown in Figure 4.2(b) indicating the mean rainfall over the northwest, west and inland regions. The highest amount of monthly mean rainfall is in October, with more than 310.7 mm month⁻¹ and the lowest monthly mean is in February of around 131.5 mm month⁻¹. On average, the peninsula received most of its rainfall during winter monsoon and the least during the summer monsoon. The APHRODITE dataset shows some similar pattern (Figure 4.2(c)) in comparison to the TRMM. From the data, the northeast part of Peninsular Malaysia received a relatively more annual rainfall, compared to the other part of the peninsula. The east and southeast coasts are also wetter, similar to TRMM. However, central Peninsular Malaysia received the least rainfall. Biannual rainfall maxima are observed in both dataset (Figure 4.2(b) and 4.2(d)) where the first maximum is in October, and the second maximum is in April. On the other hand, February is the driest month over the peninsula.

Inter-monsoon, as discussed in Section 3.3 is the time when the winds are changing from either southwesterly to northeasterly or vice versa. Wind is also one of the main indicators of seasonal change in Malaysia. Monthly winds over the Peninsular Malaysia area are given in Figure 4.3. The most prominent season in Malaysia is the boreal winter monsoon, as discussed in Section 2.1. The boreal winter monsoon is the wettest season over the peninsula, which is from November to March. The monsoon surge from the northeast brings wet and relatively colder wind surge to the peninsula. The winds are mostly northeasterly over the South China Sea region and easterly over the Andaman Sea vicinity. The whole region of the western Maritime Continent is wetter during this season, as the monsoon flow continuously moves toward northern Australia, for Australian Summer Monsoon. The western Sumatra also receives more rainfall, as the return flow (westerly wind) from the Indian Ocean influences the rainfall development over the region. A relatively drier season over the peninsula takes place during the boreal summer monsoon, from June until August. In these months, the winds are westerly and southwesterly over the western Maritime Continent. During this season, the Asian summer monsoon flow (westerly winds) brings more rainfall over the Bay of Bengal, Myanmar and east of Gulf of Thailand.

4.2. MONTHLY ANALYSIS ON RAINFALL AND WIND

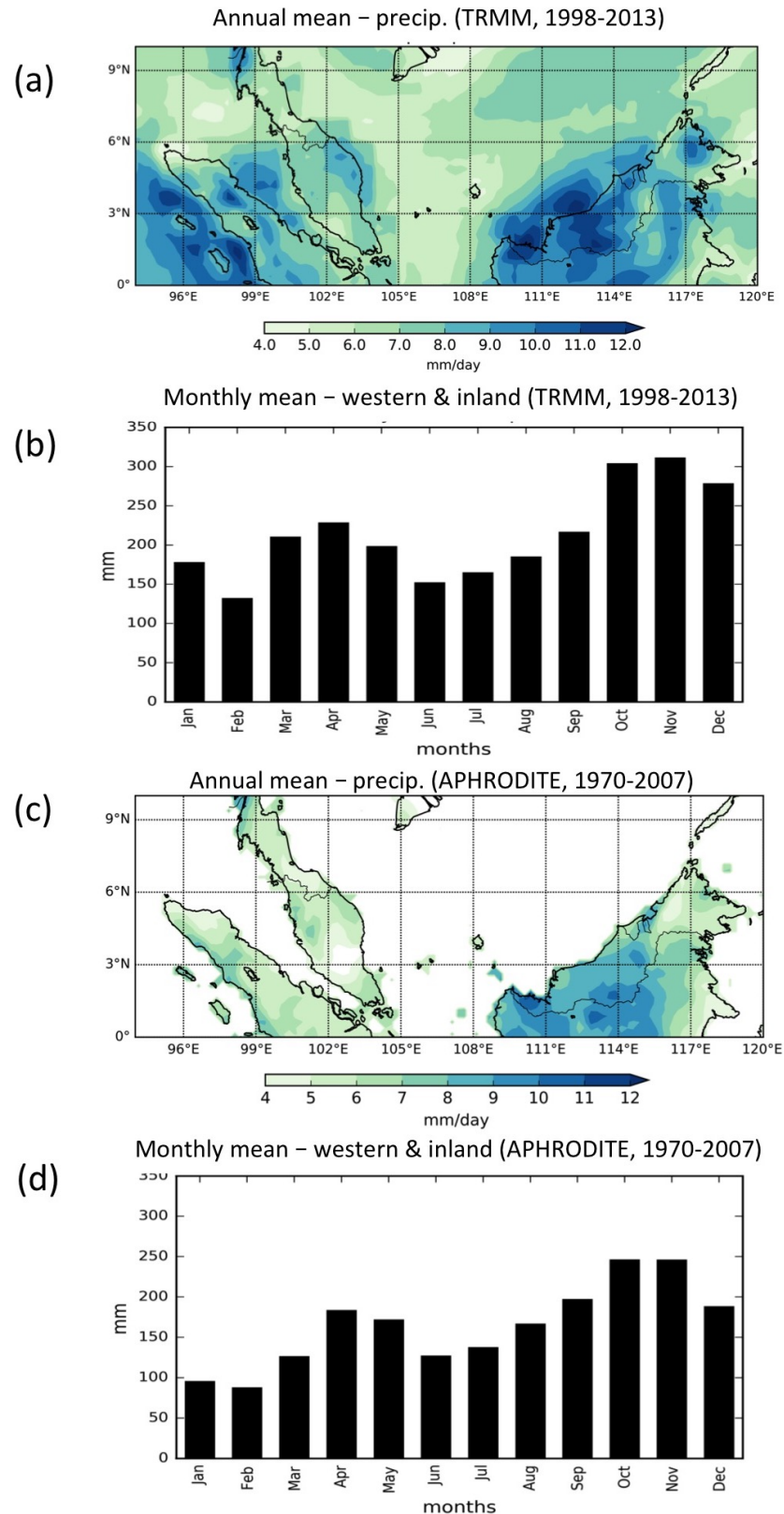


Figure 4.2: Precipitation data for Malaysia where (a) annual mean from TRMM, (b) monthly mean from TRMM (western and inland of Peninsular Malaysia only), (c) annual mean from APHRODITE, (d) monthly mean from APHRODITE (western and inland Peninsular Malaysia only). The TRMM dataset is from 1998-2013 and the APHRODITE data are from 1970-2007.

4.2. MONTHLY ANALYSIS ON RAINFALL AND WIND

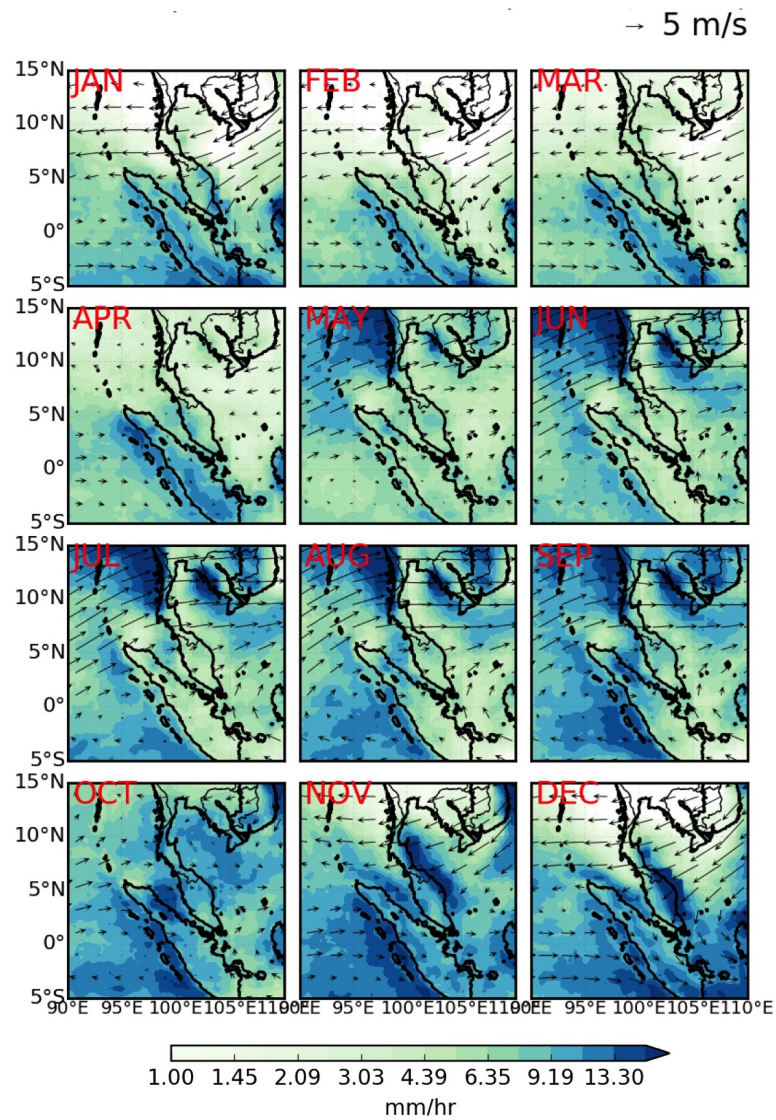


Figure 4.3: Same as in Figure 2.2, monthly mean of 850 hPa winds (from ECMWF dataset) and rainfall (from TRMM dataset) from year 1998 to 2013.

The change in wind direction is firstly observed between April and May (AM), where the winds are changing from easterly to southwesterly. This period is considered as the first inter-monsoon. The peninsula is relatively wetter over the western and inland regions. The winds are calmer over the peninsula vicinity, but normally easterly over the South China Sea and westerly over the Indian Ocean in April, and westerly in May. The second inter-monsoon is in September and October (SO). Unlike the first inter-monsoon, the winds around these months are mainly westerly and southwesterly. November is not considered as inter-monsoon (despite the wind is changing during that period) because November is the month when the boreal winter monsoon begins, and most of the onset dates are in the first two weeks of November (MetMalaysia, 2016a). Again, MetMalaysia defines the onset based on two indicators, which are the 850 hPa wind steadiness index (a magnitude and mean vector wind over a period of time at the Kota Bharu station) shall be greater than 0.6, and at least one principal station on the east coast collected a 3 inches (76.2 mm) of rainfall (Cheang, 1980; Moten et al., 2014). The region is also wetter than the first inter-monsoon. This is also the evidence for the asymmetry of the two inter-monsoon periods as discussed in Section 2.1.

Furthermore, October, November, and December are the wettest months while February is the driest. The inter-monsoon and winter monsoon onset (in November) contributed to the higher rainfall in October, November, and December. This is illustrated in Figure 4.4, which displays the annual cycle of rainfall over the Peninsular Malaysia in terms of rainfall anomaly. Western Peninsular Malaysia receives more rainfall compared to other areas of the peninsula in March and April, with more rainfall inland in May. Between October and December, the northwest of the peninsula receives more rain than other regions. A similar general pattern was observed in the APHRODITE dataset (Figure 4.5). The figure shows a slight difference from TRMM dataset, where for example in April, the area with high rainfall anomaly is not only on the west coast but most part of the mid and southern peninsula. A clear contrast in rainfall anomaly between west and east coast is observed in May. As for September and October, higher rainfall over northwest Peninsular Malaysia is observed, similar to the TRMM observation. A small difference between these datasets are expected as both of them used different methods of producing the data, as discussed in Section 3.1. The anomaly figures (Figures 4.4 and 4.5) proved that western Peninsular Malaysia receives more rainfall during inter-monsoon than the other regions, although inter-monsoon is not the highest rainfall period. Instead, November is the month with the highest rainfall.

4.2. MONTHLY ANALYSIS ON RAINFALL AND WIND

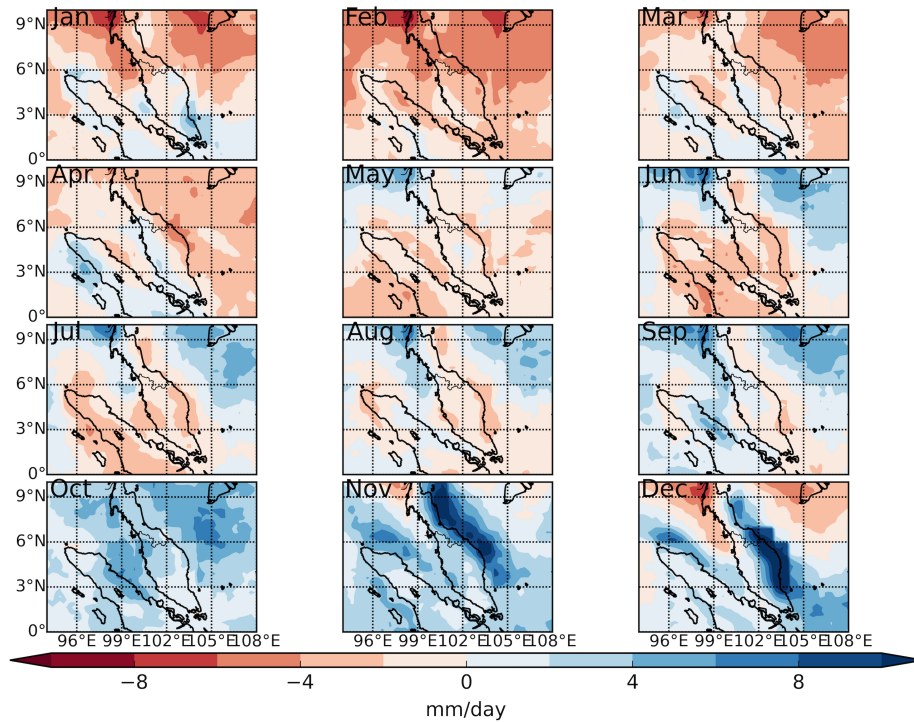


Figure 4.4: Monthly anomaly on precipitation from TRMM dataset. The anomaly was calculated by subtracting the monthly mean with annual mean for reference years: 1998-2013.

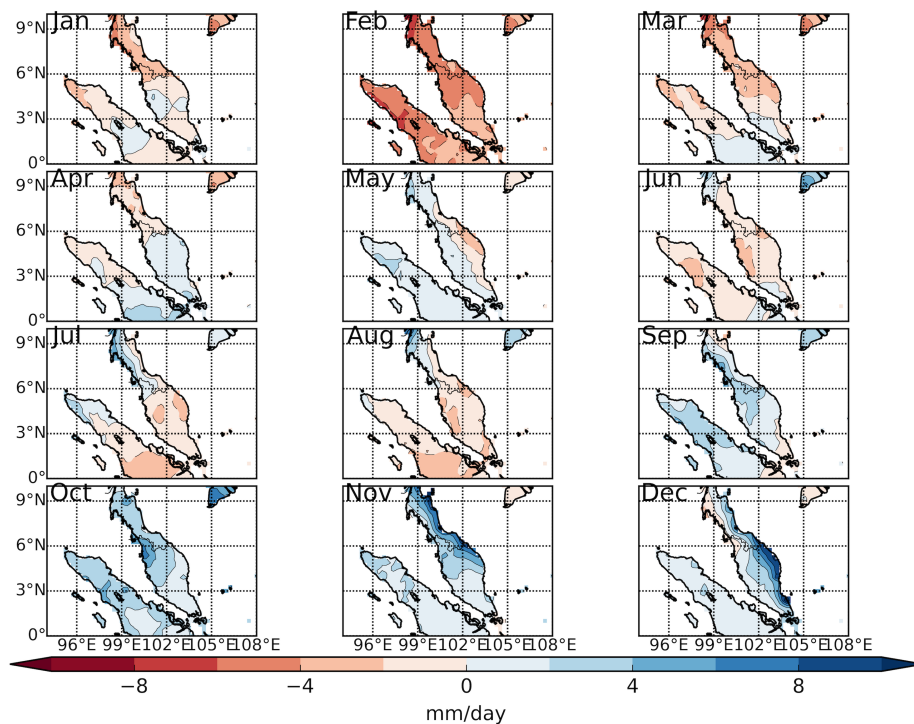


Figure 4.5: Monthly anomaly on precipitation from APHRODITE dataset. The anomaly was calculated by subtracting the monthly mean with annual mean for reference years: 1970-2007.

To investigate the months of the biannual peaks of maximum rainfall of each region, the monthly rainfall rate over the specific regions (NWC, WC, IL, SP and EC) using TRMM was analysed as illustrated in Figure 4.6 (red lines - monthly mean, blue bars - frequency). The first maximum for NWC and IL is in October (336 mm month⁻¹ and 306 mm month⁻¹, respectively) and for WC is in November (310 mm month⁻¹). Meanwhile, the first maximum for SP and EC is in December (291 mm month⁻¹ and 544 mm month⁻¹, respectively). The second maximum for NWC, WC and SP is in April (230 mm month⁻¹, 238 mm month⁻¹ and 224 mm month⁻¹, respectively) and for IL and EC is in May (223 mm month⁻¹ and 201 mm month⁻¹, respectively). Moreover, the mean rainfall of NWC, WC and IL only shows that the biannual maxima are in November and April (311 mm month⁻¹ and 228 mm month⁻¹, respectively). The maximum in November (and December) is associated with the boreal winter monsoon that affects most of the region in the peninsula. The maxima in October and second maxima in April (and May) coincide with the inter-monsoon periods, where the location of ITCZ is over the equatorial region as the solar zenith point is above the equatorial region.

In terms of frequency, the NWC region experiences the most rainfall in October with 88% of the days being rainy (≥ 1 mm day⁻¹) and followed by April with 80% of rainy days. WC region gets its most frequent rainfall in November (85%) and then April (82%). IL region experiences the most frequent rainfall in October (95%) and then May (87%). The rainfall frequency in EC and SP shows biannual peaks in May (87% and 75%, respectively) and October (95% and 81%, respectively), indicating that there are more rainfall events in these months, which coincide with the inter-monsoon periods rather than during the monsoon. As in the case of EC, rainfall events are mostly in October rather than in December (maximum rainfall amount). These results imply that the high amount of rainfall in EC does not necessarily attribute to a high frequency of rainfall events, but it can be attributed to just a few events but with a prolonged rainfall. The results also show that the IL region experiences the most frequent rainfall with a relatively high annual rainfall amount (EC received the most rainfall amount). On the other hand, NWC region experiences the least frequent rainfall and also received a relatively lower rainfall amount than the other regions.

Comparing to another gridded dataset, APHRODITE, the biannual rainfall maxima pattern is also apparent as shown in Figure 4.6 (blue lines - monthly mean, maroon bars - frequency). The first maximum is in between October to December and the second maximum is in between April and May. These coincide with the inter-monsoon periods (April-May and October) and boreal winter monsoon (November and December). The first maximum for NWC is in October with the rainfall amount of 259 mm day⁻¹ (93% of the days being rainy) and the second maximum is in May with 174 mm day⁻¹ (82% of the days being rainy). The WC

and IL receive more rain in November with 240 mm day⁻¹ and 276 mm day⁻¹, respectively and the second maxima in April with 205 mm day⁻¹ and 191 mm day⁻¹, respectively. The month with most rainy days for WC and IL, however, is October (90% and 94% of the days, respectively) and the following month with the most rainfall is April (84% and 87% of the days, respectively). Meanwhile, SP and EC regions have the most rain in December (215 mm day⁻¹ and 355 mm day⁻¹, respectively) and the second maxima are in April for SP with 174 mm day⁻¹, and in May for EC with 136 mm day⁻¹. The rainiest month is October for SP and EC, with 84% and 94% of rainy days, respectively. The second most rainy month is April for SP (78%) and May for EC (84%). The APHRODITE dataset shows a biannual pattern as in TRMM but not exactly on the same month as in TRMM. The APHRODITE dataset also shows a different biannual maximum month in terms of rainfall amount versus the biannual maximum month in terms of rainfall frequency (except the NWC region). This also supports the statement in the previous paragraph that the high rainfall frequency does not always result in a high rainfall amount.

This dataset also shows that IL experiences and receives the most rainfall than other regions, whereas NWC receives and experiences rainfall the least. Although TRMM shows that high rainfall frequency contributes to the high rainfall amount, this is not the case for APHRODITE. The difference is most probably caused by the different type of data used to produce the reanalysis (TRMM - satellite radar, APHRODITE - rain gauge), and also possibly due to the difference in temporal availability of each dataset. However, the biannual peaks in rainfall exist in APHRODITE dataset, showing that most rainfall and rain events occur during inter-monsoon (April-May and October) and at the beginning of the boreal winter monsoon (November and December). This is similar to TRMM, although some regions do not have the identical peak months (for example, WC has maximum rainfall frequency in April and November for TRMM, but in April and October for APHRODITE). It is worth mentioning that the rainfall may occur anywhere in the region, but not in the whole region at once. For example, if IL region is experiencing a rainfall on a particular day, the rainfall is just isolated within the IL region, not throughout the whole of IL region at the same time.

4.2. MONTHLY ANALYSIS ON RAINFALL AND WIND

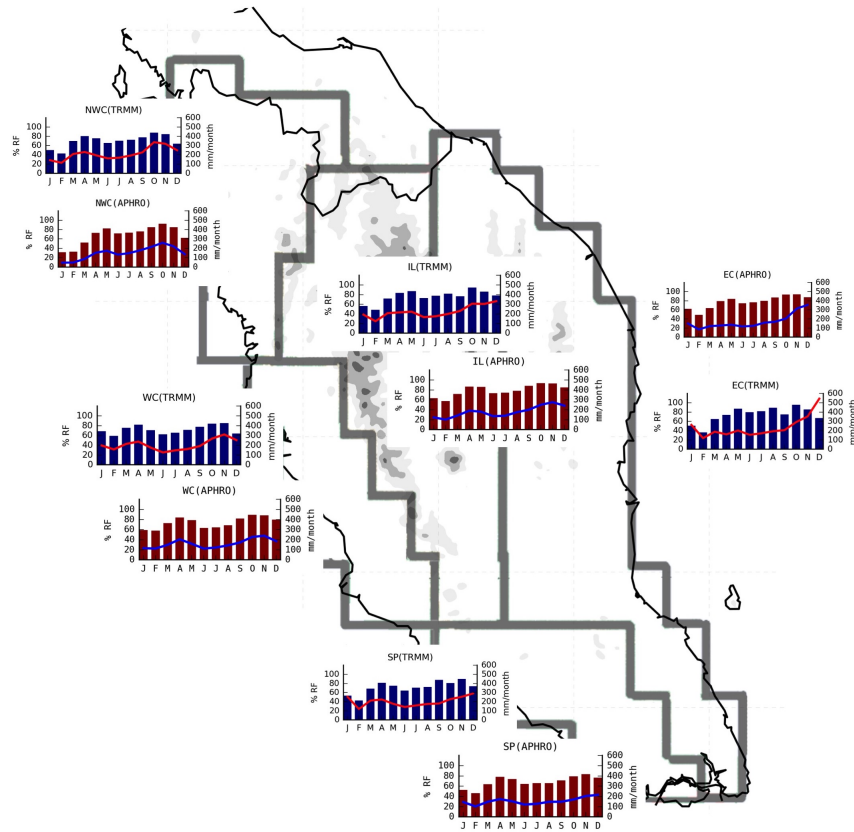


Figure 4.6: Rainfall monthly mean in mm day^{-1} (red lines - TRMM dataset, and blue lines - APHRODITE dataset) and rainfall frequency in percentage (blue bars - TRMM dataset, and maroon bars - APHRODITE dataset) for days with $\geq 1 \text{ mm day}^{-1}$ (in percentage), for northwest coast (NWC), west coast (WC), inland (IL), south peninsula (SP) and east coast (EC). Data are from TRMM (1998-2013) and APHRODITE (1970 to 2007). The rainfall amount and frequency are listed in Appendix Table A.9 and A.10, A.13 and A.14.

4.2.2 Analysis of Station Dataset

Analysing the 10-year gauge dataset retrieved from MetMalaysia, Figure 4.7 (top) reveals that the biannual maximum rainfall peaks along the west coast are in April and November, similar to the gridded datasets. The higher amount of total rainfall in November is due to the winter monsoon onset. Individual station plot in Figure 4.7 (bottom) shows that most of these stations have the biannual maximum peaks in April and November except for Alor Setar where the second peak is in October. The dataset also revealed that the Cameron Highlands station (inland station, at 1545 meter above sea level) receives more mean rainfall than other coastal or lowland stations. These results confirmed the biannual pattern of the rainfall over the west coast and revealed that the inland and highland region receives more rain than the coastal region. The definition of the regions (west coast, northwest coast, etc.) is the same as per Figure 3.6 in Section 3.3.

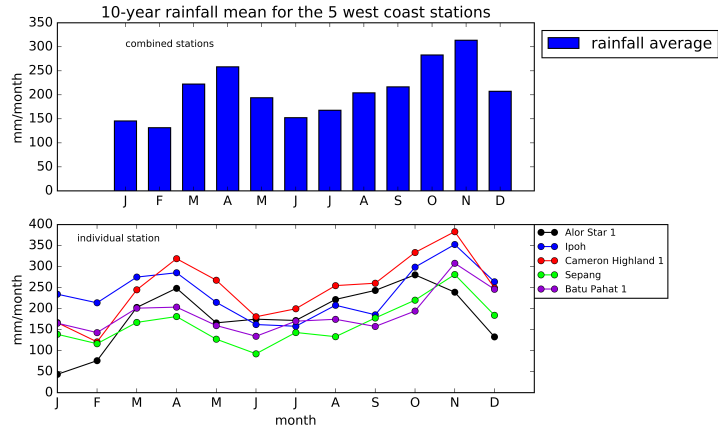


Figure 4.7: (top) Monthly mean of rainfall of the five western Peninsular Malaysia stations, (bottom) Monthly mean of rainfall of the station, individually. Daily data from MetMalaysia gauges station(2005-2014).

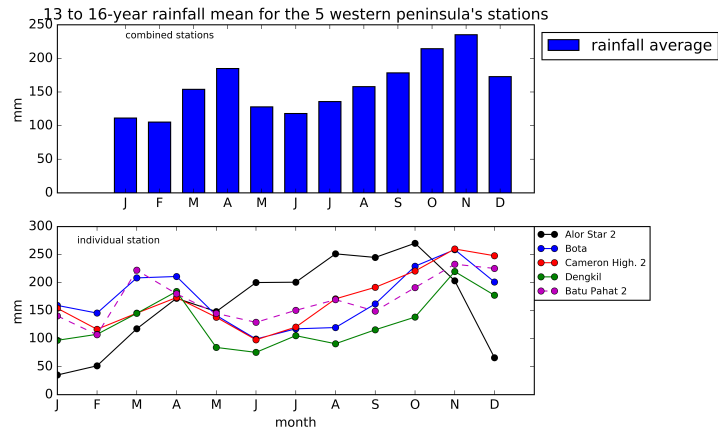


Figure 4.8: (top) Monthly mean of rainfall for the five western peninsula DID stations, (bottom) Monthly mean of rainfall of the stations, individually. Data from DID gauge stations (1998-2014).

DID dataset in Figure 4.8 (top) shows the mean rainfall over the west coast stations of the peninsula. The annual rainfall pattern is slightly different from the MetMalaysia dataset, especially for the Alor Setar 2 station (northwest). Most of the other west stations are almost similar to the climatology with rainfall peaks in between April-May and October-November. The individual station plot in Figure 4.8 (bottom) shows most of the stations, however, received the most frequent rainfall in November, except Alor Setar, which experiences the most frequent rainfall in October. Both MetMalaysia and DID datasets show a similar monthly rainfall mean at around 200 mm day^{-1} .

Generally, these datasets show the biannual maxima of rainfall total, first in November and second in April, for all the northwest, west and inland stations averaged. Individually, some dataset shows the first maxima in October (Alor Setar 1 and Alor Setar 2) instead of November, and second maxima in March (Batu Pahat 1 and Batu Pahat 2) instead of April, as shown in Figure 4.7(bottom) and 4.8(bottom). However, considering Batu Pahat is in the southern peninsula, this is negligible as we are just focusing on the western and inland regions. Rainfall is generally high in October compared to other months, except November, because it is the month of the boreal winter monsoon onset. In November, strong monsoon surge from the Siberian High-pressure system travelling toward the equator, and the colder and wetter air from the north will combine with the wetter easterly from the Pacific Ocean, bringing rain and thunderstorm over the eastern coast of Peninsula Malaysia, spreading to the west coast. Most of the rainfall in October is also associated with the ITCZ as well as the movement of convection southeastward from boreal summer monsoon to the austral summer monsoon (Chapter 2, Figure 2.1).

Comparing the rainfall frequency to the rainfall average (Figure 4.9), most stations show a double maximum of rainfall frequency which are in April and November. The highest frequency of rain is mostly in November, except for Alor Setar (northwest) where it rains the most in October. Two of the DID stations on the east coast (Kota Bharu and Mersing) recorded a high rainfall amount in NDJFM, which is the boreal winter monsoon season. From MetMalaysia dataset (rain average - blue line, rain frequency - dark green bars, Figure 4.9), 57% of the days in October was recorded to receive rainfall over Alor Setar 1, based on the 10 years MetMalaysia rain gauge data. Other stations show more rain frequency in November, with 67% in Ipoh, 77% in Cameron Highlands 1, 60% in Sepang and 54% in Batu Pahat 1. The values shown in the table suggest that there are more rainy days over the highland stations (Cameron Highlands stations) annually than those in the coastal or lowland regions. In general, Alor Setar is experiencing the least frequent rainfall annually. The gauge data from DID shows a slightly different results (rain average - blue line, rain frequency - grey bars, Figure 4.9). Their Alor Setar 2 gauge

4.2. MONTHLY ANALYSIS ON RAINFALL AND WIND

station indicates that September is the wettest month, with 53% of the days were raining. November is the wettest month for Bota (39%), Dengkil (58%), Batu Pahat 2 (44%) and Kota Bharu 2 (63%) stations. Meanwhile, December is the wettest month for Cameron Highlands 2 (58%) and Mersing (62%) stations. The total rainfall is closely following the rainfall frequency in all stations. This suggests that the rainfall frequency does contribute to the rainfall amount, for these station dataset. The correlation coefficient between the rainfall amount and rainfall frequency for both MetMalaysia and DID datasets are 0.98 and 0.97, respectively.

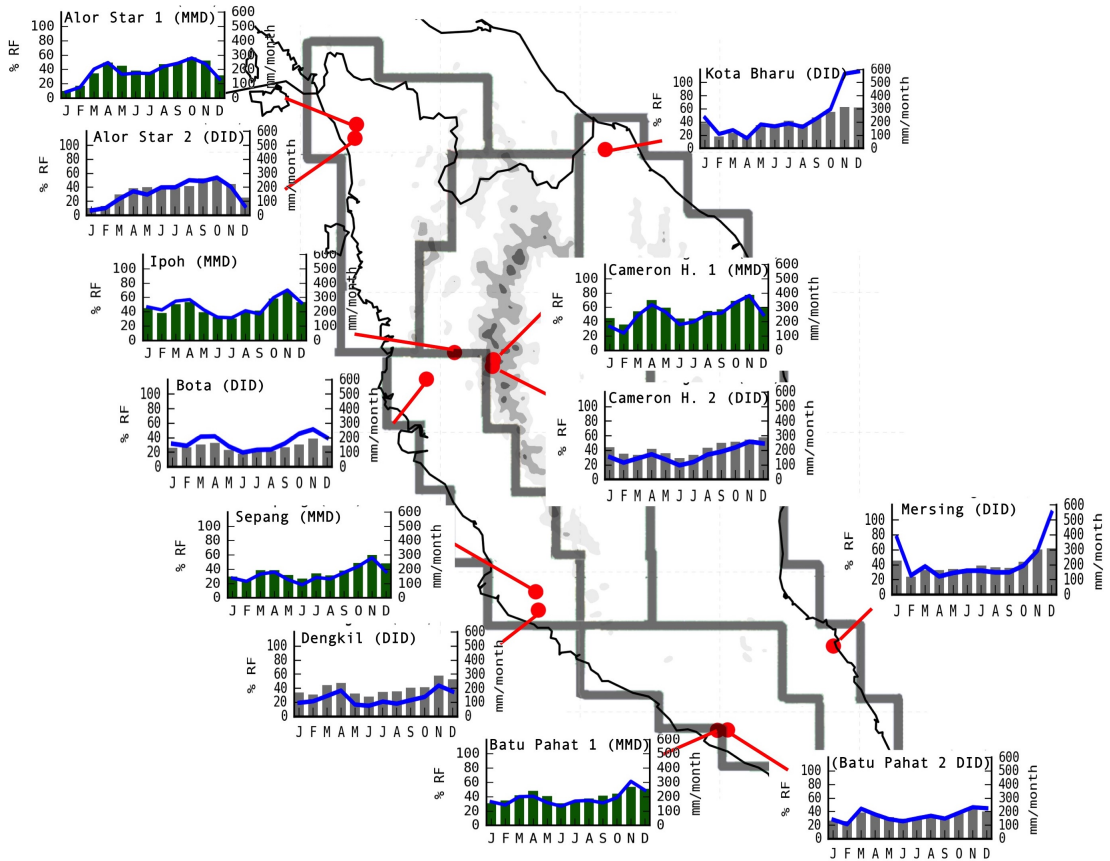


Figure 4.9: Rainfall, monthly mean (blue lines, in mm day^{-1}) and rainfall frequency for days with $\geq 1 \text{ mm day}^{-1}$ (dark greens bars - MetMalaysia dataset and grey bars - DID dataset). The rainfall frequency is the percentage of rainy day for each month for each city with respect to the monthly mean. Data are from 2005-2014 (MetMalaysia rain gauges) and 1998-2014 (DID rain gauges) dataset as listed in Table 3.1. The rainfall amount and frequency are listed in Appendix Table A.1 and A.2, A.5 and A.6.

A comparison between TRMM and MetMalaysia rain gauge data is shown in Figure 4.10. The values in TRMM dataset is the mean rainfall rate over a grid box where each rain gauge station is located. Both datasets show a similar biannual pattern and the rainfall rate values (around 0.2 mm day^{-1} difference in total), except each dataset, has different maximum peaks. The mean values (Figure 4.10 (b)) indicate that the first maximum in TRMM dataset is in October and the second maximum is in March, while the first maximum in MetMalaysia (gauge) dataset is in November and the second maximum is in April. The monthly mean rainfall and

frequency of TRMM dataset also have a strong linear correlation with other gauge datasets. The correlation coefficient of the monthly mean of the rainfall amount of TRMM with MetMalaysia gauge, DID gauge and APHRODITE are 0.89, 0.81 and 0.95, respectively. For the monthly mean of the rainfall frequency, the correlation coefficient between TRMM with MetMalaysia, DID and APHRODITE are 0.91, 0.92 and 0.89, respectively. This correlation results also show the reliability of the monthly rainfall dataset of the TRMM to be used in this study.

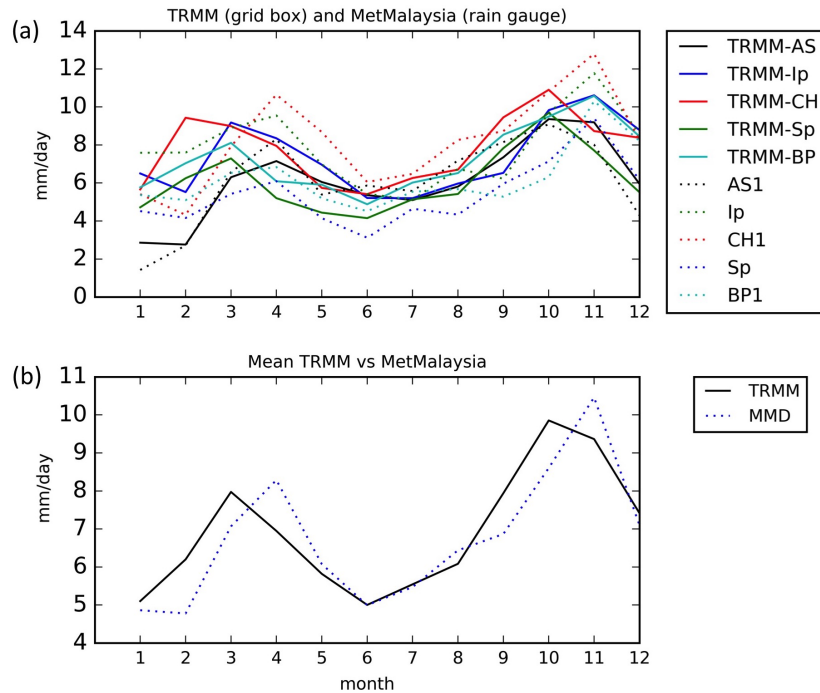


Figure 4.10: Comparison between TRMM and MetMalaysia rainfall rate for 5 cities located at the western and inland of Peninsular Malaysia. TRMM dataset was an average of a grid box where each of the MetMalaysia rain gauge stations is located. (a) All cities data were plot together, TRMM dataset is displayed by lines and MetMalaysia gauge dataset are displayed by dots, (b) mean for each dataset (TRMM mean and MetMalaysia mean). Both data are from 2005-2013 (to match data availability of both dataset).

4.3 Seasonal Analysis on Rainfall and Wind

4.3.1 Analysis of Gridded Dataset

Seasonally (Figure 4.11), a prevailing northeasterly wind is observed during November to March (NDJFM), and mostly west and southwesterly winds are observed in June to August (JJA). The AM inter-monsoon is calmer over the peninsula and Strait of Malacca areas, and the winds are mostly westerly during SO inter-monsoon. This analysis also shows that the wind conditions are different in both inter-monsoons.

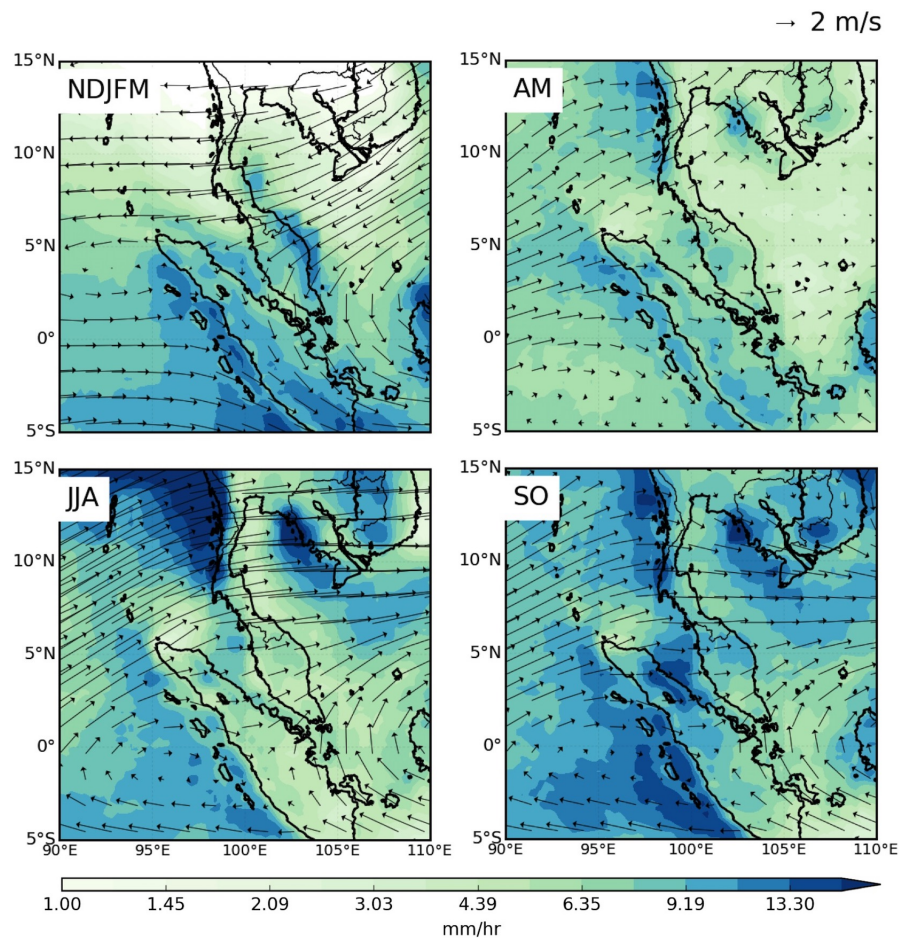


Figure 4.11: Seasonal mean of 850hPa winds from ERA-Interim and rainfall from TRMM dataset for the year 1998-2013.

The rainfall during boreal fall and winter contribute to the majority of the total rain over Peninsular Malaysia as seen in Figure 4.2. In Figure 4.12, the precipitation anomaly (from the annual mean) shows that the rainfall over the whole peninsula is higher than the annual mean in NDJFM and SO, confirming to previous studies such as by Varikoden et al. (2011). The east coast of the peninsula received most of its rainfall during boreal winter (NDJFM). This is due to the boreal winter monsoon. The west coast received a reasonably high amount of rainfall throughout the year except in JJA. The JJA season is drier over Peninsular

4.3. SEASONAL ANALYSIS ON RAINFALL AND WIND

Malaysia. This is mainly because the Asian summer monsoon flow is concentrated over the north of 5°N. The low pressure dominates South Asia with most rainfall concentrated to the north of 5°N, around the Bay of Bengal, west of Indochina, and South Asia. The Peninsula Malaysia, in general, receives more rainfall in SO, especially the northwest coast. This wet condition coincides with the movement of the convection from north to south (from boreal summer to austral summer) as discussed in Section 2.1. The same pattern is shown in APHRODITE dataset in Figure 4.13. The west coast, southern peninsula and inland receive more rainfall in AM compared to the east coast. During SO, the northwest peninsula receives more rainfall than other regions but in general, the whole peninsula receives more rainfall than the annual average. These anomaly plots show that western Peninsular Malaysia receives above average rainfall during inter-monsoons (AM and SO).

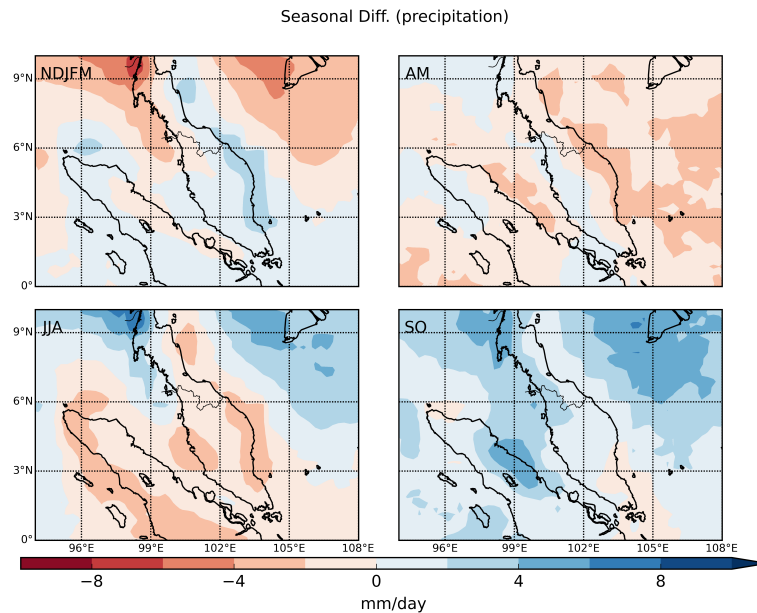


Figure 4.12: Seasonal anomaly on precipitation from TRMM dataset. The anomaly was calculated by subtracting the seasonal mean with annual mean for the reference years: 1998-2013.

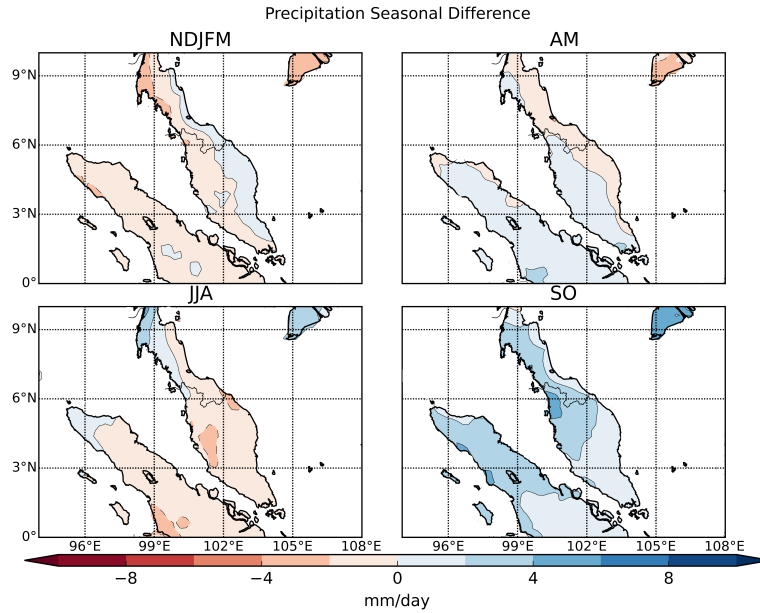


Figure 4.13: Seasonal anomaly on precipitation from APHRODITE dataset. The anomaly was calculated by subtracting the seasonal mean with annual mean for the reference year: 1970-2007.

The seasonal rainfall frequency from TRMM dataset is compared to the seasonal mean of total rainfall (Figure 4.14, red line - seasonal mean in mm month^{-1} and blue bars - frequency in %), the mean rainfall frequency was analysed based on the 5 regions. All regions experienced rainy days at least 80% of the time in SO (with total daily rain $\geq 1 \text{ mm month}^{-1}$). Seasonal mean shows that the mean rainfall in SO inter-monsoon is $281 \text{ mm month}^{-1}$ (NWC), $230 \text{ mm month}^{-1}$ (WC), $269 \text{ mm month}^{-1}$ (IL). The first maximum for SP and EC is in NDJFM, with $204 \text{ mm month}^{-1}$ (SP) and $248 \text{ mm month}^{-1}$ (EC). The second season with high rainfall amount in WC and IL regions is in NDJFM (WC: $226 \text{ mm month}^{-1}$, IL: $232 \text{ mm month}^{-1}$) and for NWC it is the AM season ($212 \text{ mm month}^{-1}$). The second maxima for SP and EC is in SO (SP: $226 \text{ mm month}^{-1}$, and EC: $293 \text{ mm month}^{-1}$) The rainfall frequency in all regions is maximum in SO season, with 83% of the days are rainy days in NWC, 81% in WC, 86% in IL, 85% in SP and 85% in EC. The first maximum in term of frequency is not the same as maximum rainfall mean (seasonally) for SP and EC, where it rains more in SO than NDJFM. The second rainfall frequency maximum is in AM for most of the region (NWC: 78%, WC: 76%, IL: 35% and SP: 78%), and in JJA for EC with 84% of the days being rainy. Again it shows that the high rainfall frequency does not always contribute to the high rainfall amount.

The same pattern is observed in APHRODITE dataset (blue lines: rainfall average, brown bars: mean of rainfall frequency, Figure 4.14), where most of the regions received most rainfall in SO (NWC: $237 \text{ mm month}^{-1}$, WC: $201 \text{ mm month}^{-1}$ and IL: $225 \text{ mm month}^{-1}$). Another region such as SP received most of the rain in AM ($163 \text{ mm month}^{-1}$), and EC received most rainfall in NDJFM (205 mm

month⁻¹). The first maximum in rainfall frequency is in SO in most regions (NWC: 89% of the days were rainy days, WC: 86%, IL: 91% and EC: 90%). The highest seasonal rainfall frequency for SP is during AM with 76% of the days being rainy days. The second maximum in rainfall amount based on APHRODITE dataset is in AM for most of the region (NWC: 163 mm month⁻¹, WC: 182 mm month⁻¹ and IL: 186 mm month⁻¹). The second maximum in rainfall amount for SP is in NDJFM (163 mm month⁻¹) and for EC is in SO (187 mm month⁻¹). The second maximum in rainfall frequency is however in AM for most of the regions (NWC: 78%, WC: 81%, IL: 87% and EC: 82%) and in SO for SP with 75% of the days being rainy days.

From both TRMM and APHRODITE, most of the inland and western regions received most of the rainfall during SO inter-monsoon and followed by AM inter-monsoon. Most of the high rainfall frequency follows with a high rainfall amount, although this is not always the case, as discussed above. Moreover, JJA receives less rainfall and experiences rainfall the least frequently, but in some instances, so does NDJFM despite being the wet monsoon season, boreal winter monsoon. This is due to the average calculation that includes the wettest month (November) and the driest month (February) in one season. In both TRMM and APHRODITE, the monthly mean of rainfall amount and the monthly mean of rainfall frequency has a strong correlation, based on linear correlation, the correlation coefficient between rainfall amount and frequency for TRMM and APHRODITE is 0.74 and 0.95, respectively. It is also worth to note that the inland region experiences the most rainfall, as well as receiving a relatively higher rainfall than the other regions. Meanwhile, the NWC region experiences rainfall the least, and relatively lower rainfall amount than the other regions.

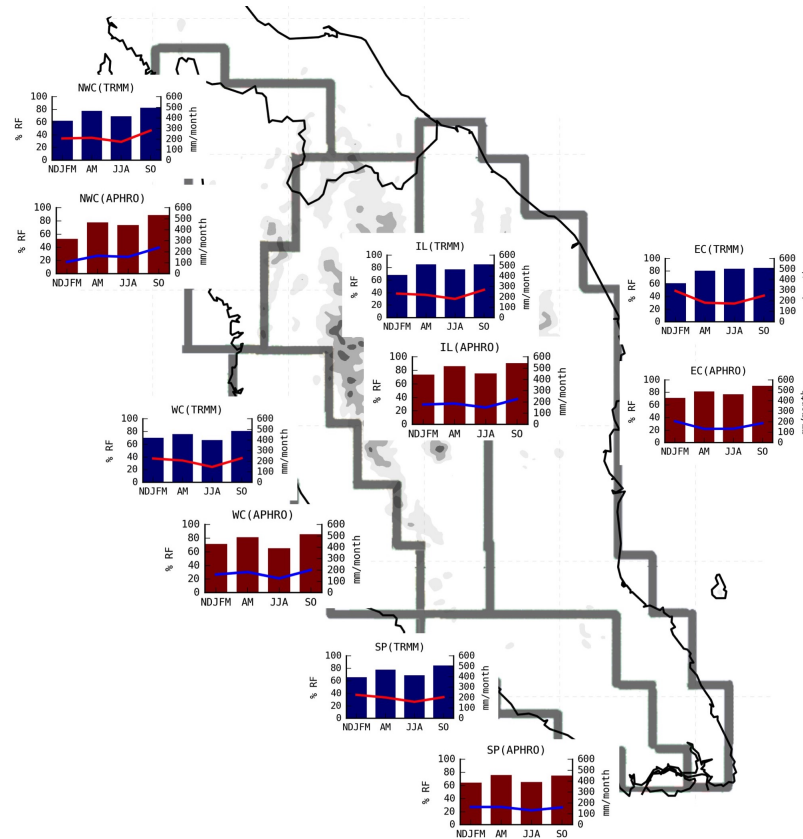


Figure 4.14: As in Figure 4.6, but seasonal mean. Rainfall seasonal mean in mm day^{-1} (red lines - TRMM dataset, and blue lines - APHRODITE dataset) and rainfall frequency in percentage (blue bars - TRMM dataset, and maroon bars - APHRODITE dataset) for days with $\geq 1 \text{ mm day}^{-1}$ (in percentage), for northwest coast (NWC), west coast (WC), inland (IL), south peninsula (SP) and east coast (EC). Data are from TRMM (1998-2013) and APHRODITE (1970 to 2007). The rainfall amount and frequency are listed in Appendix Table A.11 and A.12, A.15 and A.16.

4.3.2 Analysis of Station Dataset

Datasets from both stations consistently show that the rainfall is the highest in SO inter-monsoon and the second maximum is in AM inter-monsoon (Figure 4.15 (a) and (c)) for the northwest, west and inland stations averaged. Individually (Figure 4.15 (b) and (d)), most stations show a maximum rainfall average in SO inter-monsoon (except Dengkil in NDJFM) and the second maximum in April, except Ipoh (second maxima in NDJFM), Sepang (second maxima in NDJFM), Bota (second maxima in NDJFM), Cameron Highlands 2 (second maxima in NDJFM), and Alor Setar 2 (second maxima in JJA) stations. The second maximum in NDJFM for some stations is again associated with the boreal winter monsoon, where the monsoon surge brings more rain toward the peninsula in general.

4.3. SEASONAL ANALYSIS ON RAINFALL AND WIND

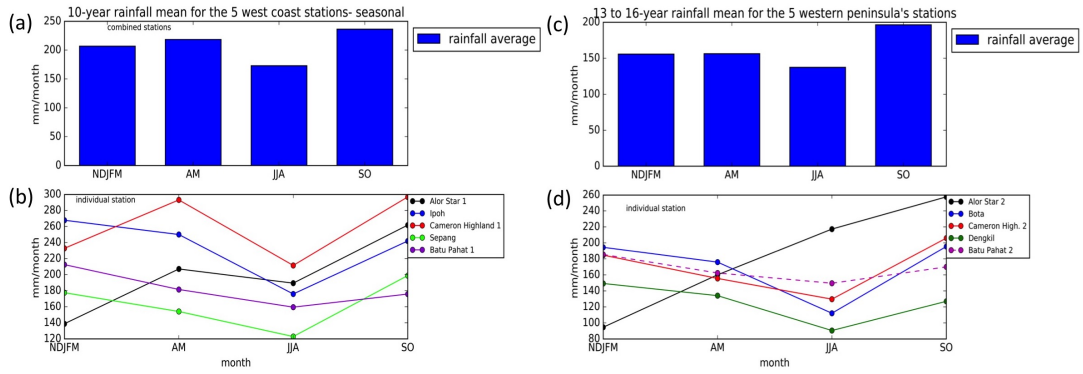


Figure 4.15: (a) seasonal mean of the 5 western and inland MetMalaysia stations, (b) seasonal mean (individual station) of the 5 western and inland MetMalaysia stations, for 10 years data from 2005-2013, (c) seasonal means of the 5 western and inland DID stations, (d) seasonal mean (individual station) of the 5 western and inland DID stations, data ranges from 1998-2014, as listed in Table 3.1.

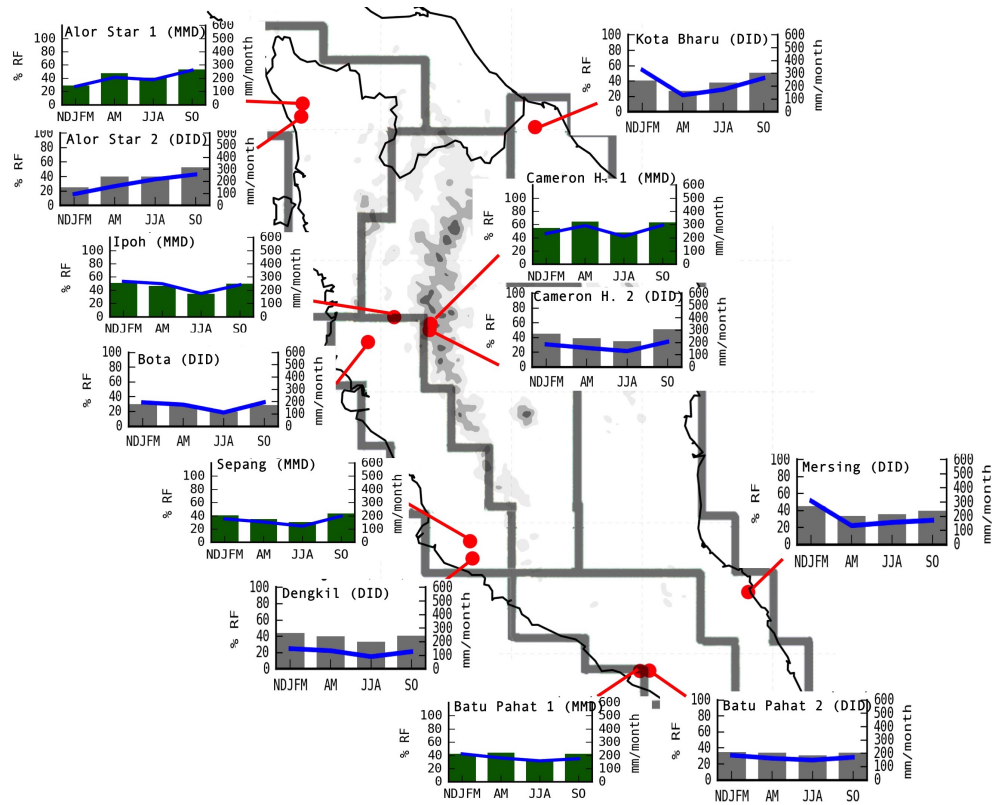


Figure 4.16: Same as Figure 4.9 but seasonal mean. Rainfall, seasonal mean (blue lines, in mm day^{-1}) and rainfall frequency for days with $\geq 1 \text{ mm day}^{-1}$ (dark greens bars - MetMalaysia dataset and grey bars - DID dataset). The rainfall frequency is the percentage of rainy day for each season for each city with respect to the seasonal mean. Data are from 2005-2014 (MetMalaysia rain gauges) and 1998-2014 (DID rain gauges) dataset as listed in Table 3.1 The rainfall amount and frequency are listed in Appendix Table A.3 and A.4, A.7 and A.8.

Focusing on northwest, west and inland stations only, seasonal mean on rainfall frequency from MetMalaysia dataset (dark green in Figure 4.16), the maximum frequency of rain occurred in SO inter-monsoon over Alor Setar 1 (53%) and Sepang (44%), AM inter-monsoon over Cameron Highlands 1 (65%), and NDJFM over Ipoh (51%). It is also important to recognise that the seasonal cycle of the rainfall over these stations is also following the trend of the seasonal mean rainfall (Figure 4.16). In the DID dataset (grey in Figure 4.16), SO is the wettest period for Alor Setar 2 (53%), Cameron Highlands 2 (51%) and Kota Bharu (51%), while NDJFM is the wettest season for Bota (30%), and Dengkil (44%). The seasonal rainfall average is also closely following the seasonal rainfall frequency in the DID dataset, suggesting that the high frequency of rainfall contributes to the high amount of rainfall. It is also worth to note that the seasonal rainfall frequency for Kota Bharu station is high in SO instead of NDJFM since Kota Bharu station is mostly affected by boreal winter monsoon, NDJFM. There are a few reasons hypothesised from this result. Firstly, the rainfall frequency over the station may not have a high impact on the total rainfall, but prolonged rainfall could be the main contribution for the large rainfall amount. Another consideration is the data availability since there are many missing data in the DID dataset.

4.4 Analysis of Diurnal Cycle of Precipitation

The diurnal cycle of precipitation as shown in Figure 4.17 reveals that most of the maximum rainfall occurrence is in the afternoon due to the solar heating on the landmass which is common in the tropics (Yang and Slingo, 2001), which induces convection activities. Alor Setar 2 station showed a mixed pattern on the diurnal maximum. Most of the seasons show a high rainfall rate between 1600 LT and 2000 LT. In JJA, the maximum rainfall is in the early morning before 0500 LT, which is associated to the Asian summer monsoon, as briefly mentioned by Oki and Musiake (1994) in their study on seasonal change of the diurnal cycle of precipitation over Malaysia (rain gauges data from 1981-1990). In their paper, the result shows a secondary peak in the early morning from 2 to 5 LST, from May to October. They hypothesised the morning peak in JJA specifically, is due to the low-level convergence between the land breeze and the monsoon flow over the coast that is perpendicular to the monsoon flow. For Dengkil station, the maximum rainfall is usually in between 1400 LT until 1900 LT. However, in JJA, its diurnal cycle of precipitation is much different from other seasons where the maximum rainfall rate is at 1300 LT. Cameron Highlands 2 station shows a distinct pattern in the diurnal cycle of precipitation throughout the year, where the highest rainfall rate was between 1400 LT and 1600 LT.

There is an exception for two of the east coast stations (Kota Bharu and

Mersing) and Batu Pahat 2. Batu Pahat 2 station shows no clear diurnal variation except during NDJFM where the maximum rainfall is normally around 1600 LT. MetMalaysia (2016a) reported that the area is influenced by the early morning *Sumatras*, which is a squall line propagated from the eastern Sumatra toward the south and southeast of the peninsula, thus a lack of diurnal variability in rainfall is observed. Mersing and Kelantan stations show the least diurnal variability during NDJFM. But in other seasons, the rainfall rate is high, in between 1400 LT and 1600 LT for Mersing station, and between 1700 LT and 1800 LT for Kota Bharu station. These stations are highly affected by boreal winter monsoon, and monsoon could have caused a prolonged rainfall over the east coast regions, as such, the rainfall may occur throughout the 24 hours of time, which is also shown in a case study investigated by Juneng et al. (2007). Moreover, this region is also affected by the incoming monsoon flow throughout the day (including in the early morning), and the low-level convergence in between the monsoon flow and the land breeze in the early morning can induce convection (Oki and Musiake, 1994), and produce rainfall. Thus a lack of diurnal variability in the precipitation during NDJFM over the east coast stations was observed. A limited dataset from MetMalaysia in Figure 4.18 shows a generally similar afternoon/evening maxima rainfall pattern.

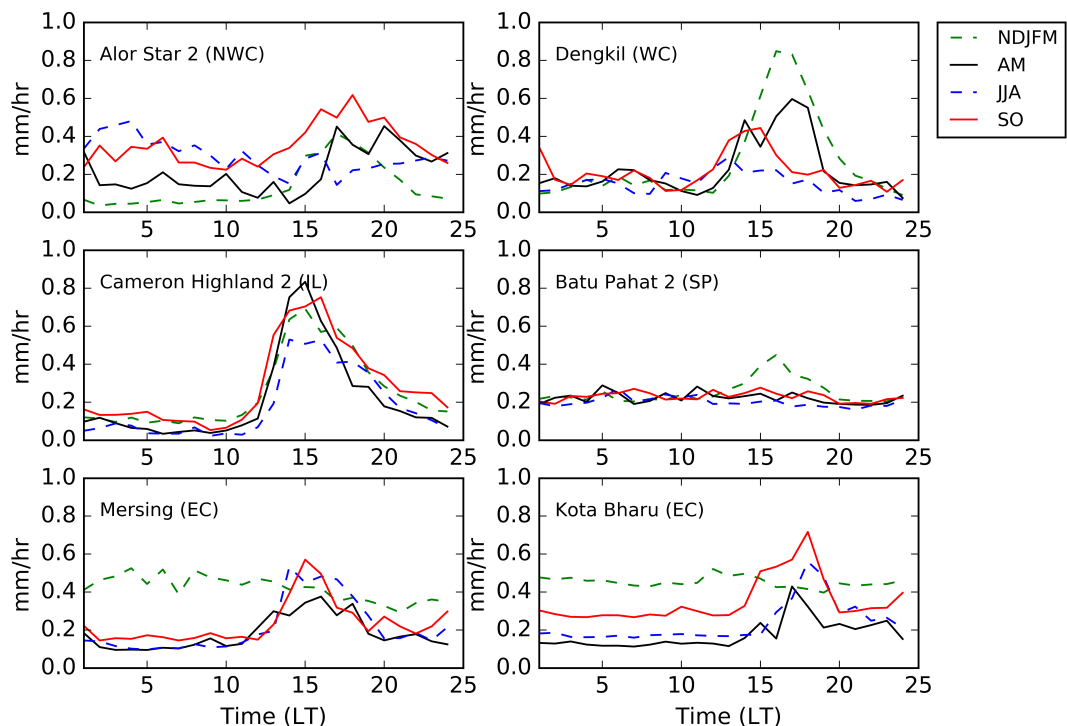


Figure 4.17: Diurnal cycle of precipitation for five DID gauge stations, plotted seasonally. This data is hourly and from 1998-2013, except Bota (1998-2012) and Dengkil (2002-2014) stations.

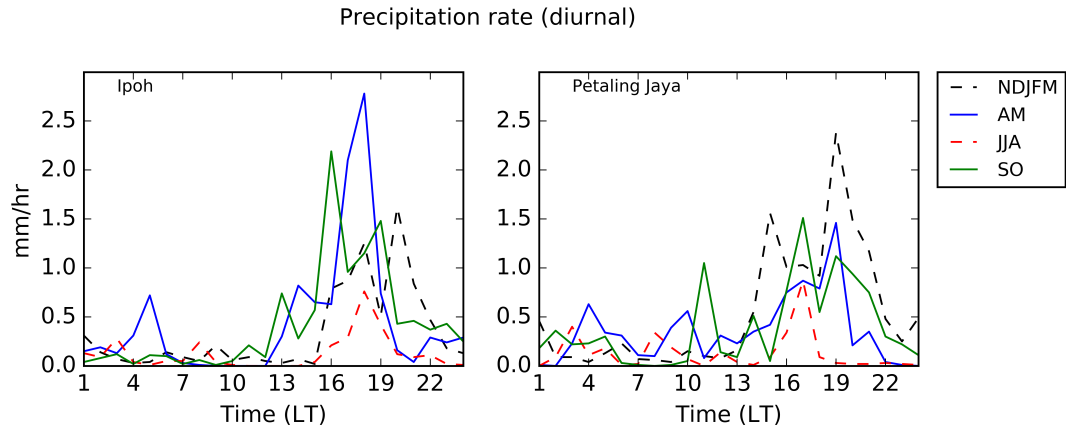


Figure 4.18: Diurnal cycle of precipitation from MetMalaysia gauge stations (Ipoh and Petaling Jaya only), representing the diurnal pattern of precipitation over the west coast of Peninsular Malaysia. Dataset is limited to one year each station; 2012 for Petaling Jaya and 2013 for Ipoh.

The TRMM dataset shows that most of the rainfall occurred around 1700 LT except in the northwest and inland of the peninsula, where the maximum rain was observed around 2000 LT, in all seasons. The same pattern was also observed in the gauge dataset in Section 4.2.2. These results are in accordance to previous literature claiming that the maximum rainfall over the tropics is during the late afternoon and early evening (for example in Johnson (2011)), after the daily maximum solar insolation which is in the early afternoon.

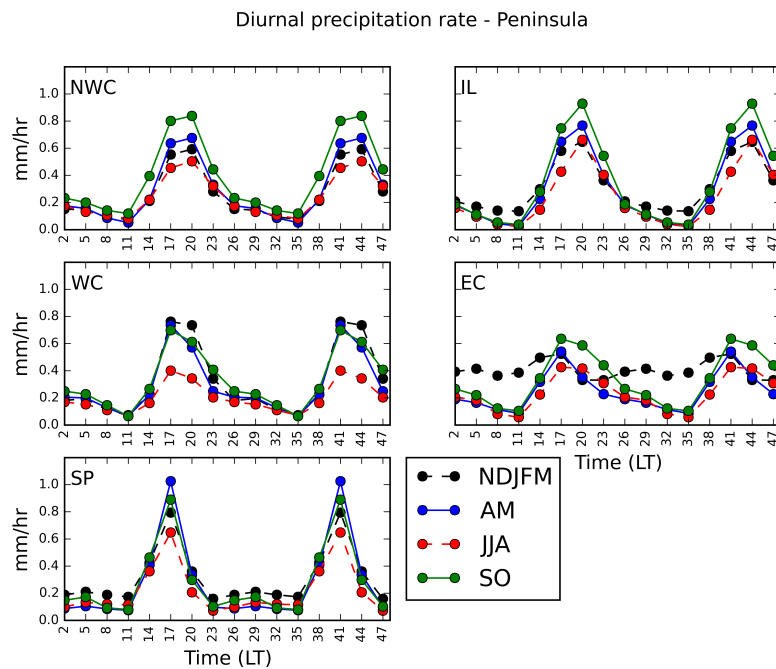


Figure 4.19: Diurnal cycle of precipitation in 48-hour plot, for the 5 regions of the Peninsular Malaysia. Data is from TRMM for the year 1998-2007.

4.5 Analysis of Air Temperature, Specific Humidity, and Sea Surface Temperature

Being in the tropics, there is not much difference in the temperature, humidity and sea surface temperature (SST) in general. Monthly data from reanalysis indicates that the mean 2-meter temperature (not shown) over the Malaysia Peninsula is around 26°C - 28°C except over the highland with 22°C - 26°C. The 2-meter temperature starts to get higher generally in April and May and getting slightly lower in June. April and May are in general the hottest months of the year. Coldest months are December and January, mostly due to the winter monsoon surge from the north. But the average cold temperature over the low land is no less than 20°C. The difference between the mean temperature is just around $\pm 2^\circ\text{C}$ annually. The mean maximum 2-meter temperature between 30°C - 36°C, that is warmer over the low-level land. The mean minimum of the 2-meter temperature is around 16°C - 25°C, where air temperature that is below 20°C is common for the highland region.

The average specific humidity over the regions is generally the same throughout the year (not shown). A seasonal difference was observed, where there was more moisture over the peninsula during the AM and lesser moisture during other seasons. The difference is just ± 0.75 g/kg. The difference may also be associated with the rainfall activity. Sea surface temperature (SST) also experience a slight change and is slightly higher around the peninsula during the AM inter-monsoon with more than 30°C and around $\pm 2^\circ\text{C}$ ($\pm 2^\circ\text{K}$) difference during SO inter-monsoon. The coldest season is the winter monsoon with a difference of around -1.5°C . It is important to note that the seasonal cycle of tropical ocean SST is not too varied in this region, but even a small difference may influence the development of severe rainfall events thus adding the amount of accumulated rainfall. As indicated in the study conducted by Lau and Wu (2011) over the tropics, a study using TRMM Microwave Imager (TMI) and Precipitation Radar (PR) from TRMM shows that a severe rainfall could increase at around 80 % to 90 % per degree increment in SST. Their study, however, had only considered a period of January until July, for the years that were not associated with moderate and strong El Niño and La Niña events.

4.6 Summary

Located in the tropics, the weather of Peninsular Malaysia is affected by the movement of Intertropical Convergence Zone (ITCZ). ITCZ is associated with the low-pressure belt around the globe, moving northward toward the Tropic of Cancer and southward toward the Tropic of Capricorn annually. The low-pressure belt is a product of the maximum solar heating due to the solar zenith point on the Earth. The ITCZ is also the location where the trade winds from the northern and southern hemisphere meet. The location of the ITCZ is dependent on the region. For example in Asia, the ITCZ in boreal summer is as far as northern India, and in boreal winter the location of the ITCZ is in between southern Maritime Continent and as far as northern Australia. In between these two seasons, the ITCZ is located close to the equator (Rutter, 2009).

The biannual peaks in maximum rainfall frequency and the amount in Peninsular Malaysia are dependent on where the station is located. When the stations (and regions - for gridded datasets) that are located in NWC, WC, and IL were averaged for both rain frequency and amount, the biannual maxima in rainfall average and frequency is in April and November (except for APHRODITE, which is in October). April in the inter-monsoon month and November is the onset month of the boreal winter monsoon. It is also worth mentioning that October also recorded a high rainfall amount and frequency in general, but the rainfall amount and frequency in November surpasses the values in October. In both April and October, these are the time when the solar zenith point is over the equator region, causing the maximum solar radiation over the equatorial. Thus, ITCZ is also located near the equatorial region, influencing and enhancing the development of convective rainfall over the equatorial region (and in this case, Peninsular Malaysia). In November, strong monsoon surge from the Siberian High-pressure system travelling toward the equator, and the colder and wetter air from the north combined with the wetter easterly from the Pacific, brings rain and thunderstorm over the eastern coast of Peninsula Malaysia, extending to the west coast.

In most stations and regions, the high frequent rainfall follows the high rainfall amount suggesting the relationship between frequent rainfall with the high amount of rain. However, this is not always the case. For example, the second maximum for Alor Setar 2 (DID station) shows a frequent rainfall in May, but the highest rainfall amount is in April. Another example is, the WC region (from APHRODITE dataset) experience the most frequent rainfall in October, but the highest rainfall amount is in November. Seasonally, SO inter-monsoon received the highest rainfall amount in all datasets, and AM is the second highest in all dataset (except in NDJFM for TRMM dataset). The results also reveal that inland stations and regions (for gridded dataset) experience the most frequent rainfall. The rainfall received by these stations and region is also relatively higher than the other regions.

This suggests the importance of orography in enhancing the rainfall activity over the region. Northwestern coast area experiences the least rainfall and thus receives the least amount of rainfall.

The differences in the peak months between the rain gauges and the gridded dataset are expected as shown in the comparison between MetMalaysia data and TRMM for the western stations at the equivalent grid point in TRMM. The reason for this is, the rain gauge dataset is based on an in-situ collection of a single-point location and the reanalysis dataset is from a grid interpolation. The data availability is also one of the reasons for the differences. Some data are limited for this study (MetMalaysia and DID) as the records are not fully available to the public, and the other datasets are either only for a short period (TRMM for 1998 until 2015 - only until 2013 in this study) or discontinued (APHRODITE data is from 1950 until 2007 only). The error is however small enough, and there are some similarities among the datasets despite the different temporal resolution and types. In the next chapter, only TRMM is used, as it is the most current and having the highest temporal resolution (3-hourly).

Diurnally, most of the rainfall events occurred in the afternoon between 1400 LT to 2000 LT, after the solar insolation reaches its maximum and this is typical in the tropics. As the east coast is affected by the Asian winter monsoon and the prolonged rainfall may be up to 24 hours and it is believed to cause the lack of variability in the diurnal cycle of precipitation over the east coast stations. Another reason is the interaction between low-level monsoon flows and the local circulation over the coastal region (such as land breeze in the early morning) that will induce convection development and eventually produce rain. Thus, rainfall is also common in the early morning instead of the afternoon only. The lack of variability in the diurnal cycle of precipitation over the southwestern station is believed to be associated with the early morning squall line phenomena (known as *Sumatras*) which affect the region throughout the year except during the winter monsoon season.

Air temperature, specific humidity and sea surface temperature (SST) studied in the regions do not vary greatly, except that the boreal winter monsoon may bring colder air and SST from the north (colder air mass from Siberian High-pressure system). The difference in SST is not more than ± 2 °K, but it is important to note that a (positive) degree difference in SST may influence the local weather, by increasing a chance for severe rainfall to occur (Lau and Wu, 2011). In general, air temperature over the peninsula is slightly higher in April and May, and generally the same in the other months. The specific humidity also does not differ much throughout the year. This is the reason for this study to focus only on rainfall and winds.

This chapter has compared the monthly and seasonal pattern of rainfall from a few stations data and gridded datasets. The study only focuses on rainfall and

provides a few discussion on the wind pattern. The variation in surface temperature and humidity is small. These results are used to determine how much is the difference the rainfall over the western and inland peninsula during inter-monsoon compared to the monsoon seasons. Since this thesis focuses on localised rainfall events, only inter-monsoon rainfall will be analysed in the next chapter, without considering the interference of large-scale events especially monsoon. Further analysis of inter-monsoon rainfall and winds will be explained in the next chapter.

Chapter 5

Severe Convection over the Western Peninsular Malaysia

5.1 Introduction

The tropics experience severe convection all year round, and they are even more severe during the wet and typhoon seasons. The Peninsular Malaysia experiences severe convection events (including thunderstorm) throughout the year. Severe convection over this region is mostly associated with the unstable tropical atmosphere due to solar heating. Localise severe convection can have a lifespan of 15 to 30 minutes but can prolong to several hours when a cluster of thunderstorms affects the region (Desa and Rakhecha, 1997). The purpose of this chapter is to analyse the common factors involved in the development of the local severe convection, without other synoptic influences such as monsoon (hence the inter-monsoon) and Madden-Julian Oscillation (MJO).

5.1.1 Chapter Structure and Aim

This chapter contains an analysis of the severe rainfall events in a monthly and seasonal mean. The heavy rainfall events which were based on the 90th percentile threshold on daily rainfall total using the observational dataset; rainfall gauge and gridded dataset. Then, just by using TRMM dataset (for consistency), the study started to focus on the April-May and September-October inter-monsoon periods. Analysis of rainfall, winds, and humidity of the interested regions (north-west, west and inland) of these heavy rainfall days are presented. The aim of this chapter is to present the mean condition of the rainfall, winds and humidity over these regions during heavy rainfall events. The results will also be useful in choosing the case study dates.

5.2 Threshold and Monthly Mean

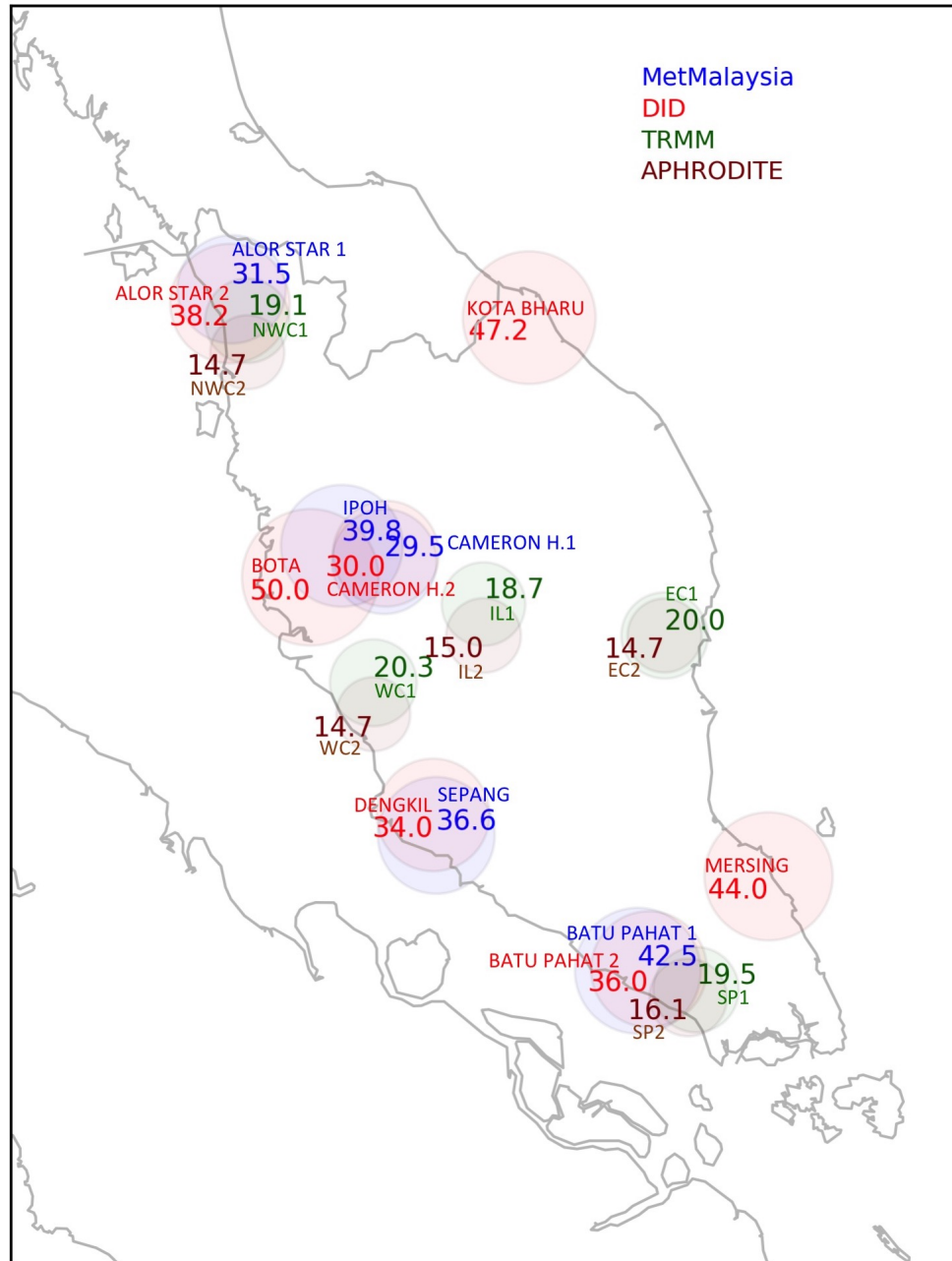


Figure 5.1: Threshold values for 90th percentile for each rain gauge station and each region, in mm day^{-1} . The percentile was calculated from all rainfall events through the year for each region or station. Data are from MetMalaysia (blue), DID (red), TRMM (green) and APHRODITE (brown) datasets. More details in Appendix, Table A.17.

As discussed in Section 3.3, a list of *heavy rainfall days* (from now on known as **HR90**, stands for the heavy rainy day above 90th percentile) is created to analyse common features (for example in terms of rainfall and winds) of the heavy rainfall events. Firstly, the *rainy day* is defined by the day with rainfall equal or greater than 1 mm day^{-1} (for each region and station). Then, the **HR90** is the day with the rainfall amount equal or greater than the 90th percentile threshold from the *rainy days* calculated earlier, also for each region and station. The 90th

percentile calculation is based on the annual rainfall events instead of monthly or seasonal, in attempt to generalise the heavy rainfall values. The 90th percentile values calculated on both gauges (MetMalaysia and DID stations) and gridded (TRMM and APHRODITE) datasets are plotted in Figure 5.1.

From Figure 5.1, the MetMalaysia gauge stations show an average of 36.0 mm day⁻¹ as the 90th percentile for all five stations. The highest value is Batu Pahat 1 station (south peninsula) with 42.5 mm day⁻¹. The lowest is Cameron Highlands 1 station (highland station) with 29.5 mm day⁻¹ of rain. The DID gauge stations show similar values for the threshold where the mean for all the western and inland stations is 37.6 mm day⁻¹. Bota station has the highest 90th percentile value which is 50.0 mm day⁻¹ and Dengkil is the lowest with 34.0 mm day⁻¹. Although both datasets have different temporal resolutions and DID dataset has more missing data, the mean values do not vary greatly.

The gridded datasets (TRMM and APHRODITE) show a significantly lower 90th percentile values than the gauge dataset. While on average, the *mean* values of rainfall in between gridded and station datasets do not differ much (for example, in monthly mean over a region), the difference in the extreme events is expected. The gridded dataset have a smaller variance since most of the data is averaged onto a coarser grid box. This is because most extreme events occur on a smaller spatial scale than a grid box, thus, such extreme events will become smaller in magnitude at the grid-scale. This gridded dataset is useful in performing the spatial analysis. TRMM dataset shows that the west coast has the highest 90th percentile value of 20.3 mm day⁻¹ and the lowest is the inland region where the 90th percentile value is 18.7 mm day⁻¹. There is a similarity between gridded and gauge datasets where the inland station has lower 90th percentile values compared to the coastal stations or regions. The APHRODITE dataset shows almost consistent threshold value, at around 14.0 mm day⁻¹ but the north-west region has the lowest value (14.7 mm day⁻¹) and southern region has the highest value (16.1 mm day⁻¹). The difference between the two gridded data may be due to the different time periods being used in the calculation of the 90th percentile in this study (TRMM: 1998-2013, APHRODITE: 1970-2007) and type of data used in the production of the dataset (TRMM: combination of satellite radar and ground readings, APHRODITE: from rainfall gauge stations).

The HR90 list from TRMM was used in the analysis from here onward for consistency and MetMalaysia gauge dataset was used as a comparison (if necessary). Only NWC, WC, and IL regions were analysed. The HR90 frequency is higher in NDJFM (46.4% for all NWC, WC and IL mean), then in SO (44.7%), and then in AM (31.7%). The lowest frequency of HR90 is in JJA (18.1%). The mean of the rainfall rate for HR90 from the highest to the lowest are 30.4 mm day⁻¹ (NDJFM), 26.9 mm day⁻¹ (SO), 26.5 mm day⁻¹ (AM) and 26.0 mm day⁻¹ (JJA). Compared

to the climatology, the highest frequency of rain (≥ 1 mm day⁻¹ on each day, for NWC, WC and IL averaged) seasonally is in SO (85.9%), followed by AM (81.4%), JJA (71.7%) and NDJFM (70.6%). The mean values of the rain rate from the highest to the lowest are 10.2 mm day⁻¹ (NDJFM), 9.9 mm day⁻¹ (SO), 8.6 mm day⁻¹ (AM) and the lowest is 7.6 mm day⁻¹ (JJA).

One of the objectives of this research is to understand the development of severe convection which was not influenced by any large-scale weather phenomena, such as monsoon (thus, inter-monsoon was selected). This also includes another large-scale event namely Madden-Julian Oscillation (MJO). The list of **HR90** was analysed and all the days associated with MJO were removed. Tables 5.1 and 5.2 show the frequency of HR90 which was not associated with MJO active phase 3, 4 and 5, for MetMalaysia and TRMM datasets, respectively. As discussed in Section 3.3, the active phase of the MJO as defined by the RMM index is when the tropics experience more convection activities, depending on the phase (Wheeler and Hendon, 2004). In this particular study, the active MJO phase 3, 4 and 5 are when the eastern Indian Ocean (phase 3) and Maritime Continent (phase 4 and 5) experience more convection activities than normal. However, a recent study (Birch et al., 2016) shows that the active MJO phases increase the probability of intense rainfall on the synoptic scale, especially over the sea, but may reduce it on the mesoscale, especially over land. The reason is, less solar insolation is received over land (in the Maritime Continent specifically) during the active phase of the MJO (in this case Phase 4) causing a weaker sea breeze, thus decreasing rainfall amount over the landmass (Peatman et al., 2014; Birch et al., 2016). This result is expressed in the Tables 5.1 and 5.2. More than 80% of the HR90 from MetMalaysia gauge dataset and at least 68% of the HR90 in TRMM dataset are not associated with MJO. As much as the MJO influences the development of convection activities in this region, most of the heavy rainfalls are not associated with the MJO active phase 3, 4 and 5.

	Alor Setar 1	Ipoh	Cameron High. 1	Sepang	Batu Pahat 1
Total (days)	184	187	274	122	111
Non-MJO (days)	159	159	230	106	96
Non-MJO (%)	86.4	85.0	83.9	86.9	86.5

Table 5.1: Number of days and percentage of days (above 90th percentile) which are and are NOT associated with Madden-Julian Oscillation's active phase (phase 3, 4 and 5) over the Maritime Continent. Data from MetMalaysia gauge (2005-2014).

To investigate how the MJO affects rainfall amount in the HR90 composite over the area, the comparison analysis was done as in Figure 5.2, using TRMM dataset. By comparing the rainfall total side by side (HR90 with the MJO - Figure 5.2 (top left) and HR90 without the MJO - Figure 5.2 (top right)), there are differences in the rainfall, especially over the sea and strait. There are also differences over the peninsula because around 30% of the days in the initial HR90 list are asso-

5.2. THRESHOLD AND MONTHLY MEAN

	NWC	WC	IL	SP	EC
Total (days)	473	423	484	427	456
Non-MJO (days)	325	319	350	313	311
Non-MJO (%)	68.7	75.4	72.3	73.3	68.2

Table 5.2: Number of days and percentage of days (above 90th percentile) which are and are NOT associated with Madden-Julian Oscillation's active phase (phase 3, 4 and 5) over the Maritime Continent. NWC: Northwest Coast, WC: West Coast, IL: Inland/Highland, SP: Southern Peninsula, EC: East Coast. Data from TRMM (1998-2013)

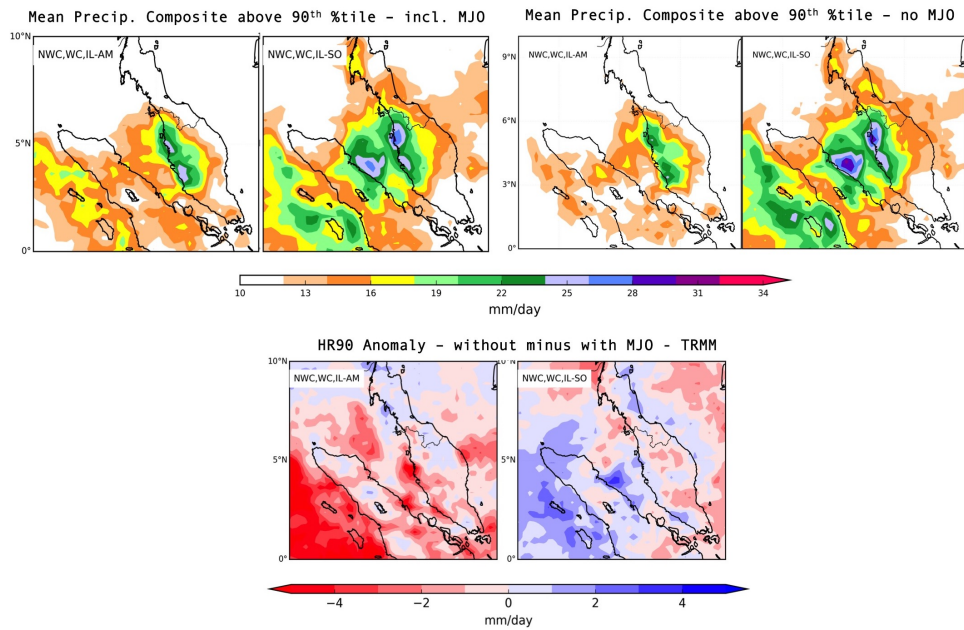


Figure 5.2: Comparison between the composite of HR90 rainfall for three regions averaged (NWC, WC and IL) for each AM and SO inter-monsoons. (Top Left) HR90 composite including the MJO and, (Top Right) without/no MJO active phase (phase 3,4 and 5) and, (bottom) the comparison between the two, without MJO minus with MJO. Blue represents a higher rainfall rate in the HR90 (no MJO), and red represents a higher rainfall rate in HR90 (with MJO). Data is from TRMM dataset, from 1998 to 2013.

ciated with MJO in the TRMM dataset. Figure 5.2 (bottom) shows the differences in the mean of HR90 for each inter-monsoon. Negative values (red) show that there is more rainfall if the MJO is passing. The differences are not that large over the peninsula, with $\pm 3 \text{ mm day}^{-1}$ in AM and $\pm 1 \text{ mm day}^{-1}$ in SO. The difference is larger over the ocean, especially over the eastern Indian Ocean. During AM period, there is more rainfall over the ocean when MJO is included. However, in SO period, there is less rainfall over the ocean when MJO is included.

Based on MetMalaysia (rain gauge), DID (rain gauge) and TRMM (gridded) datasets on Figure 5.3, there are more HR90 towards the end of the year. This is consistent with the movement of the convection from the north as discussed in Section 2.1, and also due to the beginning of the winter monsoon in November. MetMalaysia gauge dataset shows a high frequency of HR90 in November except for Alor Setar 1 which is in August. For Alor Setar 1 station, it is most likely due to its location in the north-west, facing the late summer monsoon flow and may

5.2. THRESHOLD AND MONTHLY MEAN

be due to the seasonal convection march from north to south. The DID stations show a consistently high HR90 frequency in September for the west coast and inland stations, and in December for the east coast stations. The TRMM dataset, however, shows a slightly different pattern. The NWC region received the most HR90 in October, the WC region in November and other regions are in December. Although there were differences in annual maximum between these datasets, in general, they correspond to the biannual peaks once in March-May and another in September-November in HR90 frequency. Seasonally, a higher number of rainy days were recorded over most of the north-west, west and inland stations during SO. The same pattern was also observed in the TRMM and APHRODITE datasets. The number of rainy days over the inland region exceeds the number of rainy days over the other regions, especially during SO.

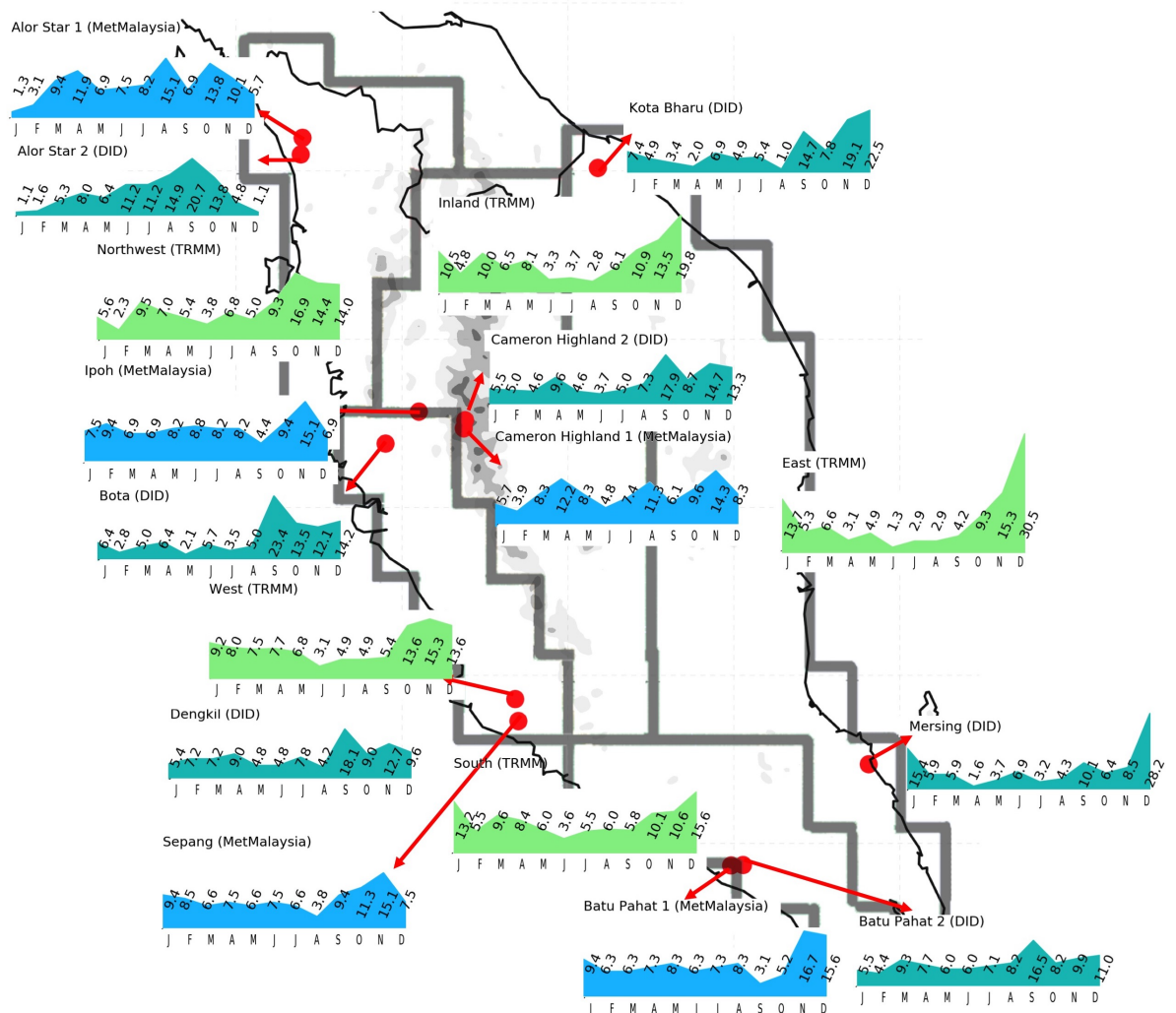


Figure 5.3: The mean distribution of HR90 frequency from MetMalaysia (Blue), DID (dark green) and TRMM (light green) dataset, monthly. Each value represents the percentage number of HR90 events occurring each month through the annual cycle (which sum to 100%). For example, $n\%$ in January means $n\%$ of the HR90 occurred in January from the total annual average. Each station (or region) were labelled on top of each graph. The table version is in Appendix Table A.18.

5.3 Inter-monsoon Outlook

Starting from this section, the analysis will only be performed for April-May and September-October periods because this study is only focusing on the inter-monsoon periods. A spatial analysis of the HR90 rain is shown in Figure 5.4. This figure helps us to determine the spatial distribution of the heavy rainfall over the regions as well as to assist in the selection of case studies. The composite images represent locations where heavy rainfalls normally occurred based on HR90. There is a noticeable difference in rainfall distribution during AM and SO. There is more rainfall over the Strait of Malacca during SO, but not during AM. The rain distribution is also widely spread over Sumatra, especially over the Indian Ocean, south-west side of the domain. This was discussed in Section 2.1, where in boreal autumn (in this case, SO), this region is the centre of the *southeastward movement of convection* from Asian boreal summer monsoon over South Asia to the boreal winter monsoon over Australia, and experiences active convective activity, stronger westerly from the Indian Ocean and produces more rainfall compared to during AM (Chang et al., 2005b). This is also associated with a more intense Walker circulation over the equatorial Pacific. The cold tongue over the eastern equatorial Pacific is stronger in boreal autumn, thus stronger descending motion over the region, and stronger ascending motion over the Maritime Continent. The cold tongue is weaker in boreal spring (Wang, 1994). Over the Indian Ocean, the eastern Indian Ocean also favours convection in fall in the Walker-like circulation over the equatorial Indian Ocean as it is warmer than the western equatorial Indian Ocean (Webster et al., 1998). Thus, SO is climatologically wetter than AM. Other than the spatial distribution, there is no significant difference in terms of rainfall rate. The standard deviation of the HR90 is shown in Figure 5.5. In all composites (except inland cases), the standard deviation is high near the coast. On the regions themselves, the standard deviation is in between 20 to 30 mm day⁻¹ in both seasons. Inland region shows a standard deviation of in between 20 to 25 mm day⁻¹ for both seasons.

To compare the location of the HR90 with the mean rainfall location of each region in each season, Figure 5.6 is referred to. On average, the WC, part of NWC and part of IL regions received more rainfall than other areas during AM. In SO, most of the northern Peninsula Malaysia received more rain on average than the other regions. Based on this figure, most of the HR90 occurred where the mean rainfall was higher. However, in cases such as in IL-SO and NWC-AM cases, the HR90 events mostly did not occur at the highest mean rainfall area. These could be that the HR90 events are isolated heavy rainfall events.

While Figure 5.4 is useful to examine the mean of heavy rainfall of each region on each inter-monsoon, the HR90 list is also useful to examine other fields, especially in terms of winds. The composite plot of 850hPa winds over the area

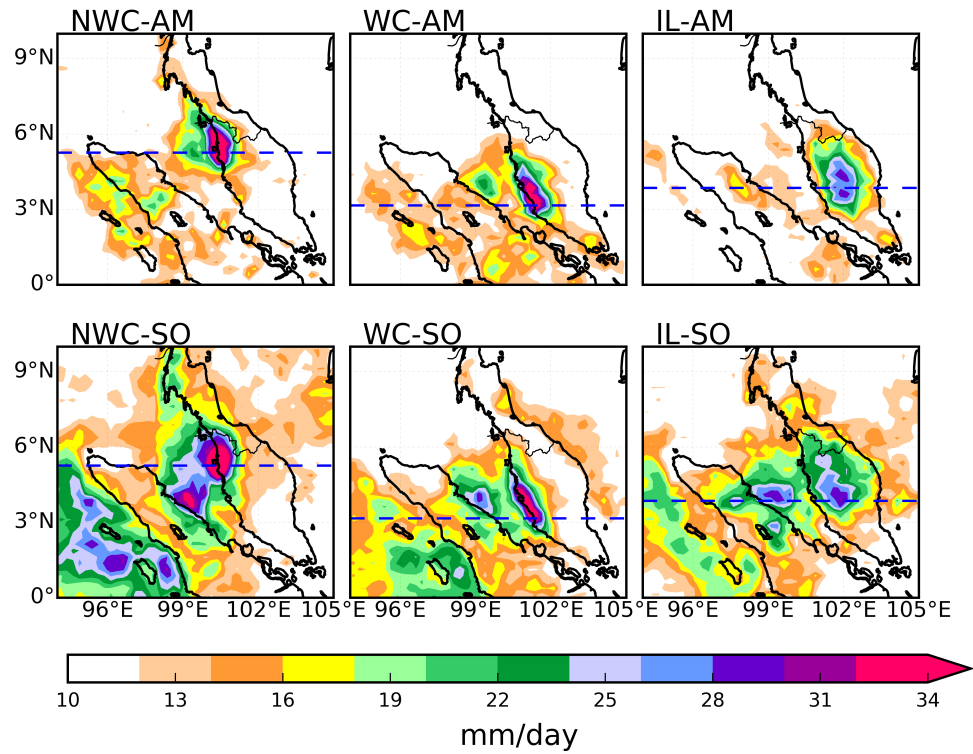


Figure 5.4: TRMM composite of precipitation distribution of the HR90, for AM and SO only, for NWC, WC, and IL regions. There are 36 days in NWC-AM, 60 days in WC-AM, 58 days in IL-AM, 88 days in NWC-SO, 77 days in WC-SO and 54 days in IL-SO. The days selected for these composite are based on HR90 value for each region. The blue dashed lines in each box are the cross-section lines of each region (NWC, WC and IL) for cross-section analysis.

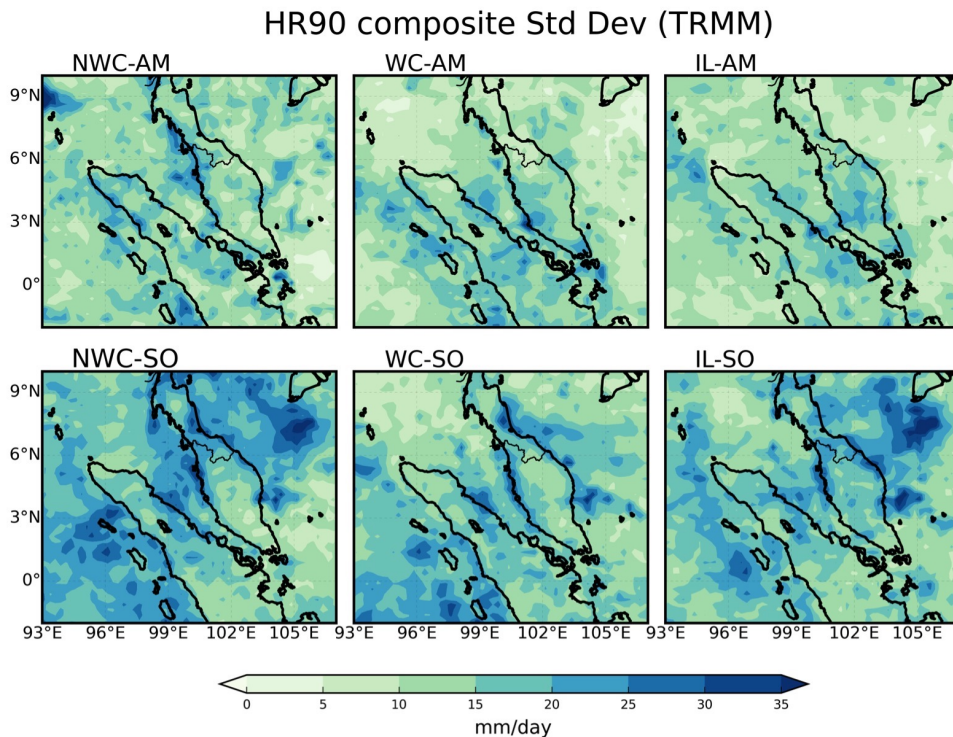


Figure 5.5: As in Figure 5.4 (without the blue dash lines), but showing the standard deviation of each rainfall composite.

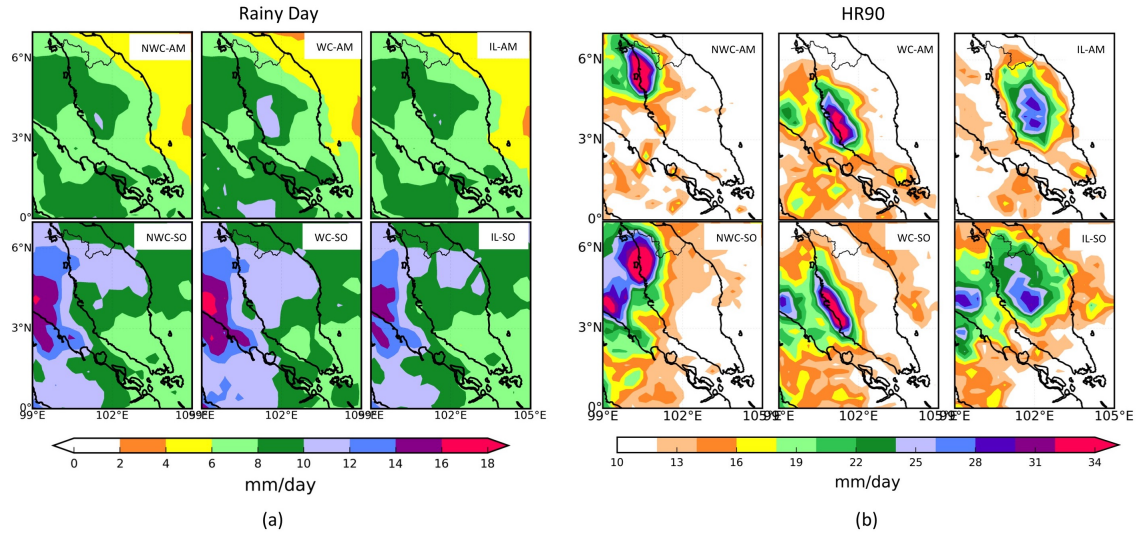


Figure 5.6: This figure compares the location of the HR90 with the mean of a rainy day ($\geq 1 \text{ mm day}^{-1}$) for each region and each season. Figure (a) shows the mean of the rainfall for the rainy day in mm day^{-1} , and (b) same as Figure 5.4. Scales are different for visualisation, as this figures are comparing the location of the HR90 to the rainy day, not their intensity.

during HR90 for each region and inter-monsoon is shown in Figure 5.7. In the case of NWC-AM, a cyclonic circulation was observed over the north-west and this may be the main characteristic of the development of severe convection over the region. In the case of WC-AM and WC-SO, easterly and westerly winds converged over the Strait of Malacca vicinity and this condition is believed to be one of the main ingredients to the severe convection development over this region. Most of the other cases (NWC-SO, IL-AM, and IL-SO) show some moderate signal of convergence over the west coast of the peninsula. A standard deviation of the wind speed, meridional and zonal wind components are shown in Figure 5.8. The figures show that in NWC cases, there is higher standard deviation of wind speed (and zonal wind component) in both cases in the northern part of the peninsula (and of the domain). The standard deviation of the meridional wind shows a higher standard deviation over the Strait of Malacca in SO season of all three regions.

Generally, stronger westerly or easterly or both may have influenced the development of heavy rainfall over the western peninsula. Stronger winds from the Indian Ocean (west) and South China Sea (east) brought more moisture and disturbance over the Strait of Malacca vicinity (in this case, western Peninsular Malaysia) and boosts the development of severe weather events. The 850hPa winds anomaly is shown in Figure 5.9, where in most cases, the stronger easterly wind may be associated with the severe rainfall events in these regions. Stronger westerly winds may be associated with the severe rainfall event in IL during AM inter-monsoon. These results also suggest a large-scale influence even without MJO. This is proven by the stronger northeasterly and westerly winds from the South China Sea and the Indian Ocean, respectively. Each composite of respective regions show

a unique large-scale wind pattern associated with the severe rainfall event at each location, and this analysis is useful in recognising the mean pattern of the 850hPa wind for severe rainfall event over these regions for each inter-monsoon.

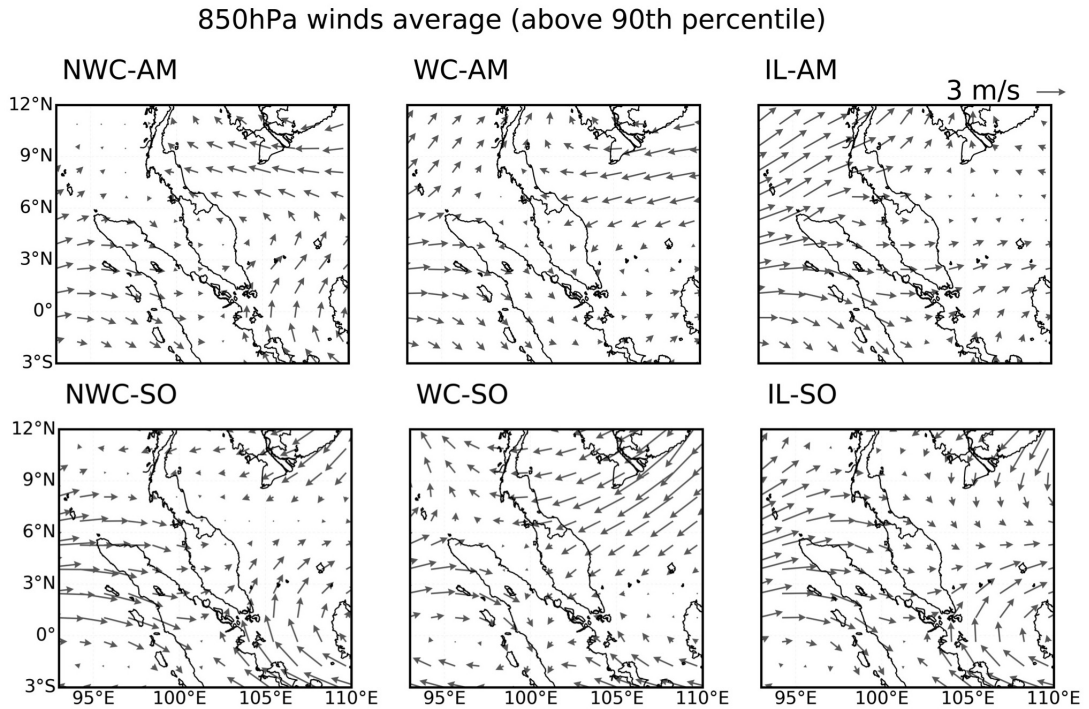


Figure 5.7: Similar to Figure 5.4 but for winds at 850hPa pressure level, from ERA-interim dataset.

Vertical cross-section analysis of the vertical motion was done to investigate the strength of the air circulation during the severe rainfall events. The cross-section for each case is based on the location of the maximum rainfall in Figure 5.4. Focusing on the western Peninsular Malaysia and Strait of Malacca regions, a relatively stronger ascending motion in the morning was observed over the west of the peninsula and Strait of Malacca vicinity in all AM and SO cases, with a lot stronger cases for both NWC cases (Figure 5.10(a)). There are also stronger descending motion near the surface over the peninsula in all cases. For afternoon circulation, the anomalies in Figure 5.10(b) show a stronger ascending motion in all cases than their morning counterpart, which can be associated with the convection and rainfall activities. There is an exception for the NWC-AM case where the stronger ascending motion is weaker in the afternoon. The stronger descending motion was also observed near the surface over the peninsula, especially over the eastern peninsula. While general pattern such as stronger ascending motion associated with strong convection activities for heavy rainfall events to occur was observed, there are still some differences in terms of strength and location. The difference is the results of varying factors involved in the development of the rainfall events, and how they behave.

Although the humidity over the tropics does not change as much as in the

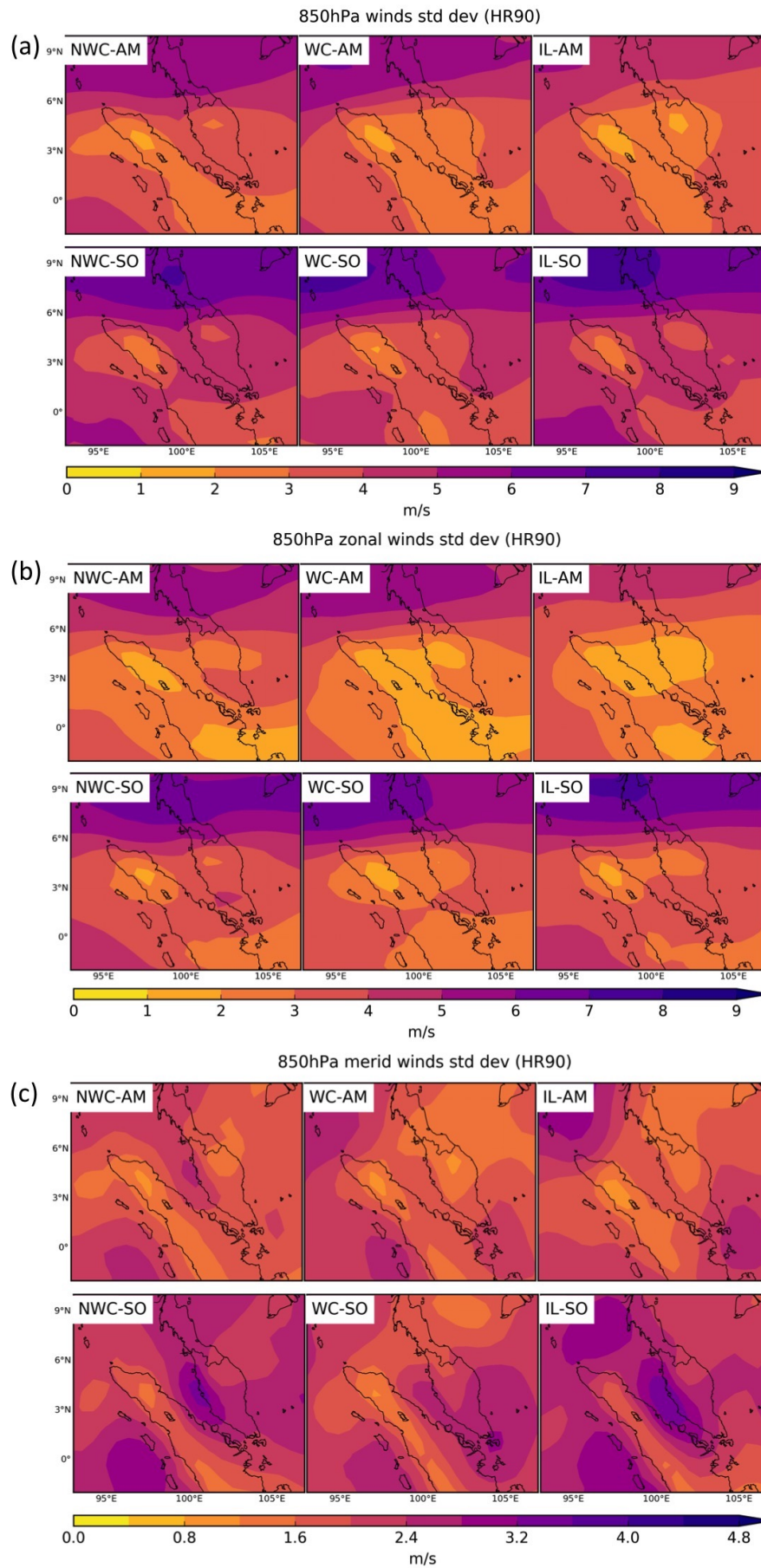


Figure 5.8: Similar to Figure 5.5 but a standard deviation for (a) wind speed (magnitude), (b) zonal wind and (c) meridional wind, from ERA-Interim.

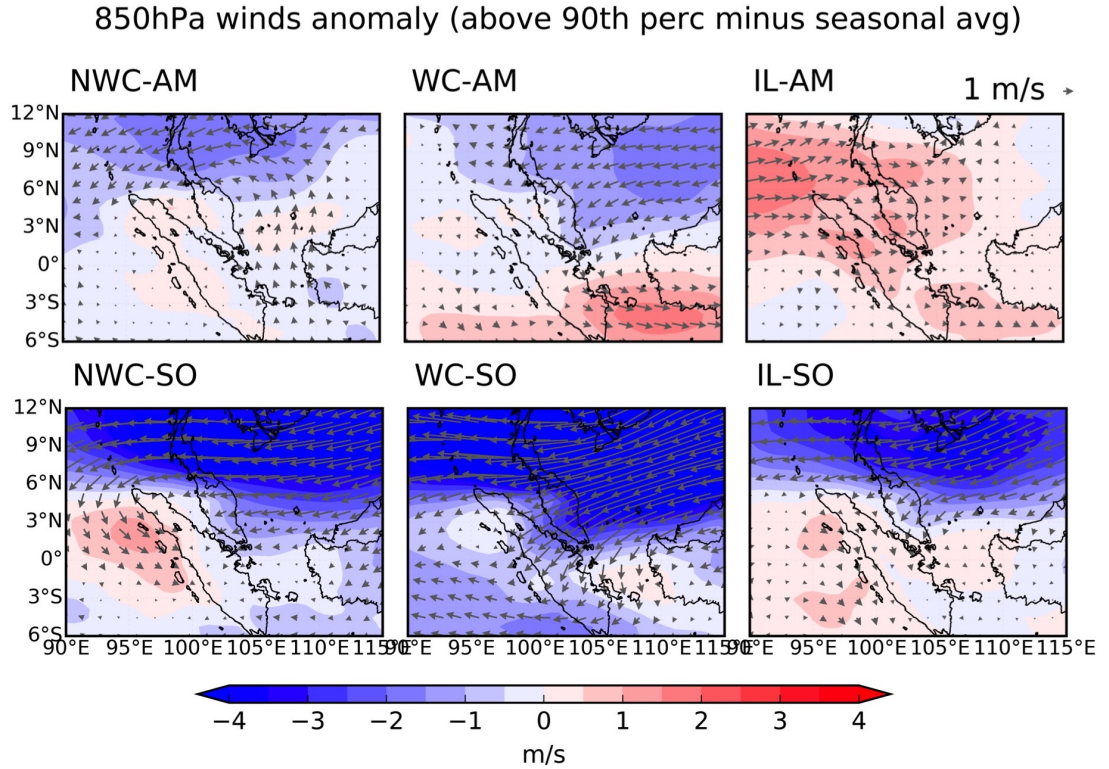


Figure 5.9: Similar to Figure 5.4 but for winds anomaly (vectors) and zonal winds anomaly (shaded) at 850hPa pressure level, from ERA-interim dataset. Calculated by subtracting the AM or SO seasonal mean (1981-2010) from each composite.

higher latitude regions, it is worth to look at the humidity anomaly associated with the severe rainfall events (or in this case, HR90). An analysis of specific humidity to examine the moisture anomaly in HR90 cases is shown in Figure 5.11(a) and 5.11(b), for NWC, WC and IL regions for each inter-monsoon. A higher humidity (around 775 hPa to 500 hPa) and anomalous dry condition near the surface were observed in all cases. A consistent pattern was observed in all cases for both inter-monsoons. The same conditions were noticed for the afternoon composite. These results also exhibit a moist anomaly in the mid-level atmosphere, consistent with deep convection activities in the HR90 days, when these convection activities over the land are intense. While most SO composites show a low-level dry anomaly and upper-level wet anomaly conditions, all regions inhibit a wetter condition at near-surface over the Peninsular Malaysia and Strait of Malacca area for the AM inter-monsoon cases. Another common pattern for all cases was the existence of a high humidity anomaly blob at around 800 hPa that is slightly tilted over the eastern peninsula. This wetter air aloft the east peninsula may be due to the extra moisture brought by the easterly winds from the South China Sea. However, this hypothesis requires an investigation potentially with modelling to determine the role of moisture carried by the wind from the South China Sea in developing of severe convection event over western Peninsular Malaysia.

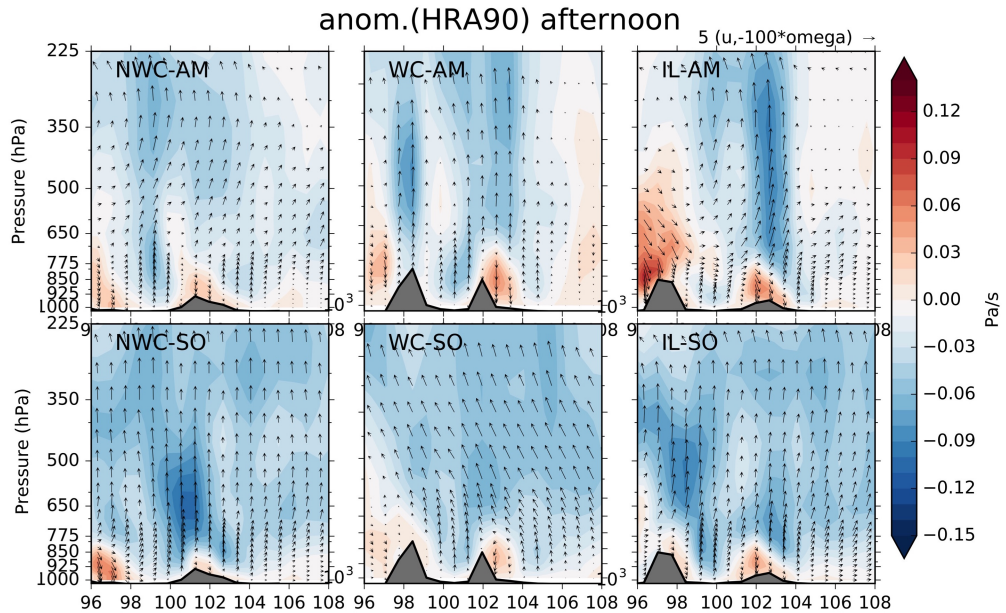
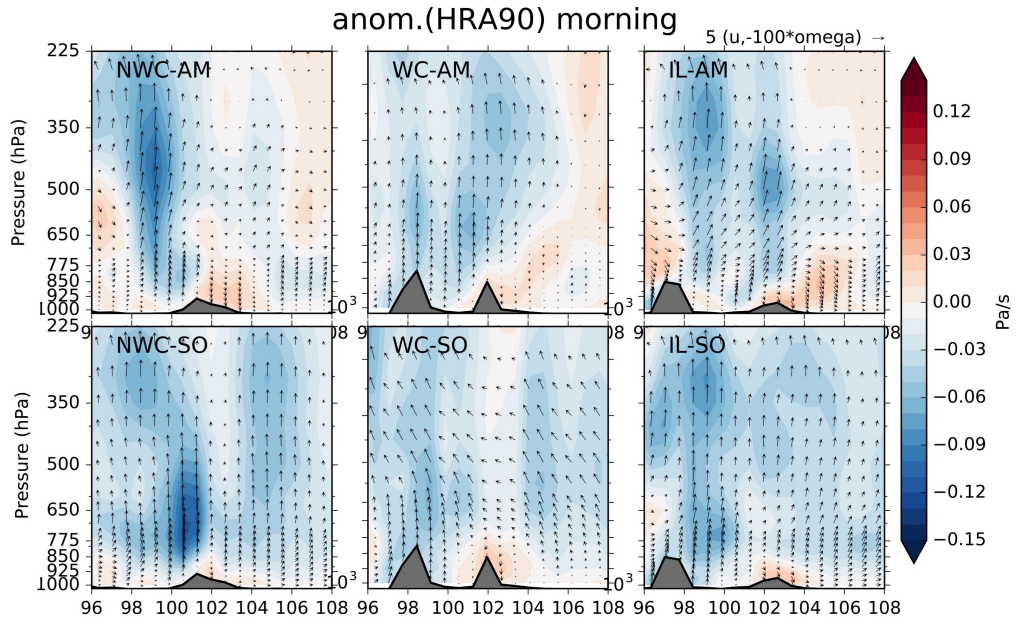
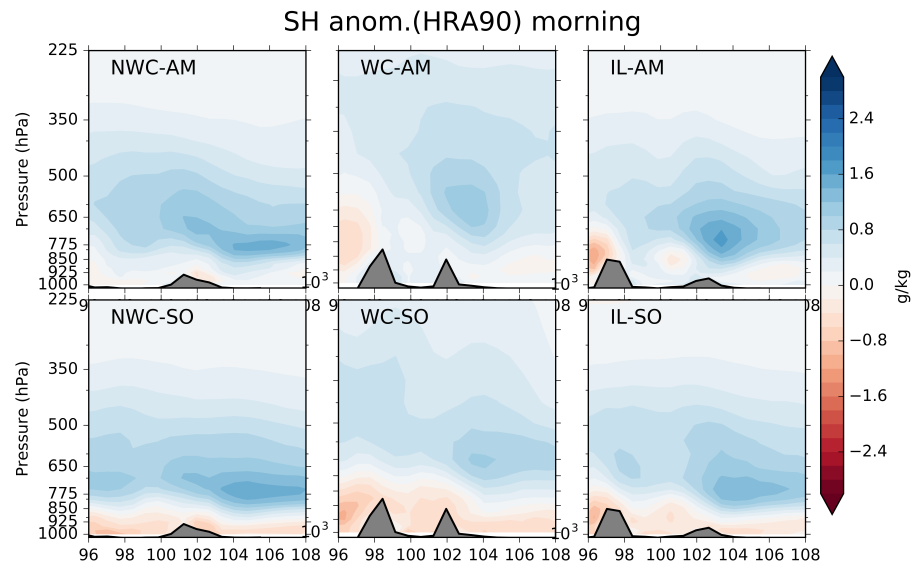
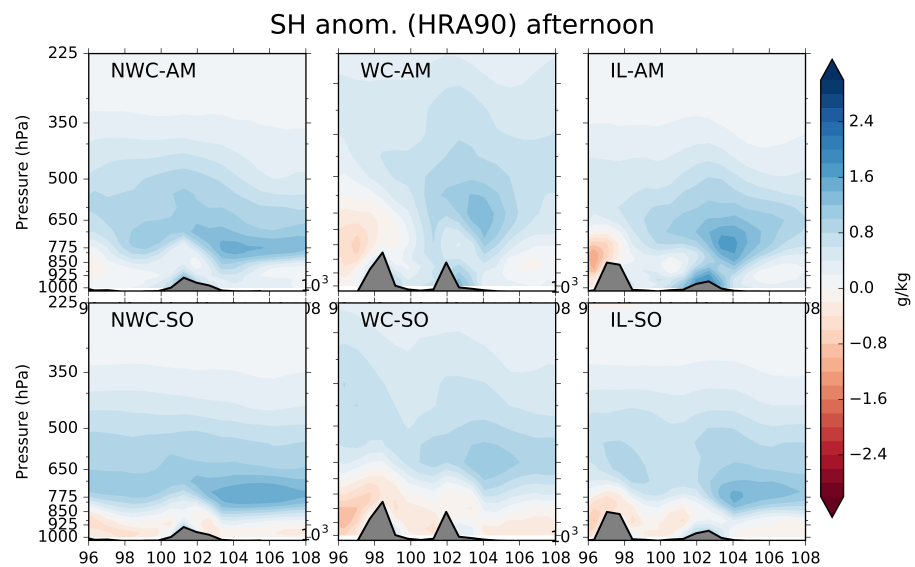


Figure 5.10: Cross section of NWC (5.26° N), WC (3.16° N) and IL (3.86° N) cases as shown in small boxes in the first row, where the cross was selected based on maximum rainfall (blue dashed lines in each box) in Figure 5.4. These plots show the composite of the anomaly of zonal wind and omega of the same HR90 days for (a) morning and (b) afternoon. The vectors represent the vertical motion anomaly and shaded colours represent omega anomaly. The dataset was taken from the ERA-interim dataset. The anomalies (of the zonal wind and omega) were calculated by subtracting the seasonal mean (AM or SO) from the HR90 composite of each morning and afternoon cases individually (reference years: 1981-2010).



(a) morning



(b) afternoon

Figure 5.11: Similar to Figure 5.10 but for the composite of specific humidity anomalies of the same HR90 days for (a) morning and (b) afternoon. Dataset was taken from the ERA-interim dataset. The anomalies were calculated by subtracting the seasonal mean (AM or SO) from the HR90 composite of each morning and afternoon cases individually (reference years: 1981-2010).

5.4 Summary

To investigate the severe rainfall events, the top 10% of the rainy days were analysed because these were considered as the heavy rainfall days (HR90) for this study. Here, the HR90 was calculated by examining the daily rainfall amount throughout the year, and not based on monthly or seasonal rainfall (for each individual station/region). The HR90 threshold for MetMalaysia and DID gauge stations are between 29.5 mm hr^{-1} to 50.0 mm hr^{-1} . The mean HR90 values for these gauge datasets are 36.0 mm day^{-1} for MetMalaysia rain gauges and 37.6 mm day^{-1} for DID rain gauges (for 5 west coast stations only). For all larger spatial averaging regions, the gridded datasets TRMM and APHRODITE show a lower mean HR90 values which are in between 14.7 mm hr^{-1} to 20.3 mm hr^{-1} , and the mean HR90 values are 19.5 mm day^{-1} and 15.0 mm day^{-1} for TRMM and APHRODITE dataset, respectively.

Analysis of the MetMalaysia dataset shows a high HR90 frequency observed in November for all stations except one station in August (Alor Setar 1 station). Analysis of the DID dataset shows a high HR90 frequency in September for all the west coast and south-west stations but two stations on the east coast have a high HR90 frequency in December. The TRMM dataset shows a high frequency of HR90 in October for north-west coast (NWC) region, November for the west coast (WC) region and December for inland (IL), south peninsula (SP) and east coast (EC) regions. Inter-monsoon was selected to study localised severe rainfall event with no large-scale weather influence (i.e. monsoon), but the inter-monsoon period is not exempted from other large-scale weather influence, especially the Madden-Julian Oscillation (MJO). However, more than 80% of the HR90 from MetMalaysia gauge dataset and more than 68% of the HR90 from TRMM dataset are not associated with active MJO 3, 4 and 5 phases. The original HR90 list has been updated by eliminating days associated with MJO. The updated list was used to analysed rainfall, winds, and humidity.

The rainfall composites from TRMM show the common area (in the peninsula) where the HR90 usually occurs and which area hit the heaviest intensity. Rainfall is more spatially distributed during SO inter-monsoon for all three selected regions than the AM inter-monsoon. Rainfall during AM in the HR90 events is more concentrated inland, while during SO, it can be either inland or over the Strait of Malacca, which may or may not be connected to each other. The spatial distribution of rainfall in SO is larger due to SO being climatologically wetter than AM. It is also associated with the *southeastward migration of convection* from the Indian summer region to the Australian monsoon region.

The values between MetMalaysia and DID (or between TRMM and APHRODITE) in the HR90 threshold do not vary much. HR90 in between MetMalaysia and DID differ in 0.8 mm day^{-1} , and the HR90 between TRMM and APHRODITE differs

in 2.1 mm day^{-1} . However, the values between the rain gauges (MetMalaysia and DID) and the reanalysis datasets (TRMM and APHRODITE) are relatively large. The difference in between the average value of gridded dataset with rain gauge dataset over the western (including southwestern) regions is 19.5 mm day^{-1} . The difference is expected, as the extreme values of the gridded dataset are averaged over a grid box size instead of a single point as in the station dataset. These extremes are sometimes cover an area smaller than the grid box, thus the values are smaller when it was averaged out. It may also have to do with the data used to produce the gridded dataset. For example, the TRMM uses radar as one of its sources. A single point to point comparison is useful to analyse and compare the difference in value. This can be done by using a single grid point where the station is located (Figure 5.2). The variation in the threshold could be due to the difference in temporal and spatial resolutions. It may also best to use the same time period wherever possible in order to compare dataset. But the sample size will be too small due to the differences in the temporal availability of each dataset for this study. An advanced method may be useful to better compare these datasets, such as collecting as much as possible rain gauge dataset and use specific software such as Geographical Information System (ArcGIS) for interpolation purpose. Other than that, there are definitely other possible analyses that can be done for the composite analysis. For example, station data of near-surface winds is useful to compare with the ERA-interim composite. Another useful analysis is an upper air data analysis, looking at the vertical profile of available stations. This will provide more useful information especially on the common features of the vertical profile for the HR90 days. While these methods are very useful for this chapter, they are out of the scope of this thesis.

No common pattern was shown in the 850 hPa winds composite. There was a cyclonic-like circulation in NWC-AM composite and could have been the main factor associated with severe convection events over NWC in AM inter-monsoon (Figure 5.7). In the other cases, wind direction over this region is either mostly westerly or both westerly and easterly. By looking at the anomaly plot, it shows that in most cases, the easterly wind from the South China Sea is stronger for most of the HR90 cases. Except for inland HR90s during AM (IL-AM) cases, where positive westerly wind from the Indian Ocean is common. Wind convergence over the Strait of Malacca vicinity is also associated with the development of the heavy rainfall events. In general, converging easterly and westerly winds are associated with the severe rainfall events over the west coast of the peninsula (Figure 5.9). These converging winds bring more moisture toward the western peninsula (and its vicinity) and create instability over the region and promote the development of severe convection. Predominantly westerly winds are common for the severe rainfall event over the inland of the peninsula. This is another example of how

westerly winds help the development of the severe convection over the peninsula by providing moisture from the Indian Ocean and lifted by the orography to develop precipitating clouds. The anomalous easterly winds also assist the development of the severe rainfall events over the western Peninsula Malaysia by providing the instability on the lee side of the mountains (west coast) and promote convection over the western peninsula, as discussed by Sow et al. (2011).

There is no consistent pattern of the vertical motion as seen from the cross-section analysis for these cases. In each inter-monsoon, each region has its own pattern with regards to the HR90 development. The cross-section anomalies plot shows a stronger vertical motion over the western peninsula and Sumatra in the morning, consistent with the diurnal heating which induces convection. The stronger upward motion on the western peninsula is associated with the development of the severe rainfall events. While stronger upward motion over land is expected in the early stage of the development of severe rainfall event, this is not shown in all composite results. The west coast (WC) and inland (IL) regions during the SO inter-monsoon show a weaker upward motion in the morning composite over the west coast, but a stronger upward motion is detected over the east Sumatra and Strait of Malacca.

Although the tropics are always humid, there is a distinct pattern of the anomaly of its specific humidity. A higher level of humidity above 775hPa was observed in all cases and a notable pattern in this composite plot is a high humidity anomaly blob around the 850 hPa over eastern Peninsular Malaysia. This high humidity anomaly aloft could be related to the events where the moisture is higher due to the convection activity. The blob of humid air anomaly over eastern Peninsular Malaysia is associated with the easterly winds from the South China Sea, bringing moisture toward the peninsula. This result also shows how the anomalous easterly winds in the discussion above are associated with the anomalous humidity over the east part of the peninsula. The anomalously high humidity is more likely to be coming from the east (South China Sea) that can enhance convection for inland and western peninsula. More studies are needed on the relationship between the humidity anomaly and the development of the HR90, for example, lag correlation study by looking at lagged composites of the specific humidity.

These results are useful to determine the common pattern of rainfall and low-level wind, specifically. The composite analysis was also extended to the cross-section analysis of the local wind circulation and specific humidity. All the results suggest that there is some aspect of large-scale flow that appear in the heavy rain events, but that local processes such as land-sea breezes, mountain-valley breezes and orographic lifting may be as important in generating the HR90 events. In the next chapter, two case studies are selected to investigate these local processes by looking at the role of local orography in the development of a heavy rainfall event.

Chapter 6

Case Studies

6.1 Introduction

The main objective of this chapter is to investigate two severe rainfall events to examine the common feature observed in Chapter 5 and to demonstrate the importance of local orography on the development of the events. The two selected case studies were chosen based on their impact on socio-economic aspects, and media reports. For example, in the first case study, the damage and loss of life were widely reported in the news. For the second case study, although there was no loss of life, the event was reported in the news. These two case studies are examples of the common severe flooding events that are caused by severe rainfall. Although general population has accepted the cause of the flooding was the severe rainfall, and is common in this region, further study on the scientific perspective is needed for the operational side to acquire knowledge and apply it for a better understanding of the local weather, and perfecting weather forecast quality in the future.

Severe rainfall events during inter-monsoon were selected because this study is focusing on the local weather events, with no large-scale influence, such as the monsoon. However, some of the severe events during inter-monsoon are also influenced by other large-scale circulation such as Madden-Julian Oscillation (MJO). Based on the discussion in Chapter 5, most of the events are not associated with the MJO active phase (phase 3, 4 and 5) and believed to be locally initiated. But since the inter-monsoon coincides with the location of the Intertropical Convergence Zone (ITCZ) over the equatorial tropical region, there are certainly some large-scale circulations play their role in the development of the severe rainfall events over this region, such as the Hadley circulation.

As discussed in Chapter 2, some mechanisms were suggested from several case studies on the development of severe rainfall events such as land-sea breeze interactions, sea breeze convergence, mountain-valley breezes, lee waves and the influence of gap winds (Joseph et al., 2008; Qian, 2008; Sow et al., 2011). These

case studies will further explore the above-mentioned mechanisms as well as other mechanisms involved. The main focus of these case studies is to look at the role of the local orography (of Peninsular Malaysia and Sumatra Island) and Sumatra Island in the development of the severe rainfall events.

6.1.1 Chapter Structure and Aims

This chapter presents an analysis of each selected case study from each inter-monsoon. However, the full analysis was only carried out for the first case study, as the models were unable to properly reproduce the rainfall event for the second case study. The first part of each case study will introduce the event including the evidence from the rainfall gauges dataset, radar and satellite images. The second part of each case study presents the computer simulation result, which is then compared to the radar (qualitatively). This comparison is important in order to validate the result and further analyse the output data. The output of this was then used to determine the possible mechanism of the development of the rainfall event in more detail. The final part of the case study involved the determination of how the local orography and Sumatra Island modify the severe rainfall events, hence the role of orography in the development of the events was analysed. The aim of this chapter is to analyse the development of the severe rainfall events in detail using the high-resolution model. This chapter also aims to present the role of local orography and Sumatra Island in the development of the severe rainfall event, and in the modification of convective activity in general. Although the two case studies are not enough to represent the general condition, it is a stepping stone toward more studies on the tropical mesoscale weather.

6.2 Case Study 1: First Inter-monsoon (April-May)

6.2.1 Introduction

On 2nd May 2012, Klang Valley (central west Peninsular Malaysia, see Figure 1.1) experienced a severe convective storm that caused flash floods and landslides in some areas. These caused financial loss and a few fatalities due to the landslide events. According to one of the stations in the affected region, the maximum hourly rainfall rate was 22 mm hr^{-1} and total rainfall of 53.2 mm within 5 hours was observed (Figure 6.1(a)). The maximum rainfall occurred at 1600 local time (LT). It weakened an hour later and stopped at 1800 LT. On the day itself, the west coast of Peninsular Malaysia experienced heavy rainfall as shown in Figure 6.1(b). This figure was retrieved from the Department of Irrigation and Drainage Malaysia (DID), the only accessible gauge data in a spatial plot for this case study. This

figure shows that the heaviest rainfall occurred mostly over the central west coast and there were some other rainfall events over the north-west and central peninsula. There was also a significant amount of rainfall over the south-east of the peninsula. The daily total rainfall on the day was above the 90th percentile threshold (as in HR90 in Chapter 5). Although it is not extremely high, it still caused a flash flood. This is also one of the reasons to investigate the development of the event from a meteorological perspective. That day was not influenced by MJO as shown in Figure 6.2, where the green lines (representing dates in the month of May 2012) are all in the non-active MJO circle (Wheeler and Hendon, 2004). The event also occurred during a neutral phase of El Nino-Southern Oscillation (ENSO). Thus, the event was believed to be locally initiated.

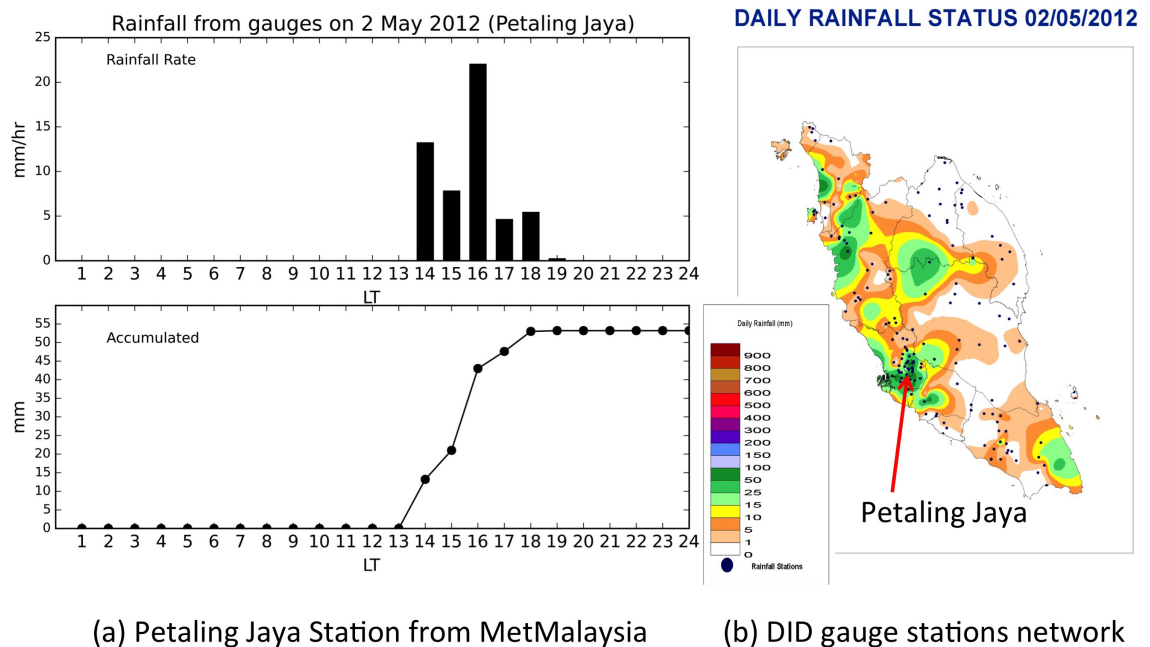


Figure 6.1: (a) Hourly rainfall rate and accumulated rainfall recorded from the gauge from one of the stations (Petaling Jaya) on the 2 May 2012 from MetMalaysia. The location is shown in the figure with a red arrow on the next map, (b) Rainfall distribution based on gauges measurement on 2 May 2012, from Dept. of Irrigation and Mitigation Malaysia database website. The black dots are the DID rainfall stations.

The radar images confirmed the event is as seen in Figure 6.3. The rainfall event over the straits in the late morning was visible in the radar image 1100 LT where there were very small-scale rainfall events around western Peninsular Malaysia. By 1200 LT, some rainfall events were observed over the western coastal line, and on the coast. There was also some rainfall or convective activity along the state border, which is where the mountain range is. By 1300 LT, the rainfall over the coast and mountain range was getting stronger. By 1400 LT, the rainfall events over the west coast were getting stronger and the rainfall over the strait had ceased. The rainfall had strengthened and spread to a larger area by 1500 LT. The

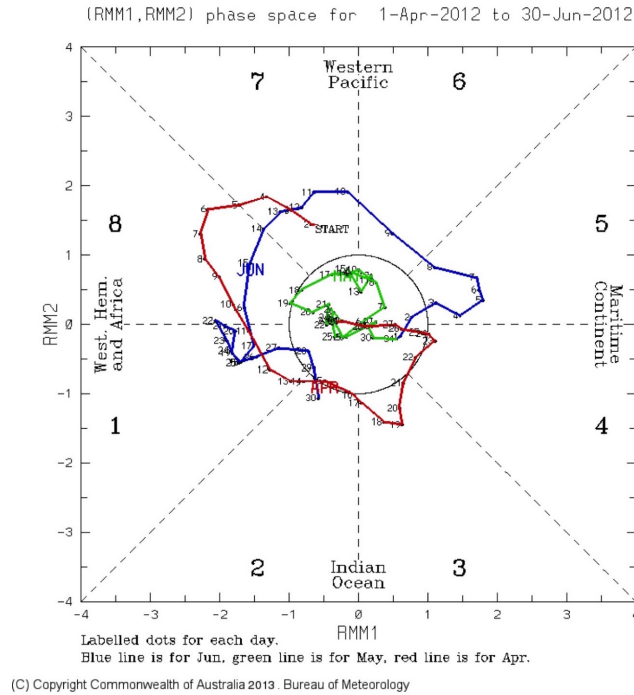


Figure 6.2: Madden-Julian Oscillation (MJO) from 1 April 2012 to 30 June 2012. Bright green is the MJO phases in May 2012, where all of the days in May are not in an active phase (inside the central circle) as in Wheeler and Hendon (2004). The figure was retrieved from Bureau of Meteorology Australia MJO webpage, available at <http://www.bom.gov.au/climate/mjo/>. Used with permission.

rainfall event stayed on the west coast until 1800 LT and had subsided by 2000 LT (not shown). The radar may have missed the inland rainfall shown in Figure 6.1(b), although there is some rainfall over the inland of the peninsula in the radar image (Figure 6.3-16:04:22) that might be the same rainfall event. As discussed in Chapter 3, it may also be related to the issues with the radar on detecting the rainfall due to the elevation angle of the radar as well as the Titiwangsa mountains that may have potentially blocked the radar from detecting the rainfall which is already being seen in rain gauge observations.

Another footprint of this event can be seen in the satellite images. The satellite images in Figure 6.4 show the development of the convective clouds over the west Peninsular Malaysia (yellow arrow). The existing convective clouds over the strait from 1100 LT to 1200 LT (0300 UTC - 0400 UTC) confirm the convective activity over the strait in the late morning of 2 May 2012. Convective clouds started to develop over the west coast at around 1300 LT and started to develop into deep convection by 1400 LT and 1500 LT. The peninsula was covered by convective clouds for the rest of the day.

This event was also confirmed in the 3-hourly data from the Tropical Rainfall Measurement Mission (TRMM). The rainfall event was captured in the 0600 UTC plot (1400 LT, Figure 6.5). TRMM captured the early morning rain over the strait early in the day and later in the afternoon. The rainfall event stayed on the west coast for a few hours before dissipating later in the evening. Some other regions

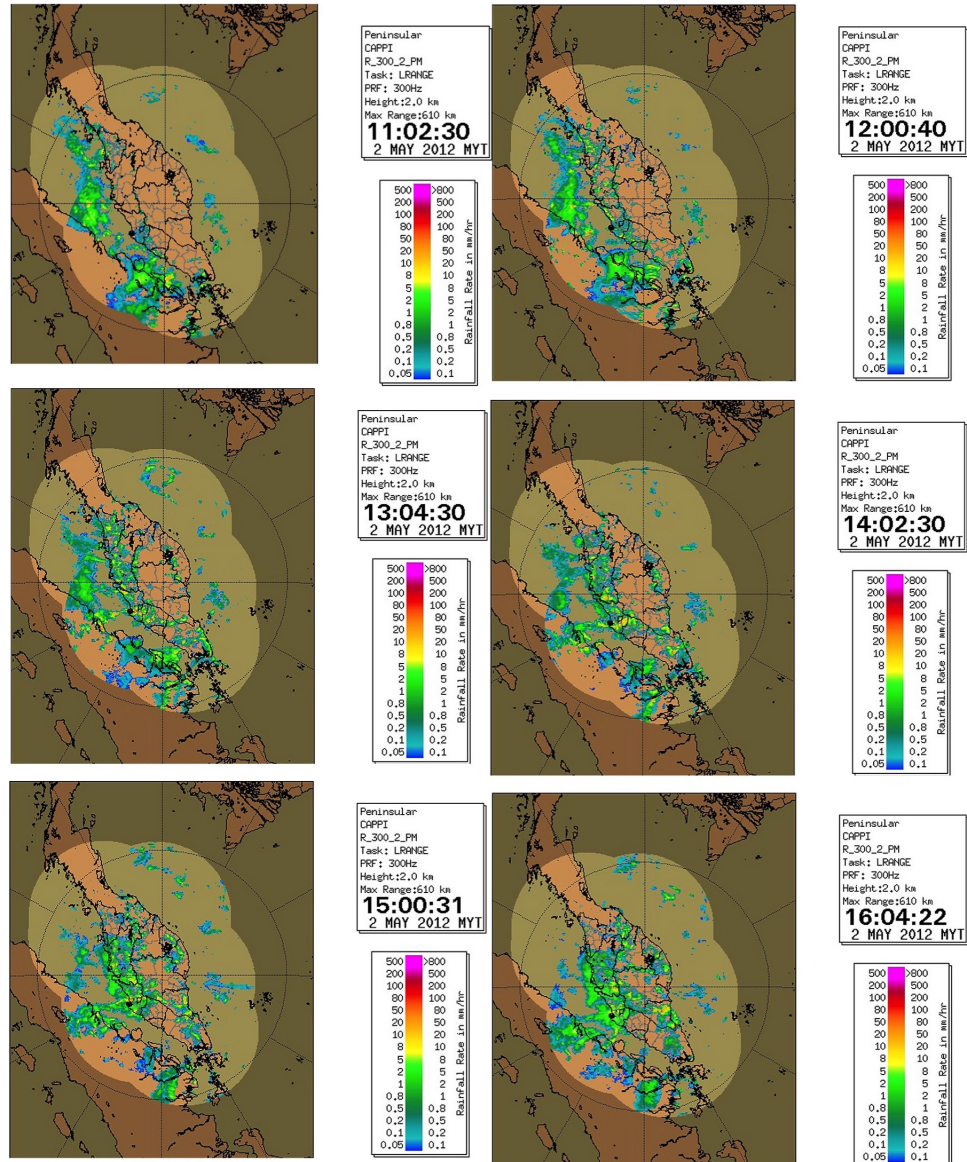


Figure 6.3: Radar images for the rainfall (in mm hr^{-1}) on 2 May 2012, from 1100-1600 LT. The images were retrieved from MetMalaysia. The radar images show the evolution of the rainfall from the Strait of Malacca to the western Peninsular Malaysia.

were also affected by the rainfall event later that day.

The mean low-level wind direction prior to the heavy rainfall was mostly northwesterly and westerly in the early night as shown in ERA-Interim's 850hPa winds plot in Figure 6.6. From this 6-hourly plot, it is clear that the winds over the region were mostly northwesterly and westerly. The mean direction of the wind was mostly northwesterly over the Strait of Malacca as it was deflected by Sumatra Island and Peninsular Malaysia. The mean wind direction is similar to the HR90 composite in Figure 5.7 (top) and most similar to the IL-AM composite. Westerly wind from the Indian Ocean changes to northwesterly over the Strait of Malacca area and then changes to westerly at the southern peninsula toward the South China Sea.

In this case study, the sounding of Sepang station (west coast station, listed

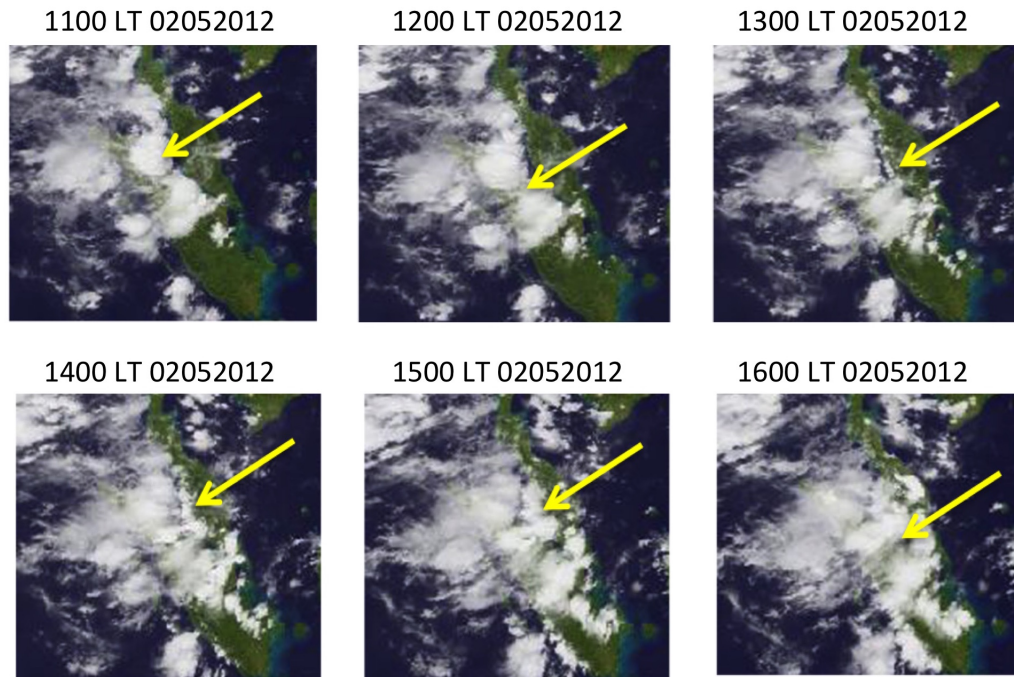


Figure 6.4: Himawari 7 (MTSAT-2) satellite images from Kochi University weather home website (infrared image IR1 (10.3-11.3 μm)), showing the evolution of the convective clouds on 2 May 2012, from 1100-1600 LT. The arrows show the location of the severe rainfall event. The landmass is coloured in green, the dark blue is the sea and the white is the clouds. Data available at <http://weather.is.kochi-u.ac.jp/archive-e.html>.

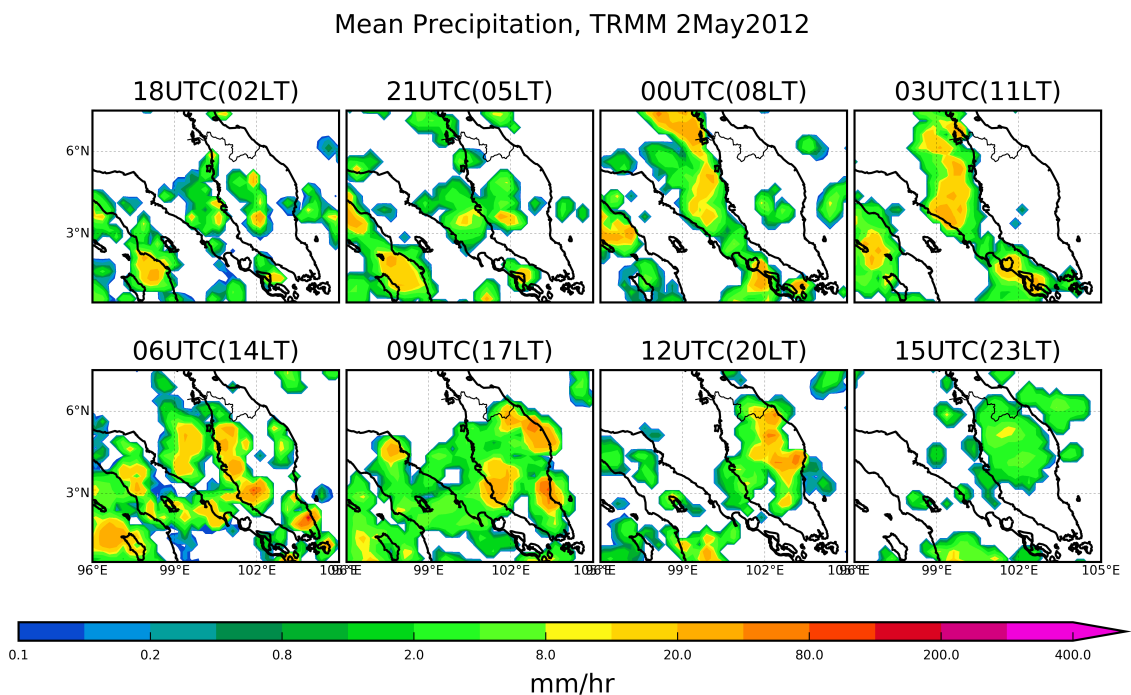


Figure 6.5: The 3-hourly precipitation from the TRMM dataset on 2 May 2012. The development of the whole event was observed from the event over the strait, 18 UTC (02 LT) and over the west coast later at 06 Z (14 LT) panel.

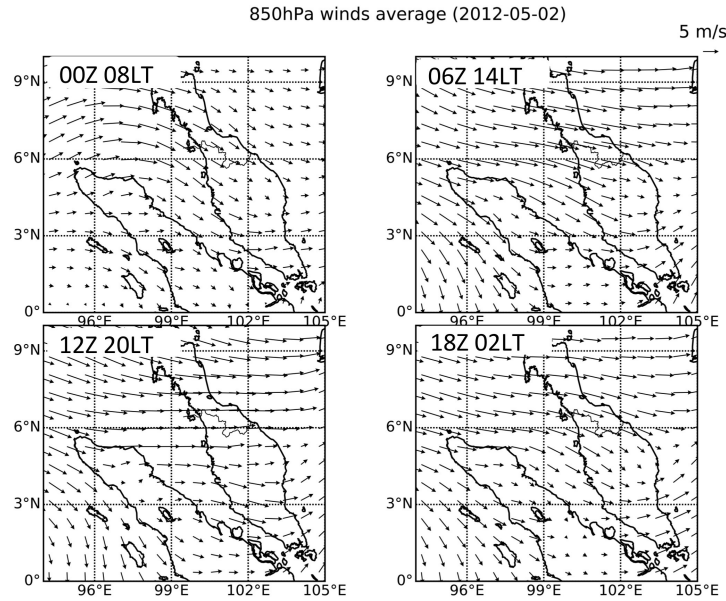


Figure 6.6: 850hPa winds 6-hourly, 2 May 2012 from ERA-Interim data. The wind over the larger area is mostly westerly. The winds over the Strait of Malacca is northwesterly as deflected by the orography of Sumatra and Peninsular Malaysia.

in Figure 3.2) was used and the CAPE shows a value of 1508 J kg^{-1} at 0000Z (or 0800 LT) 1 May 2012 signifying an unstable atmosphere, which is perfect for a storm to develop. The CIN value was weak with a reading of -39.7 J kg^{-1} and this is a morning value and after solar heating later in the day, the value may weaken to favours convection. These values are associated with the rainfall events on 1 May 2012. The CAPE value was 2361 J kg^{-1} later that night (1200Z/2000 LT 1 May 2012) with a weaker CIN value, -3.16 J kg^{-1} . Even though there were rainfall events throughout the afternoon, the CAPE values were still large and unstable with small CIN value by 2000 LT. On the morning of 2 May 2012, the CAPE value was 1786 J kg^{-1} (0000Z/0800 LT 2 May 2012), a large enough value to promote convection and the CIN value was -21.3 J kg^{-1} , which is a moderate value because it is still in the morning. After the event (1200Z/2000 LT 2 May 2012), the CAPE value has reduced significantly. The CAPE value was 318.4 J kg^{-1} with the CIN value was -124 J kg^{-1} which signifies stable conditions. Thus, on both days (1 and 2 May), the atmospheric condition was unstable in the morning (and night for the 1 May) and this favours the development of a severe rainfall event.

6.2. CASE STUDY 1: FIRST INTER-MONSOON (APRIL-MAY)

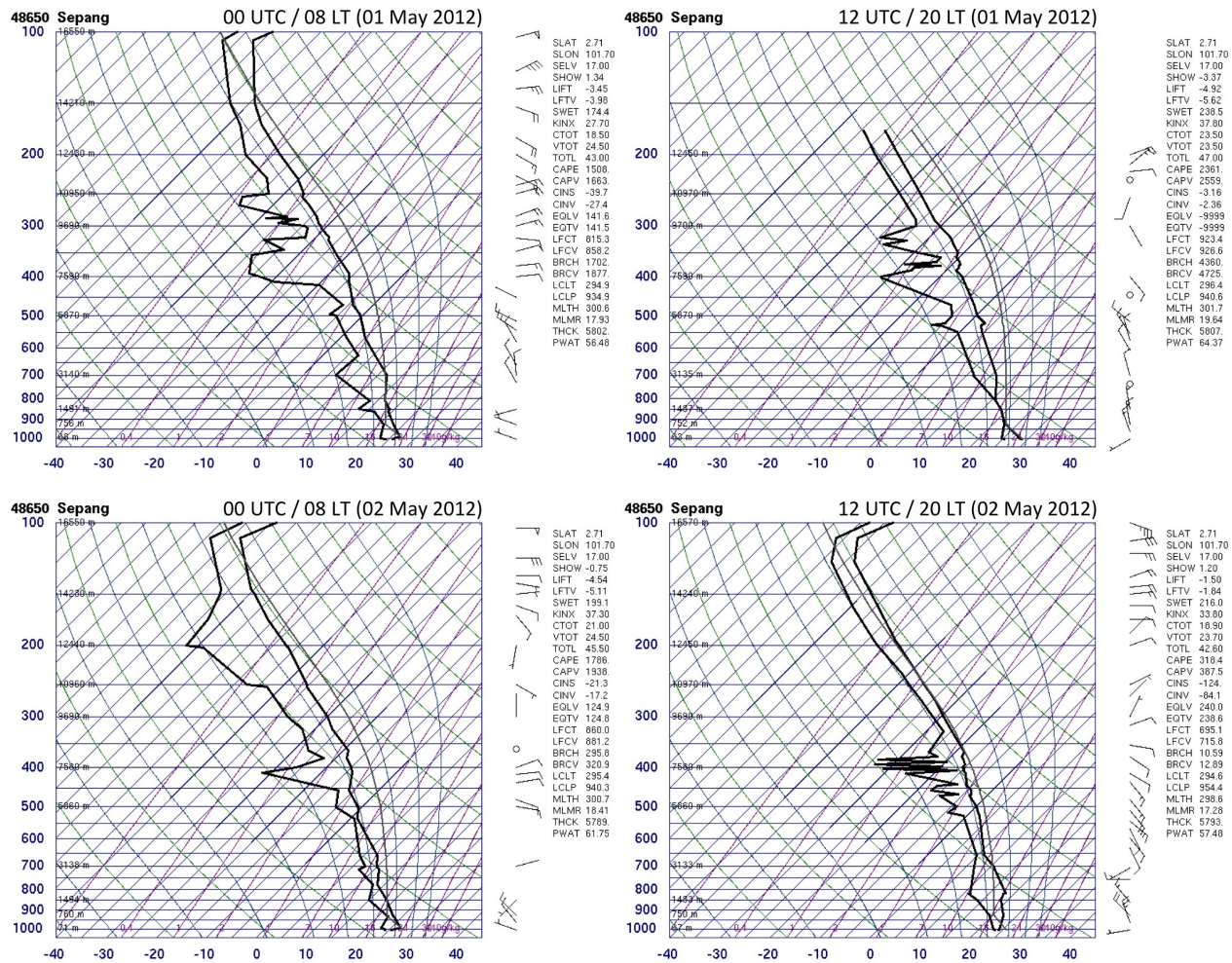


Figure 6.7: Skew-T diagrams from 1 May to 2 May 2012 showing an unstable atmosphere between 0800 LT and 2000 LT of 1 May 2012 and the morning of 2 May 2012 (0800 LT) as shown by the CAPE values. The unstable conditions were a sign of the thunderstorm events that occurred on 1 and 2 May 2012. The location of the station is shown in Figure 3.2. The sounding images from the University of Wyoming Atmospheric Sounding website in Figure 6.7 were used. The sounding time are 0800 and 2000 LT only (0000 and 1200 UTC).

6.2.2 Simulation : Control Run

The simulation of the event, as stated in Chapter 3, started from 0000UTC (0800LT) on 30 April 2012, 30 hours before the rainfall event started. The 12km model run as shown in Figure 6.8 overestimated the rainfall distribution over the region when compared to the radar images. The rain intensity was weaker than what is shown in the radar images, and the rainfall has spread more in the ocean region. It is believed that the parameterised convection scheme has contributed to the differences in spatial distribution of the rainfall in the 12km model run. The convection was parameterised at each 12 km grid box, increasing the tendencies for the model to produce a larger rainfall area although, in reality, the rainfall area could have been less than 12km in size. The output shows rainfall over the peninsula, as well as the north part of the strait, and the western and northern parts of Sumatra Island. Moreover, rainfall was also observed over the Andaman Sea and the South China Sea. Wind from the 12km model simulation is shown in Figure 6.10 (12km). The prevailing winds were westerly and the winds were mostly northwesterly over the Strait of Malacca regions. The same wind direction was also observed in the ERA-Interim plot (Fig 6.10 (ERA-Interim)).

The 1.5km model simulation result shows a better representation of the precipitation (Figure 6.9). The precipitation output was compared to the radar images retrieved from MetMalaysia. The radar images (in Figure 6.3) show the development of the convective precipitation over west Peninsular Malaysia from around 1300 LT, the start of the development into deep convection by 1400 LT and 1500 LT. The precipitation over the Strait of Malacca, which developed overnight, is believed to have helped to precondition the atmosphere to regenerate convection over the west coast Peninsular Malaysia after converging with the previously generated rainfall. This hypothesis will be further discussed in the next section. Observing the 850hPa winds in Figure 6.10 (1.5km), the prevailing wind was westerly in general and there were northwesterly winds over the Strait of Malacca region. The northwesterly winds turned into westerly winds over the southern peninsula. The wind patterns are remarkably affected by the orography of the Peninsular Malaysia and Sumatra Island. Since the 1.5km model represents the precipitation better, it will be used in the analysis from the next section onward.

A comparison between the radar images and the models (Figure 6.11) proves that the higher resolution with an explicit convective scheme (1.5km model) simulates more realistic results. The 1.5km model managed to reproduce most of the rainfall events as in the radar images, although imperfect. The main features such as the rainfall over the strait and along the Titiwangsa mountains are well represented. The main event of the rainfall over the radar shows the heaviest rainfall at about 3 °N and 101.5 °E at the time of the event. Meanwhile, the rainfall event in the 1.5 km model shows the heaviest at around 3.4 °N and 101.25 °E. The model also shows

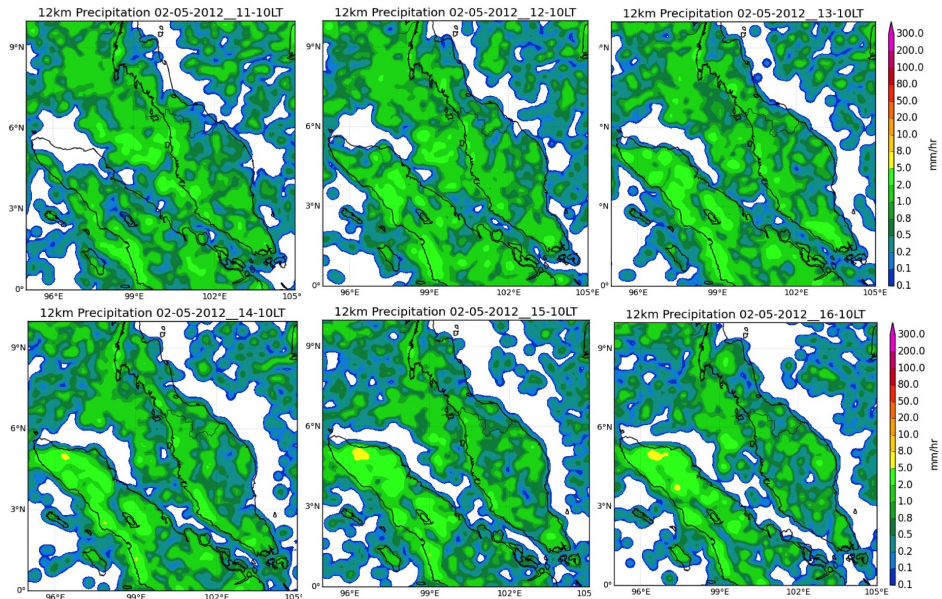


Figure 6.8: Simulated precipitation on 2 May 2012, from 1100-1600 LT, from 12km model UKMO-UM. The figure has been smoothed out to reduce noise using gaussian filter with $\sigma=1.0$.

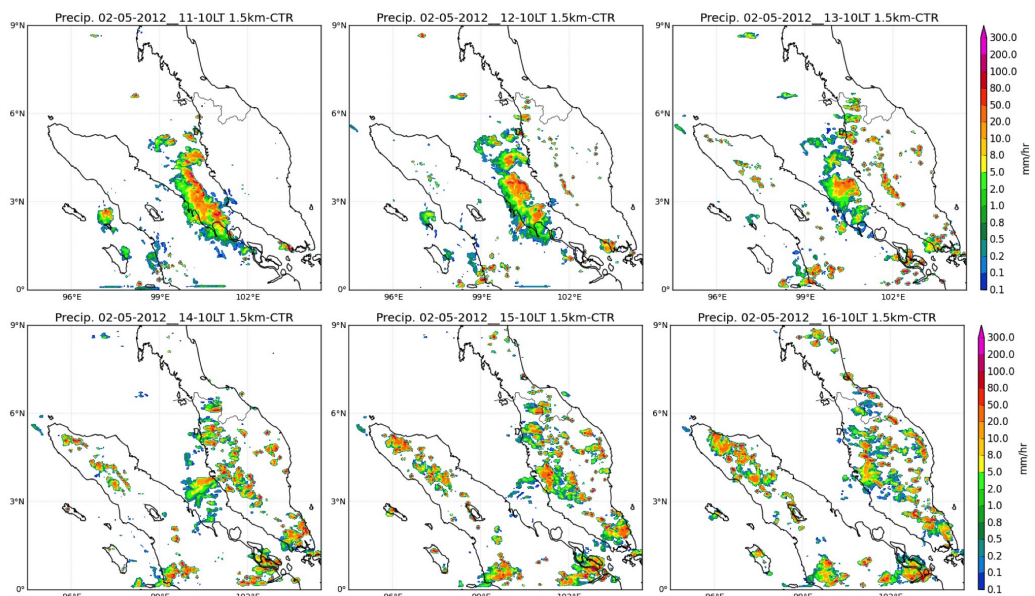


Figure 6.9: Simulated precipitation on 2 May 2012, from 1100-1600 LT, from 1.5km model UKMO-UM.

more variability in rainfall intensity over Peninsular Malaysia. The 12km model overestimates the spatial distribution of the precipitation and also underestimates the intensity. The dissimilarity between the results of the two models compared to the radar is believed to be associated with the resolution and the convection scheme differences, where the 12km model was using the parameterised convection scheme and the 1.5km model was using the explicit convection scheme. The combination of parameterisation scheme that is used in producing the rainfall over the model grid and poorly resolved orography in the 12km model may also play a role in the overestimation of the rainfall. Using convective parameterisation, for example, one

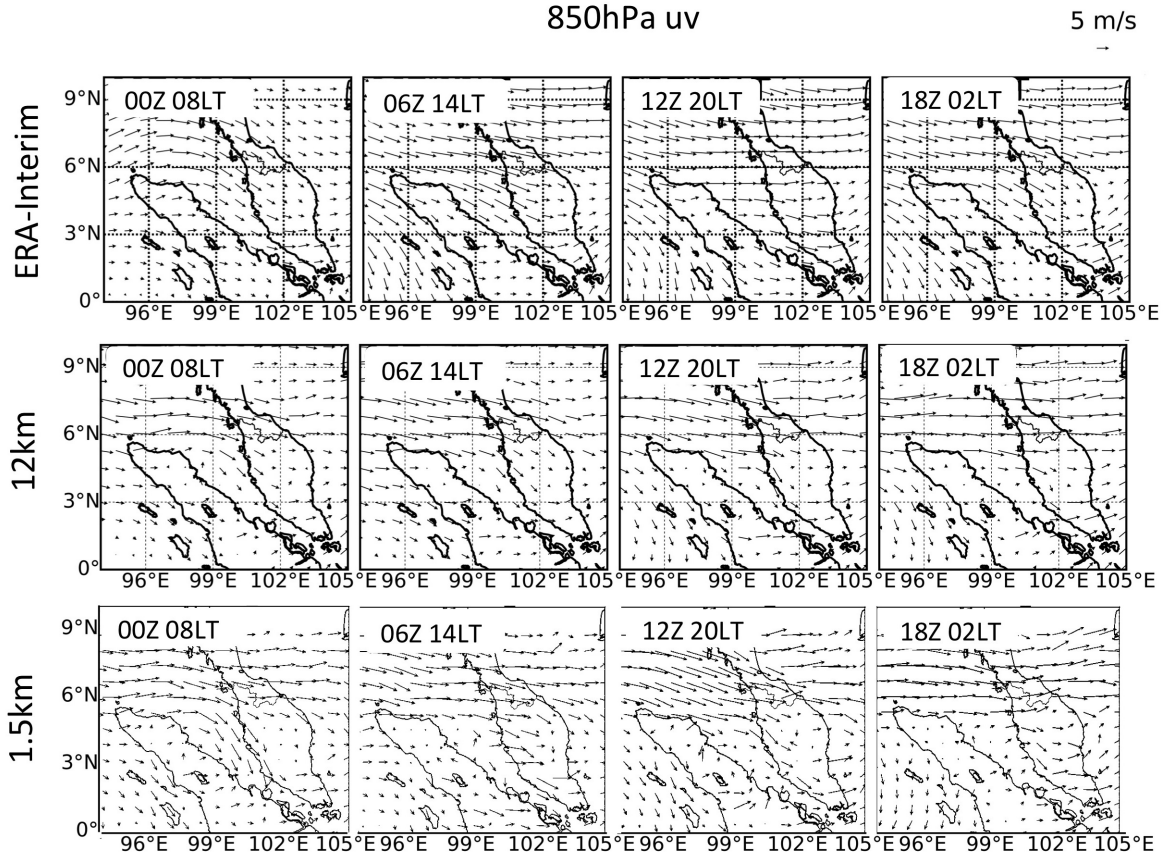


Figure 6.10: Six-hourly 850hPa winds on the 08 LT, 14 LT and 20 LT on 2 May 2012, and 02 LT on 3 May 2012, as in ERA-Interim, 12km model and 1.5km model. Generally, the wind directions are similar to the observation, except in the Strait of Malacca, where there is more disturbance in the model simulations than the ERA-Interim, due to resolution difference.

or more 12km grid box will produce at least light rainfall if there is enough instability. In addition to that, the small and individual convective rainfall events are being averaged out over the grid-scale and appear spatially larger.

A comparison between the observed and simulated 850 hPa wind (see Figure 6.10) shows that the 12km and 1.5km models managed to reproduce the wind patterns as in the ERA-Interim dataset. The wind direction, in general, was well simulated especially the deflected winds towards the Strait of Malacca from the north and then again at the southern peninsula to return to the westerly direction. There are a few details in the 12km and 1.5km models that are not found in the ERA-Interim plot. For example, the winds over the Strait of Malacca in the ERA-Interim data shows less low-level horizontal wind shear unlike in the model simulations (1.5km model). More divergence and rotation appeared in the model simulations than in the ERA-Interim dataset. The wind patterns over the centre and north of the peninsula in the model simulation are also different from the ERA-Interim data, due to the interaction with the orography. It is worth noting that the ERA-Interim is a reanalysis dataset, and comparison with observational data would be more accurate in examining the performance of these models. An example

is the observational dataset of wind speed and direction from the ground meteorological stations all over Peninsular Malaysia. The low-level winds over the ocean can also be compared to the observed surface level winds derived from microwave scatterometer satellite instruments such as ASCAT.

To compare the simulation with TRMM dataset, the 3 hourly mean precipitation was analysed and the results are shown in Figure 6.12. First of all, the TRMM dataset demonstrates a fairly good comparison with the radar images, although the temporal resolution is different (TRMM is the 3-hourly mean and the radar is an hourly instantaneous time plot). The TRMM shows the initial rainfall over the Strait of Malacca and later over the western peninsula. Comparing the TRMM and model simulations, the 12km model simulation underestimated the intensity of the rainfall but overestimated the spatial distribution especially over the ocean. The rainfall over the west coast was too early in the 12km model. The premature rainfall over land in the 12km model is a known problem related to the convective parameterisation, as mentioned in Love et al. (2011). The 1.5km model simulation produced a similar pattern to the TRMM, where the precipitation over the strait was simulated although not as spatially distributed as the TRMM, underestimating the spatial distribution of the precipitation over the ocean. The rainfall over the west coast fell at the same time according to both the TRMM and 1.5km model (see Figure 6.12 06 UTC (14 LT)) and the 1.5km model managed to simulate other events such as rainfall events in the southeast (14 LT) and rainfall events over most of the Peninsular Malaysia (17 LT). The similarities provide confidence in this study to proceed with the 1.5km model to investigate the mechanism of severe rainfall development.

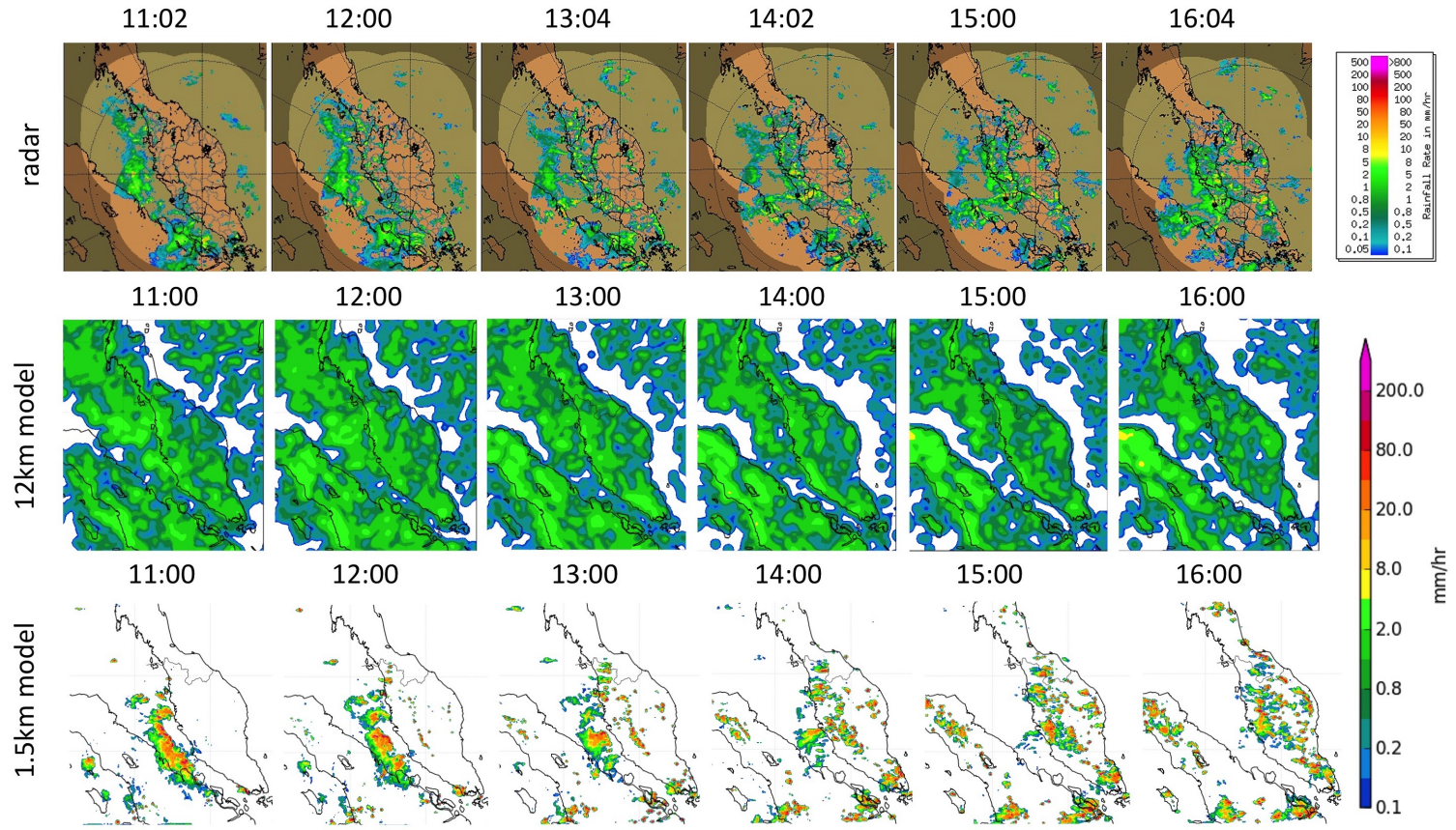


Figure 6.11: Precipitation from radar (top), 12km model (middle) and 1.5km model (bottom). Images from 1200 LT of 2 May 2012 until 1600 LT 2 May 2012. These times were selected to compare the development of the rainfall event on 2 May in the afternoon. All in mm hr^{-1} .

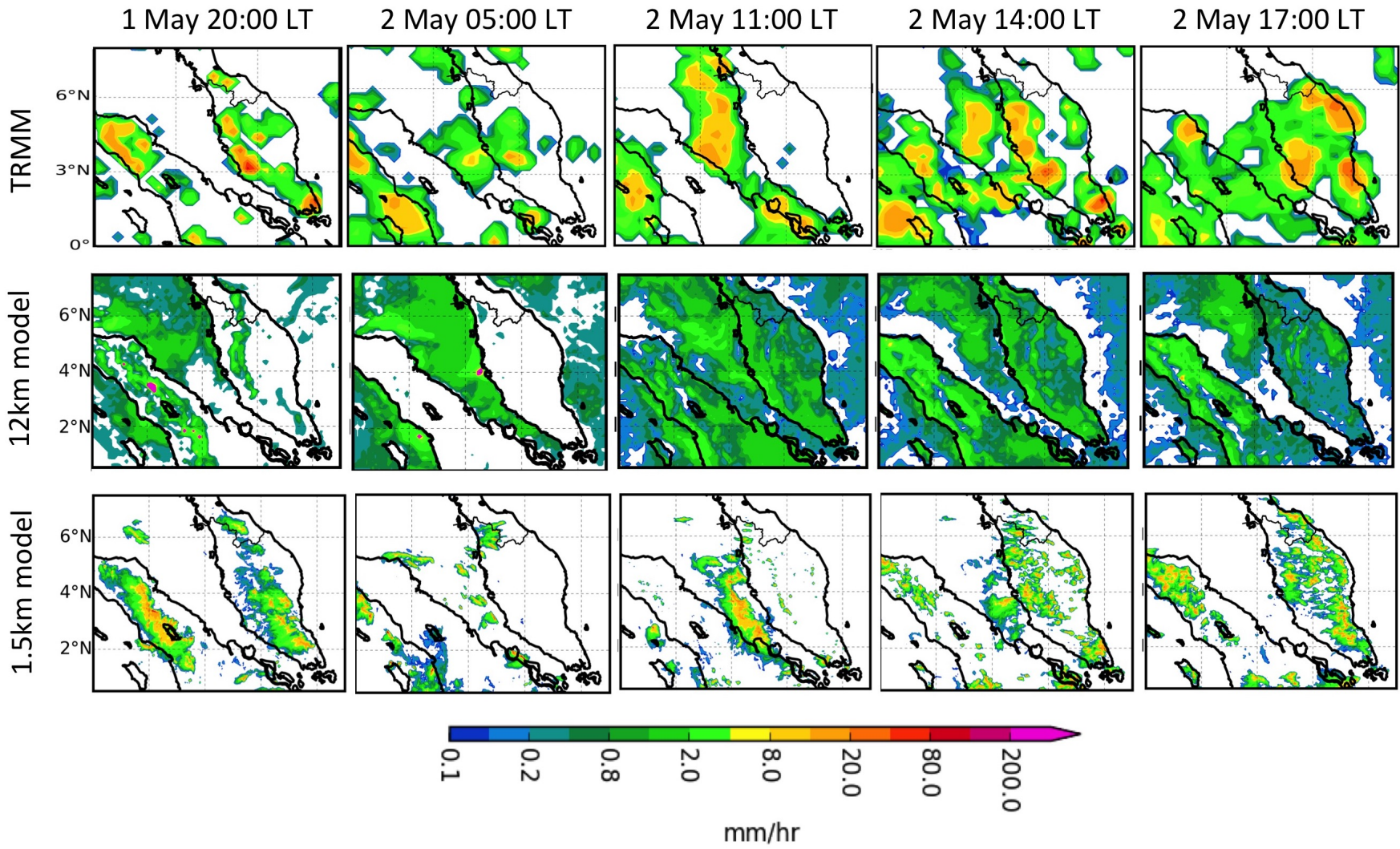


Figure 6.12: The 3-hourly precipitation images - comparison between TRMM (top), 12km model (middle) and 1.5km model (bottom). The 3-hourly mean (as calculated in TRMM) was compared to the same rainfall scale, in mm hr^{-1} .

The rainfall event in this simulation is concentrated over the west coast at around 3°N to 4°N and the evolution of the rainfall event can be viewed in the time-longitude hovmöller plot (Figure 6.14). The figure shows a clear diurnal cycle of precipitation over Sumatra Island and Peninsular Malaysia, and more prominent over the Sumatra Island. On the day of the event (red arrow on the left of the figure), the rainfall over the strait had started earlier, at around 0500 LT on 2 May 2012 and appeared to propagate eastward within 9 hours for about 100km (around 3 m s⁻¹)(labelled A, on the figure). It deteriorated before reaching the coast. The rainfall over the Titiwangsa Mountains (101.75°E, (labelled B)) started at around 1100 LT and appeared to propagate westward and eastward. A closer look at the hovmöller plot of rainfall indicates that the rainfall occurred over the Titiwangsa mountains for about an hour and beginning to move east before decayed and vanished after almost 30 mins. The rainfall also spread toward the west and remains longer and less intense. The westward rainfall combined with the rainfall event developed over the coast at around 1400 LT (labelled C) and remained over the west coast for a couple of hours. The eastward rainfall (which was generated from the Titiwangsa mountains) propagated and regenerated eastward due to the mean westerly winds (labelled D). This figure also shows the rainfall event that occurred on the previous day in both Sumatra Island and Peninsular Malaysia, could be one of the main factors contributing to the development of the severe event on 2 May 2012.

The wind circulation over the same 3°N to 4°N latitudinal mean was also analysed as in Figure 6.15 at 233 m model (hybrid) level. The wind vectors in the figure represent the wind direction and speed. An additional contour line represents the rainfall above 1 mm hr⁻¹, to observe the wind-precipitation relationship. The shaded area represents the zonal winds, which show a clear diurnal cycle over the Peninsular Malaysia and a slightly weaker diurnal cycle over Sumatra Island. In the morning before the event (red arrow on the left of the figure), the winds over the Strait of Malacca are mostly northwesterly (labelled A, in the figure). The westerly winds are stronger and penetrated across the peninsula during the event (labelled B). The northwesterly winds are stronger over the peninsula before the rainfall event, on both 1 and 2 May 2012 (labelled C). Although there are not enough days of analysis to draw a conclusion, stronger northwesterly winds could be one of the main factors in the development of the heavy rainfall over the peninsula. This is similar to the result in Chapter 5, where strong northwesterly over the Strait of Malacca region is associated with severe rainfall event over western Peninsular Malaysia. The winds converged near the coast of the peninsula before the event (labelled D). The convergence may be associated with the rainfall event but it was not necessarily the cause of the event. The same goes for the stronger westerly over the west coast before the event. The stronger winds may be a sign of stronger

convection over the peninsula before the event occurred.

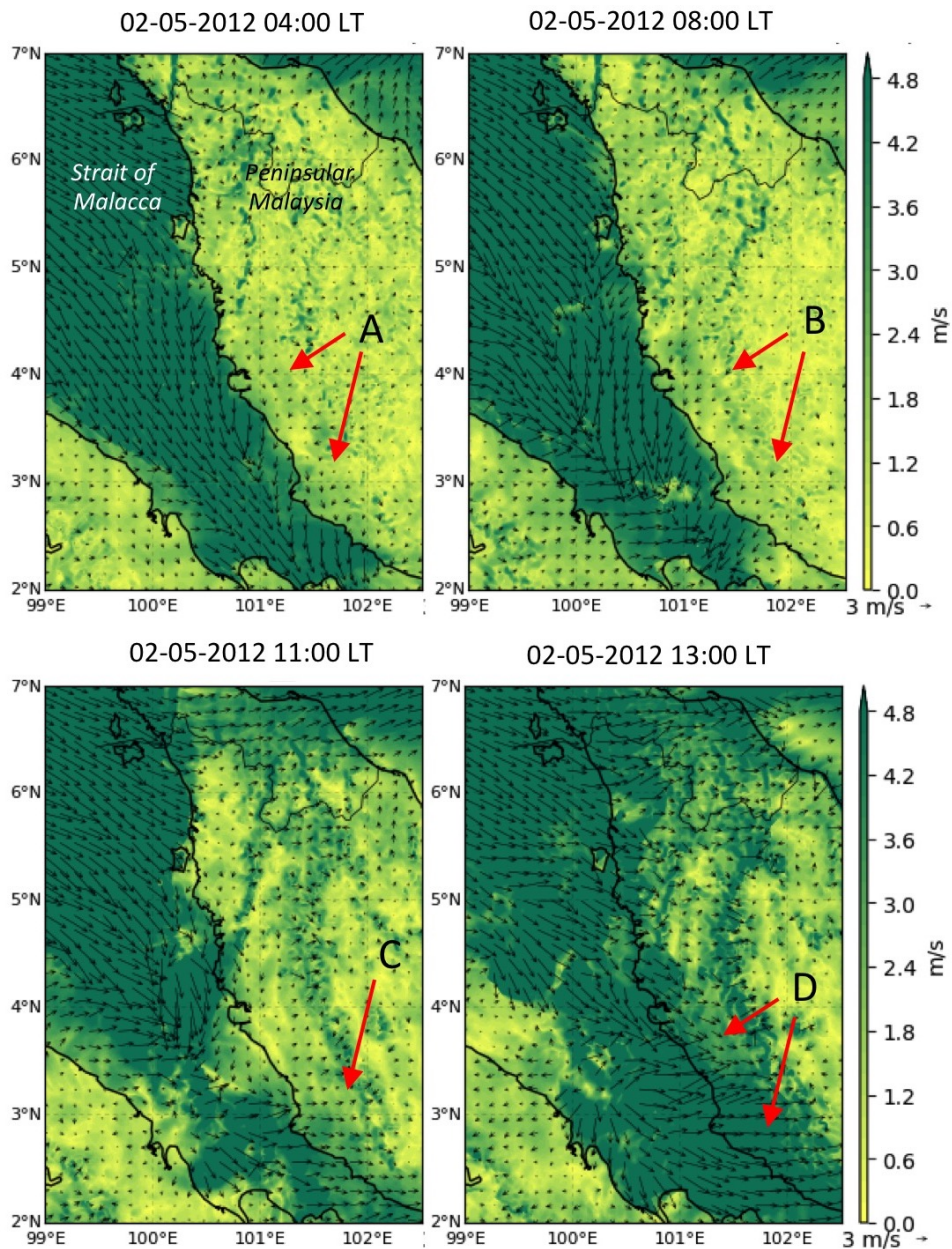


Figure 6.13: 10-meter wind vectors (in m s^{-1}) and wind speed (shaded, in m s^{-1}) from the 1.5 km model of the control run. The figures show the land breeze formed in the early morning of the event, at 04:00 LT (A), as well as in the morning at 08:00 LT (B). The sea breeze later formed in the late morning prior to the event (11:00 LT, C) and then stronger during as the rainfall event started at 13:00 LT (D).

The simulation was also able to show the changing of land and sea breeze as shown in a 10-meter wind plot in Figure 6.13. On the early morning of the event (2 May, 04:00 LT), a slower land breeze was observed in Figure 6.13 (A) but slightly weaker. The condition was also similar in the mid-morning at 08:00 LT (Figure 6.13 (B)). Prior to the event, the westerly wind over the western peninsula started to strengthen and this indicates a strengthening sea breeze over the region. When the rainfall event started, the westerly winds over the western peninsula strengthened as the prevailing northwesterly wind merged with the sea breeze. The

result indicates that the development of this event is associated with the strong northwesterly winds over the Strait of Malacca on that day.

The diurnal cycle of land-sea breeze is observed using the zonal wind component. Red shades represent westerly zonal winds and blue shades represent the easterly zonal wind. An apparent sea breeze is observed on both sides of the peninsula during the daytime. In the west coast of the peninsula, the sea breeze generally becomes stronger by 1200 LT, with the northwesterly winds condition, the sea breeze is enhanced and blew further inland. On the east coast, the sea breeze was seen to have initiated near the coast and gradually became stronger from off coast toward inland. Note that the sea breeze over the east coast on the day of the case study, was constrained (spatially, not blowing inland further) and it could be affected by the severe rainfall event over the western peninsula, especially stronger northeasterly winds coming from the Strait of Malacca and western peninsula. The land breeze in both west and east coasts were weaker except in the early morning of 3 May. The land and sea breezes over Sumatra Island are generally weaker than in Peninsular Malaysia.

To investigate the convective activities in this event, the wind convergence and divergence at a 13-metre height were analysed and this is shown in Figure 6.16. When atmospheric convection occurs, the air in the lower level atmosphere is transported toward the upper level of the atmosphere, and induce an air movement in the lower level to replace the transported air (converging air). Hence, convergence, as in wind convergence in a lower level is associated with an upward motion, thus, inferring convective activity where the convergence occurs. Moreover, converging air can also be a lifting mechanism as in when two air flows meet and forcing the merging air to be lifted upward. The figure shows the evolution of the convergence (negative, reds) and divergence (positive, blues) activities before, during and after the event. A strong convergence and some other divergence over the Strait of Malacca was observed at 1100 LT (labelled A, in the figure) and this is associated with converging winds and the rainfall event over the strait at that time. Weaker convergence activities are also visible over the Titiwangsa mountains (labelled B), which are also associated with the mountain breeze and rainfall activities over the mountainous region, as can be seen in the radar images (Figure 6.3). As the land reached its maximum heating, the convergence over the mountainous area of the peninsula had intensified (labelled C). The sea breeze became stronger and most of the convective activities started to occur near the coast at around 1300 LT (labelled D). The convergence near the coast (over the central Strait of Malacca) had weakened by 1300 LT and intensified convergence activity was observed over the coast (central west) at 1400 LT (labelled E). The convergence activity later deteriorated, by 1500 LT onwards. These results strongly suggest that the rainfall activity was not a moving system from the strait to the land, but rather an interaction

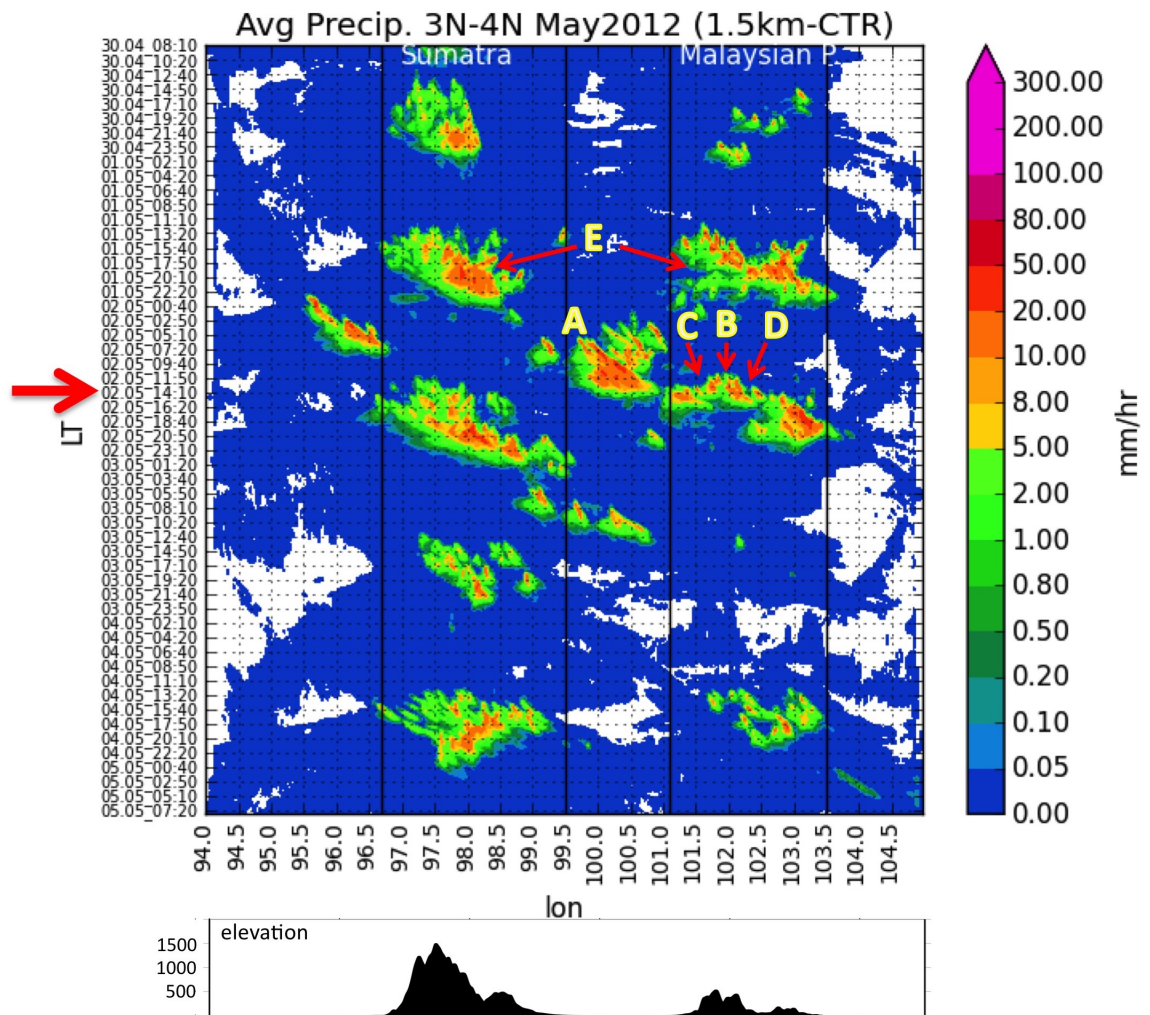


Figure 6.14: Time-longitude hovmöller plot of precipitation from 1.5km model, averaged over $3^{\circ}N$ to $4^{\circ}N$. The red arrow shows the time of the event. The lines $96.7^{\circ}E$ and $99.5^{\circ}E$ represent the west and east coastlines of Sumatra Island, respectively. The lines $101.1^{\circ}E$ and $103.5^{\circ}E$ represent the west and east coastlines of the Peninsular Malaysia, respectively.

between the mountain-induced convection, the sea breeze, the mountain breeze and the mean northwesterly winds.

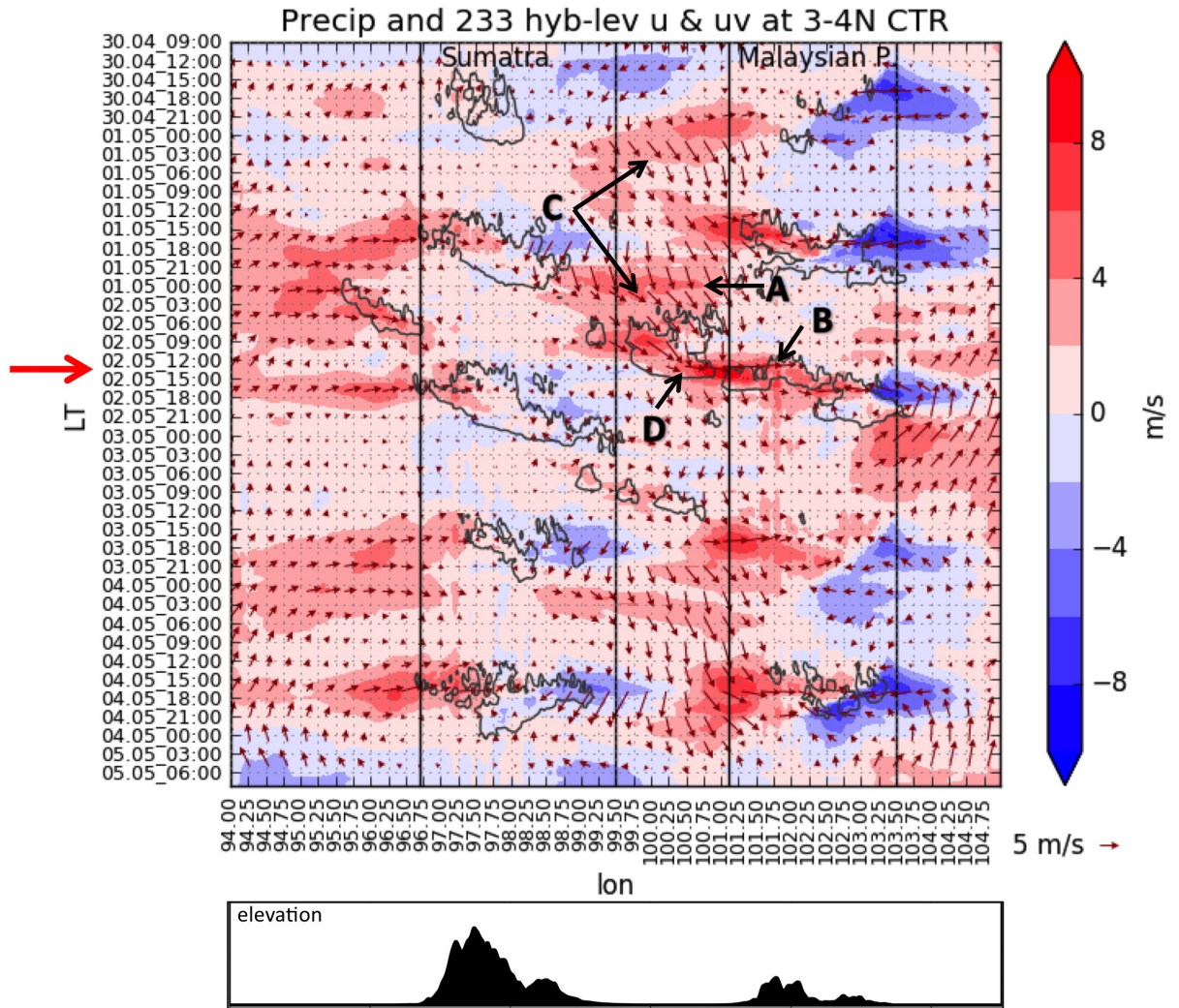


Figure 6.15: Time-longitude hovmöller plot of zonal wind (shaded) and wind direction and magnitude (vectors) from the 1.5km model, averaged over 3°N to 4°N. The red arrow shows the time of the event. The lines 96.7°E and 99.5°E represent the west and east coastlines of Sumatra Island respectively. The lines 101.1°E and 103.5°E represent the west and east coastlines of the Peninsular Malaysia, respectively. The land was also averaged over 3°N to 4°N. The red colour represents westerly, and the blue represents easterly zonal winds. Wind vectors show the direction and strength of the winds. The dark contour represents rainfall with the amount above 1 mm hr⁻¹, for additional reference on winds and precipitation relationship.

6.2. CASE STUDY 1: FIRST INTER-MONSOON (APRIL-MAY)

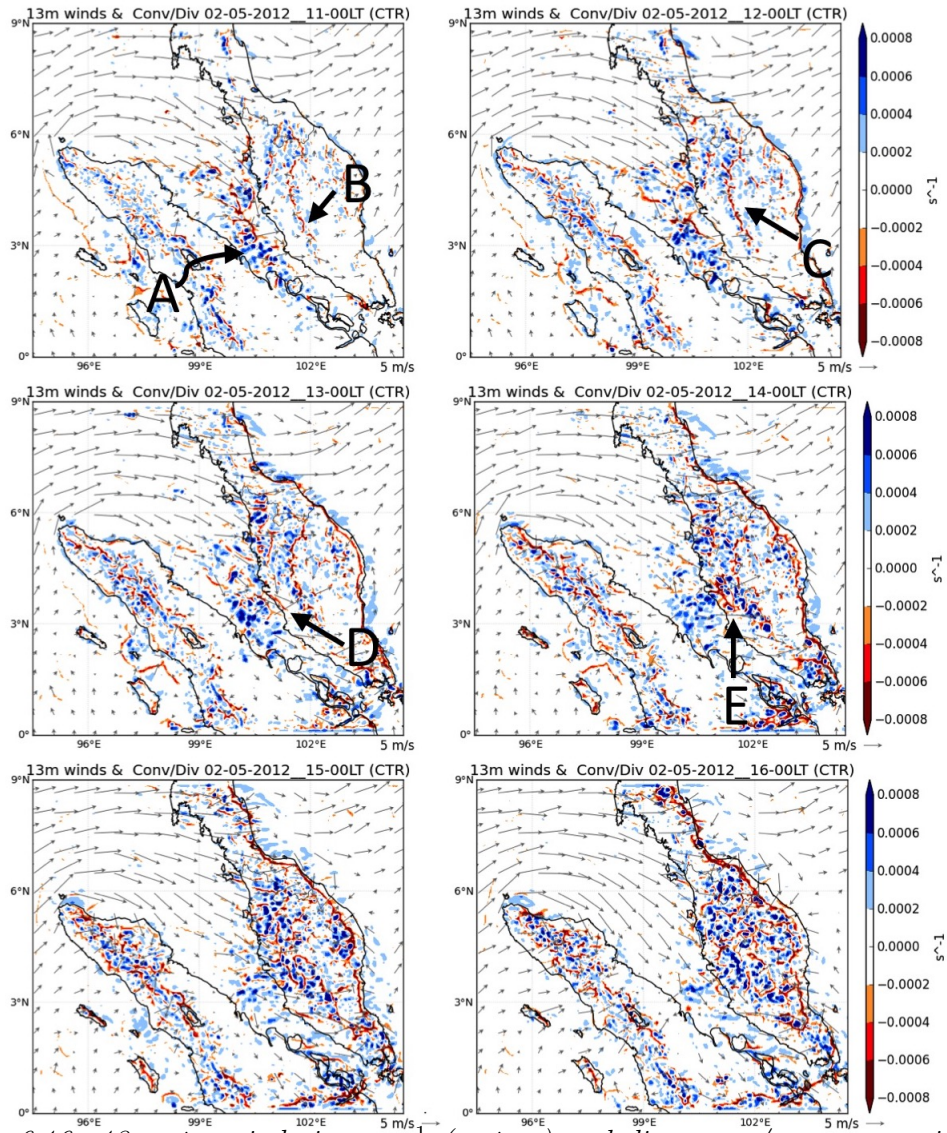


Figure 6.16: 13 metre winds in $m s^{-1}$ (vectors) and divergence/convergence in s^{-1} at 13 metre level (shaded), from the 1.5km model simulation. Blue represents divergence (descending movement) and red represents convergence (ascending movement) of air. The photos show the convergence/divergence before, during and at the end of the rainfall events.

6.2.3 Possible Mechanism

The event is considered well simulated by the 1.5km model and therefore it can be used for detailed study of the rainfall event development. The rainfall development can be viewed in Figure 6.17 based on the radar and 1.5km model simulation. The exact place of the rainfall area is not accurate, but some of the key features of the rainfall event development are considered properly represented. The key features mentioned are the rainfall over the Strait of Malacca and the mountainous region in the peninsula as well as the stationary rainfall over the west coast. The arrows in the 1200 and 1400 LT Figure 6.17 show the similar characteristic in between radar and the 1.5km model. Rainfall over the strait and rainfall over the Titiwangsa mountains are visible in both radar and 1.5km model as pointed by the arrows in figure 1200 LT. The spreading rainfall over the west coast and near the coast is pointed out in figure 1400 LT. There is also a rainfall along the east coast in the 1.5km model plot. The rainfall is developed as in 1400 LT figure. The intensification of the rainfall along the east coast is visible by 1600 LT. The easterly sea breeze, along with the mean westerly winds over from the Strait of Malacca has enhanced the rainfall. The convergence of sea breeze along the east coast can also be seen in the previous figure, Figure 6.16. This result is concurrent with the previous studies on the important role of local orography in the development of rainfall events in this region (Qian, 2008; Fujita et al., 2010). Sumatra Island plays an important role in the nocturnal precipitation over the Strait of Malacca where the cold flows from both the peninsular and Sumatra enhance convection over the strait (Fujita et al., 2010). Orography plays an important role in the rainfall activity over tropical landmass and the orography enhances convection by enhancing sea breezes and mountain-valley breezes (Qian, 2008). Information from these studies will be useful to investigate this event.

For further investigation of this case study, the rainfall event in the late afternoon of 1 May 2012 over both Peninsular Malaysia and Sumatra Island is believed to induced the convection and rainfall activities over the Strait of Malacca overnight. This is also mentioned in Fujita et al. (2010) in their study in relation to morning precipitation over Strait of Malacca. Cold flow (a density current mechanism) coming from both Sumatra and Peninsular Malaysia around midnight due to the afternoon rainfall on the previous day often converge over the Strait of Malacca and create a new convection over the strait to produce rain. To test this in our case, we are looking at the dew point temperature to determine if there is moisture change or transport from both land masses toward the Strait of Malacca. Figure 6.18(a) shows the movement of the cold flow from the temperature anomaly plot (blue shades) as pointed out by the arrows. Both cold flow from Sumatra and peninsula moving toward Strait of Malacca beginning around 2300 LT. The cold flow merged in the central Strait of Malacca to assist the development of convection.

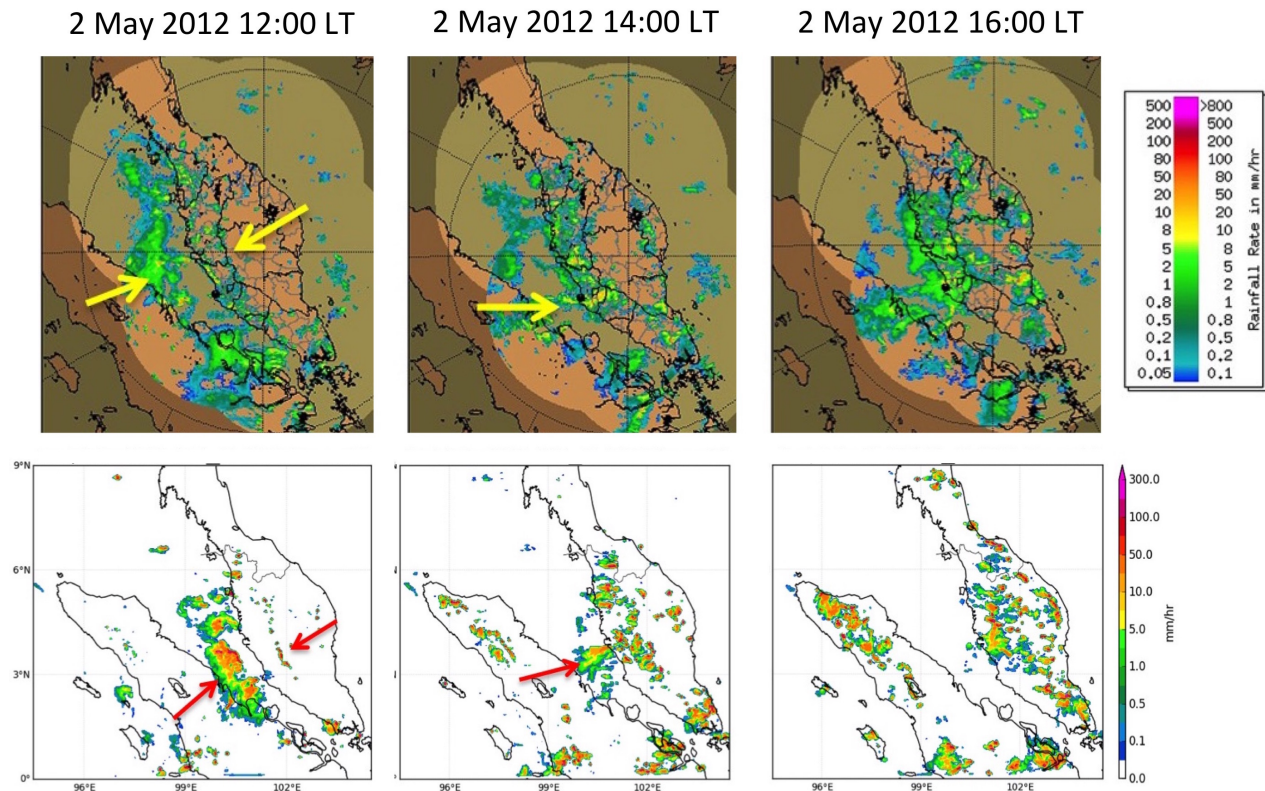


Figure 6.17: Precipitation as represented in the radar (top) and 1.5km model (below). Key features are shown by the arrows. The first image shows the rainfall over the strait. The Titiwangsa Mountains may have combined with (or influenced) the development of rainfall over the west coast of the peninsula later that day (arrow in the second figure). The model managed to replicate this development as in the radar.

The moisture from previous rainfall could have been transported toward the strait and to show the moisture movement from Sumatra and peninsula toward Strait of Malacca, dew point temperature was used as shown in Figure 6.18(b). The higher the dew point temperature, the higher the moisture of the atmosphere at the area. Based on the red shades representing a moist air, the moist air is still concentrated near the coast of Sumatra and peninsula at 2200 LT of 1 May (red arrows). By 2300 LT, the moist air had moved toward the strait (red arrows) and eventually merged by 0100 LT (2 May) and filling the strait atmosphere. The dew point temperature became higher over time (not shown) and thus the air moisture over the strait. Hence, these conditions favour the development of convective rainfall.

This mechanism is also shown in Figure 6.19. Rainfall from an afternoon of 1 May (A and B, 1900 LT 1 May) may have provided extra water on land, saturating the land especially over the west coast of the peninsula. The rainfall events in both Sumatra Island and Peninsular Malaysia may have influenced the development of the rainfall over the Strait of Malacca and the rainfall activity intensified after sunrise (C, 1000 LT 2 May). The incoming northwesterly winds from the Indian Ocean and the Andaman Sea may also have enhanced the convective activity over the strait. In the early afternoon (1300 LT), convective activity was also observed

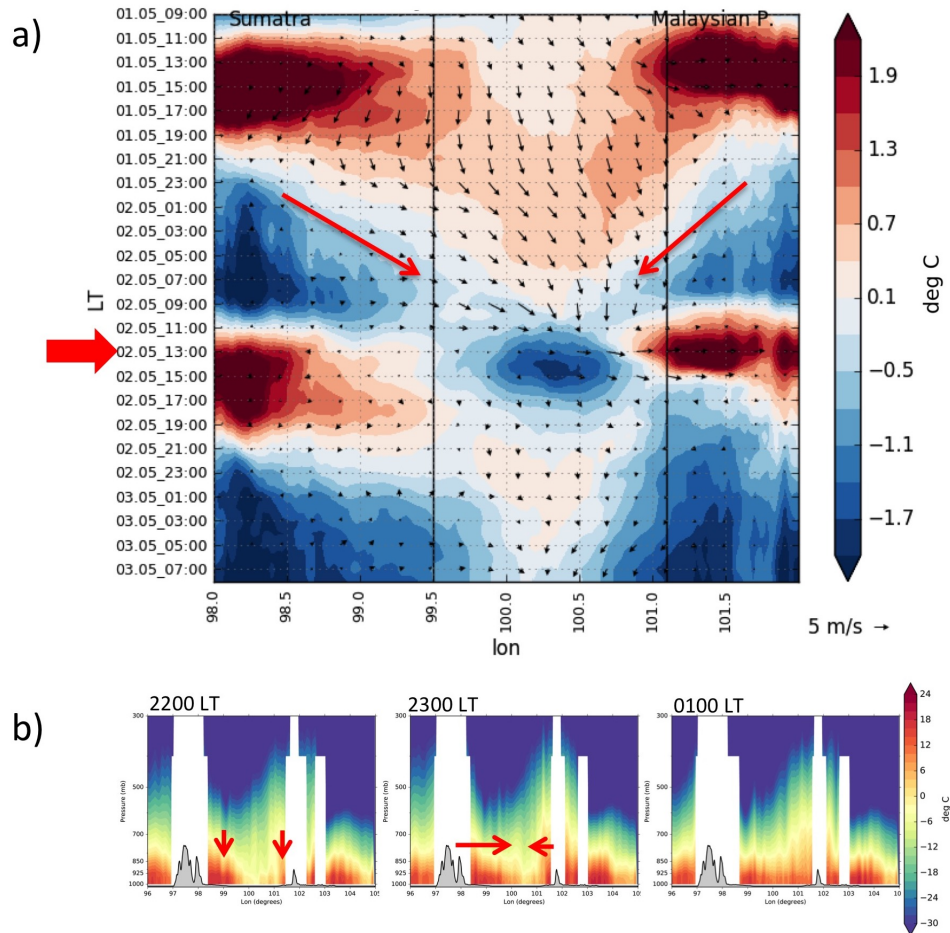


Figure 6.18: (a) Time-longitude hovmöller plot of near-surface air temperature anomaly (shaded) and near-surface winds (vectors) averaged over $3^{\circ}N$ to $4^{\circ}N$ from the 1.5km model. The red arrows show the cold flow moving toward the centre of Strait of Malacca. This cold flow is a result of the previous day (1 May) late afternoon rainfall. (b) cross-section plots (at $3.5^{\circ}N$, from 1.5km model) of the late night of (1 May) showing the dew point temperature (used here as a measure of moisture in the atmosphere) showing the high dew point temperature moving from the land toward the Strait of Malacca depicting the movement of moisture toward the Strait of Malacca. Higher dew point temperature means higher moisture amount in the atmosphere.

over the Titiwangsa Mountains of the Peninsular Malaysia (1300 LT 2 May). Over time, these two rainfall events influenced the development of convection over western Peninsular Malaysia, especially over the central west region (D, 1600 LT 2 May). Based on this observation, it can be hypothesised that the local orography and Sumatra Island played an important role in the development of the rainfall event on 2 May 2012. To investigate how the local orography and Sumatra Island affected the rainfall development in this event, sensitivity experiments were done and these will be discussed in the next section.

While it is hard to clearly look at the influence of the winds on the development of the event in this figure (Figure 6.19), rainfall events do affect the wind circulation over the region. The 850 hPa wind as simulated by the 1.5km model shows a westerly wind in general, with a northwesterly over the Strait of Malacca as a result of its interaction with Sumatra and Peninsular Malaysia. The west-

erly winds from the Indian Ocean were deflected towards the Strait of Malacca by Sumatra Island and the Titiwangsa mountains over Peninsular Malaysia kept the wind northwesterly until it turned to westerly again at the southern Peninsular Malaysia, where the Titiwangsa Mountains range ends. The winds over the west coast of Peninsular Malaysia remained northeasterly all day despite the convective activities over the straits and the west coast later that afternoon. The northwesterly winds may also have influenced the convection to move or re-develop eastward.

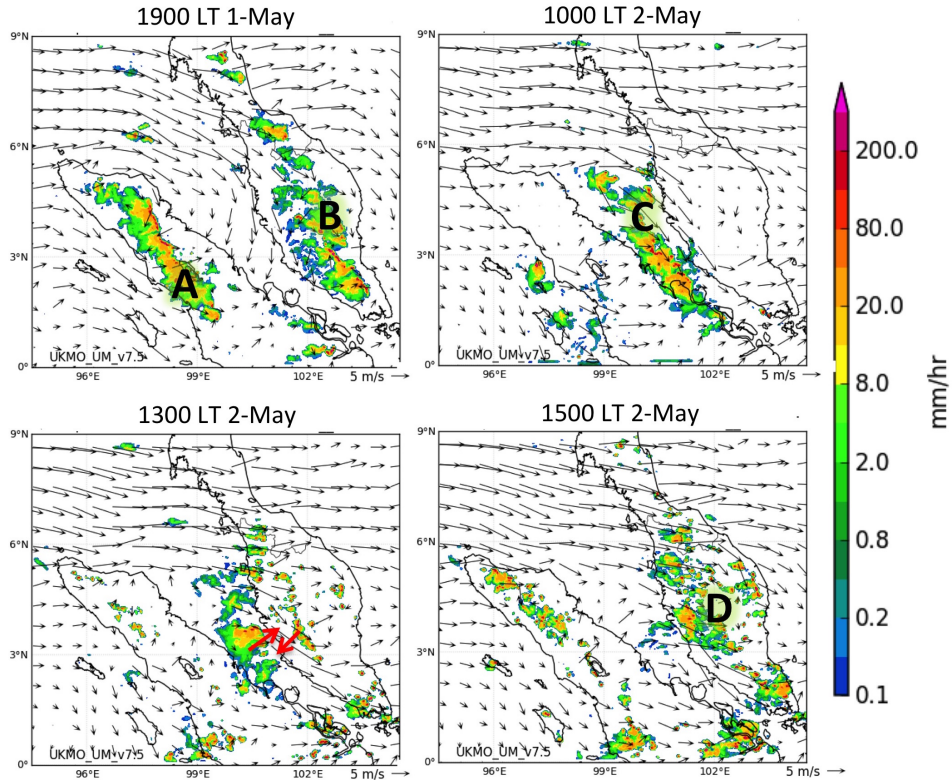


Figure 6.19: Precipitation and 850hPa winds from the 1.5km model showing the possible mechanism for this event. Rainfall from afternoon of 1 May (A and B, 1900 LT 1 May) provided extra moisture to the region to produce convective rainfall over the Strait of Malacca overnight (C, 1000 LT 2 May) and later the convection over the strait combined with rainfall in the mountain region over the peninsula (1300 LT 2 May) produced the rainfall events over the west coast (D, 1600 LT 2 May).

The zonal wind cross-section is shown in Figure 6.20. This shows how the orography modified the convection system by examining the zonal wind. Strong convection is seen at around 100°E at 1000 LT 2 May and is seen to move eastward by 1100 LT 2 May. This is probably due to the northwesterly winds as well as the developing sea breeze. The northwesterly wind influences the convective system to move eastward toward the western coast of Peninsular Malaysia. The sea breeze that is developing over the area could have caused the convective system to dissipate before reaching the land. The strengthening of sea breeze circulation at this point means the strengthening of the downward movement of air over the strait (as part of the sea breeze circulation) and suppressing the convective activity over the strait. Thus, the further development of the convective clouds and rainfall

was halted. The land heating favours more convection to occur on the peninsula, causing a lower atmospheric pressure near the surface. The low surface pressure favours low-level convergence. The surface air pressure over the Strait of Malacca is relatively higher by then, and higher surface pressure favours low-level divergence, thus halting convection to continue over the strait. By 1200 LT 2 May, due to insolation, the land heated up faster especially inland where the Titiwangsa Mountains range is, and convection appeared over the orography (before 102°E). At 1300 LT, the convection over both Titiwangsa and the Strait of Malacca had intensified. Due to the combination of sea breeze and convective activity over the Titiwangsa mountains, the westerly zonal wind over the west coast became stronger (1400 LT). The stronger westerly zonal wind here is also an indication of stronger convective activity over the west coast. This is because convection leads to stronger low-level convergence and upper-level divergence and this increases the low-level winds toward the convective region, thus the low-level westerlies that are coming toward the coast become stronger. While the orography enhances both convection and sea breeze circulation, this figure also shows how the orography stalled the westerly zonal wind from penetrating across the peninsula, at least during the early afternoon. Sea breezes over the east coast had developed by 1100 LT and got stronger by 1200 and 1300 LT. By 1400 LT, stronger westerly moving eastward and disturbed the easterly sea breeze. This could also be the main reason for the development of east coast rainfall associated with sea breeze as seen and discussed in Figure 6.17.

To compare the mechanisms suggested by the previous studies, more analysis is needed. Not all of the mechanisms were observed in this case study because of some of the mechanisms, such as the gap wind interaction with the convection system, require a model sensitivity experiment, which is not the main objective of this thesis. The interaction between mountain breezes and sea breezes was indirectly manifested by the convective activity (thus rainfall activity) and zonal winds as discussed earlier. Solar insolation influences the development of convection over the Titiwangsa mountains, thus enhancing the sea and mountain breezes.

Based on the discussion above, the mechanism involved in this severe rainfall event development can be represented in Figure 6.21. In Figure 6.21(a), Sumatra Island and Peninsular Malaysia experienced heavy rainfall in the late afternoon of 1 May 2012. By midnight (Figure 6.21(b)), the cold flow from both Sumatra and peninsula, together with land breeze had merged over the Strait of Malacca and triggers convection. Furthermore, the northwesterly wind over the strait enhanced the convection. By the morning of 2 May 2012, rainfall occurred over the Strait of Malacca (Figure 6.21(c)). By midday (Figure 6.21(d)), convective rainfall occurred over the peninsula due to solar radiation (while the rainfall over the strait is still occurring). Both rainfall systems produced cold pool that will be merged by the coastal region of the west coast and enhanced by the sea breeze that is already

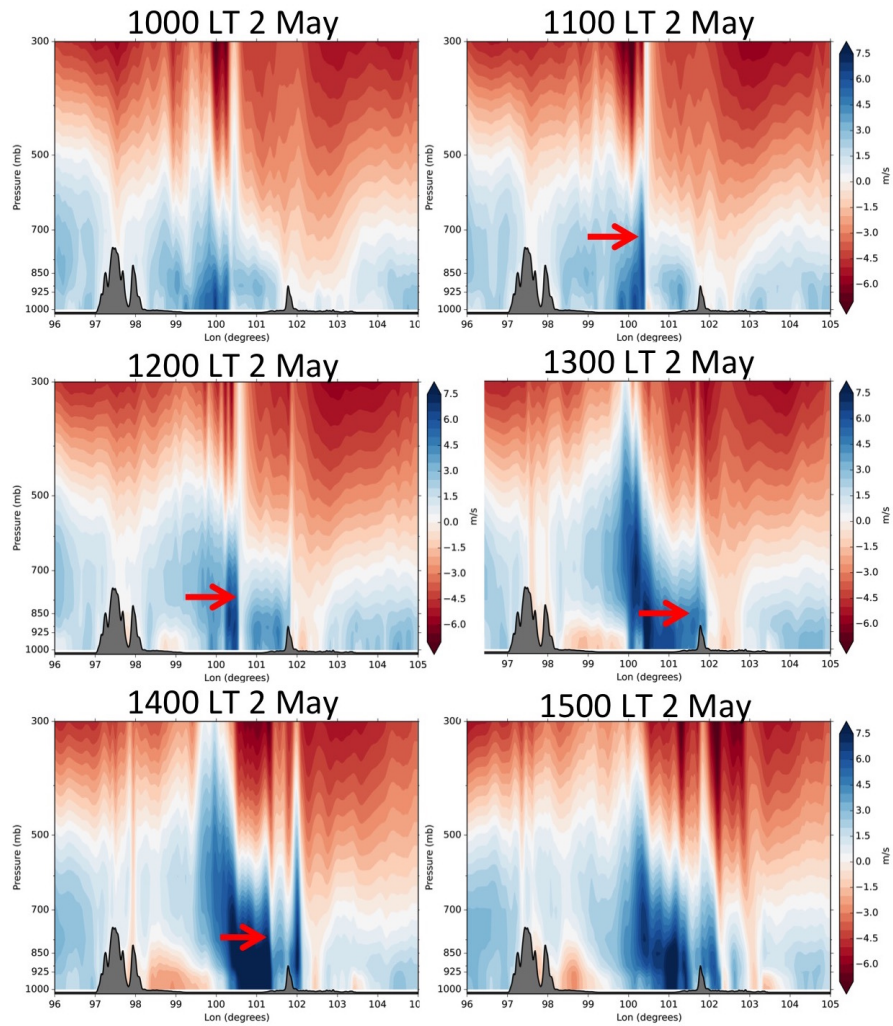


Figure 6.20: Zonal winds from the control run representing the zonal flow at 3.5°N cross section from 1000 LT 2 May until 1500 LT 2 May. The arrows show the evolution of the winds in the development of the rainfall event, from the precipitation over the strait (1100 LT), strengthening westerly as it merged with the large-scale northwesterly winds (1200 LT) and with the sea breezes (1300 LT). Then the westerly is blocked by the Titiwangsa Mountains (1400 LT), causing the pre-existing convective activities to remain on the west coast of the peninsula.

occurring. The northwesterly winds over the region enhance the development of convective clouds over the west coast of the peninsula. Over time, the convective clouds matured and produced rainfall over the west coast of the peninsula. Additionally to that, the inland rainfall is still occurring, and the merging of both rainfall systems produced a spatially large rainfall area.

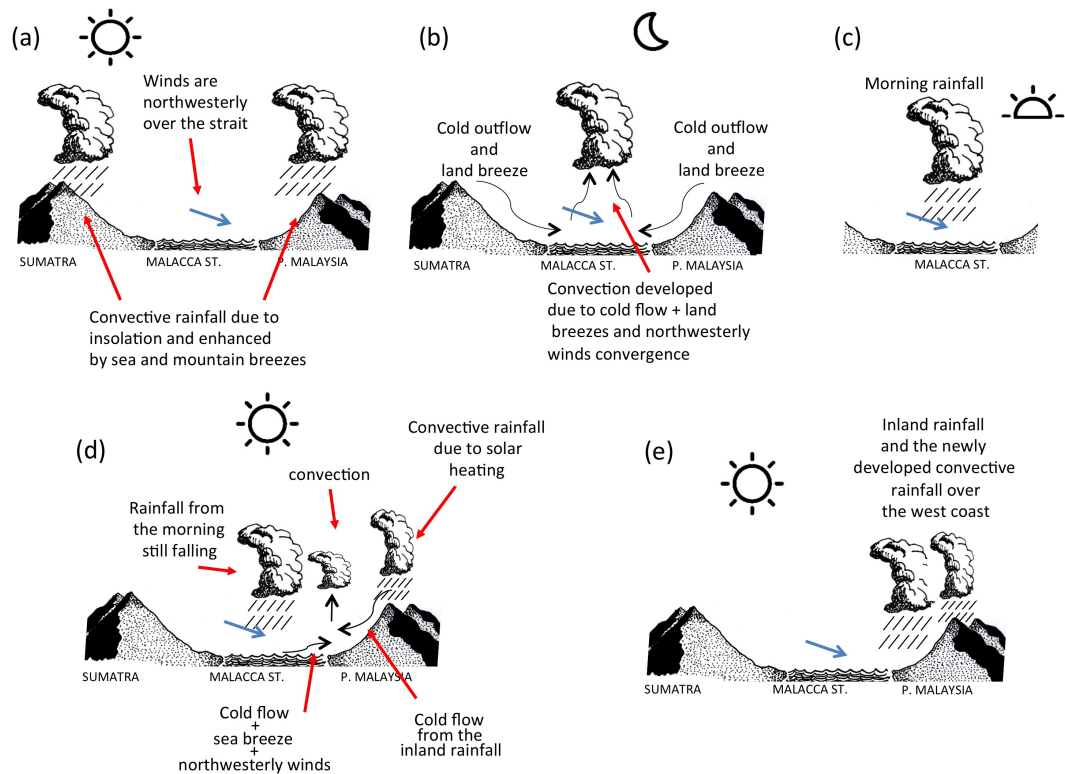


Figure 6.21: The figures show the mechanism involved in the development of the severe rainfall event over the west coast Peninsular Malaysia on the 2 May 2012. (a) In the late afternoon of 1 May 2012, Sumatra Island and Peninsular Malaysia experienced heavy rainfall. (b) By midnight, the cold flow, land breeze and northwesterly wind over the strait assist convection over the strait. (c) midnight convection produced convective rainfall over the strait in the morning of 2 May 2012. (d) By noon, convective rainfall occurred inland of the peninsula due to solar radiation, and cold pool from the inland rainfall, rainfall over Strait of Malacca, sea breeze and northwesterly wind helps convection to develop over the west coast of the peninsula. (d) The convection over the western peninsula develops to produce rainfall and combined with inland rainfall to produce spatially large area of rainfall. Figures are illustrated by author.

6.2.4 The Role of Local Orography and Sumatra Island

The local orography and Sumatra Island are believed to have played a major role in this event. The topography features over these regions have proved to have an impact on the weather activities here, as stated by Qian (2008) and Fujita et al. (2010). The orography of an island induces convective activity, which is common in tropical islands (Qian, 2008). The rainfall activity over the Strait of Malacca is commonly associated with the cold flows from Sumatra and the Peninsular Malaysia (Fujita et al., 2010). Thus, for this study, a few sensitivity experiments were done to investigate the attribution of local orography and Sumatra to a severe weather event. Four sensitivity experiments were undertaken to investigate the role of local orography and Sumatra Island:

1. Experiment 1: Flat Peninsular Malaysia orography (**flatPM**)
2. Experiment 2: Flat Sumatra orography (**flatSI**)
3. Experiment 3: Flat Peninsular Malaysia and Sumatra orography (**flatALL**)
4. Experiment 4: No Sumatra (**noSI**)

Exp. 1: The Role of the Titiwangsa Mountains in Peninsula Malaysia

It is believed that the Titiwangsa mountain range has a major impact on the weather activities over western Peninsular Malaysia. In the first experiment (**flatPM**), the whole orography of Peninsular Malaysia was flattened to sea level height and the results are shown in Figure 6.22). In this experiment, the peninsula and Sumatra Island experienced rainfall events in the early evening of the previous day as seen in Figure 6.22 (A, 01 May 1900 LT). These events are also believed to have influenced the development of the later morning rainfall over the Strait of Malacca (Figure 6.22 (B) 02 May 1000 LT). Because of the flattened peninsula, there is no barrier to block the wind from propagating eastward over the peninsula, and this has affected the northern part of the rainfall system over the Strait of Malacca to be tilted toward the peninsula, rather than in the centre of the strait. In the early afternoon (Figure 6.22 - 02 May 1300 LT), winds over the peninsula and northern part of the Strait of Malacca have turned westerly, and rainfall over the strait decreases. No rainfall over the inland of the peninsula, due to the absence of the Titiwangsa Mountains (Figure 6.22) (C)). However, rainfall still occurs over the peninsula by afternoon, due to the convection from the land heating process, and the interaction between the convective activity with the sea breeze. The event was less intense and later that day the rainfall system was pushed to the south-east by the northwesterly winds (Figure 6.22 - 02 May 1500 LT).

Since the rainfall event in the control run is concentrated between 3°N-4°N over the west coast, an analysis of time-longitude hovmöller plot for this experiment (and other following experiments) was also done by analysing the hovmöller plot at the same latitudinal average. The rainfall over the Strait of Malacca is still

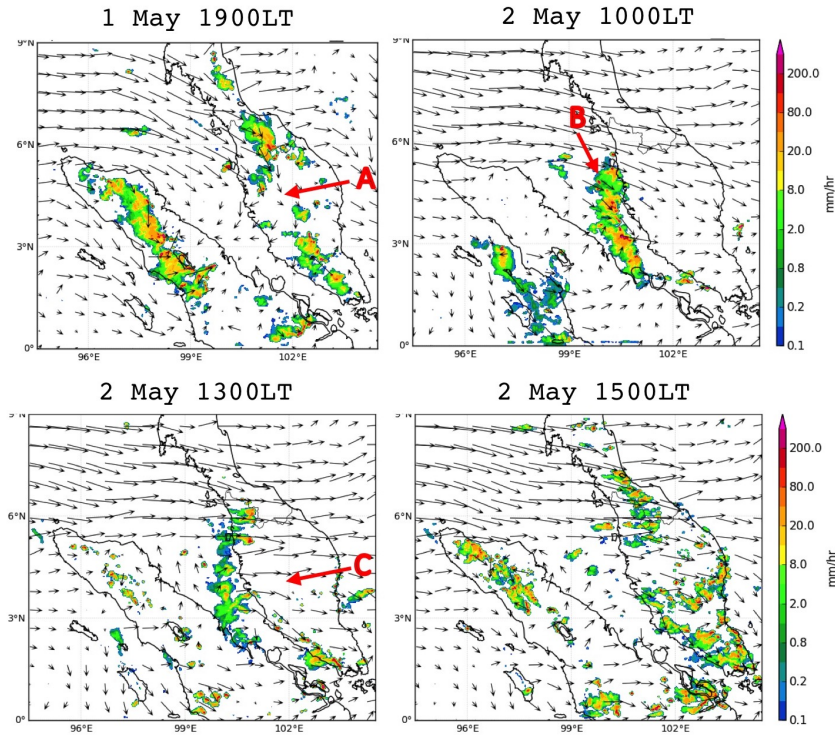


Figure 6.22: Precipitation and 850hPa winds on control run as compared to all of the experiments, flat Peninsular Malaysia (**flatPM**). The figures only compare the main mechanisms in the development of the rainfall on 2 May 2012.

occurring, as discussed earlier in Figure 6.22. The rainfall over the western peninsula is weak (Figure 6.23 (A)) and the rainfall is seen to be progressing eastward over time. This is the effect of the flat peninsula, and thus, the northwesterly wind could easily propagate eastward and influence the rainfall to move eastward. This is also the reason for the smaller amount of rainfall over the west coast of Peninsular Malaysia because most of the rainfall was pushed toward the east.

The hovmöller plot for the mean zonal wind, wind speed and wind direction at the 233 model level (which is 233 m for points at sea level) over 3-4°N is shown in Figure 6.24. This figure also includes the rainfall (above 1 mm hr⁻¹) contour to examine the rainfall and surface wind relationship. The same northwesterly winds were observed over the Strait of Malacca the day before and early morning before the event. With no Titiwangsa Mountains in the peninsula, the low-level winds are mostly westerly by the afternoon on the day of the event, as shown by the strong westerly zonal wind which lingers over the west coast until midnight (Figure 6.24 (A)). Due to the absence of the Titiwangsa mountains, the westerly wind advances further inland of the peninsula on the day of the event Figure 6.24 (B). A weak easterly sea breeze on the east coast (Figure 6.24 (C)) is also associated with the absence of the Titiwangsa Mountains, by reducing the land-sea temperature gradient, and also the absence of orographic convection inland of the peninsula. The plot also shows some important wind-rainfall relationship in this experiment. For example, rainfall over the Strait of Malacca is associated with the converging low-level winds near the west coast of the peninsula (Figure 6.24 (D)).

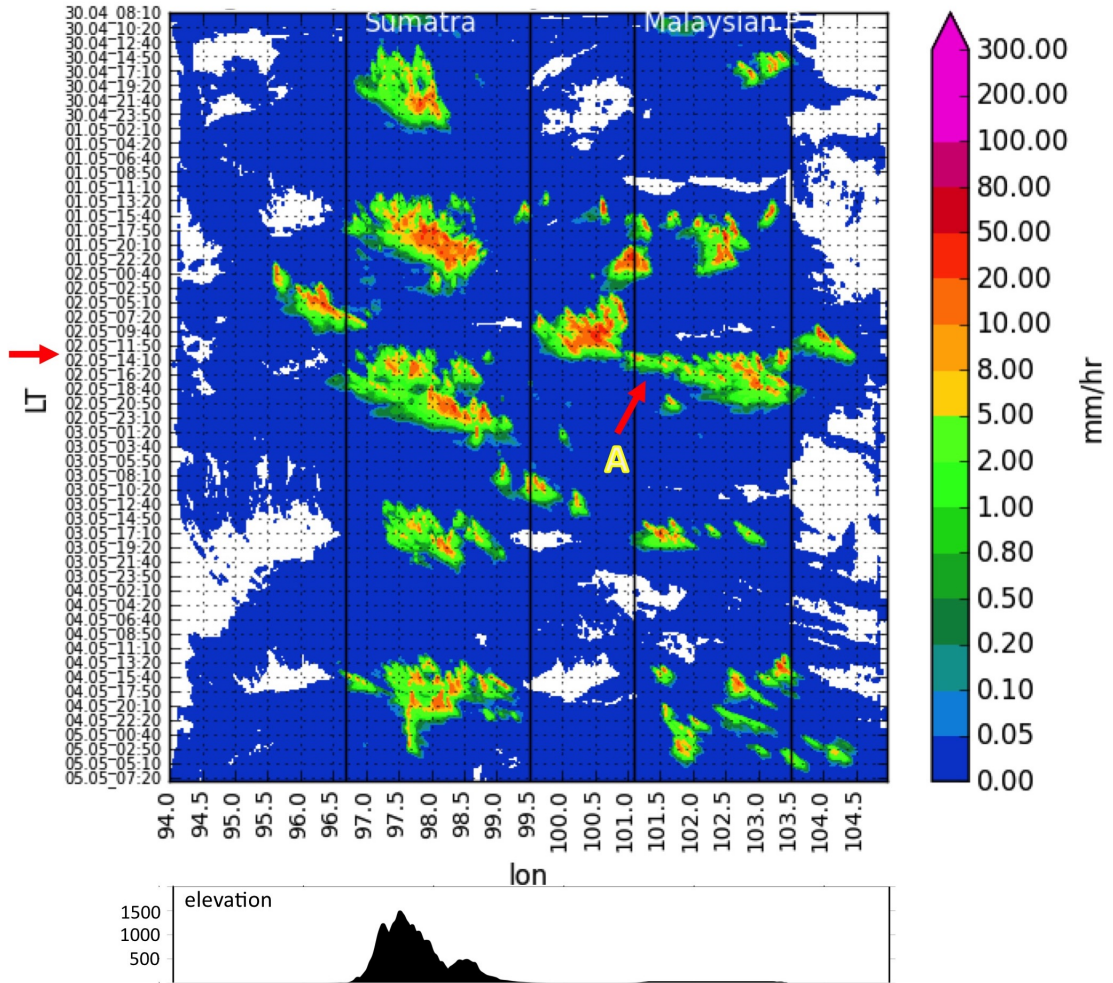


Figure 6.23: Time-longitude hovmöller plot from the **flatPM** experiment (1.5km model), averaged over $3^{\circ}N$ to $4^{\circ}N$. The orography of the Peninsular Malaysia was flattened to sea level. The red arrow on the left side of the box is pointing to the time of the event. The lines $97^{\circ}E$ and $98.75^{\circ}E$ represent the west and east coastlines of Sumatra Island respectively. The lines $101^{\circ}E$ and $103.5^{\circ}E$ represent the west and east coastlines of the Peninsular Malaysia, respectively.

The convergence/divergence plot in Figure 6.25 shows how the converging winds, orographic lifting and other processes influencing the convective activities in this case study. The main findings of this analysis are there was no orographic convection over the peninsula by noon (Figure 6.25 (A)). The absence of the Titiwangsa mountains prevents the development of orographic induced convective activity over the peninsula (Figure 6.25 (B)). The convective activity over the western coast of the peninsula is still occurring, and this is due to the interaction between the northwesterly winds from the Strait of Malacca, the developing sea breeze circulation from solar insolation and the land surface. However, the convection over the central west coast of the peninsula was not intense and propagated to the east and south-east following the northwesterly winds. The convergence over the eastern coast of the peninsula is very pronounced, as seen in Figure 6.25 (1200 LT - 1600 LT), unlike in the western coast of the peninsula.

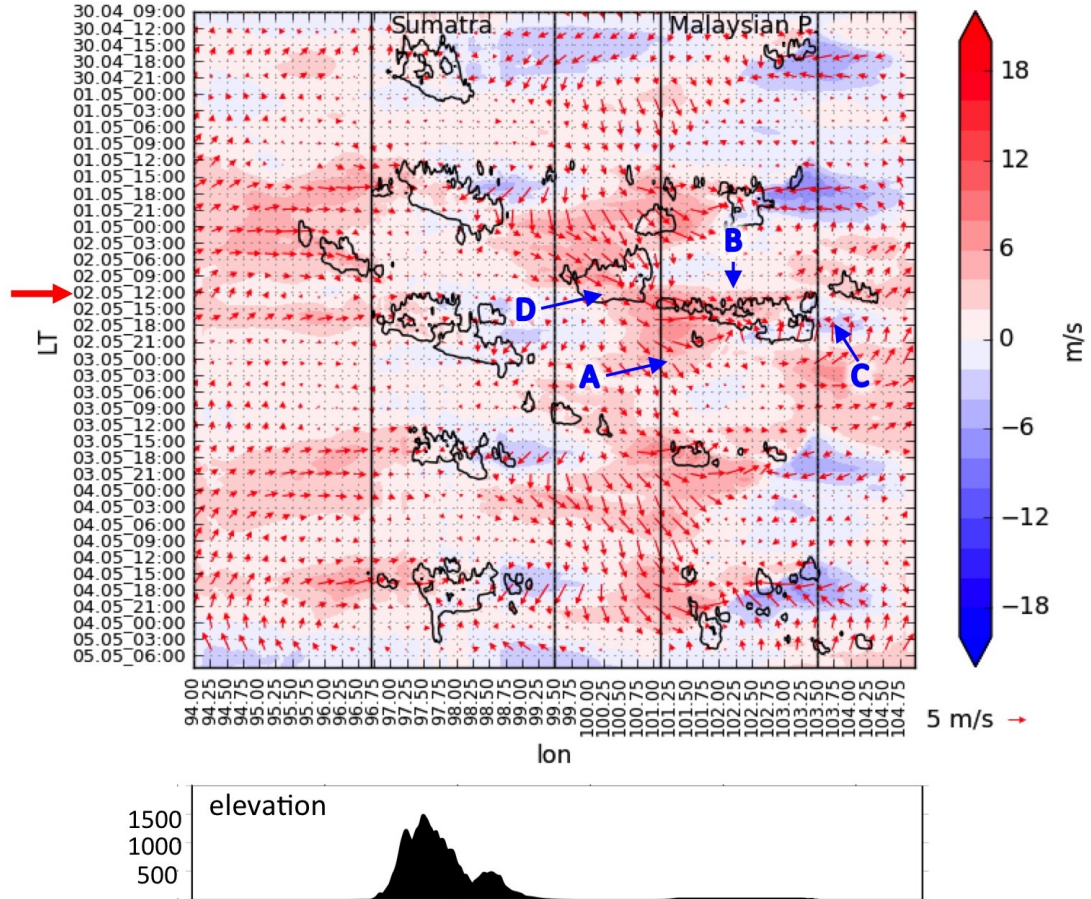


Figure 6.24: Time-longitude hovmöller plot of zonal wind (shaded) and wind direction and magnitude (vectors) at 233 model level from the **flatPM** experiment, averaged over 3°N to 4°N . The red arrow on the left side of the box is pointing to the time of the event. The lines 96.7°E and 99.5°E represent the west and east coastlines of Sumatra Island respectively. The lines 101.1°E and 103.5°E represent the west and east coastlines of the Peninsular Malaysia, respectively. The red colour represents westerly, and the blue represents easterly zonal winds. Wind vectors show the direction and strength of the winds. The dark contour represents rainfall with amount above 1 mm hr^{-1} , for additional reference on winds and precipitation relationship.

To investigate how the Titiwangsa Mountains affecting the zonal winds and convective activity over the peninsula, the analysis on the zonal winds over the 3°N to 4°N cross section was done. This is to track the convection movement along the 3°N to 4°N beginning at 0000 LT (after the 1 May evening rainfall), at 0600 LT (earlier time of convective rainfall over the strait) and then 1100 until 1400 LT (the event hours). A strong northwesterly wind over the western peninsula is noticeable in (Figure 6.26 (A)) where the westerly zonal winds dominated the peninsula. The land breeze is also seen in Figure 6.26(B) but weaker than the dominating northwesterly wind. This is also an indication of a convective activity that is occurring at midnight (or 0000 LT 2 May) as observed in the hovmöller plot in Figure 6.23. Convection has developed over the Strait of Malacca by 0600 LT and matured by mid-morning. This is when the morning rainfall over the strait has begun. By 1100 LT, the convection over the strait (indicated by stronger zonal

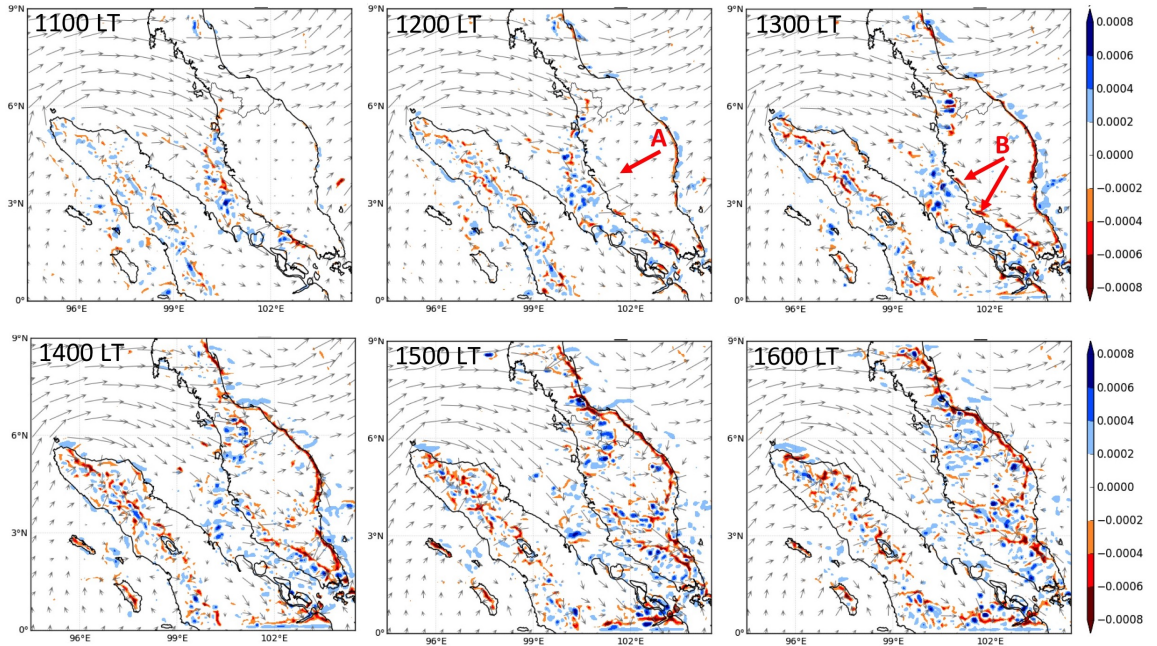


Figure 6.25: 13 metre winds in $m s^{-1}$ (vectors) and divergence/convergence in s^{-1} at 13 metre level (shaded), from the **flatPM** experiment. Blue represents divergence (descending movement) and red represents convergence (ascending movement) of air. The photos show the convective activities from 1100 LT until 1600 LT.

winds in this plot) moves towards the peninsula by 1200 LT. The convective activity still occurs over the peninsula, near the coast rather than inland (Figure 6.26 (C)) Later, the convection spreads across the peninsula, as there is no mountain range to block it from propagating eastward.

The development of the rainfall event in this experiment can be explained by Figure 6.27. In the **flatPM** experiment, the rainfall in the late afternoon of 1 May 2012 was developed due to insolation and possibly synoptic influence that enhanced the development of the event (Figure 6.27(a)). The rainfall is less organised and relatively weaker over the peninsula, mostly developed from sea breeze circulation over land (from insolation) and no mountain ranges to enhance convection and to keep it over the west coast. By late night (Figure 6.27(b)), cold flows, land breezes had merged over the strait and established atmospheric convection, and northwesterly enhances the convection. By mid-afternoon (Figure 6.27(c)), the convection matured and yielded precipitation. By late morning (Figure 6.27(d)), insolation and sea breeze begin to promote atmospheric convection over the land (nearer to the coast than inland) and the ongoing rainfall over the strait beginning to move eastward due to the northwesterly wind. By midday (Figure 6.27(e)) the convection over the strait dissipated as the sea breeze enhanced and the convection near the coast matured and yielded precipitation. No mountain ranges to block the rainfall system thus the rainfall system moving eastward before dissipating to the east coast.

6.2. CASE STUDY 1: FIRST INTER-MONSOON (APRIL-MAY)

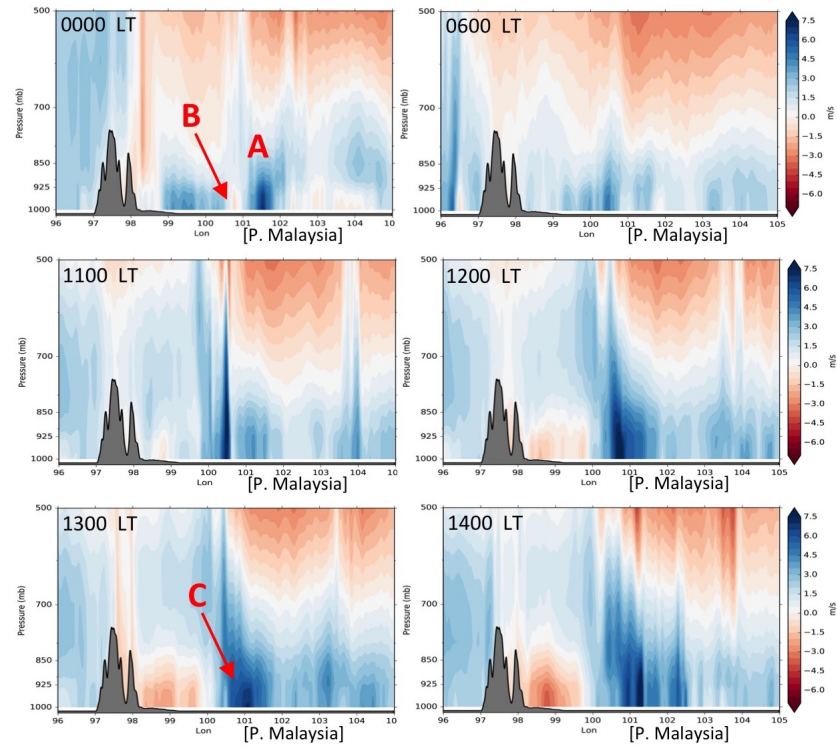


Figure 6.26: Zonal winds cross section, averaged over $3^{\circ}N$ to $4^{\circ}N$ for (a) control run, (b) **flatPM** experiment and (c) **flatSI** experiment of the 1.5km model. The bracket "[P. Malaysia]" indicates the limit of the flattened Peninsular Malaysia landmass.

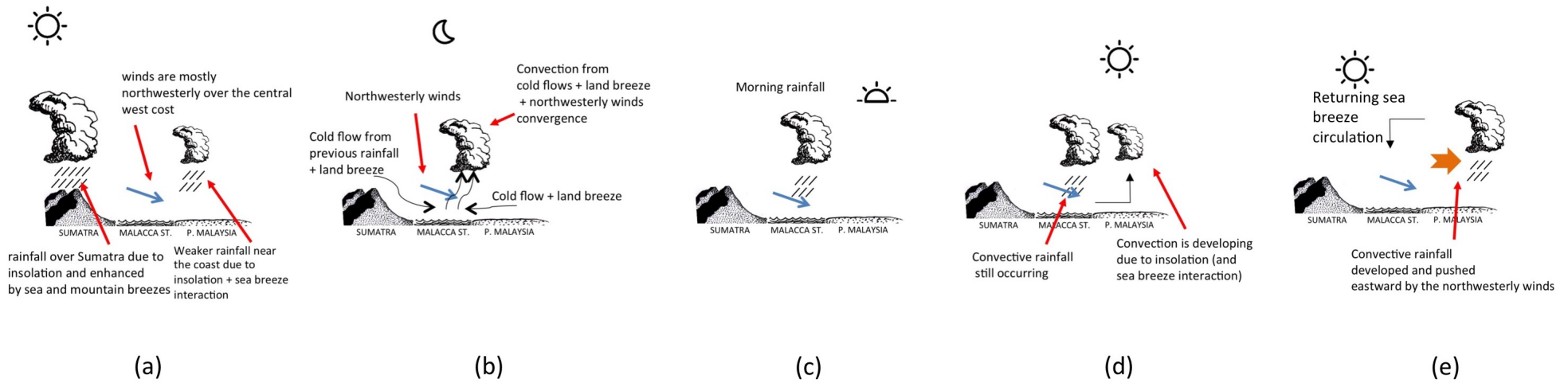


Figure 6.27: Schematic figures explaining the process of the development of rainfall on the 2 May in the *flatPM* experiment. (a) insolation and possibly synoptic influence drive the development of rainfall event in the late afternoon of 1 May 2012. Weaker rainfall over the peninsula, mostly developed from sea breeze interaction and no mountain ranges to enhance convection, and keep it over the west coast. (b) by late night, cold flows, land breezes and northwesterly wind generate convection over the Strait of Malacca and (c) the convection matured by mid-morning and yielded precipitation. (d) by late morning, insolation and sea breeze begin to promote convection over the land (nearer to the coast than inland) and the ongoing rainfall over the strait beginning to move eastward due to the northwesterly wind. (e) the convection over the strait dissipated as the sea breeze enhanced by the afternoon, and the enhancing convection over the coast matured and yielded precipitation. No mountain ranges to block the rainfall system thus the rainfall system moving eastward before dissipating on the east coast. (Images were illustrated by the author.)

Exp. 2: The Role of the Barisan Mountains in Sumatra Island

Sumatra Island and its higher altitude mountains (Barisan Mountains) plays an important role in the local weather activities over the Strait of Malacca and western Peninsular Malaysia. The second sensitivity experiment investigated the effect of the development of the event when the Barisan Mountains was flattened to sea level. There are rainfall events over the peninsula and Sumatra in the late afternoon of the day before the event (Figure 6.28 (A) - 01 May 1900 LT) and influencing the development of rainfall event over the Strait of Malacca in the morning of 2 May (Figure 6.28(B) 02 May 1000 LT). Orographic convective rainfall was observed over the peninsula (Figure 6.28(C) 02 May 1300 LT). The cold front from the rainfall event at the Strait of Malacca together with the developing sea breeze merge with the orographic rainfall over the peninsula to generate rainfall along the western coast of the peninsula. The rainfall event remains stationary on the west coast as it is blocked by the Titiwangsa Mountains for a couple of hours (Figure 6.28) 02 May 1500 LT).

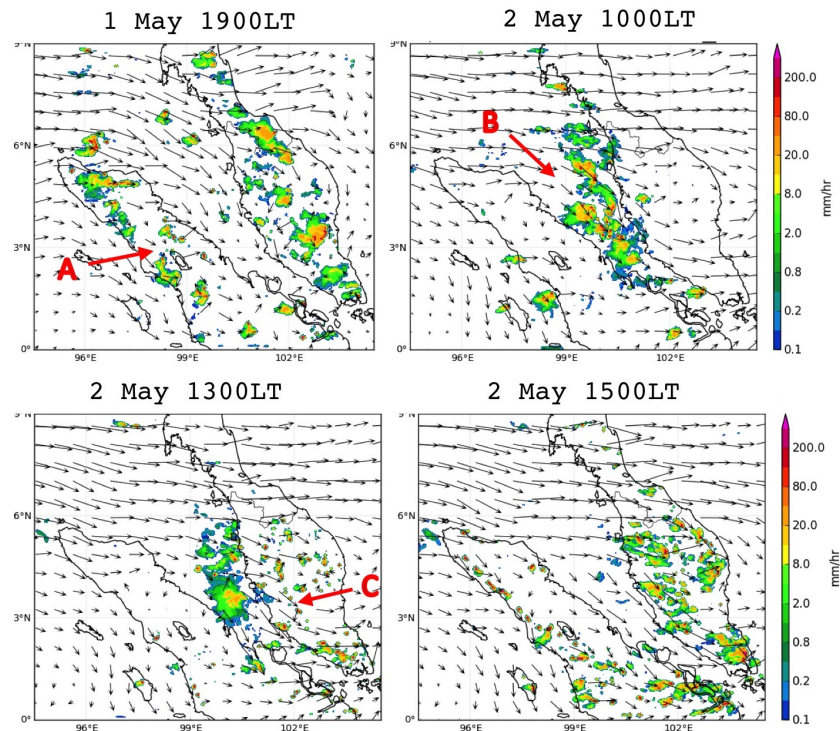


Figure 6.28: Precipitation and 850hPa winds on *flatSI*. The figures only compare the main mechanisms in the development of the rainfall on 2 May 2012.

The evolution of the rainfall between the 3°N to 4°N latitude is shown in Figure 6.29. There were rainfall events over the peninsula and Sumatra, but weaker over the Sumatra Island (Figure 6.29(A)). These events still influencing rainfall over the Strait of Malacca. Rainfall starting from the eastern of the Sumatra Island (Figure 6.29 (B)) was most probably developed from the late afternoon rainfall of the previous day and moving toward the strait throughout the early morning. Moreover, the rainfall over the west coast occurred earlier (around 1150 LT, Figure 6.29

(C)) and propagated inland. The orographic convective rainfall over the peninsula is also moving both sides (westward and eastward) and merged with the rainfall that was developing over the western coast. The rainfall event stays mostly on the western coast, and the eastward-propagated rainfall from the mountains developed and expanded throughout the east coast.

The hovmöller plot of the lower level wind showed that the absence of Barisan mountains in Sumatra allows the westerly winds from the Indian Ocean to advance inland of Sumatra as per Figure 6.30(A). The sea breeze over the east coast of Sumatra is generally weak on both days. However, a stronger sea breeze is observed over the west coast of the peninsula (B) and stay longer for at least until midnight. The winds over the strait (near to the west coast of the peninsula) are northerly before the event as shown in Figure 6.30(C), and strong westerly during the event. The Titiwangsa Mountains enhanced the convective activity over the peninsula on the day and influence the sea breeze to become stronger, on both the west and east coasts of the peninsula. Rainfall over the peninsula and Strait of Malacca in Figure 6.30 (D) is an example of the rainfall that is associated with the converging winds. However, converging winds does not always produce rain, for example in (E).

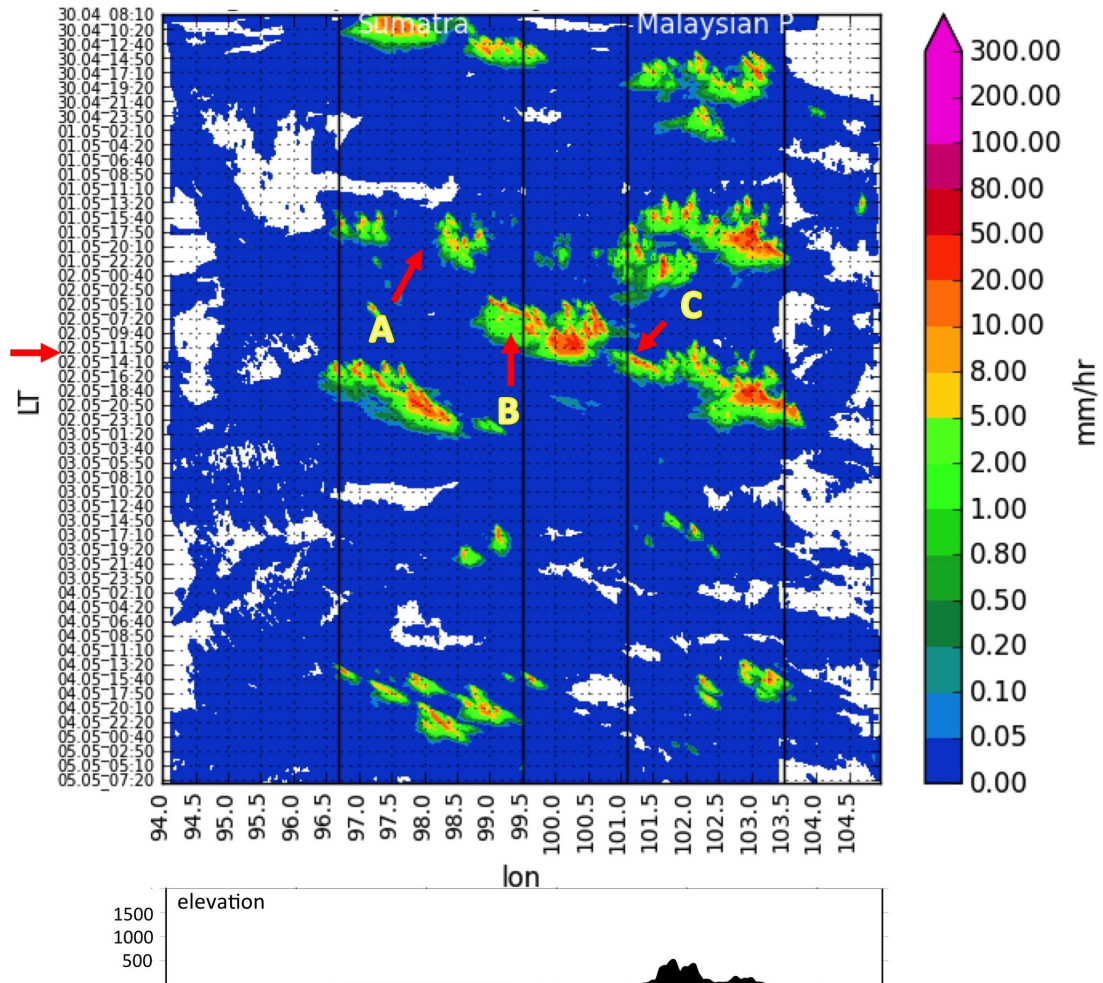


Figure 6.29: Time-longitude hovmöller plot from the **flatSI** experiment (1.5km model), averaged over $3^{\circ}N$ to $4^{\circ}N$. The orography of the Sumatra Island was flattened to sea level. The red arrow on the left side of the box is pointing to the time of the event. The lines $97^{\circ}E$ and $98.75^{\circ}E$ represent the west and east coastlines of Sumatra Island respectively. The lines $101^{\circ}E$ and $103.5^{\circ}E$ represent the west and east coastlines of the Peninsular Malaysia, respectively.

In the absence of the Barisan Mountains, less convective activity was observed over the Sumatra Island before noon (Figure 6.31 1100 LT and 1200 LT). The absence of the orography also caused the winds to flow towards the peninsula with less deflection (Figure 6.31 (A)), which is usually pronounced over the northern Sumatra. The orography over the peninsula induces orographic convection over the peninsula, as well as blocking the convective system from moving eastward following the prevailing northwesterly wind. In 1500 LT, there is a lot of convergence and divergence over the western peninsula showing that there are active convective activity over the western part of the mountains. This experiment also shows a pronounced sea breeze convergence over the east coast by afternoon, the same as previous experiment and control run.

The cross-section of the zonal wind shown in Figure 6.32 indicates that the westerly zonal wind dominating the western side of the peninsula (including the

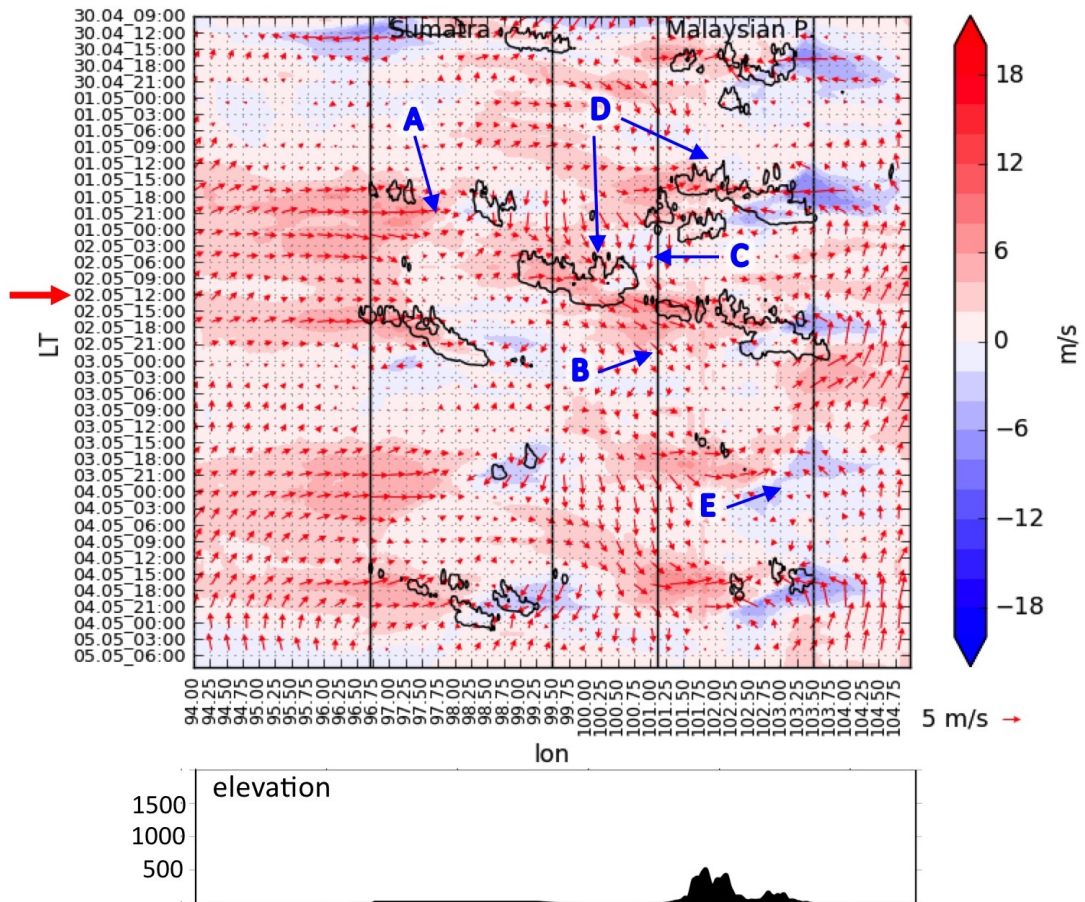


Figure 6.30: Time-longitude hovmöller plot of zonal wind (shaded) and wind direction and magnitude (vectors) at 233 model level from the *flatSI* experiment, averaged over 3°N to 4°N . The red arrow on the left side of the box is pointing to the time of the event. The lines 96.7°E and 99.5°E represent the west and east coastlines of Sumatra Island respectively. The lines 101.1°E and 103.5°E represent the west and east coastlines of the Peninsular Malaysia, respectively. The red colour represents westerly, and the blue represents easterly zonal winds. Wind vectors show the direction and strength of the winds. The dark contour represents rainfall with amount above 1 mm hr^{-1} , for additional reference on winds and precipitation relationship.

whole Sumatra) at midnight (Figure 6.32 - 0000 LT). This is also due to the dominating westerly-northwesterly winds over the western part of the domain box. A weak land breeze is visible over the west coast of the peninsula by the mid-morning (Figure 6.32 (A)), and this is also the beginning time of the morning rainfall over the strait (Figure 6.32 (B)) and got stronger by 1100 LT. By noon (Figure 6.32 - 1200 LT), the convection dissipated (Figure 6.32 (C)), and convection developed over the western peninsula and gets stronger (Figure 6.32 (D)). The stronger westerly over the western coast of the peninsula is also influenced by the strong northwesterly wind. The convection stayed over the west coast as it is blocked by the Titiwangsa Mountains from moving eastward following the prevailing northwesterly wind. The easterly sea breeze over the east of the peninsula is weaker in the afternoon despite the convective activity inland. The westerly winds may have dominated the mean wind direction and reduced the effect of the sea breeze, due to the absence of

6.2. CASE STUDY 1: FIRST INTER-MONSOON (APRIL-MAY)

Barisan Mountains (in Sumatra).

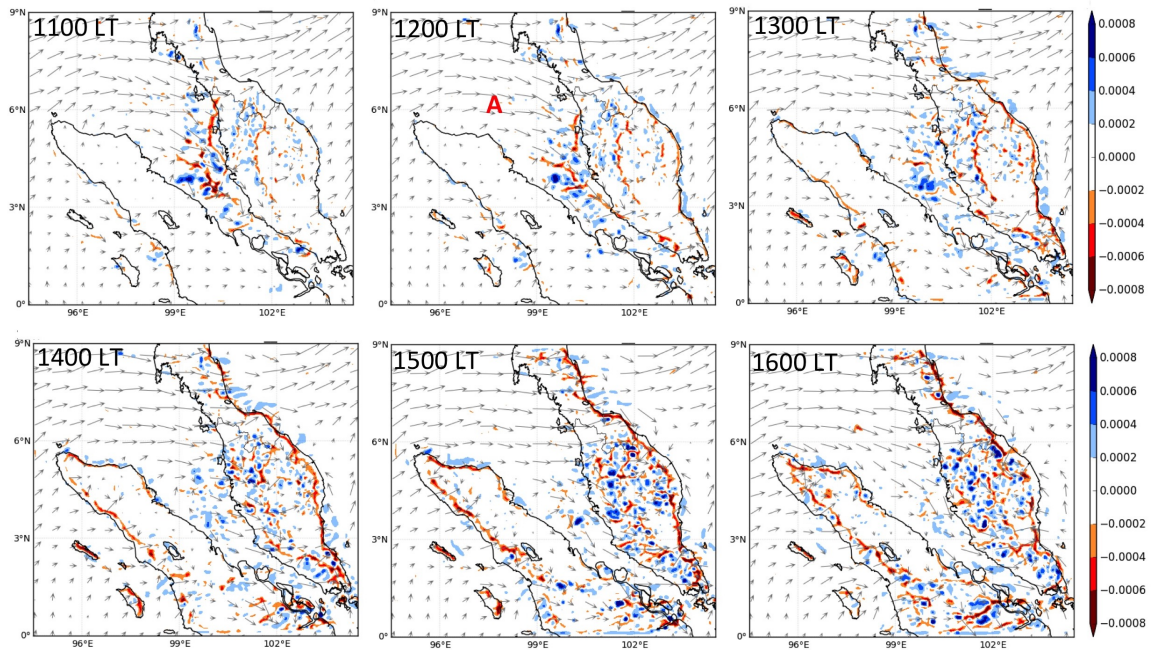


Figure 6.31: 13 metre winds in $m s^{-1}$ (vectors) and divergence/convergence in s^{-1} at 13 metre level (shaded), from the **flatSI** experiment. Blue represents divergence (descending movement) and red represents convergence (ascending movement) of air. The photos show the convective activities from 1100 LT until 1600 LT.

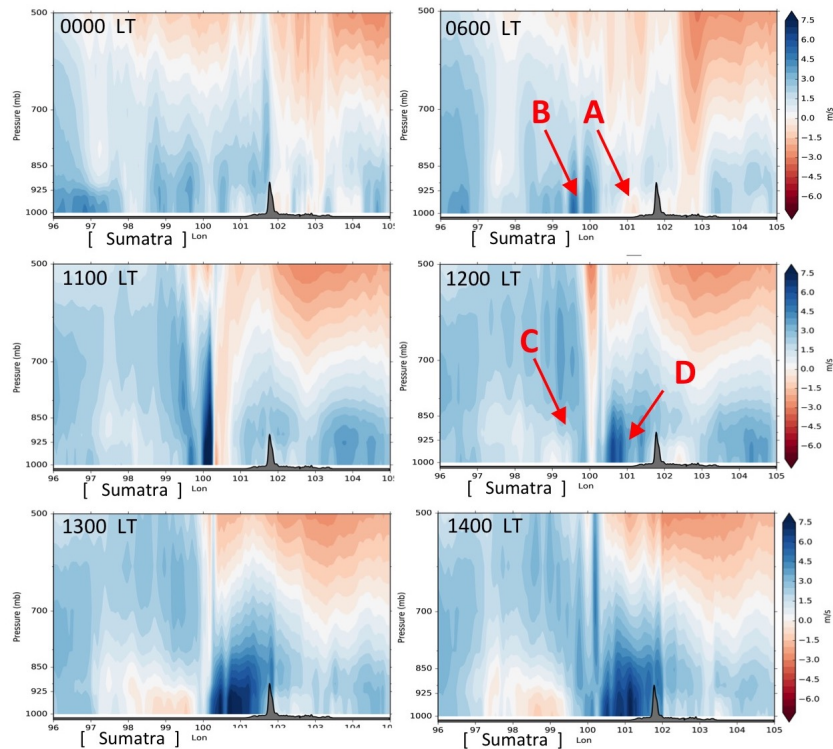


Figure 6.32: Zonal winds cross section, averaged over $3^{\circ}N$ to $4^{\circ}N$ for **flatSI** experiment of the 1.5km model.

The development of the rainfall event in the **flatSI** experiment can be explained in Figure 6.33. In the **flatSI** experiment, the rainfall on the 1 May (Figure

6.33(a)) is developed by insolation and a possibly synoptic influence, over the peninsula and Sumatra. Most of the rainfall over Sumatra is induced by the sea breeze and nearer to the coast instead of inland. Winds are northwesterly over the Strait of Malacca. By midnight (Figure 6.33(b)), land breeze and cold flow from both lands merged in over the strait to develop atmospheric convection and northwesterly wind enhances the convection. By mid-morning (Figure 6.33(c)), convection over the strait has matured and produced rainfall. By midday (Figure 6.33(d)), convection has developed over the peninsula due to insolation and sea breeze circulation then yielded to rainfall while the rainfall over the strait is still ongoing. As the sea breeze enhanced (Figure 6.33(e)), the rainfall system over the strait was suppressed and dissipated, and rainfall over the peninsula enhance. The rainfall system is enhanced by the sea and land breezes as well as the northwesterly winds. Titiwangsa mountains blocked the rainfall system for a few hours from moving eastward.

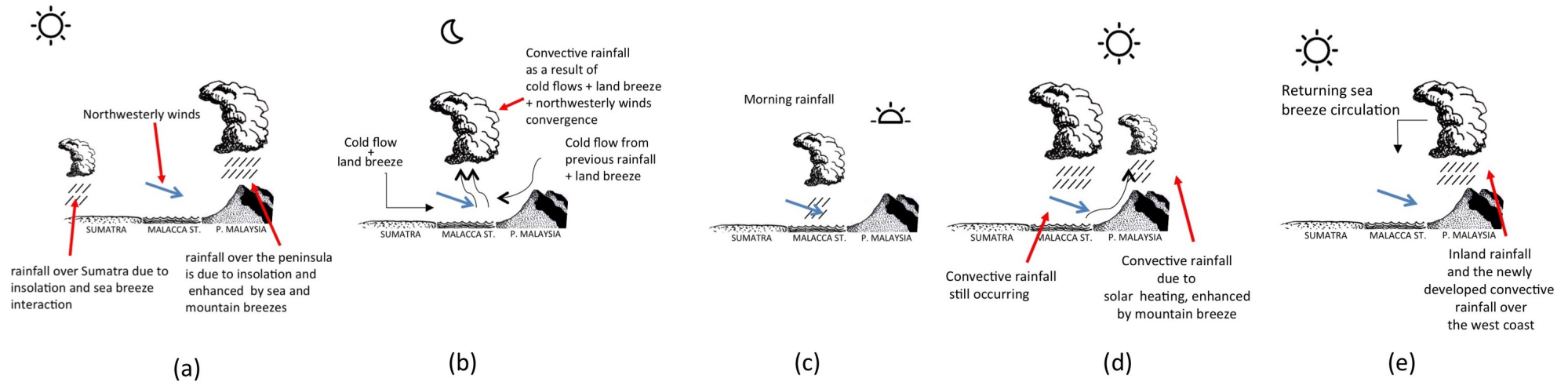


Figure 6.33: Schematic figures explaining the process of the development of rainfall on the 2 May in the **flatSI** experiment. (a) insolation and sea breeze influence the development of rainfall in the late afternoon over the peninsula and Sumatra. Most of the rainfall over Sumatra is induced by the sea breeze and nearer to the coast. Winds are northwesterly over the Strait of Malacca. (b) by midnight, land breeze and cold flow, as well as northwesterly wind, induce convection over the strait, and (c) convection matured by mid-morning on the 2 May and produced rainfall. (d) by midday, convection developed over the peninsula and yielded rainfall while the rainfall over the strait is still ongoing. (e) as the sea breeze enhanced, the rainfall system over the strait was suppressed and dissipated, and rainfall over the peninsula enhance. The rainfall system enhanced by the sea and land breezes as well as the northwesterly winds. Titiwangsa mountains blocked the rainfall system for a few hours from moving eastward. (Images were illustrated by the author.)

Exp. 3: The Role of Titiwangsa and the Barisan Mountains

The third sensitivity experiment involved a flattened orography of both Peninsular Malaysia and Sumatra Island to sea level height (Figure 6.34). This was done to investigate the effect of high altitude orography on the rainfall pattern over the region, especially this event. The lack of orography causes a weaker inland rainfall on 1 May (Figure 6.34 (A) - 01 May 1900 LT). These rainfall events (1 May afternoon) however still influences the development of the rainfall over the Strait of Malacca (Figure 6.34 - 02 May 1000 LT). However, the absence of higher mountains in both Peninsular Malaysia and Sumatra Island caused the rainfall system over the strait disrupted by the westerly winds and pushed towards the coast. No orographic rainfall present over the peninsula and Sumatra as expected (Figure 6.34 - 02 May 1300 LT). However, there is still rainfall occurring over the west coast later that afternoon (Figure 6.34 - 02 May 1500 LT), and it is most probably due to the interaction between the westerly wind, the land friction and sea breeze. Rainfall events were observed across the western coast by 1500 LT and dissipated as it was pushing eastward by the westerly wind (not shown).

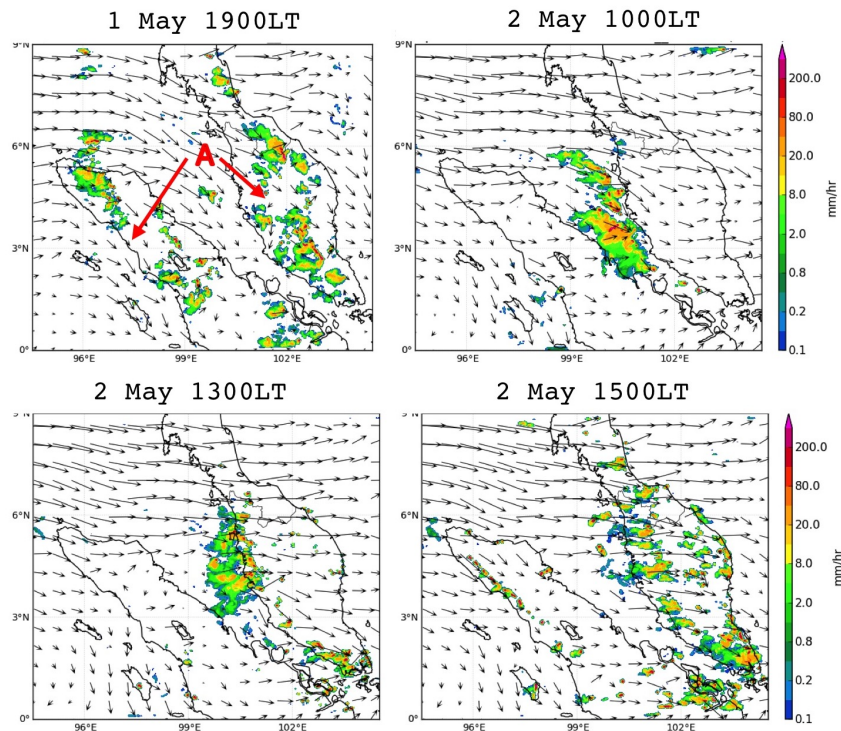


Figure 6.34: Precipitation and 850hPa winds on *flatPM* experiment. The figures only compare the main mechanisms in the development of the rainfall on 2 May 2012.

The hovmöller plot in Figure 6.35 shows a generally weak rainfall over the Sumatra Island and Peninsula Malaysia. The absence of the Barisan Mountains and Titiwangsa Mountains also reducing the amount of rainfall development in both landmasses on the 1 May afternoon (Figure 6.35 (A)). There is also a rainfall event over the west coast throughout the night between 1 May and 2 May. Despite an absence of high mountain, the rainfall over the Sumatra has still developed

6.2. CASE STUDY 1: FIRST INTER-MONSOON (APRIL-MAY)

(Figure 6.35 (B)) in the morning of 2 May. The rainfall over the western coast of the peninsula developed due to solar insolation and sea breeze interaction with the land surface, and dissipated as it propagated inland (Figure 6.35 (C)). There is also rainfall event developed over the eastern peninsula, and this is most probably due to the solar insolation and sea breeze interaction with the land surface.

In the hovmöller plot of the low-level wind in Figure 6.36, the absence of the mountains in both Sumatra and peninsula causes the westerly wind to be able to advance inland. The winds are mostly westerly in the early morning before the event (Figure 6.36 (A)). Without the orography, the westerly wind advances inland smoothly across the peninsula (Figure 6.36(B)). The rainfall over the peninsula (the day before) and in the Strait of Malacca (early morning of 2 May) are also associated with convergence as seen in Figure 6.36(C).

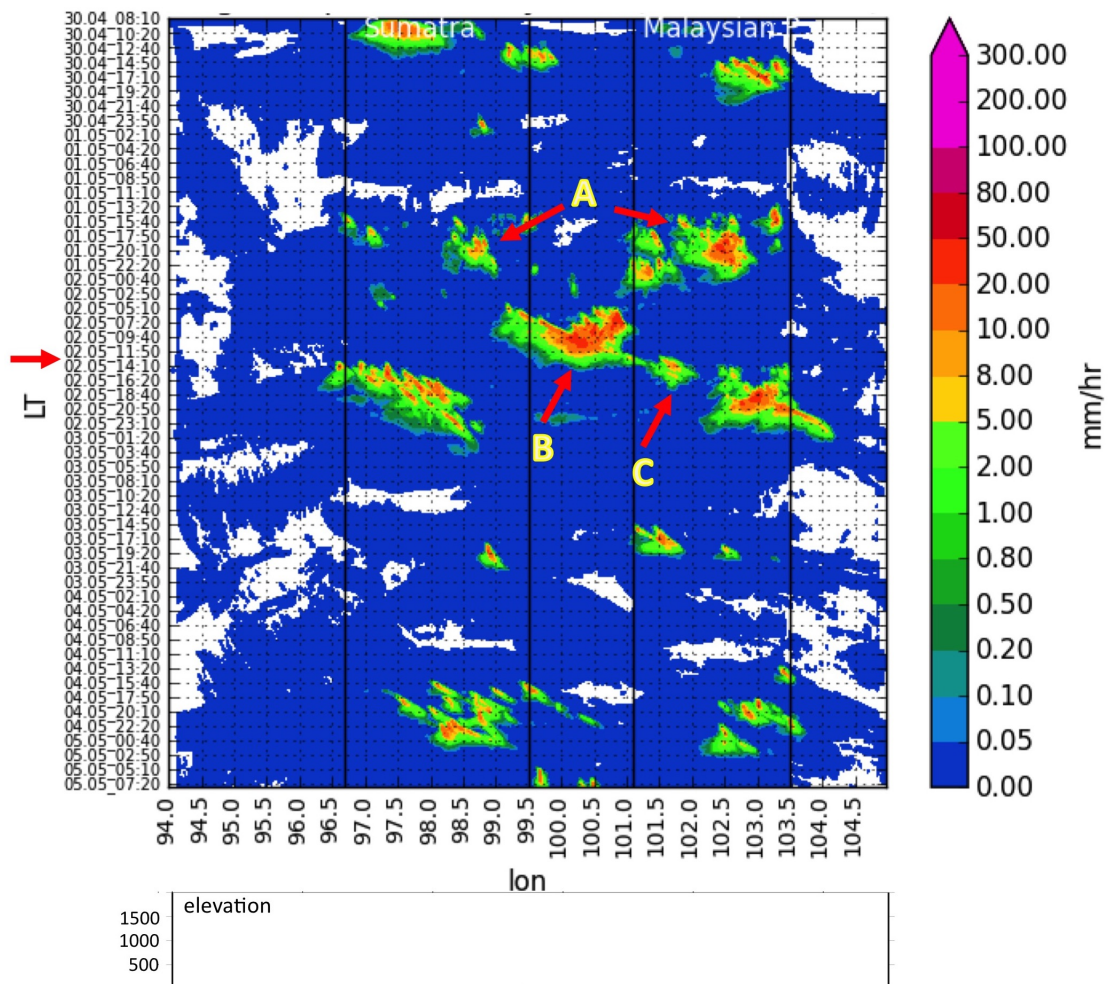


Figure 6.35: Time-longitude hovmöller plot from the **flatALL** experiment (1.5km model), averaged over $3^{\circ}N$ to $4^{\circ}N$. The orography of the Peninsular Malaysia and Sumatra were flattened to sea level. The red arrow on the left side of the box is pointing to the time of the event. The lines $97^{\circ}E$ and $98.75^{\circ}E$ represent the west and east coastlines of Sumatra Island respectively. The lines $101^{\circ}E$ and $103.5^{\circ}E$ represent the west and east coastlines of the Peninsular Malaysia, respectively.

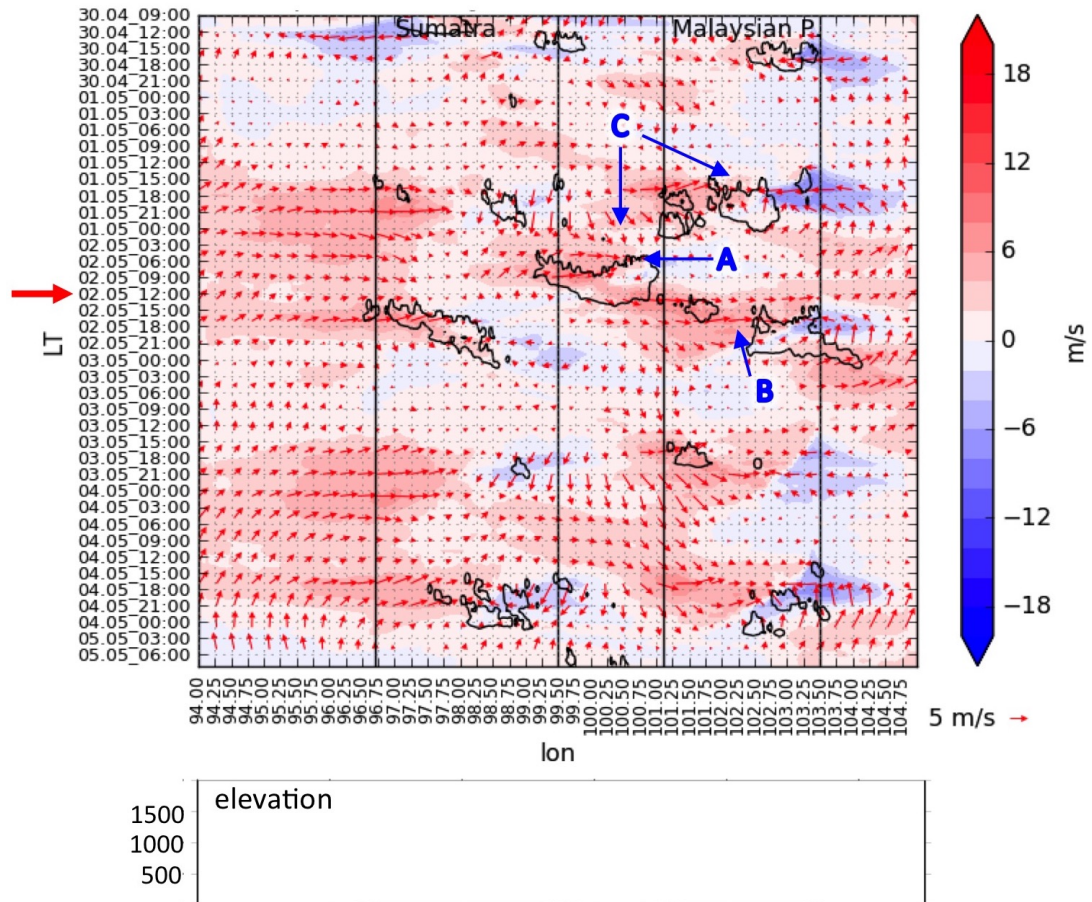


Figure 6.36: Time-longitude hovmöller plot of zonal wind (shaded) and wind direction and magnitude (vectors) from the **flatALL** experiment, averaged over 3°N to 4°N . The red arrow on the left side of the box is pointing to the time of the event. The lines 96.7°E and 99.5°E represent the west and east coastlines of Sumatra Island, respectively. The lines 101.1°E and 103.5°E represent the west and east coastlines of the Peninsular Malaysia, respectively. The red colour represents westerly, and the blue represents easterly zonal winds. Wind vectors show the direction and strength of the winds. The dark contour represents rainfall with amount above 1 mm hr^{-1} , for an additional reference on winds and precipitation relationship.

When both Peninsular Malaysia and Sumatra Island were flattened, there were no convergence or divergence activities inland in the late morning of 2 May as seen in Figure 6.37 1100 LT and 1200 LT. There were convective activities observed over the Strait of Malacca as there was morning rainfall. The convection over the strait moved westward towards the peninsula and moving inland (Figure 6.37 (A)). There was also convection over the coastal area, in both west and east coasts. Later that afternoon, the convection over the west coast moved eastward following the mean westerly winds (Figure 6.37 1400 LT - 1600 LT). The convection over the Sumatra Island was also concentrated on the coast, not inland, and propagated eastward over time.

Looking at the zonal winds through the cross section in (Figure 6.38), the whole western part of the domain box was dominated by the westerly zonal wind around midnight (Figure 6.38 0000 LT). However, it is interesting to observe that the

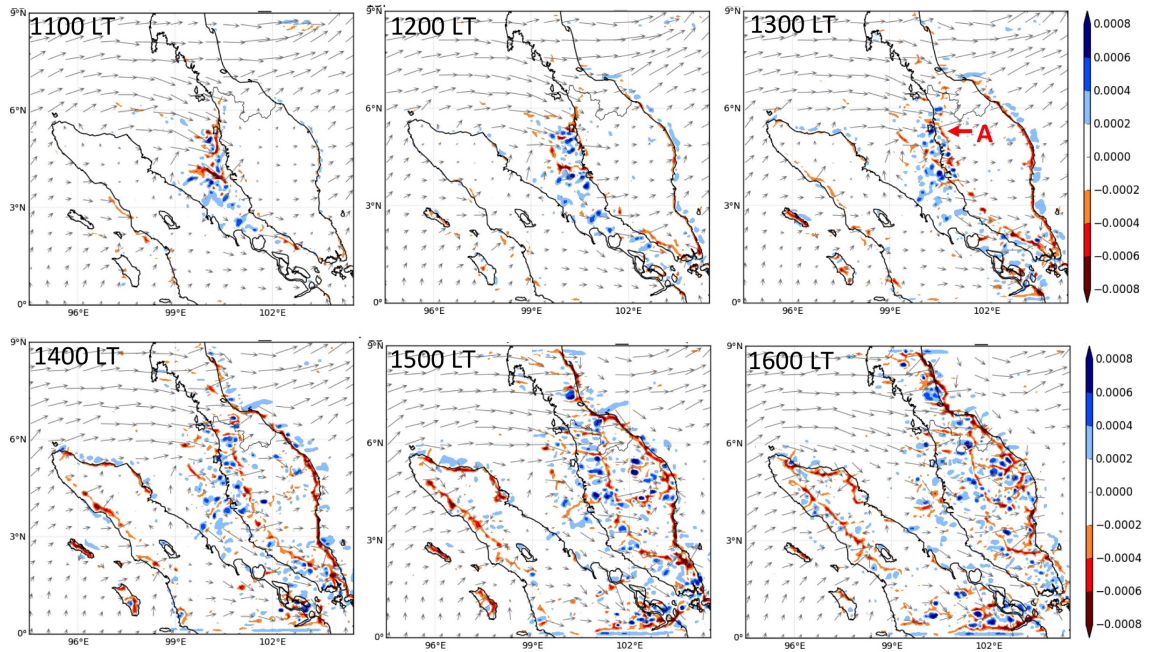


Figure 6.37: 13 metre winds in $m s^{-1}$ (vectors) and divergence/convergence in s^{-1} at 13 metre level (shaded), from the **flatALL** experiment. Blue represents divergence (descending movement) and red represents convergence (ascending movement) of air. The photos show the convective activities from 1100 LT until 1600 LT.

land breeze and westerly zonal wind merged near the western coast of the peninsula by mid-morning (Figure 6.38 (A)). This is also the beginning of the morning rainfall over the strait. The convection has developed over the strait (Figure 6.38 (B)), and moves eastward. The westerly wind and the developing sea breeze over the western coast of the peninsula induce convection over the western peninsula and as the convection over the coast of the peninsula develops, the westerly strengthens as it combines with the sea breeze (Figure 6.38 (C)). The dominating westerly winds over the region also reducing the intensity of the sea breeze over the east coast of Sumatra and the Peninsular Malaysia (Figure 6.38 1100-1400 LT). The convective activity stayed mostly over the peninsula before slowly propagated eastward across the peninsula.

The development of rainfall event in this experiment can be explained in Figure 6.39. For the **flatALL** experiment, (Figure 6.39(a)), a weaker convective rainfall near the coast over both peninsula and Sumatra had developed due to insolation and sea breeze. The wind at the centre of the strait is mostly northwesterly. By midnight (Figure 6.39(b)), land breezes from both lands merged over the strait and favour convection, furthermore incoming northwesterly wind enhanced the convection. By mid-morning (Figure 6.39(c)), the convection matured and yielded precipitation. By midday (Figure 6.39(d)), sea breeze enhanced over the peninsula and promotes convection on the land near the coast. The ongoing rainfall over the strait is slowly dissipating as the sea breeze enhances. By afternoon (Figure 6.39(e)), the convection over the peninsula enhanced and matured to yield

6.2. CASE STUDY 1: FIRST INTER-MONSOON (APRIL-MAY)

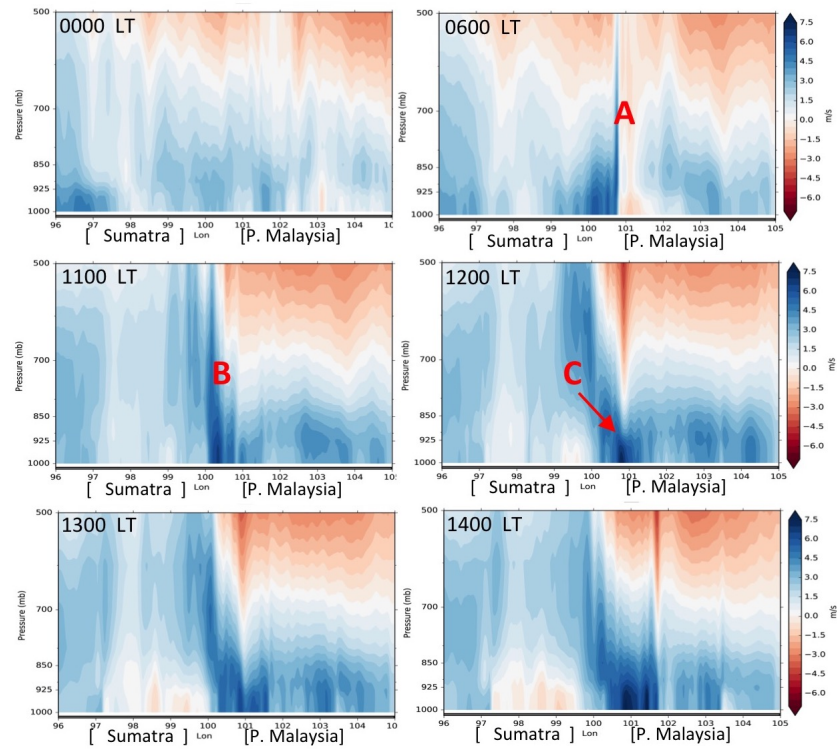


Figure 6.38: Zonal winds cross section, averaged over $3^{\circ}N$ to $4^{\circ}N$ for *flatALL* experiment of the 1.5km model.

precipitation in the afternoon and moving eastward as there are no mountain ranges to sustain the system in the west.

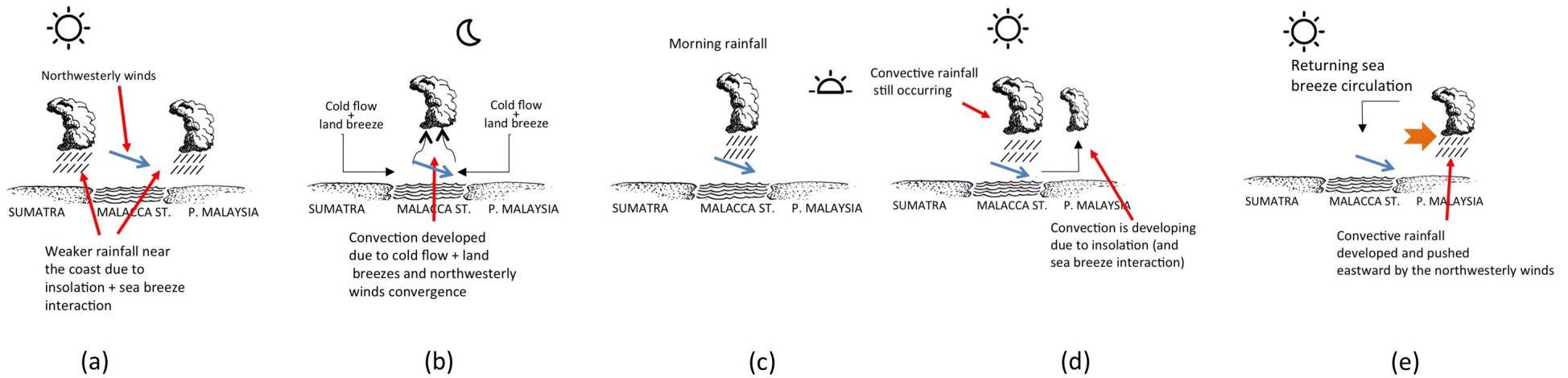


Figure 6.39: Schematic figures explaining the process of the development of rainfall on the 2 May in the **flatALL** experiment. (a) A weaker convective rainfall near the coast over both peninsula and Sumatra developed due to insolation and sea breeze. The wind at the centre of the strait is mostly northwesterly. (b) by midnight, land breezes from both lands and incoming northwesterly wind induce convection over the strait. (c) By mid-morning, the convection matured and yielded precipitation. (d) By midday, sea breeze enhanced over the peninsula and promotes convection near the coastal region. The ongoing rainfall over the strait is slowly dissipating as the sea breeze enhances. (e) The convection over the peninsula enhanced and matured to yield precipitation in the afternoon and moving eastward as there are no mountain ranges to sustain the system in the west. (Images were illustrated by the author.)

Exp. 4: The Role of Sumatra Island

As previously mentioned, Sumatra Island plays an important role in the weather activities over the Strait of Malacca and western Peninsular Malaysia. The fourth sensitivity experiment is looking at the effect of removing the whole of Sumatra Island on the development of the rainfall event on 2 May 2012. The land was replaced by the ocean, and the result of precipitation and 850 hPa wind of this experiment are shown in Figure 6.40. Figure 6.40 (01 May 1900 LT) shows that there are rainfall events occurred in the afternoon of the previous day. A few rainfall events are developing off the western coast by late morning, and some rainfall over the northwestern peninsula (Figure 6.40 02 May 1300 LT). However, lack of the early morning rain over the ocean does not prevent the rainfall development over the west coast on the afternoon of 2 May (Figure 6.40 - 02 May 1300 LT). There are also rainfall events over the Titiwangsa Mountains from the orographic convection which lead to a heavy rainfall over the western peninsula later in the afternoon of 2 May (Figure 6.40 - 02 May 1300 LT). Due to the open ocean on the west, there is an assumption that the rainfall events are fuelled by a large amount of moisture from the Indian Ocean especially in the afternoon of 2 May, aided by the orographic lifting over the Titiwangsa Mountains (Figure 6.40- 02 May 1500 LT). The 850 hPa wind in these figures are mostly northwesterly near to the western peninsula and stronger over the southern peninsula as it was deflected by the Titiwangsa mountain toward the South China Sea.

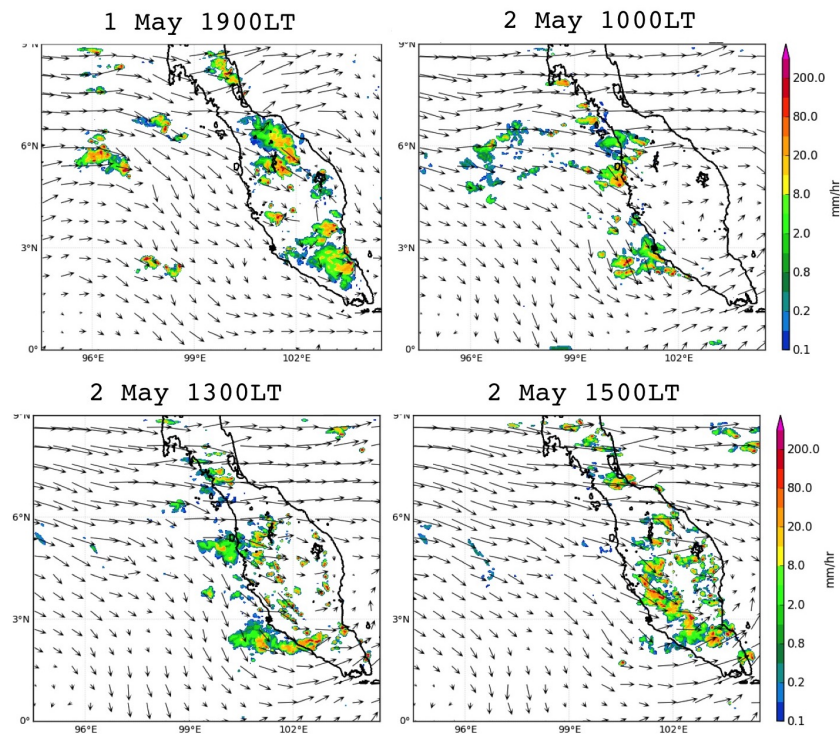


Figure 6.40: Precipitation and 850hPa winds on No Sumatra (*noSI* experiment). The figures only compare the main mechanisms in the development of the rainfall on 2 May 2012.

Analysing the rainfall through the hovmöller diagram in Figure 6.41 shows that the rainfall events were mostly concentrated over the peninsula and the adjacent sea on 1 and 2 May (Figure 6.41), with a large events (in both afternoons) across the peninsula. A few ocean rainfall events were observed in the figure, and the rainfall over the peninsula on 2 May occurred almost simultaneously across the peninsula and began earlier, at around 1150 LT, on the event day. There was also an early morning rainfall event over the west coast, at around 0250 LT, for more than 4 hours, and another rainfall event later that day at around 1900 LT, which may have started from the ocean and moved to the land. These three rainfall events (Figure 6.41 (A)) are believed had contributed to a large amount of daily rainfall on the 2 May. Rainfall is more frequent over the west coast, from the 1 May until the 2 May.

The winds are mostly westerly in the **noSI** experiment as expected due to the absence of Sumatra Island Figure 6.42 (A). Interestingly, the winds over the eastern part of the peninsula are also affected. The wind over the east of the peninsula coast seems to be a stronger southwesterly most of the time on the 2 May (Figure 6.42 (B)). This is probably due to the stronger westerly winds from the Indian Ocean. When there is no Sumatra, the peninsula faces a strong westerly and northwesterly from the Indian Ocean, which deflected by the Titiwangsa Mountains at the south of the peninsula toward the South China Sea. Stronger westerly wind in both 1 May and 2 May over the ocean of the western peninsula indicate an association of the rainfall event development over the peninsula, especially over the western coast.

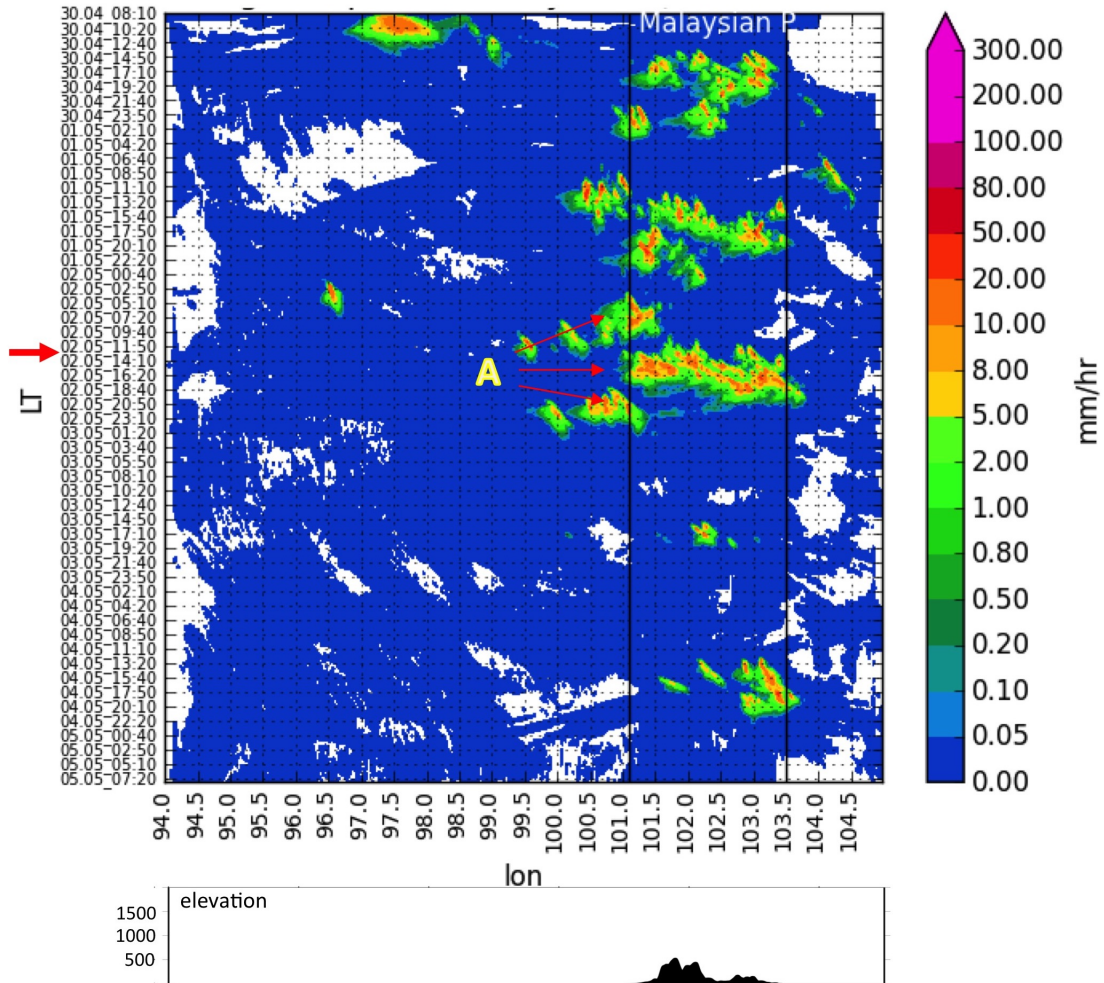


Figure 6.41: Time-longitude hovmöller plot from the *NoSI* experiment (1.5km model), averaged over $3^{\circ}N$ to $4^{\circ}N$. The red arrow on the left side of the box is pointing to the time of the event. The lines $101^{\circ}E$ and $103.5^{\circ}E$ represent the west and east coastlines of the Peninsular Malaysia, respectively.

The convective activities in this experiment are shown in Figure 6.43. When the Sumatra was removed, there were more convective activities concentrated closer to the coastal region of Peninsular Malaysia. The convective activities were visible over the west coast as well as over the ocean before the event. The convective activity is also visible from the 1100 LT across the Titiwangsa Mountains. A convective activity over the west coast (Figure 6.43 (A)) moves inland to merge with the orographic convection (Figure 6.43 (B)) by 1400 LT. The convective activity stays over the west coast as it is blocked by the Titiwangsa Mountains, preventing it from moving eastward. The convergence over the east coast is also visible starting in 1200 LT until later, demonstrating the sea breeze interaction with the land surface.

Looking at the zonal cross section in Figure 6.44, the process of rainfall development over the western peninsular on the 2 May is totally different. The winds over the western part of the domain are generally westerly (Figure 6.44 0000 - 1400 LT). A weaker land breeze is visible on the western coast of the peninsula by mid-morning (Figure 6.44 (A)), which is when the land breeze reaches its maximum

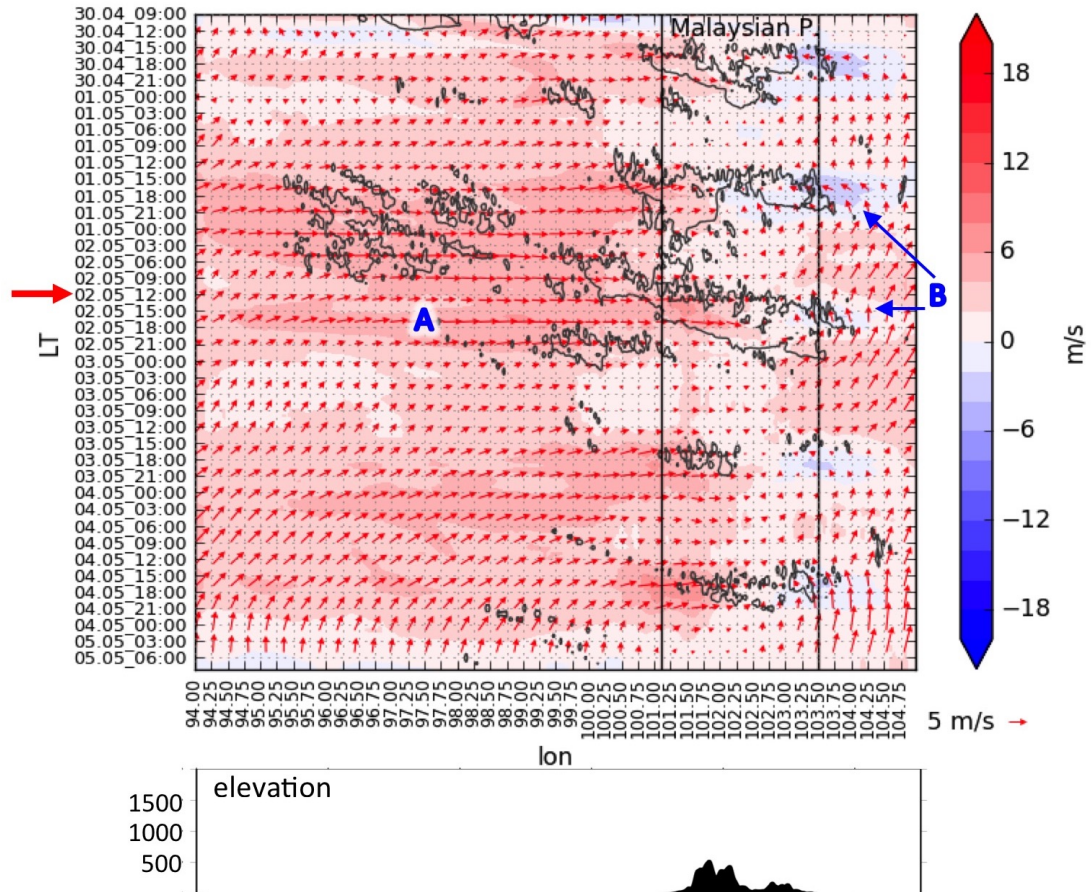


Figure 6.42: Time-longitude hovmöller plot of zonal wind (shaded) and wind direction and magnitude (vectors) from the **NoSI** experiment, averaged over 3°N to 4°N . The red arrow on the left side of the box is pointing to the event time. The lines 101.1°E and 103.5°E represent the west and east coastlines of the Peninsular Malaysia, respectively. The red colour represents westerly, and the blue represents easterly zonal winds. Wind vectors show the direction and strength of the winds. The dark contour represents rainfall with amount above 1 mm hr^{-1} , for an additional reference on winds and precipitation relationship.

and also coincides with the development of several rainfall events along the west coast. The westerly zonal wind is consistent over the west of the domain at 1100 LT and 1200 LT (Figure 6.44). By 1300 LT, there was convective activity over the west coast of the peninsula and strengthened by 1400 LT. The convective activity remained over the western peninsula as it is blocked by the Titiwangsa Mountains from moving eastward following the westerly and northwesterly winds.

The process of the development of the rainfall event in this experiment can be explained in Figure 6.45. For the no Sumatra (**noSI**) experiment in Figure 6.45, solar insolation, sea breeze and the westerly winds induced convection and yielded precipitation over the peninsula in the late afternoon of 1 May 2012 (Figure 6.45(a)). By midnight (Figure 6.45(b)), cold flow and land breeze enhance convection over the ocean near the coast and is enhanced by the incoming westerly winds. By mid-morning (Figure 6.45(c)), the convection had matured and yielded precipitation over the ocean near the coast. By midday (Figure 6.45(d)), the land was heated

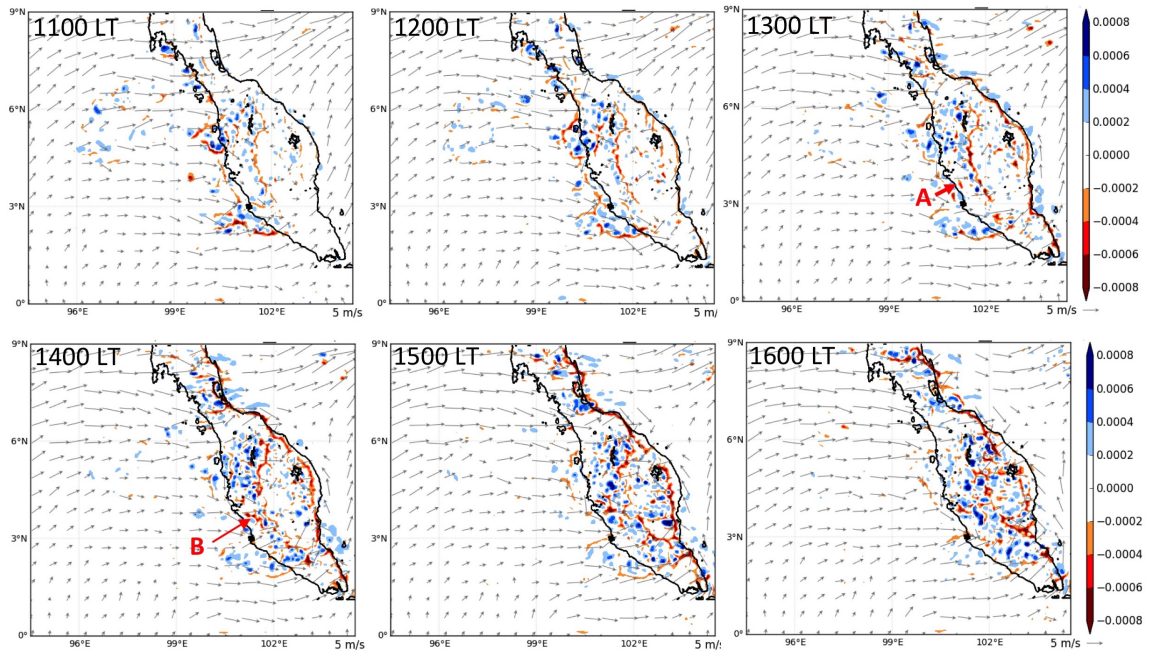


Figure 6.43: 13 metre winds in $m s^{-1}$ (vectors) and divergence/convergence in s^{-1} at 13 metre level (shaded), from the *noSI* experiment. Blue represents divergence (descending movement) and red represents convergence (ascending movement) of air. The photos show the convective activities from 1100 LT until 1600 LT.

and induces convection as the sea breeze developed. The convective activity was then enhanced by mountain breeze and rainfall over the ocean dissipated as the sea breeze circulation enhanced. Convection over the peninsula had matured and yielded precipitation. The Titiwangsa Mountains blocked the rainfall system for a few hours from propagating eastward.

6.2. CASE STUDY 1: FIRST INTER-MONSOON (APRIL-MAY)

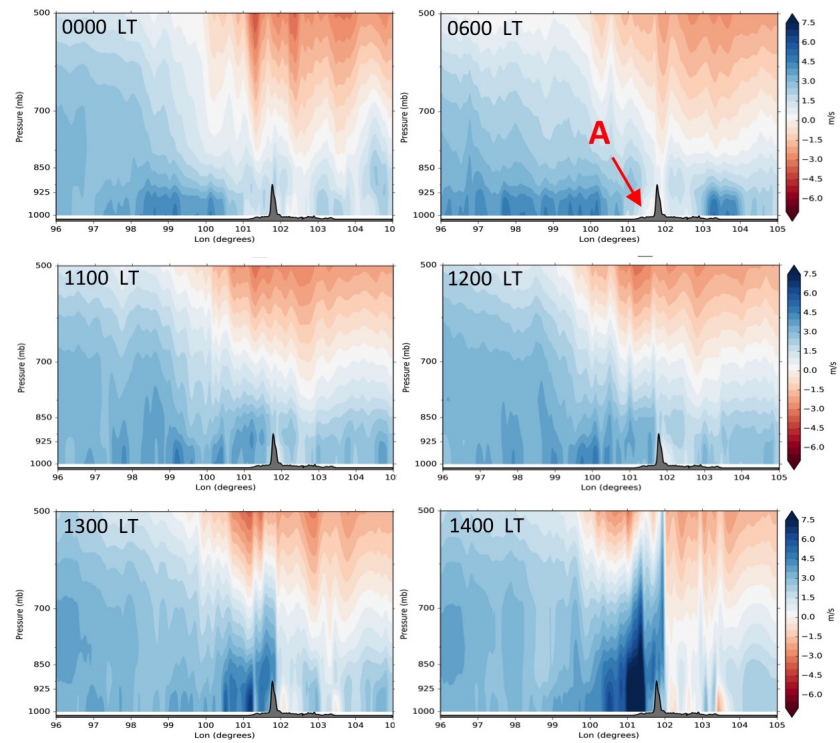


Figure 6.44: Zonal winds cross section, averaged over $3^{\circ}N$ to $4^{\circ}N$ for **NoSI** experiment of the 1.5km model.

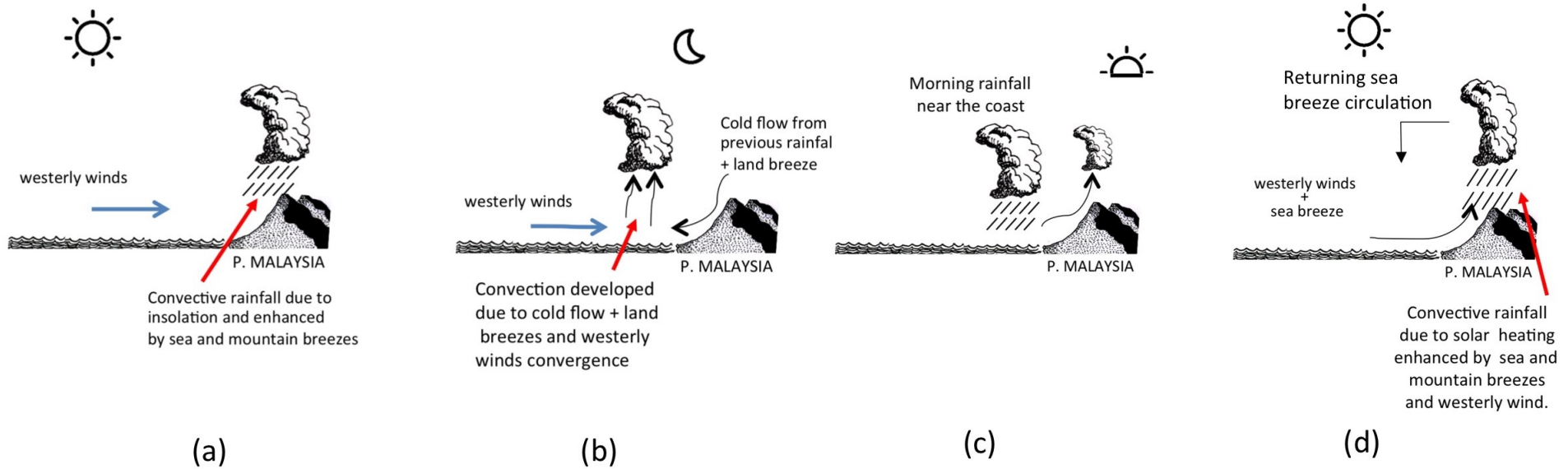


Figure 6.45: Schematic figures explaining the process of the development of rainfall on the 2 May in the *noSI* experiment. (a) Insolation, sea breeze and westerly winds induced rainfall over the peninsula in the late afternoon of 1 May 2012. (b) By midnight cold flow and land breeze enhance convection over the ocean near the coast and is enhanced by the incoming westerly winds. (c) By mid-morning, the convection had matured and yielded precipitation over the ocean near the coast. (d) By midday, the land was heated and induces convection, and sea breeze develops. The convective activity was then enhanced by mountain breeze and rainfall over the ocean dissipated as the sea breeze circulation enhances. Convection over the peninsula had matured and yielded precipitation. The Titiwangsa Mountains blocked the rainfall system for a few hours from propagating eastward. (Images were illustrated by the author.)

Comparison

This part compares the experiments with the control run and will be highlighting the main differences. Quantitatively, the results of the experiments can be viewed as daily total rainfall as in Figure 6.46. The figure shows the total rainfall over the north-west, west and inland regions (NWC, WC, and IL respectively) for the day -2,-1,0,1,2. In the focus region, WC, the rainfall on the event day in the control run shows a higher regional mean of total precipitation with **flatPM** and **flatSI** where the **flatPM** was 4.36 mm less than the control, and the **flatSI** was 1.77 mm less than control run. However, the **flatALL** and **NoSI** experiments show a higher total rainfall over the WC, where if we remove Sumatra, the rainfall is 18.19 mm more, and if both Peninsular Malaysia and Sumatra Island are flattened, the rainfall over this region is 2.87 mm more than the control run. One of the reasons for higher rainfall over the region in the **NoSI** experiment was mentioned earlier, there were rainfall events occurred before and after the event which contributed the higher daily rainfall amount for the 2 May 2012. The change in rainfall amount for the west coast Peninsular Malaysia (in **flatPM**) and the whole Sumatra in the domain of the study (in **flatSI**) is statistically significant at 95% level of significance (the calculation is not shown).

Looking at the other regions of interest, namely NWC and IL, the total rainfall shows a different result. The rainfall over NWC is higher in most of the experiments except **flatPM**. In the **flatPM** experiment, the rainfall is 1.34 mm less than the control run. The **flatSI**, **noSI** and **flatALL** experiments show 6.10 mm, 3.60 mm and 4.29 mm higher in total rainfall, respectively. The IL region shows a less rainfall except when we remove Sumatra Island. The rainfall is 7.91 mm more when Sumatra Island was removed. The rainfall average was less than the control in the **flatPM**, **flatSI**, and **flatALL** experiments, with value of 2.83 mm, 1.35 mm and 5.63 mm, respectively. These experiments affect each region differently, but two common results were observed. Removing the Peninsular Malaysia orography reduced the rainfall in all three regions, and removing Sumatra Island caused more rainfall.

In all flattened experiments, no orographic convection exist, and this is shown by the rainfall plot and convergence plot in Figure 6.47 and Figure 6.48, respectively. These results indicate that the Titiwangsa Mountains in Peninsular Malaysia and Barisan Mountains in Sumatra Island plays an important role in providing orographic rainfall (Figure 6.47 - red arrows), and this is also shown by the convergence plot Figure 6.48 (red arrows), in this case study, and possibly in all of the severe rainfall events over this region. This is, of course, need further experiment with more case studies included to be tested using the same method. Even if without the orography, there are still rainfall over the flattened landmass (Peninsula Malaysia or Sumatra or both, Figure 6.47 - blue arrows). This rainfall was developed by the

6.2. CASE STUDY 1: FIRST INTER-MONSOON (APRIL-MAY)

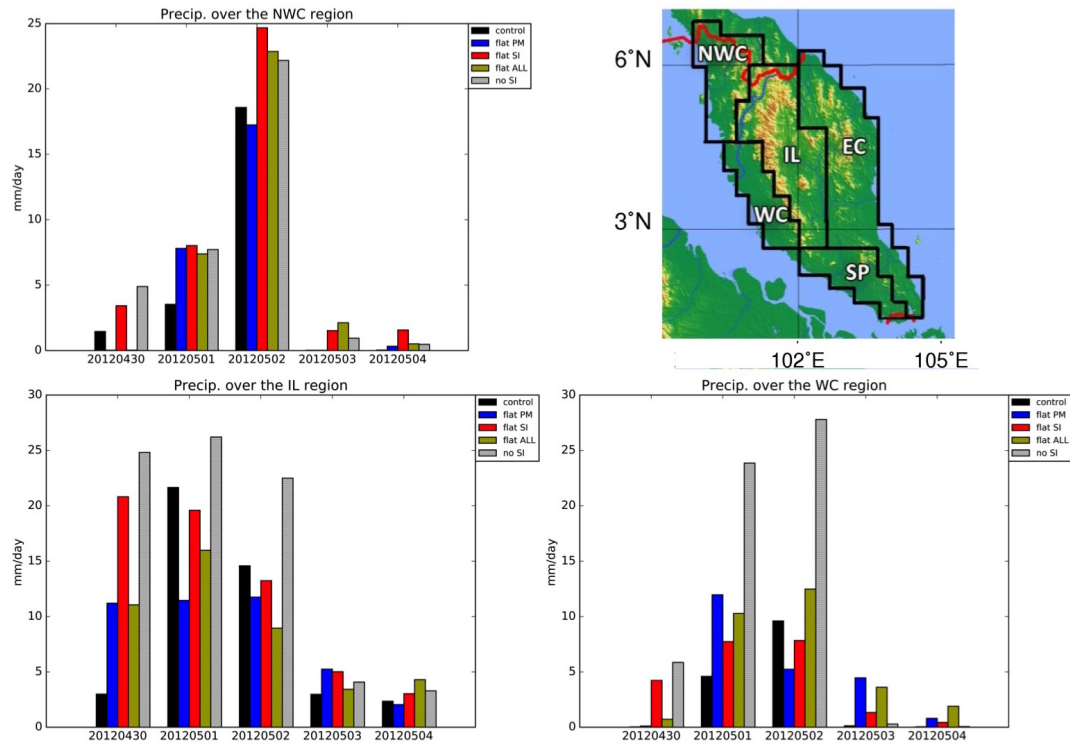


Figure 6.46: Daily precipitation total for the three regions of interest: northwest coast (NWC), west coast (WC) and inland (IL).

sea breeze interaction with the land surface.

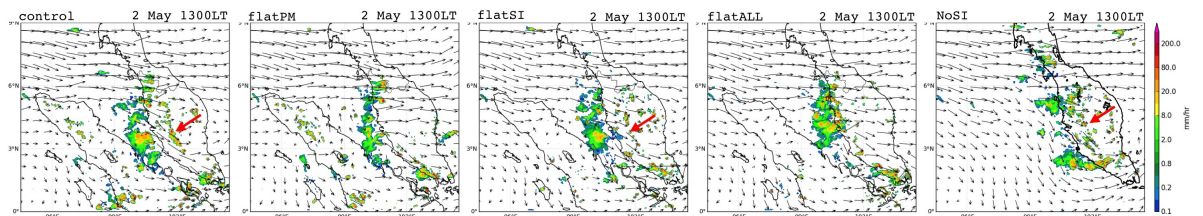


Figure 6.47: Rainfall and 850 hPa wind of control run, **flatPM**, **flatSI**, **flatALL** and **noSI** experiments, comparing the orographic rainfall in between the experiments by looking at the plot at 1300 LT on 2 May 2012. Red arrows showing the orographic induced rainfall.

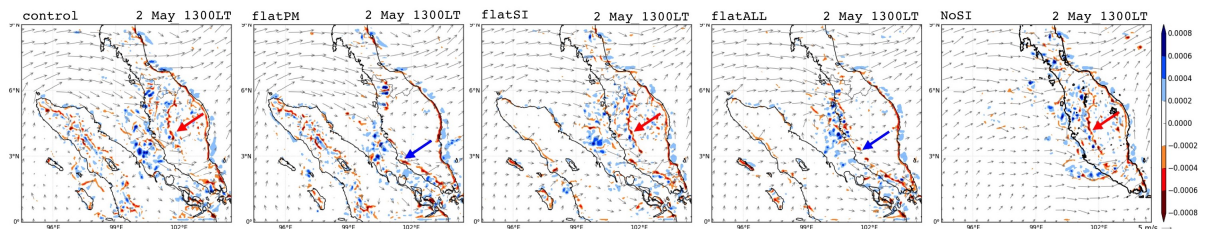


Figure 6.48: Convergence and 233 model level wind of control run, **flatPM**, **flatSI**, **flatALL** and **noSI** experiments, comparing the orographic rainfall in between the experiments by looking at the plot at 1300 LT on 2 May 2012. Red arrows showing convective activity over the Titiwangsa Mountains and blue arrows indicate the convergence over the coastal region from sea breeze interaction with land surface.

Another important finding in these experiments is, the importance of the peninsula and Sumatra Island on the development of the nocturnal or morning rainfall over the Strait of Malacca. As seen in Figure 6.49 (red arrows), in all experiments with or without the mountains, the morning rainfall will still developed, with a slight difference in intensity and location. Without Sumatra Island (NoSI), there are still rainfall events over the adjacent sea but not as intense as in the control run. The morning rainfall in the NoSI experiment is more likely caused by the northwesterly wind interaction with the land breeze and cold flow in the early morning of 2 May. The cold flow is the effect of the rainfall from the previous midnight in Peninsular Malaysia. The morning rainfall is also enhanced by the northwesterly winds from the north of the Strait of Malacca by enhancing the convection at the strait. It is also worth to note that there is a possible large-scale influence on the development of the morning rainfall over the Strait of Malacca, and the occurrence of rainfall on 1 and 2 May afternoon because both events occurred in all experiments. This also needs a further analysis such as larger scale domain experiment.

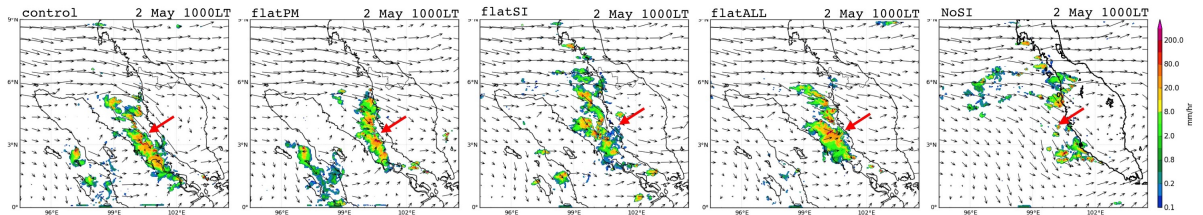


Figure 6.49: Rainfall and 850 hPa wind of control run, *flatPM*, *flatSI*, *flatALL* and *noSI* experiments, comparing the morning rainfall over the Strait of Malacca in between the experiments by looking at the plot at 1000 LT on 2 May 2012. Red arrows showing the morning rainfall over the Strait of Malacca.

To analyse the change in moisture for the *noSI* experiment compared to the control run, a vertical plot of a selected grid box over the west coast of the Peninsular Malaysia (3.5°N , 101.2°E) was plotted in Figure 6.50. The daily mean of the dew point temperature on the 2 May and the mean of the dew point in the afternoon of the 2 May are both higher than the CTR run. These results show that the extra moisture exists at western Peninsular Malaysia when there is no Sumatra on the west. The difference in the dew point temperature between CTR and *noSI* is 5.67°C .

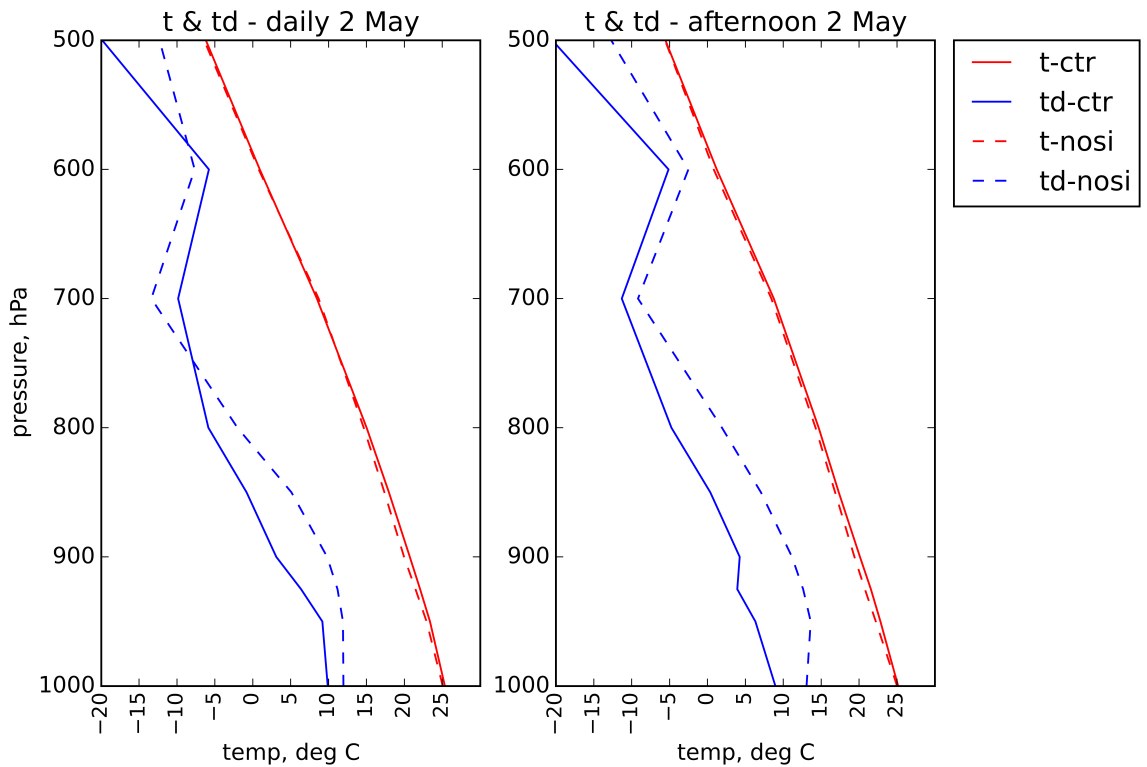


Figure 6.50: A comparison of temperature and dew point temperature in between CTR run and **noSI** experiment for a grid box in the western Peninsular Malaysia (3.5°N , 101.2°E). Solid line represent the CTR run and the dash lines represent the **noSI** run (solid: air temperature, dash: dew point temperature). This is a vertical plot and not a tephigram.

6.2.5 Summary

Based on Case Study 1, the 12km and 1.5km models of the Met-UM managed to reproduce the rainfall event. However, the 12km model overestimated the spatial distribution and underestimated the rainfall rate. The 1.5km model represents the rainfall event better, although the rainfall event is not at the exact location. The main event of the rainfall over the radar shows the heaviest rainfall at about 3 °N and 101.5 °E at the time of the event. Meanwhile, the rainfall event in the 1.5 km model shows the heaviest at around 3.4 °N and 101.25 °E. It also underestimated the rainfall rate. Using the 1.5km model to investigate the mechanism in detail, the 1.5km model managed to present the rainfall events over the Strait of Malacca and over the Titiwangsa mountains over the peninsula as observed in the radar images. The 1.5km model managed to get the rainfall on 1 May 2012 over the Peninsular Malaysia and Sumatra Island, and the rainfall over the Strait of Malacca in the morning of 2 May 2012. The 1.5km model also managed to reproduce the rainfall over the Titiwangsa Mountains of the Peninsular Malaysia on 2 May 2012. Although the rainfall event was not exactly where it should have been, the mechanism was properly simulated. The other fields such as wind are also properly simulated. The winds over the Andaman Sea diverted to the Strait of Malacca to be northwesterly, and westerly over southern Thailand. The wind turning from northwesterly to westerly over southern Peninsular Malaysia was also properly simulated. As shown from the previous studies, the most common mechanisms for the development of convective storms are sea breeze collisions, the combination of sea breezes and mountain breezes, the combination of lee waves and sea breezes and also the role of wind gaps in maintaining the convection over the west coast of Peninsular Malaysia. Not all of the mechanisms listed here were observed in this study. But the most common mechanism for the development of convective storms was observed, which is the combination of the sea breeze and mountain breeze. Based on these results, the 1.5km model performed better than the 12km model and been used to analyse the mechanism of the severe rainfall development for this case study.

As in Case Study 1, the amount of daily rainfall was definitely above the 90th percentile threshold and it was considered a heavy rainfall day. The rainfall amount was not extreme but it still caused flash floods over the west coast. One possible cause of the flash flood could have been the saturated land (on the west coast of the peninsula) from the rainfall event on the previous day. The mechanism can be explained by the following process:

1. On the afternoon of 1 May 2012, the western and inland regions of the Peninsular Malaysia, and northern and inland Sumatra experienced heavy rainfall. This is the result of convection due to solar insolation and was enhanced by northwesterly winds from the Indian Ocean and the Andaman Sea.
2. This afternoon rainfall influenced the development of convective activity over

the Strait of Malacca overnight. The cold flows (a density current mechanism) from both lands merged over the Strait of Malacca and develop convection, assisted by the land breeze circulation from both lands.

3. At the same time, a strong northwesterly wind coming from Indian Ocean/Andaman Sea enhanced the convergence and convection over the strait.
4. Then, on the morning of 2 May 2012, the Strait of Malacca experienced a heavy rainfall event that continued for most of the morning until noon.
5. By noon of 2 May 2012, convection developed over the Titiwangsa mountains due to solar insolation and matured to produce rainfall over the mountain ranges.
6. Cold pool from the rainfall system over the Strait of Malacca together with the sea breezes over induced convection over the west coast (of the peninsula).
7. The sea breezes combined with the cold pool from the rainfall over the Titiwangsa mountain range enhanced the convective activity over the west coast.
8. As the sea breeze circulation enhanced, the rainfall over the strait suppressed and convection over the west coast enhanced, and later matured to produce rainfall.
9. As the rainfall over the west coast enhanced, the rainfall over the Titiwangsa mountains spreading. The two rainfall system merged.
10. As the prevailing winds were northwesterly the rainfall system was prevented from moving eastward by the presence of the mountains, and thus it stayed stationary over the west coast.
11. The rainfall system continued for a couple of hours and then dissipated.

Elaborating on the mechanisms listed above, the Peninsular Malaysia and Sumatra experienced heavy rainfall on the late afternoon of the 1 May and these events are more likely due to the enhanced convection (from insolation) by the stronger northwesterly and westerly winds. Enhanced convection by the sea breeze and mountain breeze favour convective rainfall to occur in both peninsular and Sumatra. Later that night, after the rainfall subsides, the cold flow (a density current mechanism) response from the rainfall downdrafts propagated toward the Strait of Malacca and merged in the middle of Strait of Malacca to induce convection. This is also enhanced by the land breeze that is already developing, as a response to the change of air pressure between lands and the strait. The convection over the strait is also enhanced by the incoming northwesterly winds. After the convection had matured and produced rainfall in the mid-morning of the next day (2 May), the land is starting to heat and the land breeze is becoming a sea breeze. The heating land also induces convection over the peninsula (Titiwangsa mountains) and produced rainfall. The sea breeze and cold pool from the rainfall over the strait propagated toward the land (in this case the western peninsula) and the cold pool

from the rainfall over the Titiwangsa Mountains enhanced convection over the west coast of the peninsula. Later, as the sea breeze enhances, the rainfall over the strait dissipated, and convection over the west coast enhanced. The convection is fully developed to produce rainfall in the early afternoon and then merged with the rainfall over the Titiwangsa Mountains that is still occurring and expanding toward both sides of the mountains range. Rainfall over the west coast of the peninsula stayed over the west coast region despite the northwesterly winds as it is blocked by the Titiwangsa Mountains. While there are more factors involved in the development of this event, local orography plays one of the important roles.

With regard to investigating the role of local orography, the sensitivity experiment was done by flattening the orography in three ways. First, the orography of Peninsular Malaysia was removed (**flatPM**), then the orography of Sumatra Island was removed (**flatSI**), and finally the orography of both Peninsular Malaysia and Sumatra Island was removed (**flatALL**). The modification shows a significant difference in the amount of rainfall on the day over the west coast area.

In the first experiment, the flat Peninsular Malaysia received less rainfall on 2 May 2012 with the mean rain total is 5.2 mm day^{-1} for the WC region (54.6% of the control run), 11.8 mm day^{-1} for the IL region (64.1% of the control run) and 17.2 mm day^{-1} for the NWC region (92.8% of the control run). It is believed that the absence of the orography caused no afternoon rainfall over the inland peninsula due to the absence of the rainfall that initiated over the Titiwangsa mountains. Another reason for the observation in less rainfall is the absence of the Titiwangsa mountains, which may have caused the prevailing northwesterly winds to push the rainfall system across the peninsula resulting in less rainfall over the west coast. The convection over the Strait of Malacca still exists because the rainfall over Sumatra Island and the small-scale rainfall over Peninsular Malaysia on 1 May still occurs. However, the rainfall intensity over the Strait of Malacca is less than in the control run.

In the second experiment, the flattened Sumatra Island orography (**flatSI**) causes the rainfall over Sumatra on 1 May 2012 to be reduced significantly, but the rainfall over the peninsula still occurs. This condition causes the rainfall activity over the Strait of Malacca to be less intense on the morning of 2 May 2012, as the rain total mean is 7.8 mm day^{-1} (81.5% of the control run) for WC and 13.2 mm day^{-1} for IL (90.8% of the control run). However, it has increased in NWC with the mean rainfall of 24.7 mm day^{-1} (132.8% of the control run). The rainfall over the Titiwangsa Mountains is also observed. The combination of the rainfall event over the strait and that over the Titiwangsa mountains enhances the severe rainfall event over the west coast Peninsular Malaysia on 2 May 2012. However, the rainfall is less than in the control run over the west coast and inland.

As the orography of Sumatra Island and Peninsular Malaysia was flattened

(**flatALL**), the mean total rainfall over the west coast on 2 May 2012 was higher than in the control run by 2.87 mm day^{-1} over the WC and 4.29 mm day^{-1} over the NWC. The mean total rainfall was less in the inland region (IL) than in the control run by 5.63 mm day^{-1} . The absence of the Titiwangsa Mountains is believed to reduce the inland rainfall. It is not totally clear why there is a higher amount of rainfall over the west coast, but the absence of both mountain ranges may have influenced the rainfall system over the strait to move towards the west coast earlier and the combination with the convection over the coast may have added to the total rainfall in that region.

To investigate the role of Sumatra Island, the island was removed in the final experiment (**noSI**). The daily total rainfall increased significantly. The total rain on the 2 May is 27.8 mm day^{-1} over the WC (289.4% of the control run), 22.5 mm day^{-1} over the IL (154.3% of the control run) and 22.2 mm day^{-1} (119.4% of the control run) over the NWC. Rainfall over the west coast only occurred three times on 2 May 2012. The rainfall over the west coast occurred as early as 0300 LT on 2 May and stopped after 1000 LT. Then another rainfall event occurred at 1200 LT for almost six hours. At 2000 LT, another rainfall event occurred near and over the west coast. These events contributed to the high total rainfall over the region. The frequent rainfall events were also influenced by the higher moisture available as discussed from Figure 6.50, based on a dew point temperature values. A higher dew point temperature when the Sumatra Island was removed indicates a higher moisture available to develop precipitating cloud over the western peninsula, as compared to the control run. Although there is no clear evidence, it is hypothesised that the westerly wind from the Indian Ocean brings the extra moisture to the peninsula.

Although the rainfall event on the day may have influenced the flooding and landslide events over the west coast of the peninsula, it was not the sole reason. The rainfall event from the previous day may have caused the land to be partially saturated with water and the additional water from the rainfall on 2 May 2012 may have saturated the land and caused the floods and landslides. Other considerations should also be included such as drainage and irrigation issues. There is more to look at from this case study, but the results presented here are enough to initiate more studies in the future for more in-depth investigation in terms of dynamics and thermodynamic aspects of the development of the rainfall event. In particular, the role of local orography and Sumatra Island in the development of the rainfall event over Peninsular Malaysia could be further investigated.

6.3 Case Study 2 : Second Inter-monsoon (Sept.-Oct.)

6.3.1 Introduction

Unlike Case Study 1, this event occurred in the morning over the land where the heaviest rainfall occurred in northwestern Peninsular Malaysia. This event also occurred during the second inter-monsoon season, in September-October. A study from MetMalaysia by Phang and Shaari (2011) using 4 northwestern peninsula rain gauge stations data from 1985-2009 shows that on average, an extreme rainfall event ($\geq 80 \text{ mm day}^{-1}$) over northwestern Peninsular Malaysia occurred 4 times annually, with September and October being the months most inclined to the extreme rainfall event. In this case study, the event was relatively recent and some of the observational data are limited. The gauge data (Figure 6.51 (a)) shows a maximum rainfall over the Alor Setar station at 0100 LT on 24th September 2014 of 23.8mm and the final accumulated amount of 81mm. The rainfall started at 2300 LT the previous day and continued for the next 5 hours and dissipated after sunrise. Figure 6.51 (b) shows the high amount of rainfall over northwestern Peninsular Malaysia. This event was not associated with the active MJO phases 3, 4 and 5, and was in a neutral phase of ENSO.

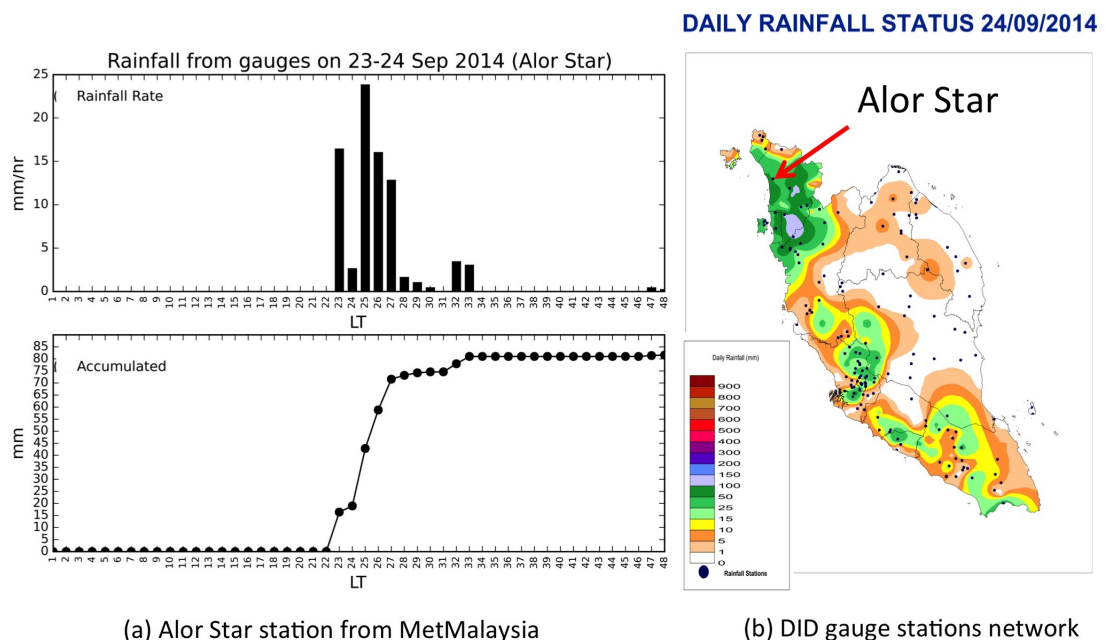


Figure 6.51: (a) Rainfall recorded from the gauge from Alor Setar station on 24th Sept 2014. (b) Rainfall distribution based on gauges measurement on 24 Sept. 2014. Figure was retrieved from Dept. of Irrigation and Mitigation Malaysia database website.

This event was detected on the radar network as shown in Figure 6.52 around 0400 LT (no radar images are available before 0400 LT). The rainfall events were observed over the north-west coast of the Peninsular Malaysia and central Strait of

Malacca. They dissipated around 0900 LT and cleared by noon, except over some areas on the strait. The same can be observed in the satellite figures (Figure 6.53). A group of convective clouds was observed over the northern part of the Strait of Malacca and the north-west coast of the Peninsular Malaysia (yellow arrow). The same evolution as in the radar images was also observed; the convective clouds over the northwestern part of Peninsular Malaysia were observed at around 0400 LT and dissipated by 0900 LT. As seen in gauge dataset from Alor Setar station (Figure 6.51(a)), the rainfall event started at around 2300 LT on 23 September 2014 (previous day) and extended overnight and for at least 10 hours afterwards.

Based on the TRMM dataset, the rainfall over the north-west region started as early as 1700 LT on 23 September 2014 (Figure 6.54) and lasted for more than 10 hours. The rainfall started to become more severe near the coast and on the land of northwestern Peninsular Malaysia by 0200 LT on 24 September 2014, when it spread over the north part of the Strait of Malacca. It eventually stopped raining over land by 1100 LT on 24 September 2014 (Figure 6.54). The rainfall was still observed over the strait at 1100 LT and again a rainfall event was observed over northwestern Peninsular Malaysia with some other rainfall over the southwestern peninsula. However, the focus of this case is on the morning rainfall on the northwestern peninsula. The 850 hPa winds as observed in the ERA-Interim dataset (Figure 6.55) show as prevailing southeasterly wind over the Strait of Malacca, where the winds were mostly turning from easterly in the equator to westerly around 9 °N. Comparing to the HR90 composite of 850 hPa wind in Chapter 5, the mean winds, in this case, were not similar to the NWC-SO case composite (mean the wind is westerly with northwesterlies over the Strait of Malacca region in Figure 5.7). However the anomaly composite in Figure 5.9 shows an easterly anomaly for NWC cases.

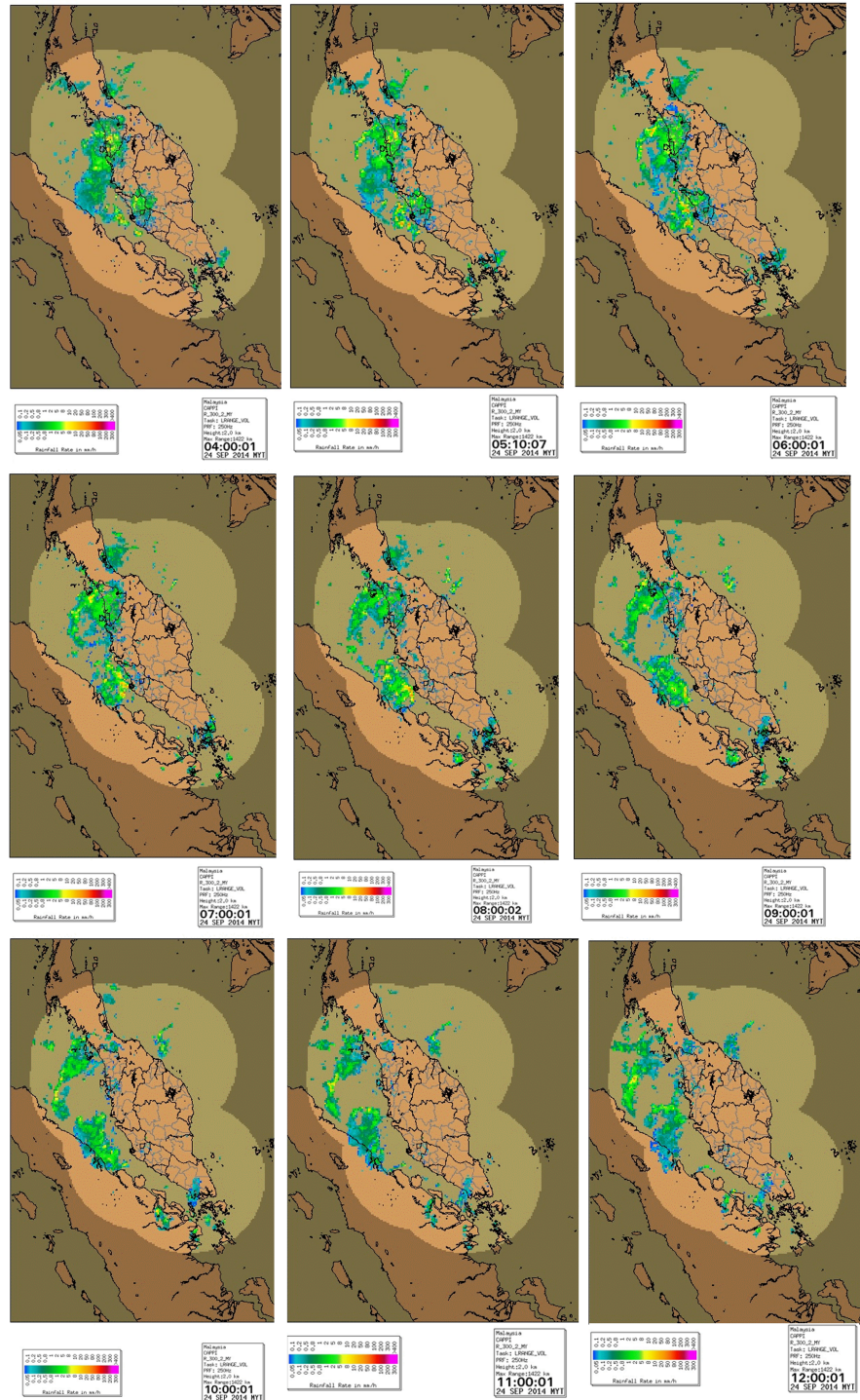


Figure 6.52: The radar images show the evolution of the rainfall over the northwestern Peninsular Malaysia in the morning of 24 September 2014. The images are from the MetMalaysia website from 0400 LT to 1200 LT on 24 September 2014. No images before 0400 LT were available.

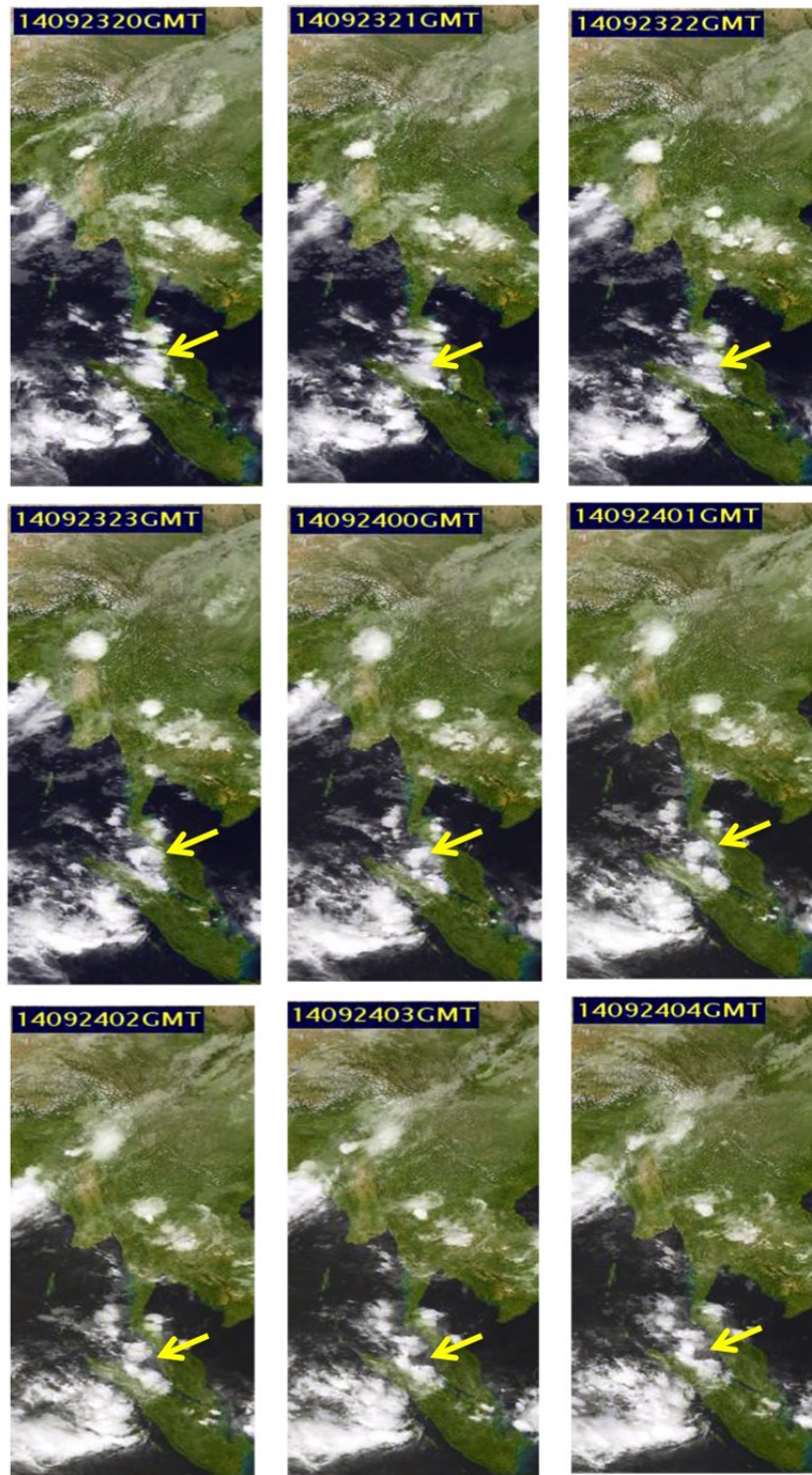


Figure 6.53: The satellite images show the evolution of the convective clouds in the morning of 24th September 2014 over the northwestern Peninsular Malaysia (yellow arrow). The images are from the Kochi University Weather archive from 2000 UTC 23 Sept 2014 (0400 LT 24 Sep 2014) to 0400 UTC (1200 LT) 24 September 2014.

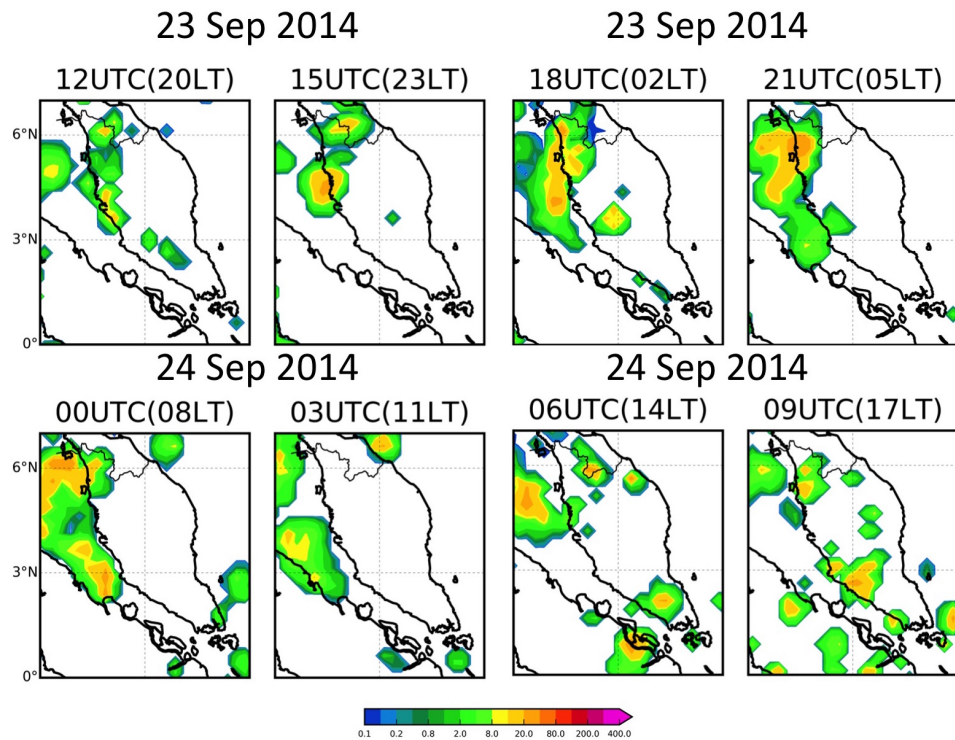


Figure 6.54: Precipitation from TRMM (3-hourly mean) from 2000 LT on 23 September until 1700 LT on 24 September 2014. The images agree with the radar and satellite images on the location and time of the event.

850 hPa winds (ERA-Interim)

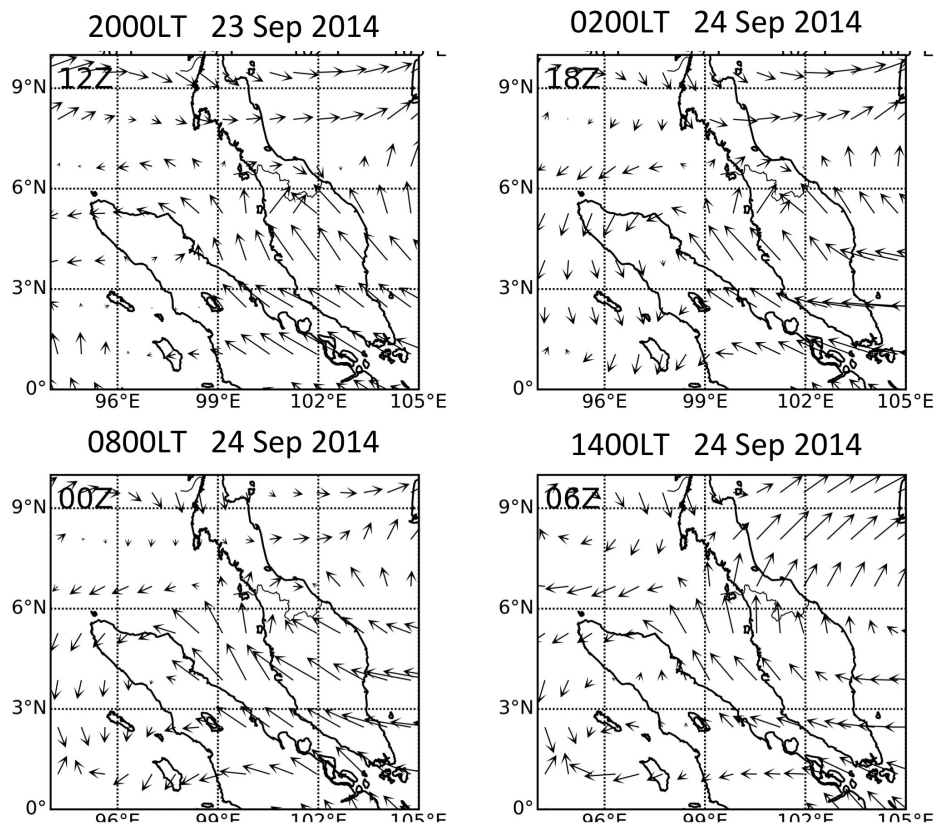


Figure 6.55: 6-hourly 850hPa winds from 2000 LT 23 September to 1400 LT 24 September 2014. The winds were mostly southeasterly over the Strait of Malacca and in the vicinity.

6.3.2 Simulation: Control Run

The 12km model captured the convective activity over the Strait of Malacca and over the north-west of the peninsula. However, the rainfall was not quite over the region as observed in the radar images. A light rainfall event was observed over part of the northwestern area, but this was not as strong as the observation. As shown in Case Study 1, the 12km model overestimated the rainfall distribution (spatially) over the region. On the other hand, the precipitation produced in the 1.5km resolution model did not capture the event over the north-west of the peninsula (Figure 6.56). A few little patches of rainfall appeared at 0400 LT near the north-west coast, but they did not last for more than an hour and did not grow into a severe event.

Compared to the TRMM dataset (Figure 6.57), the 3-hourly mean shows that the 12km model poorly simulated the rain over the northwestern peninsula and the north Strait of Malacca. The TRMM shows a rainfall event over north-west Peninsular Malaysia in the early morning (0200, 0500, and 0800 LT as in the event of interest). The only consistent feature between the TRMM and the 12km model is the rainfall over the Strait of Malacca. However, the model underestimated the intensity. The 12km model overestimated the rainfall over both Peninsular Malaysia and Sumatra Island in the afternoon. The 1.5km model was also unable to simulate the event properly. The model underestimated the spatial distribution of the rainfall, where there are only a few patches of rain observed in the simulation over the northwestern peninsular and the Strait of Malacca (0200, 0500, and 0800 LT). The rainfall over the western Sumatra seems to be realistically simulated, but not over the Strait of Malacca and Peninsular Malaysia.

The general wind pattern is not very different between the models and the ERA-Interim dataset (Figure 6.58). The wind is southeasterly in most of the Peninsular Malaysia area and the Strait of Malacca. The winds over the Andaman Sea and the Indian Ocean are however slightly different in the model compared to the ERA-Interim. The winds are mostly westerly over the Indian Ocean and Andaman sea in both the observation and the models but are slightly different over at the north-west and west of Sumatra Island. The winds over the areas are more northeasterly in the observation (ERA-Interim) but more westerly in both models and there is a visible wind disturbance on the west coast. While the models do manage to get the right wind direction over the Peninsular Malaysia and Strait of Malacca, the difference over the Indian Ocean may be a sign of an error in the model physics, which has led to an error in the other diagnostic fields, namely rainfall.

At this point, the reason for the unrealistic simulation is still unclear, and it is hard to only look at one case to speculate the reason. The rainfall event over northwestern Peninsular Malaysia is also reproduced in the forecast field output from the ERA-Interim (not shown) indicates that the ERA-Interim atmospheric

model managed to capture the event. This suggests that the error in the experiment of this thesis is possibly an isolated error made while simulating the case using Met-UM. Since this thesis does not focus on finding the reason for the model error, the reason for the error can only be hypothesised. The inability of the model to reproduce the rainfall event may be because of its physics (the convection scheme), the land surface model used in the UM and some less accurate initial (or boundary) conditions. Because of the unrealistic simulation produced by the models, it is difficult to further investigate in detail the mechanism involved in the development of the severe rainfall event for this case study.

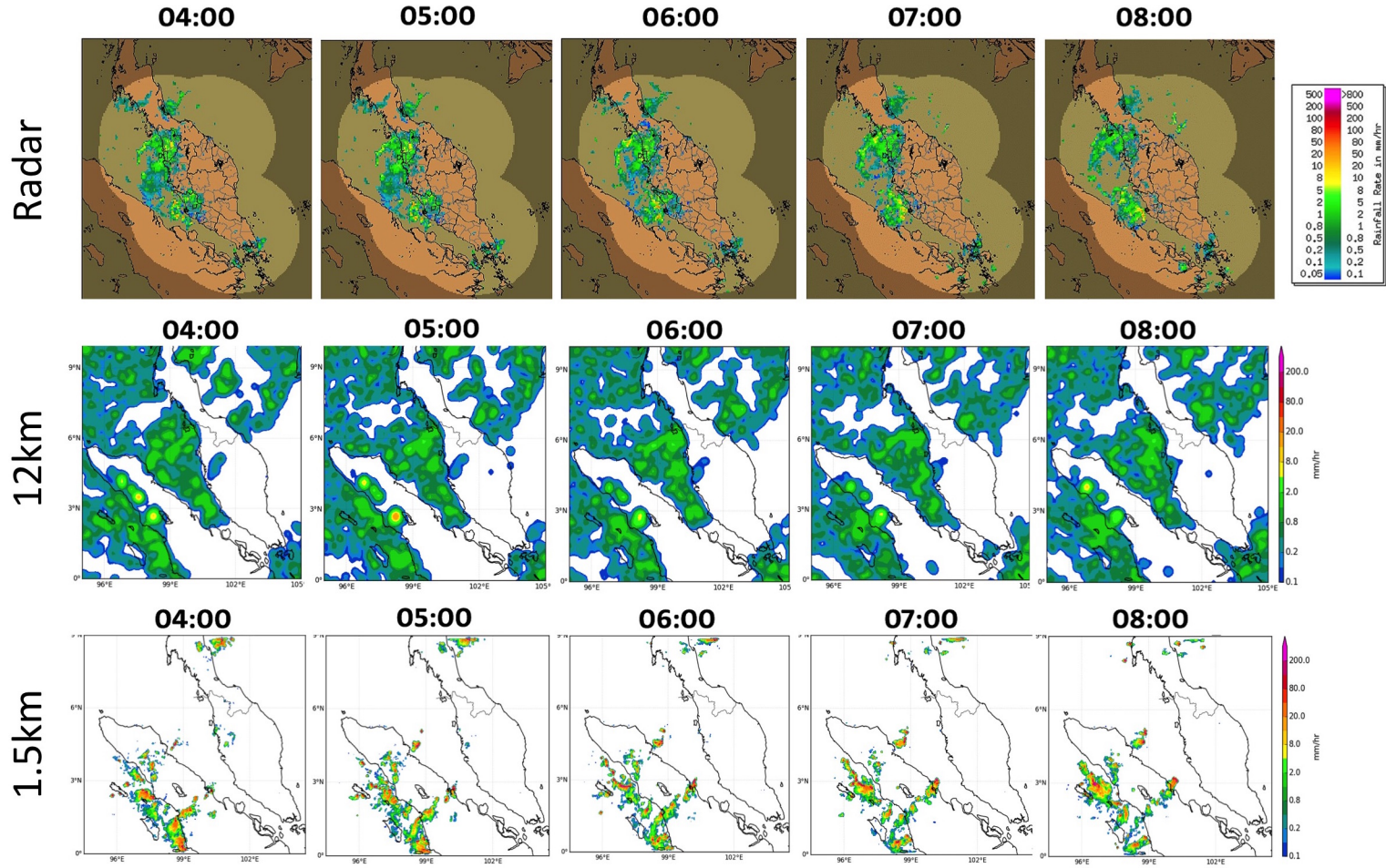


Figure 6.56: (top) Radar images on the morning of 24th September 2014 from 0400 LT to 0800 LT. (middle) Precipitation from the 12km model for the same period. (bottom) Precipitation from the 1.5km model run for the same period.

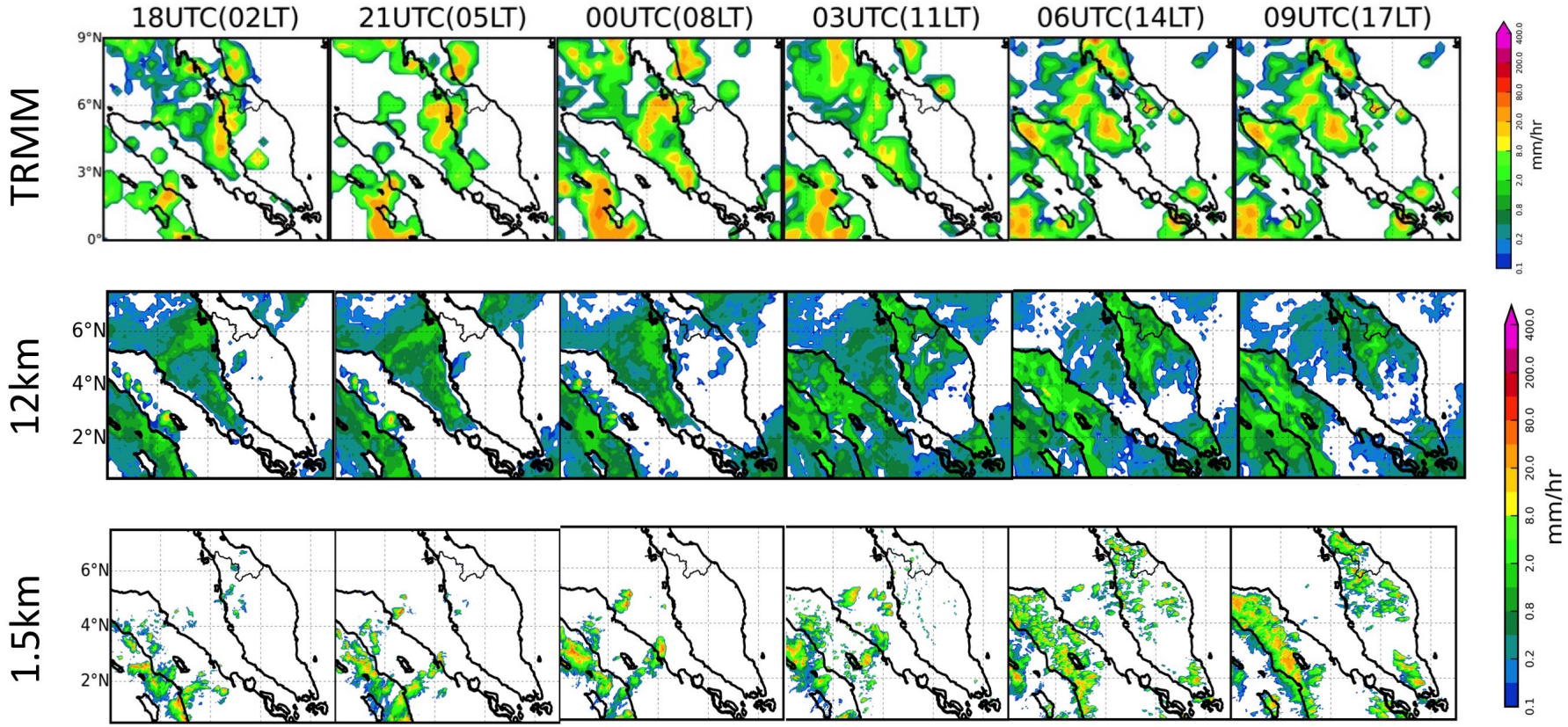


Figure 6.57: (top) 3-hourly TRMM on the 24th September 2014 from 0200 LT to 1700 LT. (middle) Precipitation from the 12km model for the same period. (bottom) Precipitation from the 1.5km model run for the same period.

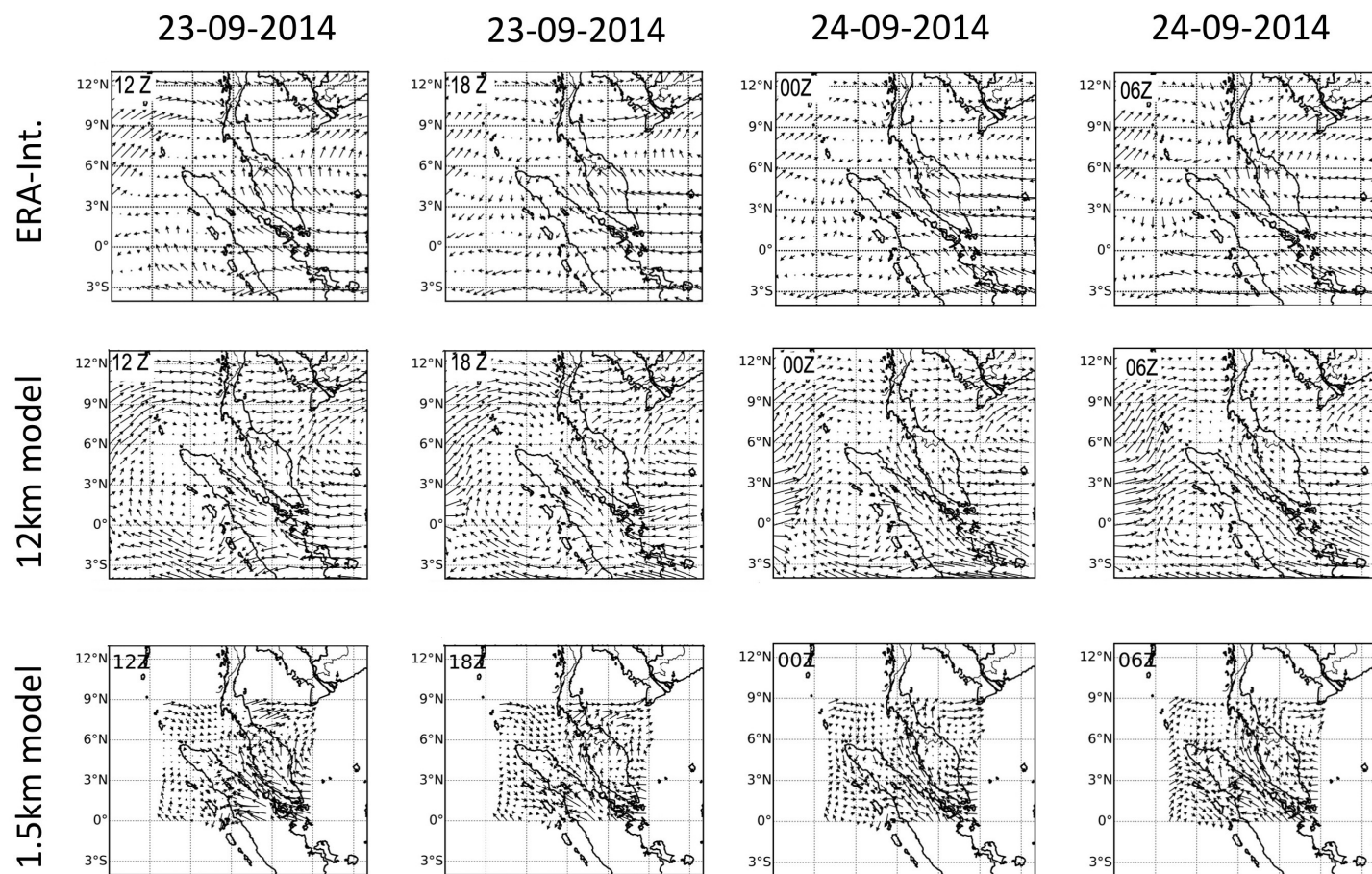


Figure 6.58: 850hPa winds as compared between ERA-Interim, the 12km model and the 1.5km model. Six-hourly from 1200 Z /2000 LT on 23 Sept 2014 to 0600 Z /1400 LT.

6.3.3 The Role of Orography and Sumatra Island

Even though the control run did not produce a realistic rainfall pattern in the 1.5km model, the sensitivity experiment, which involved adjusting the orography, was still performed with only the 1.5km model. The same experiments were done as listed below:

1. Experiment 1: Flat Peninsular Malaysia orography (**flatPM**)
2. Experiment 2: Flat Sumatra orography (**flatSI**)
3. Experiment 3: Flat Peninsular Malaysia and Sumatra orography (**flatALL**)
4. Experiment 4: No Sumatra (**noSI**)

Although this event was not properly simulated in the control run, this experiment can provide an insight into how orography affects the wind flows. This is different from Case Study 1, because the winds are from southwesterly over Peninsular Malaysia, and it is an early morning event. However, the discussion will not be more than just a rainfall and surface wind.

6.3.3.1 Exp. 1: The Role of the Titiwangsa Mountains in Peninsular Malaysia

The **flatPM** experiment will be looking at the role of the Titiwangsa Mountains on the rainfall and the winds over the region. A significant amount of rainfall in northern Peninsular Malaysia was observed and it dissipated immediately after another system developed near the coast of north-west Peninsular Malaysia (Figure 6.59). The prevailing southeasterly winds over the peninsula may have influenced the rainfall development over the northern and north-west Peninsular Malaysia as this is the region where the southeasterly winds and westerly winds from the Indian Ocean converge and turn to westerly across the Thai Gulf (northeast part of the domain). The converging southeasterly wind from the south of Strait of Malacca and the northwesterly wind from the Andaman Sea over the north of Strait of Malacca could be the main factor to develop convective cloud over the northern Strait of Malacca area that eventually produced rainfall. Without the orography over Peninsular Malaysia (**flatPM**), the wind is stronger inland as expected, but more southerly over the west coast.

It is indeed strange to observe that the rainfall took place longer until 0900 LT in this experiment when the rainfall in the control run dissipated by 0500 LT and in a slightly different location. Without the Titiwangsa Mountains, the convective activity which was developed from the converging southeasterly wind from the southern Strait of Malacca and northwesterly from the Andaman Sea is moving inland and matured over time to produce rainfall. There is no detailed analysis to find the reason why rainfall is produced in this experiment but not in the control run. The change in the orography of Peninsular Malaysia definitely modified the local circulation and condition to favour rainfall.

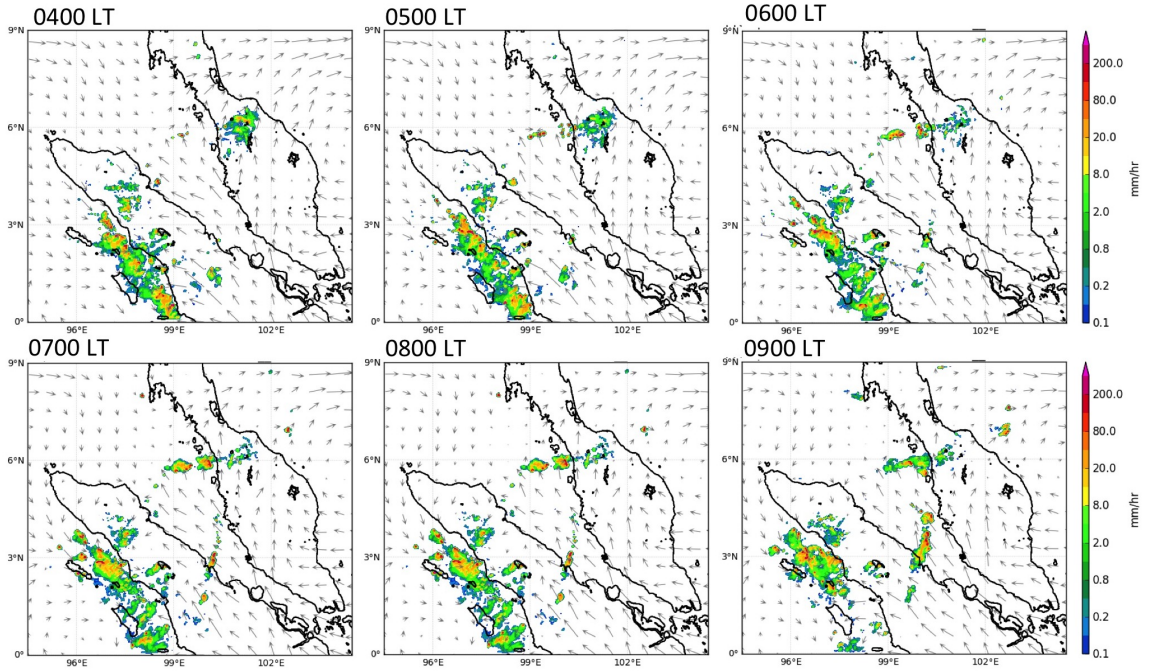


Figure 6.59: Rainfall in the flat Peninsular Malaysia orography (**flatPM**) experiment. The images shown were from 0400 LT until 0900 LT 24 September 2014.

6.3.3.2 Exp. 2: The Role of the Barisan Mountains in Sumatra Island

In the **flatSI** experiment (Figure 6.60), the patches of rainfall over the northern Peninsular Malaysia are smaller than in the **flatPM** experiment. The rainfall system is staying in the northwestern region as it was blocked by the Titiwangsa Mountains before dissipated by mid-morning. When there is no orography over Sumatra (**flatSI**), the northwesterly winds are stronger than the southeasterly wind (unlike in **flatPM** experiment). The rainfall over the western Sumatra is also more toward the landmass, as there is no Barisan Mountains. Furthermore, the strong southeasterly at the central Sumatra producing rainfall as it converges with the easterly winds from the Strait of Malacca.

This experiment is also producing a longer rainfall over the northwestern peninsula, unlike in the control run. The rainfall over the northwestern peninsula is also believed to be produced by the converging southerly wind (over the northwestern peninsula) and the westerly winds from the west. The rainfall is also over the right area (as in the radar) but smaller in spatial size. This result also shows that the change in the orography modifies the circulation and more conducive to produce rainfall over the northwestern peninsula.

6.3.3.3 Exp. 3: The Role of Titiwangsa and the Barisan Mountains

In the **flatALL** experiment (Figure 6.61), the patches of rainfall over northwestern Peninsular Malaysia are weaker than in the **flatPM** experiment and the rainfall over the western Sumatra is also weaker than the rainfall in the **flatSI** experiment.

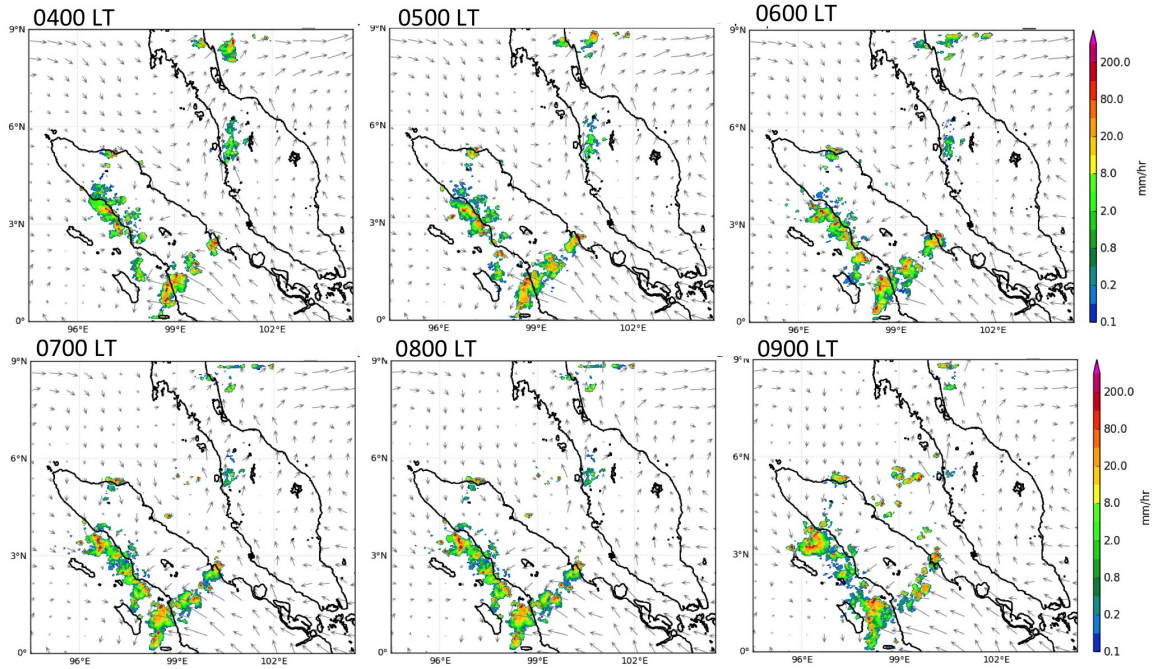


Figure 6.60: Rainfall in the flat Peninsular Malaysia orography (**flatSI**) experiment. The images shown were from 0400 LT until 0900 LT 24 September 2014.

The rainfall is also longer and dissipated by noon. The winds are expected to be stronger inland with no strong southeasterly over the Strait of Malacca as in the control run. The converging southeasterly from the southern Strait of Malacca and northwesterly from the Andaman Sea as well as the overturning wind from Strait of Malacca to the Gulf of Thai are believed to produce a favourable condition to produce rainfall over the northwestern Peninsula Malaysia.

This experiment shows a combination of **flatPM** and **flatSI** experiments but with slightly less intense rainfall. The absence of the Barisan Mountains in Sumatra and Titiwangsa Mountains in Peninsular Malaysia is believed to modifies the weather circulation over this region. This is, of course, need in-depth analysis to understand how. The experiments still show some of the important roles of orography based on the three experiments above. It is also difficult to understand the role of the local orography and Sumatra Island in modifying the rainfall due to the unrealistic result in the control run. But the modified orography does make a difference over north-west Peninsular Malaysia.

6.3.3.4 Exp. 4: The Role of Sumatra Island

Several rainfall events can be observed near the coast of western Peninsular Malaysia in the **noSI** experiment (Figure 6.62). These rainfall events did not spread inland (specifically over north-west Peninsular Malaysia) and appeared to move westward. The rainfall is also more than the other experiments and control run. The overturning southeasterly winds from the west of the peninsula to the Gulf of Thai

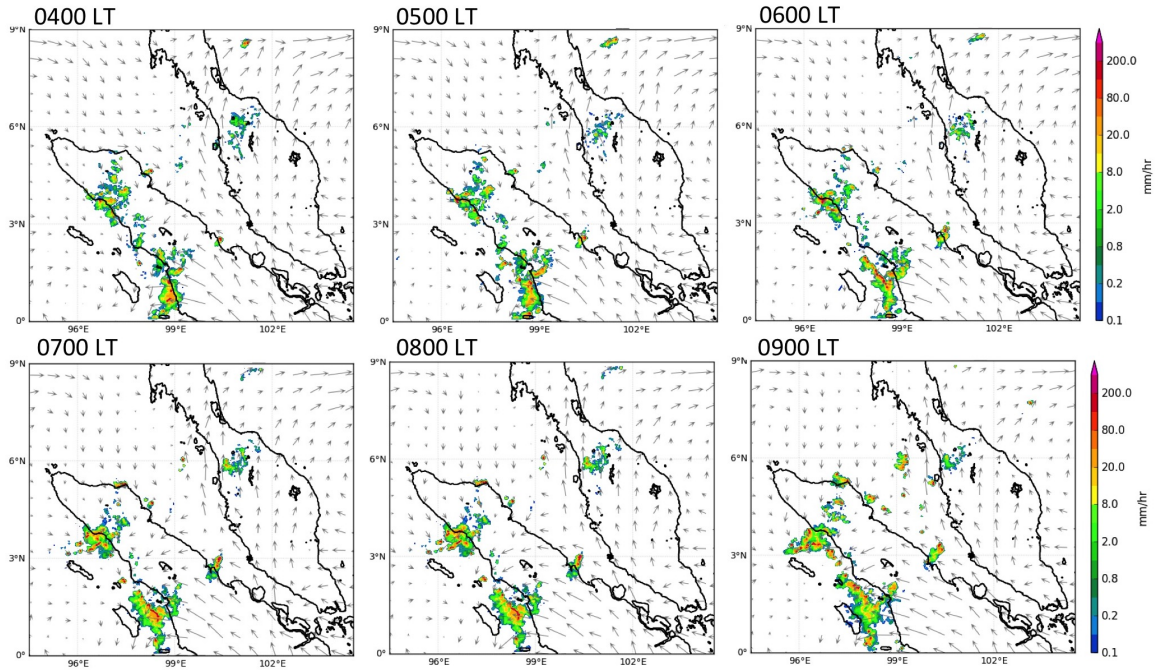


Figure 6.61: Rainfall in the flat Peninsular Malaysia orography (**flatALL**) experiment. The images shown were from 0400 LT until 0900 LT 24 September 2014.

over the northern peninsula as well as the converging northwesterly winds from the Andaman Sea and southeasterly winds from the south of the peninsula producing convective activity over the north-west and western peninsula which eventually producing rainfall. The winds are also calmer on the west side of the domain, which is where the northwesterly and southeasterly winds met, but not producing any rainfall over the ocean. The small patches of rainfall over the edge of the western of the domain is most probably from the initial boundary condition.

This experiment is expected to have more rain, because of the vast open ocean on the west that will provide more moisture from the ocean. The rainfall observed in this experiment is not over the land and more on the adjacent ocean, and this is also expected from the early morning rainfall. The gravity wave plays its role by providing the atmospheric instability over the adjacent sea and combined with the land breeze circulation, induce convective activity.

In all of the experiments, the rainfall over north-west Peninsular Malaysia was not prolonged until mid-morning on 24 September and was not as large (spatially) as the observation (radar). These results can also be used as a hint regarding the role of orography and Sumatra in assisting the severe rainfall development, although this issue needs a more in-depth study to be properly understood.

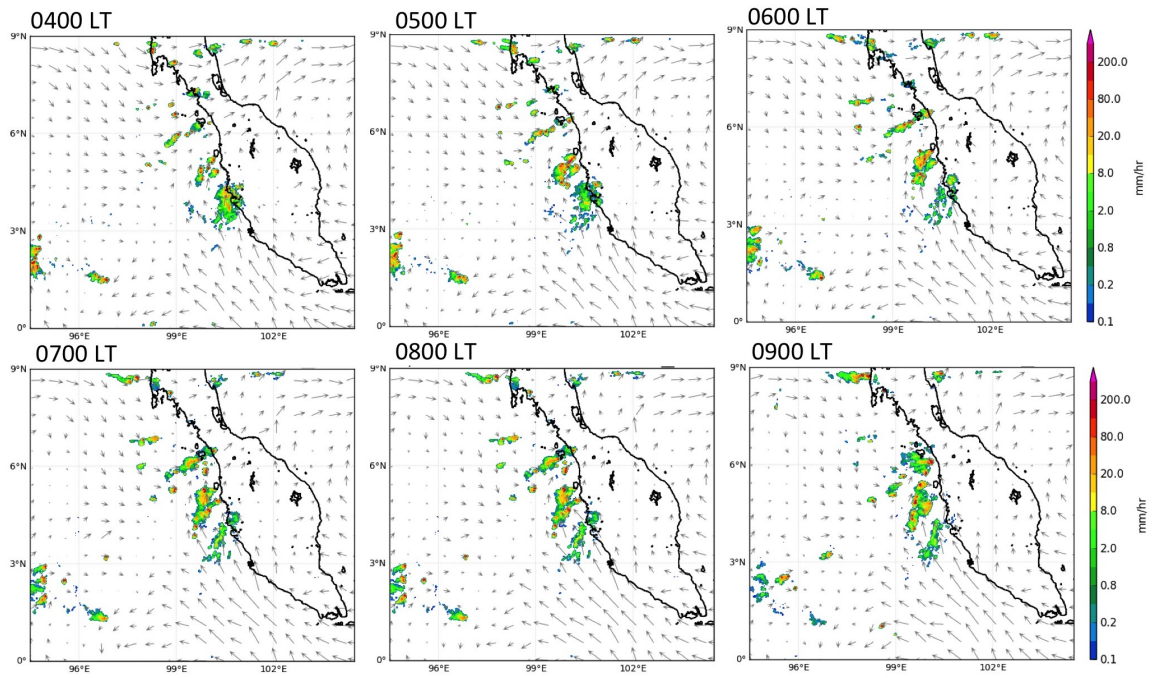


Figure 6.62: Rainfall in the flat Peninsular Malaysia orography (*noSI*) experiment. The images shown were from 0400 LT until 0900 LT 24 September 2014.

6.3.4 Summary

It is unfortunate that this simulation did not reproduce the rainfall event over northwestern Peninsular Malaysia, especially in the 1.5km model. The 12km model managed to reproduce the rainfall over the Strait of Malacca, but not spreading over land (northwestern Peninsular Malaysia) as in the observation (radar and TRMM). Even in the 1.5km model, the rainfall is not properly simulated even in the strait and over Peninsular Malaysia. The model failed to simulate the overnight rainfall over northwestern Peninsular Malaysia. The comparison with the winds between the ERA-Interim data and the model simulation shows a mostly similar wind pattern over the Peninsular Malaysia and Strait of Malacca, which is southeasterly. The slight difference over north-west Sumatra may be another signal that the model did not manage to accurately simulate the weather conditions on the day over the domain.

Sensitivity experiments in the 1.5km model were also performed and the result may give an insight into the role of local orography and Sumatra in the weather over western Peninsular Malaysia. All of the flattened-orography experiments managed to reproduce the rainfall over northwestern Peninsular Malaysia but it is not as intense as in the observation (radar). The patches of rainfall events dissipated early and were not prolonged until mid-morning on the 24 September. In the no Sumatra experiment, the rainfall over western Peninsular Malaysia was observed but it was not as strong as in the observation and it was not on the land, in particular over the northwestern peninsula. This experiment also shows the role of Sumatra in the weather conditions over western Peninsular Malaysia. No Sumatra means a wetter Peninsular Malaysia west coast. These experiments also reveal that the combination of southeasterly winds over the peninsula and the strait with the westerly winds from the Indian Ocean may have influenced the development of rainfall over the northern and northwestern Strait of Malacca and Peninsular Malaysia. These results show the influence of the orography on the severe rainfall development. However, it is difficult to draw conclusions as the model did not produce the right rainfall event in the control run. The odd results in the sensitivity experiments also raise the question of how much the orography affects the severe rainfall development over western Peninsular Malaysia (with the exception of the **noSI** experiment).

While modelling and forecasting of weather are improving, it is still an approximation of the real physical processes and thus the reason for the error could be from the failure in the model physics (such as the convection scheme), the land-surface model used, and less accurate initial (or boundary) values. For example, a slight error in the initial phase of the model calculation such as the difference in cloud cover in the initial stage may disturb the radiation calculation and eventually lead to miscalculations in the rainfall process. Further study on this matter is needed. Using a high-resolution model with the explicit convection scheme is

generally better to simulate rainfall to represent reality, but this is not always the case. As in Case Study 2, the 1.5km model did not manage to realistically simulate the event, but the 12 km model did simulate the rainfall even though it was not as realistic as in the observation. These results also raise the question of how much the resolution change can improve the model result. This matter should be investigated with a proper study focusing on the model, the model physics and the convection schemes in order to understand it better.

The main objective of this thesis is not to explore the model error, but it is important, in the future, to investigate this issue. While to investigate more on both larger domain and lengthier timescale are computationally expensive and time-consuming, another approach may be easier. Checking against other forecast product such as Weather Research and Forecast (WRF) products of ERA-Interim (a model analysis) may help us determine if that particular case study is able to be reproduced by another model, and also to check the radiosonde profile and compare it with the simulation result especially the hours or days before the event to check the model consistency. The limited time available to finish the problem constrains the ability to explore this issue in more detail. Perhaps, future research could explore this issue and eventually explain the problem.

Chapter 7

Conclusion

7.1 Conclusion

The key findings are summarised in the first part of this Chapter (7.1). The questions that we raised at the beginning of this thesis (Chapter 1, Section 1.1.3) will be answered based on the results presented. The concluding remarks and future outlook will be discussed in the final section, Section 7.2.

7.1.1 Summary of Findings

This thesis has discussed severe rainfall events over western Peninsular Malaysia during the inter-monsoon seasons and it includes two case studies. Based on the rain gauge data from MetMalaysia, the west coast of Peninsular Malaysia experiences biannual rainfall maxima, one in between April and May and another in between October and November every year. This is also concurrent with the findings discussed in Chapter 4. Having closely examined the data from rain gauge (MetMalaysia and DID) and gridded datasets (TRMM and APHRODITE) it can be seen that the biannual total rainfall maxima are commonly in April and November. April is the inter-monsoon period and November is the start of the boreal winter monsoon. The same biannual pattern was also observed in the rainfall frequency, in April and November (or October in the north-western peninsula). These results are consistent with the climate report by MetMalaysia (MetMalaysia, 2016a) and confirmed by results from other studies such as in Nieuwolt (1986), Oki and Musiaka (1994), Lim and Samah (2004), and Varikoden et al. (2011).

One of the motivations for this study was to investigate localised heavy rainfall events, which are not associated with large-scale weather events such as monsoons and the Madden-Julian Oscillation (MJO). Most of the extreme rainfall events in this study (Chapter 5) appeared to be localised, but the composite of rainfall and 850 hPa winds reveals that there may also be some large-scale influence such as the ITCZ. As the rainfall composite shows large amounts of rainfall in other regions than

the peninsula, there are the possibilities of large-scale influence affecting some (but not all) heavy rainfall events. These localised events are hard to predict especially in terms of the timing and location of the heavy rainfall (Suhaila et al., 2011).

To understand these local severe rainfall events, a case study is essential. Two case studies selected in this thesis are the 2 May 2012 and 24 September 2014 cases. To investigate these in more detail, a high-resolution model (Met-UM) was used. The first case study was realistically simulated using the high-resolution model (1.5km model) but the second case study was poorly simulated. In the first case study, the model reveals that the event on 2 May 2012 is likely to have been influenced by the rainfall event on the previous day. The rainfall on the previous day in both Sumatra Island and Peninsular Malaysia plays a major role in the development of the rainfall over the Strait of Malacca the next morning. Then, the rainfall over the strait influenced and enhanced the rainfall event in the afternoon over the western peninsula.

The above-mentioned mechanism is one of the probable reasons why the severe rainfall event on 2 May 2012 caused flash floods and landslides, despite the moderate amount of heavy rainfall. One case study is definitely not enough to generalise the mechanism for the development of the rainfall event, but this study will definitely supplement the previous literature, for example, those of Joseph et al. (2008), Qian (2008), Fujita et al. (2010), and Sow et al. (2011), which investigated rainfall development over the western Maritime Continent, particularly in the vicinity of Peninsular Malaysia.

Revisiting the research questions listed in Chapter 1, Section 1.1.3, the answers to these questions will deliver a better insight into the whole thesis.

1. How different is the rainfall amount over western Peninsular Malaysia during inter-monsoon periods compared to the monsoon seasons?

This study confirms the biannual maximum total rainfall (as in Section 4.1 Figure 4.1) from the available rain gauge and gridded datasets. As addressed in Varikoden et al. (2010) and also in reports from MetMalaysia (MetMalaysia, 2016b), the inter-monsoon periods are the time when the west coast of Peninsular Malaysia experiences frequent rainfall and afternoon severe convective storms. By examining the rain gauge and gridded datasets, this study confirms the high total rainfall during the inter-monsoon (April) and the onset of winter monsoon (November) in the west coast areas. It also confirms the finding of Varikoden et al. (2010) and the MetMalaysia (2016b) report by cross-examining additional datasets (DID and APHRODITE).

The double rainfall maximum is associated with the ITCZ which is also associated with the movement of maximum solar radiation on the earth surface. Based on rain gauge and gridded datasets, the first rainfall maxima is in Novem-

ber (October in APHRODITE dataset) and the second maximum is in April, for western Peninsular Malaysia. Most datasets show the highest in rainfall means over the western peninsula and inland in November, with 314 mm month⁻¹ from MetMalaysia dataset, 235 mm month⁻¹ from DID dataset 311 mm month⁻¹ from TRMM and in October for APHRODITE with 246 mm month⁻¹ (western and inland stations and regions averaged). In November, strong monsoon surge from the Siberian High-pressure system travelling toward the equator, and the colder air from the north combined with the wet easterly winds from the Pacific Ocean, brings rain and thunderstorm over the eastern coast of Peninsular Malaysia, extending to the west coast. Most of the rainfall in October is associated with the ITCZ and also the movement of convection southeastward from boreal summer monsoon to the austral summer monsoon (Chapter 2, Figure 2.1). Thus, a large amount of rainfall is expected over the peninsula.

The rainfall frequency shows the region experiences rainfall for 89% of the days in a month in November from MetMalaysia dataset and in October for TRMM dataset (89% of the days in the month). For the second maxima, April, the western and inland MetMalaysia stations (combined) experiences rainfall on 53% of the day, and the western and inland regions from TRMM experiences rainfall on 82% of the days in a month. The seasonal rainfall average closely follows the seasonal rainfall frequency, but in some stations (for example, the MetMalaysia's east coast station of Kota Bharu), the rainfall amount was higher in NDJFM but experiences more rainfall (frequency) in SO. This suggests a high rainfall frequency is not necessarily contributing to the high amount of rainfall. Infrequent but heavy rainfall could also contribute to the high amount of rain.

Seasonally (NDJFM, AM, JJA and SO, as discussed in Chapter 3 section 3.3.1), the mean rainfall from all of the datasets is higher in the SO inter-monsoon. The second maximum is in AM inter-monsoon. The second maximum in TRMM dataset is in NDJFM which is the boreal winter monsoon season. In the rainfall frequency analysis, all dataset shows that the maximum rainfall frequency is in SO inter-monsoon and the second maxima in AM inter-monsoon (Section 4.1, Figures 4.16 and 4.14). These results suggest the rainfall frequency and total are higher over the western coast of the peninsula during inter-monsoon periods (SO and AM), coincidentally with the ITCZ that is located over the equatorial region. Thus, these results suggest more rainfall occurred during inter-monsoon periods over the western and inland part of Peninsular Malaysia.

In summary, based on these datasets, western and inland Peninsular Malaysia received higher rainfall amounts and experience more rainfall during inter-monsoon, which is in April-May and October-November. The highest is in November (or October in APHRODITE dataset) and the second is in April. The high amount of rainfall in April coincides with the position of the ITCZ, which is associated with

the location of the solar maximum on the surface of the earth. The highest rainfall amounts in November is due to the fact that November is the onset month for the boreal winter monsoon and the monsoon surge is affecting the amount of rainfall over the whole peninsula. However, the frequent rainfall may not always be associated with large rainfall amount. Nonetheless, western Peninsular Malaysia during inter-monsoon periods (April-May and September-October) is generally receiving a relatively higher rainfall amount and experiencing a relatively higher rainfall frequency than the other months (except November).

2. What are the common conditions during heavy rainfall events over this region during the AM and SO inter-monsoon?

Using the total daily rainfall above the 1 mm day^{-1} threshold from both the rain gauge and gridded dataset, the 90th percentile was calculated (Section 5.2, Figure 5.1). The calculation was done by considering each day of all available years (each dataset consists of a different length of years), not seasonally. The days with daily rainfall equal to or above the 90th percentile threshold for each region are categorised as heavy rainfall days (HR90). The 90th percentile of the daily rainfall rate for each rain gauge and gridded dataset was analysed. The gauge dataset shows the values of the 90th percentile threshold at around 36.2 mm day^{-1} and the gridded dataset shows an average of 17.1 mm day^{-1} . Values calculated from the TRMM were chosen for the rest of the analysis for consistency and this work focuses on the western Peninsular Malaysia which is the Northwestern (NWC), Western (WC) and Inland (IL) regions. As we are only looking at localised events, the days associated with active Madden-Julian Oscillation (MJO) phases were removed. Based on the TRMM dataset, around 72.14 % of the days were not associated with active MJO phases 3, 4 and 5 (Section 5.2 Table 5.2). The mean area of heavy rainfall and the intensity is shown in Section 5.3 Figure 5.4.

From TRMM dataset, most of the HR90 occurred at the end of the year, between October and December (Section 5.2 Table 5.3). There is no prominent biannual signal in the mean frequency of heavy rainfall days in these datasets. Based on TRMM, the NWC, WC and IL regions experienced most of their heavy rainfall in October, November and December, respectively. The HR90 frequency is higher in NDJFM, then in SO and followed by AM. The lowest frequency of HR90 is in JJA. The mean of the rainfall rate for HR90 from the highest to the lowest is NDJFM, SO, AM and JJA. Compared to the climatology, the highest frequency of rain ($\geq 1 \text{ mm day}^{-1}$ on each day, for NWC, WC and IL mean) seasonally is in SO, followed by AM, JJA and NDJFM. The mean value of the rain rate from the highest to the lowest is NDJFM, SO, AM and the lowest is in JJA. The HR90 frequency and rainfall total have similar seasonal peaks which are the highest in NDJFM and the lowest in JJA. Compared to the daily rainfall, the frequency of the rainfall has a different peak from the total rainfall. There is more frequent rainfall

in SO, but more rainfall amount in NDJFM. The same goes with the least frequent rainfall, which is in NDJFM, but the least rainfall total is in JJA (for NWC, WC and IL combined). These results bring us back to the first research question. The high rainfall frequency does not always mean a high total rainfall.

The mean 850hPa winds for these heavy rainfall days were also analysed. By analysing the wind anomalies (Section 5.3 Figure 5.9), a stronger northeasterly or easterly associated with the heavy rainfall event over the western peninsula was observed in most cases. There is an exception for the IL region in the AM inter-monsoon, where a stronger westerly wind is associated with the severe rainfall events. The stronger easterly suggests that a stronger wind from the east (South China Sea) influences the development of severe convection over the western peninsula, which favours the development of lee waves over the Titiwangsa Mountains and influences the development of convective clouds inland due to instability. It is also hypothesised that the lee wave influences the development of the convective clouds when merged with the sea breeze over the western peninsula (as explained in Joseph et al. (2008)). As in IL-AM case, stronger and moist northwesterly or westerly winds from the Indian Ocean induces convective activity over the peninsula as it influences the development of convective clouds from orographic lifting as it combined with local sea and mountain breezes and eventually lead to a heavy rainfall event. In the vertical winds analysis, each region in each inter-monsoon shows a unique condition (Section 5.3, Figure 5.10). The stronger morning sea breeze circulation is associated with the development of convection later in the afternoon. This is observed in the NWC region cases (AM and SO) and the IL region case (AM). A weak vertical motion was observed for the west coast cases (AM and SO) and in the inland region (SO) case (Section 5.3, Figure 5.10(a)). In the afternoon, each region for each inter-monsoon shows a different condition. Stronger upward vertical motion is observed in all regions during the SO inter-monsoon. Weak vertical motion over the north-west in AM and slightly higher vertical motion in the west and inland regions occurred in the AM inter-monsoon (Section 5.3, Figure 5.10(b)).

No distinct difference in the humidity anomaly was seen over the region during these heavy rainfall days. However, the upper-level atmosphere over the peninsula (at around 700 hPa pressure level), particularly the eastern part of Peninsular Malaysia was more humid than the rest of the area, in the morning and the afternoon. (Section 5.3, Figure 5.11). This feature can also be associated with the stronger easterly wind from the South China Sea, bringing excess moisture toward the peninsula.

To summarise, the dataset from the station shows a heavy rainfall threshold (as in the 90th percentile) of between 29.5 mm day⁻¹ and 50.0 mm day⁻¹ of rainfall. The gridded dataset shows a range of 14.7 mm day⁻¹ to 20.3 mm day⁻¹ of daily rainfall. Most of the heavy rainfall days are not associated with any known large-

scale weather phenomena, such as monsoon and MJO. Heavy rainfall is frequent at the end of the year, from August to December. Most of the heavy rainfall in the inter-monsoon time is associated with stronger northeasterly or easterly anomalous wind. Each region in each inter-monsoon shows a unique vertical wind structure and these individual conditions are assumed to be the common condition associated with heavy rainfall events for each region. The same circumstances were observed in the vertical cross-section of the specific humidity. A unique condition was observed for each region and each inter-monsoon, with one exceptionally pronounced characteristic in all cases, which is the wetter upper atmosphere over the eastern part of the peninsula. This condition can be associated with the strong anomalous northeasterly and easterly wind in most of the HR90 cases.

3. How well are heavy rainfall events simulated by the UK Met Office Unified Model (UM)?

Based on Case Study 1 (2 May 2012), the 1.5km UK Met Office Unified Model version 7.5 has managed to reproduce the important mechanisms that lead to the event, as seen in the radar and TRMM dataset (Section 6.2.2 Figure 6.11 and 6.12 respectively). For example, the rainfall over the strait in the morning, rainfall over the mountains at noon and rainfall over the west coast in the afternoon (Figure 6.11 and Figure 6.17). However, the location of the rainfall was not exactly accurate. It is impossible to compare the rain intensity accurately using the radar images with the model output, but a qualitative comparison may be useful. The 1.5km model seems to have overestimated the rain intensity, with the maximum around 10.0 to 20.0 mm hr⁻¹ instead of 8.0 to 10.0 mm hr⁻¹ in the radar. For the 12km UM model, the model overestimates the spatial distribution of the rainfall although the intensity is almost at the same intensity, around 5 mm hr⁻¹. The model shows the rain covers a large area of the region in the afternoon of the event, which is not shown on the radar. These differences may also indicate how radar can inaccurately measure the rainfall over the mountainous regions due to the radar rain retrieval limitation as discussed in Section 3.1.4.

The other fields such as wind are properly simulated as in the reanalysis dataset, ERA-Interim (Section 6.2.2 Figure 6.10). The winds from the Indian Ocean diverted into the Strait of Malacca to be northwesterly at the northern tip of Sumatra Island and flow through southern Thailand to be westerly toward the South China Sea. The northwesterly wind at the Strait of Malacca turning from northwesterly to westerly at the southern peninsula was also properly simulated.

However, the rainfall event in Case Study 2 (24 September 2014) was not realistically represented. The morning heavy rainfall event over the north-west Peninsular Malaysia was not reproduced, especially in the 1.5km model (Section 6.3.2 Figure 6.56). The 12km model managed to show relatively higher rainfall

near the coast of the north-west, but not over the north-west coast itself. Some low-intensity rainfall was observed over part of the north-west but it was not as strong as expected. The 1.5km model did not reproduce the rainfall in either the Strait of Malacca or the north-west coast of Peninsular Malaysia. There were some patches of rainfall but these were too small and did not grow into a heavy rainfall event.

The UK Met Office Unified Model performed better in Case Study 1 in simulating a heavy rainfall event. Although the rainfall event was not exactly where it should have been, the mechanism was properly simulated. However, unrealistic simulation is also common, for example in Case Study 2. The unrealistic simulation may have been caused by the limited area domain, complex orography, failure in the model physics, convection scheme, the land-surface model used in the model, and a possibly less accurate initial (or boundary) condition that affect the final result. This issue requires further study to properly understand why the model fails.

4. What are the mechanisms involved in the development of the rainfall event based on Case Study 1 ?

As shown in previous studies, the most common mechanisms for the development of convective storms are the interaction between sea breeze and mountain breeze (Fujita et al., 2010; Sow et al., 2011), the interaction between lee waves (and gravity waves) with sea breeze (Joseph et al., 2008; Love et al., 2011) and also the role of wind gaps in maintaining the convection over the west coast of the Peninsular Malaysia (Joseph et al., 2008) as discussed in Section 2.4, Figure 2.4. Another mechanism which usually describes the precipitation or convection development offshore is gravity waves, propagated from inland toward the sea, as discussed in Love et al. (2011). Sea breeze collision (Joseph et al., 2008; Qian, 2008; Fujita et al., 2010; Sow et al., 2011) is common in the southern part of the Peninsular Malaysia where the land is relatively flat with no high mountains. This is specifically the collision of the westward and eastward sea breeze from east and west coast respectively. But this was not observed specifically related to the event. Not all of the mechanisms listed here were observed in this study. But the most common mechanism for the development of convective storms was observed, namely sea breeze collisions and the combination of sea breezes and mountain breezes.

As in Case Study 1 (Section 6.2), the amount of rainfall during the event day was definitely above the 90th percentile and it was considered a heavy rainfall day. The rainfall amount was not extreme but it still caused flash floods over the west coast. The rainfall event the previous day may also have influenced the flash floods and landslides to occur. In this case study, the mechanism (Figure 6.19 and Figure 6.21) can be explained by this process:

1. On the afternoon of 1 May 2012, the western and inland regions of the Penin-

sular Malaysia, and northern and inland Sumatra experienced heavy rainfall. This is the result of convection due to solar insolation and was enhanced by northwesterly winds from the Indian Ocean and the Andaman Sea.

2. This afternoon rainfall influenced the development of convective activity over the Strait of Malacca overnight. The cold flows (as a density current mechanism) from both lands merged over the Strait of Malacca and develop convection, assisted by the land breeze circulation from both lands.
3. At the same time, a strong northwesterly wind coming from Indian Ocean / Andaman Sea enhanced the convergence and convection over the strait.
4. Then, on the morning of 2 May 2012, the Strait of Malacca experienced a heavy rainfall event that continued for most of the morning until noon.
5. By noon of 2 May 2012, convection developed over the Titiwangsa mountains due to solar insolation and matured to produce rainfall over the mountain ranges.
6. Cold pool from the rainfall system over the Strait of Malacca together with the sea breezes over induced convection over the west coast (of the peninsula).
7. The sea breezes combined with the cold pool from the rainfall over the Titiwangsa mountain range enhanced the convective activity over the west coast.
8. As the sea breeze circulation enhanced, the rainfall over the strait is suppressed and convection over the west coast enhanced, and later matured to produce rainfall.
9. As the rainfall over the west coast enhanced, the rainfall over the Titiwangsa mountain range was spreading. The two rainfall systems merged.
10. As the prevailing winds were northwesterly the rainfall system was prevented from moving eastward by the presence of the mountains, and thus it stayed stationary over the west coast.
11. The rainfall system continued for a couple of hours and then dissipated.

Elaborating the mechanisms listed above, the Peninsular Malaysia and Sumatra experienced heavy rainfall on the late afternoon of 1 May and these events are more likely due to the enhanced convective activity from insolation and sea breeze circulation. Later that night after the rainfall subsides, the cold flow from the mountainous region propagated toward the Strait of Malacca and merged in the middle of Strait of Malacca to induce convection (Chapter 6, Figure 6.18). This is also enhanced by a land breeze that is already developing in the early morning as a response to the change of air pressure between lands and the strait. The convection over the strait is also enhanced by the incoming northwesterly winds.

After the convection matured and yielded rainfall in the mid-morning of the next day (2 May), the land is starting to heat and a land breeze is changing into the sea breeze. The heating landmass also induces convection over the peninsula (Titiwangsa Mountains) and produced rainfall. Sea breeze and cold pool from the

rainfall over the strait propagated toward the land (in this case the western peninsula) and the cold pool from the rainfall over the Titiwangsa Mountains enhanced convective activity over the west coast of the peninsula. Later, as the sea breeze enhances, the rainfall over the strait dissipated, and convective activity over the west coast intensified. The convection matured to produce rainfall in the early afternoon and then merged with the rainfall over the Titiwangsa Mountains that is still occurring and spreading toward both sides of the mountain range. Rainfall over the west coast of the peninsula stays over the west coast region despite the northwesterly winds as it was blocked by the Titiwangsa Mountains. While there are more factors involved in the development of this event, local orography plays one of the important roles.

5. How important was the orography over both Peninsular Malaysia and Sumatra Island in the development of the rainfall event in this region, particularly from these case studies?

To investigate the role of orography, a few sensitivity experiments were done by flattening the orography in three ways. First, the orography of Peninsular Malaysia was removed (**flatPM**), then the orography of the Sumatra Island was removed (**flatSI**) and finally the orography of both the Peninsular Malaysia and Sumatra Island was removed (**flatALL**). The modification shows a significant difference in the amount of rainfall received on the day of the event over the region of interest or the west coast area in general.

The **flatPM** experiment reduced the amount of rainfall on 2 May 2012 with the mean total of 5.2 mm day⁻¹ for the WC region (54.6% of the control run), 11.8 mm day⁻¹ for the IL region (64.1% of the control run) and 17.2 mm day⁻¹ for the NWC region (92.8% of the control run) as shown in Section 6.2.4 Figure 6.46. The difference is statistically significant at the 95% significance level. The absence of the orography, which caused no afternoon rainfall over the Titiwangsa mountains, influenced the reduction in total rainfall inland and the west coast. Another possible reason for the smaller amount of total rainfall over the west coast is that the convective system was pushed eastward by the prevailing northwesterly wind. The convection over the Strait of Malacca still developed but dissipated earlier than in the control run.

The **flatSI** experiment caused the rainfall over the western and inland peninsula on the 2 May 2012 to reduce significantly, with mean rainfall of 7.8 mm day⁻¹ (81.5% of the control run) for WC and 13.2 mm day⁻¹ for IL (90.8% of the control run). However, it increased in NWC with the mean rainfall of 24.7 mm day⁻¹ (132.8% of the control run) as shown in Section 6.2.4 Figure 6.46. The difference is statistically significant at 95% significance level. The rainfall amount on the 1 and 2 May 2012 over Sumatra (in the included domain, north and middle Sumatra)

was lesser than in the control run when the Barisan Mountains were flattened. The mean total rainfall on 1 May was 29.9 mm day⁻¹ (45.5% of the control run). The mean total rainfall on 2 May was 70.0 mm day⁻¹ (84.8% of the control run). The reduced amount of the rain is also contributing to the less intense rainfall over the central Strait of Malacca on the morning of 2 May 2012.

A weak rainfall over Sumatra on the previous day resulted in a smaller amount of total rainfall over the WC and IL. The weak rainfall over the Sumatra on the previous day affected rainfall over the central Strait of Malacca on the morning of 2 May 2012, thus affecting the rainfall activity over the west coast on the afternoon of 2 May. It is hypothesised that the lower rainfall over the Strait of Malacca in this experiment was due to the less intense afternoon precipitation on 1 May which makes the cold flow converging at Strait of Malacca weaker than in control run. As in Fujita et al. (2010), the cold flow from the afternoon precipitation of the previous day induces cold flow convergence with the cold flow from Peninsular Malaysia on the midnight. The weaker cold flow combined with land breeze moving to the Strait of Malacca at midnight and converge with the cold flow and land breeze coming from Peninsular Malaysia. The weaker flow from Sumatra caused a less intense rainfall over the Strait of Malacca. The higher rainfall over the NWC was due to the early rainfall around 0200 LT, which was not observed in the control run.

In the **flatALL** experiment, the mean rainfall over the west coast on 2 May 2012 was higher than in the control run by 2.87 mm day⁻¹ over the WC and 4.29 mm day⁻¹ over the NWC, but it reduced over the IL by 5.63 mm day⁻¹. (Section 6.2.4 Figure 6.46). The higher total rainfall over the WC and NWC was probably due to the early rainfall events over these regions, which were not observed in the control run. Less total rainfall over the IL was expected, as there was no orographic convection. Although both Peninsular Malaysia and Sumatra Island are flat, the morning rainfall over the Strait of Malacca still developed.

Thus, the local orography plays an important role in modifying the rainfall event in this case study, especially over the west and inland regions. The **flatPM** experiment resulted in less total daily rainfall over the WC and IL due to the absence of orographic induced rainfall. The **flatSI** experiment resulted in slightly less total daily rainfall over the WC and IL than in the control run, due to there being less intense rainfall over the Strait of Malacca. The **flatALL** experiment resulted in a higher total daily rainfall over the west coast but not inland. One possible reason for this was an additional short early morning rainfall event at around 0100 LT over the west coast, which was not observed in the control run. The additional rainfall made the total daily rainfall over the west coast region higher than in the control run. In all three experiments, the rainfall over the Strait of Malacca in the morning of 2 May still developed although the orography was modified. This shows the importance of both Peninsular Malaysia and Sumatra Island in influencing the

development of rainfall events over the strait.

6. How important is Sumatra Island in the development of severe rainfall events over western Peninsular Malaysia?

In addition to the **flatSI** experiment, the final experiment, which involved removing Sumatra Island (**noSI**) and replacing it with ocean, was done to investigate the influence of Sumatra Island on severe rainfall events over western Peninsular Malaysia. As mentioned previously, flattening Sumatra Island caused the rainfall over the west coast Peninsular Malaysia to be slightly less than in the control run. This is likely to be due to the weak rainfall over the Strait of Malacca because of the less intense rainfall in both the Strait of Malacca and Titiwangsa mountains the previous day.

When Sumatra Island was removed, the total rainfall on 2 May are 27.8 mm day⁻¹ over the WC (289.4% of the control run), 22.5 mm day⁻¹ over the IL (154.3% of the control run) and 22.2 mm day⁻¹ (119.4% of the control run) over the NWC (Section 6.2.4 Figure 6.46). The significant increase total rainfall over the WC is due to the higher frequency of rainfall events over the WC region on 2 May; one in the early morning of the 2 May, one in the afternoon and another one in the evening. The more frequent rainfall over the WC is associated with the vast amount of moisture provided by the Indian Ocean, but this is yet to be proven. However, daily and afternoon means of dew point temperature (T_d profile of a column over the central western Peninsular Malaysia) on the 2 May indicate that the T_d in the **noSI** experiment is higher than in the control indicating the excess moisture present (Chapter 6, Figure 6.50). The westerly wind from the Indian Ocean, which is usually restrained by Sumatra Island, now directly impacts Peninsular Malaysia, bringing more chance of rainfall development over Peninsular Malaysia.

Thus, Sumatra Island has a huge impact on the severe rainfall activity and development over western Peninsular Malaysia, for example in this case study on 2 May 2012. Flattening Sumatra causes less total rainfall over western Peninsular Malaysia but without Sumatra Island, western Peninsular Malaysia receives a large amount of rainfall. Sumatra Island is also important in influencing the development of night-time or early morning rainfall events over the Strait of Malacca. It is also likely that Sumatra Island is important in preventing western Peninsular Malaysia from receiving a huge amount of rainfall, throughout the year.

7.1.2 Concluding remarks and future outlook

Climatologically, western Peninsular Malaysia experiences biannual rainfall maxima, one in April and one in November. April is the inter-monsoon period and November is the onset of the boreal winter monsoon. These are similar to the report from MetMalaysia (MetMalaysia, 2016a). The biannual maxima in the rainfall amount also closely follow the movement of the Inter-Tropical Convergence Zone which follows the movement of the solar maxima that crosses the equatorial tropics twice a year (roughly in between March-April and September-October).

While monsoon seasons attract more attention for heavy rainfall events over the whole peninsula generally, inter-monsoon periods are given less attention. However, it is made aware by MetMalaysia to the public that afternoon thunderstorms are more common during inter-monsoon periods. In an analysis based on TRMM dataset, most of the heavy rainfall events (in this study, above the 90th percentile threshold, HR90) are toward the end of the year. In NWC, the month with more HR90 is in October. In WC, most of the HR90 is in November and in IL, most of the HR90 is in December. These results show that heavy rainfall is common in NWC during second inter-monsoon and common in WC and IL during boreal winter monsoon. These heavy rainfall events are mostly localised and orography plays a major role in their development. Thus, a case study is essential, to study how the local orography influenced the development of the heavy rainfall event over western Peninsular Malaysia.

To understand the role of local orography in the development of severe rainfall event, two case studies were selected. However, only one case study (Case Study 1) was realistically simulated by the MetUM. In Case Study 1 (2 May 2012), the combination of the rainfall events over the Peninsular Malaysia the previous day and the rainfall events over the Strait of Malacca has been a major influence in the development of the severe rainfall events over the west coast on 2 May 2012. The late evening rainfall over the peninsula and Sumatra on the 1 May 2012 influenced the development of morning rainfall over the Strait of Malacca in the morning of 2 May 2012. By noon, another rainfall event over the Titiwangsa mountains developed. By afternoon, the rainfall over the strait dissipated and with the influence of northwesterly winds and sea breeze, convection over the western coast developed and producing rain. This rainfall system developed further and combined with the rainfall system over the Titiwangsa mountains and stay stationary over the western peninsula as the Titiwangsa mountains prevented it to propagated eastward (to follow the prevailing northwesterly wind).

Other than rainfall, other fields such as 850 hPa zonal and meridional winds were realistically simulated in 12 km and 1.5 km models as compared to the reanalysis dataset, ERA-Interim. As the models have a higher horizontal, vertical and temporal resolution, more details of the wind dynamic were displayed. The details

will also help the study to determine how local orography and circulation affecting the development of the severe rainfall event. Since local orography and Sumatra Island are important in this event, sensitivity experiments were done by flattening the orography (Peninsular Malaysia and Sumatra) to the sea level and removing Sumatra Island.

The **flatPM** resulted in less total rainfall over the west coast and inland on the event day, due to the weaker rainfall event over the strait in the morning and the absence of orographic associated rainfall over Malaysia. The absence of orography caused the rainfall system over the west coast to be pushed eastward and deteriorate. The **flatSI** experiment resulted in slightly less rainfall over the west coast on the event day, due to the less intense rainfall over the strait. The total rainfall is still higher than in the **flatPM** experiment because of the orographic influenced rainfall over the Titiwangsa mountains. The **flatALL** experiment reveals that the rainfall over the west coast on the event day was higher than in the control run, but there was less rainfall over the inland region. The higher total daily rainfall was caused by the additional rainfall event in the morning.

Removing Sumatra Island and replacing it with ocean (**noSI** experiment) reveals how important the island is in the weather activity on the west coast of Peninsular Malaysia. The experiment shows that the rainfall over the peninsula during the event is triple the amount in the control run. The reason for the high total daily rainfall is that there were three rainfall events on the day, one in the early morning, one in the afternoon and another in the late afternoon. The vast open ocean in the west is believed to have an influence on the frequent rainfall events over the region. Overall, both Peninsular Malaysia and Sumatra Island are important in the development of rainfall events over the strait, regardless of the height of the orography. Orography is important in enhancing the convection activity over western Peninsular Malaysia as in this case study. Sumatra Island plays a crucial role in influencing the local weather. As shown in the case studies, it prevents western Peninsular Malaysia from being wetter than normal, which may lead to more severe flooding and landslides.

This thesis essentially provides an additional insight into the development of severe rainfall events, which adds to previous studies that have looked at the development of rainfall events over western Peninsular Malaysia, especially events that were not associated with large-scale weather events such as MJO and monsoons (as in Joseph et al. (2008), Fujita et al. (2010), and Sow et al. (2011)). Continuous study to understand the tropical weather is important, especially in the changing climate; specifically the study of weather events that matter to human life and the economy. While the inter-monsoon in this study is defined as the time when wind direction is changing, it is still not perfect. There are possibly more sophisticated ways of determining the inter-monsoon period, for example by carefully analysing

observational data for the exact time when the direction of the prevailing wind changes. The inter-monsoon is mostly the ‘grey period’ in between monsoons with no official start and end time in any publication, at least for Malaysia. Hence, it would be interesting to conduct more studies to understand the inter-monsoon, not only because of the lack of studies but also because a lot of severe convective storm events occur during the inter-monsoon periods in Malaysia.

More analysis is also needed of the common characteristics of severe or heavy rainfall events (as in Chapter 5). This analysis could be done not only with the Tropical Rainfall Measurement Mission (TRMM) dataset but also by using other observational data such as rain gauges and other gridded datasets. Thus, more rain gauge datasets are needed from MetMalaysia or DID. Using hourly rainfall data from the rain gauge could provide more in-depth information about heavy rainfall event, especially the temporal scale of the events. Daily rainfall can be a combination of one or more rainfall events, but with hourly data, a study on individual storm events would be possible. In this study, the use of the 90th percentile on the daily total value for the HR90 selection using TRMM may not be as accurate in determining an individual event as the extreme event usually lasts in less than 24 hours. Thus, the HR90 may be a group of a few extreme events on a particular day. There should be a better way of selecting the extreme event from the TRMM itself such as considering the 3 hourly data instead of 24-hour mean. The combination of these datasets and more statistical analysis could improve the understanding of the common behaviour of severe rainfall events in terms of precipitation, winds and other fields such as humidity.

There is definitely a lot of work that could be done with the model output. An overall understanding of how this event (Case Study 1) developed is still to be completed, but a possible mechanism is discussed in the previous section. This possible mechanism could be a guide for more study in the future to verify its accuracy and it will definitely be useful in expanding the current knowledge on severe convective storm genesis in the tropics. More study on the dynamics and thermodynamics of the severe convective storm event genesis is also recommended and might be useful for forecasting in the future. The more case studies are investigated, the more an understanding can be acquired of the mechanisms involved in the development of severe weather in the tropics, specifically over Malaysia. The mechanism may not be the same every time. This thesis is one of many studies that will eventually be aggregated in order to generalise an important common mechanism for the development of severe weather not only in Malaysia but also in the Maritime Continent.

Due to time constraints, the simulations described in this thesis have not been analysed in every possible respect and there are possibly more mechanisms could be revealed from the MetUM simulation output. The use of this high-resolution

state-of-the-art Numerical Weather Prediction (NWP) model, MetUM, is definitely possible to test the importance of different mechanisms by manipulating the physics and dynamics of the model. There are definitely more studies that could be done other than just two case studies. More than two case studies are better to properly understand the role of orography in the development of severe rainfall event over western Peninsular Malaysia. Other than that, more useful data such as radiosonde data could be added to the lateral boundary condition file in the model as in a study by Zhu et al. (2012) in their study on Hector thunderstorm development. Not only is examining the effects of local orography important, there are also other sensitivity tests could be done in the future, such as the change in land-use and vegetation, as well as the change in moisture (including soil moisture). It would also be sensible to conduct similar studies using more than one NWP model to examine and hopefully eliminate biases in individual models. An intercomparison between the behaviour of different models for the same case studies, forced with the same boundary conditions, would allow the identification of any errors which might be due to the boundary conditions rather than the models themselves. Sensitivity to different parametrisation schemes, in particular, the convective and boundary layer schemes could also be diagnosed from model inter-comparison studies.

There are also previous studies that have investigated the role of orography in severe rainfall events over in this region. More studies on specific cases should be done to add more new information to the current knowledge on the effect of orography on the development of severe weather. Most importantly, this thesis can be the beginning of understanding the role of Sumatra Island in modifying the weather over Peninsular Malaysia. Although the role of orography and Sumatra Island in modifying severe weather event was investigated in this thesis, it is not enough. More analysis on the model simulation output is needed to fully understand the development of the severe weather event over western Peninsular Malaysia associated with the local orography and Sumatra Island.

Severe rainfall events in the tropics such as those presented in this thesis have a clear socioeconomic impact on the region. This it is of key importance that the findings of this study are developed with the need to improve the forecasting of such events in mind. Further studies, conducted in conjunction with the operational forecasters in the region, would allow for a two-way exchange of information between researchers and forecasters. Forecasters need to know about the limitations of NWP models to simulate these severe weather events, but they can also learn about the local factors that lead to their development, recognising the precursor signals in the region such as heavy rain events on neighbouring islands in the previous 24 hours and sea or land breeze development. The forecasters can train themselves to recognise the precursor signals in their model forecast event when the model did not actually predict the heavy rainfall event. The transfer of knowledge

between forecaster and modeller in such collaboration is important, and the transfer of knowledge can be in two ways. Forecasters, who are familiar with the real world, could have useful information to be conveyed to the modeller, in order to improve the forecasting of severe events by monitoring NWP forecasts and feeding back information to model developers on aspects of the forecast that the models either capture well or fail to represent.

This study could also add value to previous studies involving climate modelling and short-term forecasting studies, for example on the role of the high-resolution models in improving climate models. Climate models struggle to simulate precipitation over the tropics, especially in the Maritime Continent region (eg. Yang and Slingo (2001)) and this causes errors in the global circulation. High-resolution model studies such as in this thesis can help climate modellers develop better convective parameterisations and thus improve climate models. It may be useful in suggesting further study on the interaction of convective parameterisations with the land-surface and orographic features. This thesis also presents an example of a successful and an unsuccessful result of the explicit convection scheme (1.5km model) and parameterised convection scheme (12km model). The 1.5km model successfully simulated the rainfall event close to the observation in Case Study 1, but not in Case Study 2. In Case Study 2, the 12km model performed better than the 1.5km model. This result shows that moving to a high-resolution model with an explicit convection scheme is not always better at simulating tropical convection. From a local forecasting perspective, there are a lot of improvements needed for day to day weather forecasting and this study suggests that these improvements will likely come from better understanding of mechanisms involving both large-scale condition and local flow on the development of severe convection.

Appendix A

Appendix

	Jan	Feb	Mar	Apr	May	Jun	Jul	Aug	Sep	Oct	Nov	Dec
Alor Star 1	43.5	76.0	202.7	248.3	166.0	174.7	171.7	221.7	243.2	280.2	239.0	132.6
Ipoh	234.2	213.7	274.9	285.2	214.8	162.0	157.9	207.9	185.2	298.6	352.4	263.7
Cameron High. 1	166.5	120.8	244.7	318.7	267.5	180.5	199.5	254.6	260.3	333.4	383.0	249.0
Selang	138.8	116.4	167.1	181.0	127.2	92.4	143.1	133.1	177.6	220.0	281.0	184.1
Batu Pahat 1	165.2	142.8	200.9	203.4	159.6	134.1	170.0	174.5	157.4	194.1	307.8	245.9

Table A.1: Monthly rainfall average from MetMalaysia rain gauge dataset, 5 stations from 2005-2014. Each value is in mm month⁻¹.

	Jan	Feb	Mar	Apr	May	Jun	Jul	Aug	Sep	Oct	Nov	Dec
Alor Star 1	10.3	17.4	34.5	50.0	45.5	38.7	36.5	47.4	49.3	57.1	52.3	31.6
Ipoh	45.2	38.3	50.7	53.7	39.7	33.0	30.7	41.3	41.7	58.4	67.3	53.6
Cameron High. 1	45.2	36.2	54.8	70.3	59.7	44.7	44.8	55.2	57.3	69.4	77.3	61.0
Selang	30.0	25.2	38.7	38.7	31.9	27.0	34.2	31.6	38.3	48.7	60.3	48.4
Batu Pahat 1	31.0	35.1	42.3	48.0	41.0	31.0	32.6	37.7	41.3	44.2	53.7	51.3

Table A.2: Rainfall frequency (monthly mean) for days with ≥ 1 mm day⁻¹. Each value represents the percentage of rainy day of each month. Data are from 2005-2014, from MetMalaysia gauge dataset.

	NDJFM	AM	JJA	SO
Alor Star 1	138.8	207.1	189.4	261.7
Ipoh	267.8	250.0	175.9	241.9
Cameron High. 1	232.8	293.1	211.5	296.8
Selang	177.5	154.1	122.9	198.8
Batu Pahat 1	212.5	181.5	159.5	175.8

Table A.3: Same as in Table A.1 but seasonal.

	NDJFM	AM	JJA	SO
Alor Star 1	29.3	47.7	40.9	53.3
Ipoh	51.1	46.6	35.0	50.2
Cameron High. 1	55.1	64.9	48.3	63.4
Selang	40.7	35.2	31.0	43.6
Batu Pahat 1	42.7	44.4	33.8	42.8

Table A.4: Same as in Table A.2 but seasonal.

	Jan	Feb	Mar	Apr	May	Jun	Jul	Aug	Sep	Oct	Nov	Dec
Alor Star 2	35.0	51.4	117.5	171.9	148.2	200.0	200.6	251.2	244.8	270.1	203.2	65.9
Bota	159.2	145.5	208.3	210.8	141.3	99.2	117.4	119.7	161.9	229.1	258.7	201.0
Cameron High. 2	154.1	116.6	145.4	173.2	138.1	97.8	120.5	170.9	191.5	220.5	259.9	247.8
Dengkil	96.9	107.6	145.0	184.0	84.2	75.4	105.2	90.8	115.7	138.3	219.6	177.3
Batu Pahat 2	140.5	106.9	222.0	179.9	144.9	129.0	150.4	169.4	149.0	191.0	232.7	225.2
Mersing	381.4	128.8	189.6	122.1	145.8	160.5	160.7	149.1	149.8	193.7	293.9	548.6
Kota Bharu	232.8	109.6	139.4	77.9	182.2	168.2	189.8	164.0	227.7	298.7	567.2	585.3

Table A.5: Monthly rainfall average from Department of Irrigation and Drainage (DID) rain gauge dataset, 7 stations from 1998-2013 (except Bota (1998-2012) and Dengkil (2002-2014)). Each value is in mm month⁻¹.

	Jan	Feb	Mar	Apr	May	Jun	Jul	Aug	Sep	Oct	Nov	Dec
Alor Star 2	10.5	13.3	29.6	38.8	40.5	37.9	39.5	42.1	53.3	53.0	44.8	25.2
Bota	26.2	26.9	30.5	33.1	23.0	18.4	20.9	22.2	27.3	30.5	38.9	29.2
Cameron High. 2	44.4	35.4	33.9	41.9	36.1	29.2	33.7	43.5	50.6	52.0	54.8	57.9
Dengkil	34.0	30.8	44.4	47.4	32.5	28.5	35.0	35.7	41.0	41.9	58.2	52.9
Batu Pahat 2	27.0	25.7	38.9	36.7	31.9	29.8	28.6	33.3	31.7	36.9	44.4	40.3
Mersing	46.0	23.7	33.3	32.7	34.5	34.0	38.7	36.7	35.8	44.2	60.8	62.1
Kota Bharu	38.5	18.4	23.6	19.4	35.3	34.8	41.7	36.7	47.5	55.2	63.3	62.3

Table A.6: Rainfall frequency (monthly mean) for days with ≥ 1 mm day⁻¹. Each value represents the percentage of rainy day of each month. Data are from 1998-2013 (except Bota (1998-2012) and Dengkil (2002-2014)), from DID gauge dataset.

	NDJFM	AM	JJA	SO
Alor Star 2	94.6	160.1	217.3	257.5
Bota	194.5	176.0	112.1	195.5
Cameron High. 2	184.7	155.6	129.7	206.0
Dengkil	149.3	134.1	90.5	127.0
Batu Pahat 2	185.5	162.4	149.6	170.0
Mersing	308.5	134.0	156.8	171.8
Kota Bharu	326.9	130.1	174.0	263.2

Table A.7: Same as in Table A.5 but seasonal.

	NDJFM	AM	JJA	SO
Alor Star 2	25.0	40.0	40.0	53.0
Bota	30.0	28.0	20.0	29.0
Cameron High. 2	45.0	39.0	35.0	51.0
Dengkil	44.0	40.0	33.0	41.0
Batu Pahat 2	35.0	34.0	31.0	34.0
Mersing	45.0	34.0	36.0	40.0
Kota Bharu	41.0	27.0	38.0	51.0

Table A.8: Same as in Table A.6 but seasonal.

	Jan	Feb	Mar	Apr	May	Jun	Jul	Aug	Sep	Oct	Nov	Dec
NWC	141.2	112.7	207.8	230.4	193.8	161.0	168.4	192.2	226.2	336.2	318.6	248.6
WC	198.0	157.7	213.9	237.5	176.3	126.9	147.9	161.4	191.4	267.7	310.2	252.3
IL	193.0	124.1	208.1	216.3	223.2	166.6	176.2	200.4	230.9	306.2	303.3	332.4
SP	253.3	119.6	211.9	224.2	176.8	141.9	159.1	175.3	179.7	228.1	253.5	290.5
EC	261.5	119.0	188.6	159.7	201.3	154.9	171.1	193.5	204.9	291.6	353.7	544.1

Table A.9: Monthly rainfall average for days with ≥ 1 mm/day (in mm month⁻¹), for northwest coast (NWC), west coast (WC), inland (IL), south peninsula (SP) and east coast (EC). Data are from TRMM dataset, 1998-2013.

	Jan	Feb	Mar	Apr	May	Jun	Jul	Aug	Sep	Oct	Nov	Dec
NWC	50.2	42.5	69.8	80.2	75.6	65.7	70.2	72.2	77.8	87.9	84.9	63.9
WC	68.8	58.9	75.6	81.7	70.6	62.5	65.7	71.6	77.8	84.1	84.9	63.9
IL	56.7	48.4	72.0	83.3	87.3	73.0	77.6	82.1	76.4	94.8	86.1	78.4
SP	53.0	42.9	68.5	81.3	75.0	64.3	70.6	72.2	87.9	81.0	90.1	74.0
EC	50.6	36.5	64.7	74.0	87.3	79.6	81.9	89.1	74.8	95.4	85.5	66.9

Table A.10: Rainfall frequency (monthly mean) for days with ≥ 1 mm day⁻¹ for northwest coast (NWC), west coast (WC), inland (IL), south peninsula (SP) and east coast (EC). Each value represents the percentage of rainy day of each month. Data are from 1998-2013, from TRMM dataset.

	NDJFM	AM	JJA	SO
NWC	205.8	212.1	173.8	281.2
WC	226.4	206.9	145.4	229.5
IL	232.2	219.7	181.0	268.6
SP	225.8	200.5	158.8	203.9
EC	293.4	180.5	173.1	248.2

Table A.11: Same as in Table A.9 but seasonal.

	NDJFM	AM	JJA	SO
NWC	62.3	77.9	69.4	82.9
WC	70.4	76.1	66.6	81.0
IL	68.3	85.3	77.6	85.6
SP	65.7	78.1	69.0	84.5
EC	60.9	80.7	83.5	85.1

Table A.12: Same as in Table A.10 but seasonal.

	Jan	Feb	Mar	Apr	May	Jun	Jul	Aug	Sep	Oct	Nov	Dec
NWC	45.9	47.5	85.8	152.4	173.7	132.4	148.3	178.4	215.3	259.2	220.3	135.7
WC	115.6	112.8	149.6	204.7	159.8	112.1	122.7	144.3	173.7	227.6	239.6	185.8
IL	123.8	101.4	142.1	191.4	180.4	135.3	139.9	175.7	200.6	250.0	276.1	241.2
SP	145.3	102.1	147.7	173.8	152.3	120.2	127.9	147.5	148.0	169.9	203.6	215.1
EC	150.8	85.0	120.6	128.3	136.3	117.5	123.9	158.4	169.1	204.0	314.3	354.8

Table A.13: Monthly rainfall average for days with ≥ 1 mm day⁻¹ (in percentage), for northwest coast (NWC), west coast (WC), inland (IL), south peninsula (SP) and east coast (EC). Data are from APHRODITE dataset, 1970-2007.

	Jan	Feb	Mar	Apr	May	Jun	Jul	Aug	Sep	Oct	Nov	Dec
NWC	31.6	32.9	52.5	73.1	82.3	71.9	73.4	76.4	85.3	92.5	85.4	62.1
WC	58.9	58.3	73.0	83.9	78.9	63.3	64.7	68.5	81.8	89.6	88.4	80.0
IL	63.1	57.5	71.6	86.7	86.2	73.5	74.7	78.4	88.1	93.7	93.2	84.9
SP	52.8	46.3	64.0	78.1	74.2	64.3	65.9	66.2	71.3	79.5	83.7	76.4
EC	62.1	48.8	64.0	79.3	83.8	74.2	76.3	79.8	87.4	93.3	94.0	87.6

Table A.14: Rainfall frequency (monthly mean) for days with ≥ 1 mm day⁻¹ for northwest coast (NWC), west coast (WC), inland (IL), south peninsula (SP) and east coast (EC). Each value represents the percentage of rainy day of each month. Data are from 1970-2007, from APHRODITE dataset.

	NDJFM	AM	JJA	SO
NWC	107.0	163.0	153.0	237.2
WC	160.7	182.3	126.4	200.6
IL	176.9	185.9	150.3	225.3
SP	162.8	163.0	131.9	159.0
EC	205.1	132.3	133.3	186.6

Table A.15: Same as in Table A.13 but seasonal.

	NDJFM	AM	JJA	SO
NWC	52.9	77.7	73.9	88.9
WC	71.7	81.4	65.5	85.7
IL	74.0	86.4	75.6	90.9
SP	64.6	76.2	65.5	75.4
EC	71.3	81.5	76.8	90.3

Table A.16: Same as in Table A.14 but seasonal.

MetMalaysia gauges	Period	90th percentile
Alor Star 1 (NWC)	2005-2013	31.5
Ipoh (WC)	2005-2013	39.8
Cameron Highland 1 (IL)	2005-2013	29.5
Sepang (WC)	2005-2013	36.6
Batu Pahat 1 (SP)	2005-2013	42.5
DID gauges	Period	90th percentile
Alor Star 2 (NWC)	1998-2013	38.2
Bota (WC)	1998-2012	50.0
Cameron Highland 2 (IL)	1998-2013	30.0
Dengkil (WC)	2002-2014	34.0
Batu Pahat 2 (SP)	1998-2013	36.0
Mersing (EC)	1998-2013	44.0
Kota Bharu (EC)	1998-2013	47.2
TRMM gridbox	Period	90th percentile
Northwest Coast (NWC)	1998-2013	19.1
West Coast (WC)	1998-2013	20.3
Inland/Highland (IL)	1998-2013	18.7
South Peninsula (SP)	1998-2013	19.5
East Coast (EC)	1998-2013	20.0
APHRODITE gridbox	Period	90th percentile
Northwest Coast (NWC)	1970-2007	14.7
West Coast (WC)	1970-2007	14.7
Inland/Highland (IL)	1970-2007	15.0
South Peninsula (SP)	1970-2007	16.1
East Coast (EC)	1970-2007	14.7

Table A.17: Threshold values for 90th percentile for each rain gauge station and each region, in mm/day. Data are from MetMalaysia, DID, TRMM and APHRODITE datasets. Temporal scale for each dataset is listed under 'Period'.

(a) MetMalaysia	Jan	Feb	Mar	Apr	May	Jun	Jul	Aug	Sep	Oct	Nov	Dec
Alor Star 1	1.3	3.1	9.4	11.9	6.9	7.5	8.2	15.1	6.9	13.8	10.1	5.7
Ipoh	7.5	9.4	6.9	6.9	8.2	8.8	8.2	8.2	4.4	9.4	15.1	6.9
Cameron Hig. 1	5.7	3.9	8.3	12.2	8.3	4.8	7.4	11.3	6.1	9.6	14.3	8.3
Sepang	9.4	8.5	6.6	7.5	6.6	7.5	6.6	3.8	9.4	11.3	15.1	7.5
Batu Pahat 1	9.4	6.3	6.3	7.3	8.3	6.3	7.3	8.3	3.1	5.2	16.7	15.6
(b) DID	Jan	Feb	Mar	Apr	May	Jun	Jul	Aug	Sep	Oct	Nov	Dec
Alor Star 2	1.1	1.6	5.3	8	6.4	11.2	11.2	14.9	20.7	13.8	4.8	1.1
Bota	6.4	2.8	5	6.4	2.1	5.7	3.5	5	23.4	13.5	12.1	14.2
Cameron High.2	5.5	5	4.6	9.6	4.6	3.7	5	7.3	17.9	8.7	14.7	13.3
Dengkil	5.4	7.2	7.2	9	4.8	4.8	7.8	4.2	18.1	9	12.7	9.6
Batu Pahat 2	5.5	4.4	9.3	7.7	6	6	7.1	8.2	16.5	8.2	9.9	11
Mersing	15.4	5.9	5.9	1.6	3.7	6.9	3.2	4.3	10.1	6.4	8.5	28.2
Kota Bharu	7.4	4.9	3.4	2	6.9	4.9	5.4	1	14.7	7.8	19.1	22.5
(c) TRMM	Jan	Feb	Mar	Apr	May	Jun	Jul	Aug	Sep	Oct	Nov	Dec
Northwest,NWC	5.6	2.3	9.5	7	5.4	3.8	6.8	5	9.3	16.9	14.4	14
West,WC	9.2	8	7.5	7.7	6.8	3.1	4.9	4.9	5.4	13.6	15.3	13.6
Inland,IL	10.5	4.8	10	6.5	8.1	3.3	3.7	2.8	6.1	10.9	13.5	19.8
South,SP	13.2	5.5	9.6	8.4	6	3.6	5.5	6	5.8	10.1	10.6	15.6
East,EC	13.7	5.3	6.6	3.1	4.9	1.3	2.9	2.9	4.2	9.3	15.3	30.5

Table A.18: HR90 frequency from (a) MetMalaysia, (b) DID and (c) TRMM dataset. Each value represents the percentage (%) of HR90 from the annual total. Highlighted numbers represent the highest number of HR90 for each station/region.

Bibliography

- Ambaum, Maarten (2010). *Thermal Physics of the Atmosphere*. Wiley-Blackwell, p. 123. ISBN: 978-0-470-74515-1.
- Ariff, N.M., A.a. Jemain, K. Ibrahim, and W.Z. Wan Zin (2012). “IDF relationships using bivariate copula for storm events in Peninsular Malaysia”. In: *Journal of Hydrology* 470-471, pp. 158–171. ISSN: 00221694. DOI: 10.1016/j.jhydrol.2012.08.045.
- Barnes, Gary (2001). “Severe Local Storms in the Tropics”. In: *Severe Convective Storms*. Ed. by Charles A Doswell. Boston, MA: American Meteorological Society, pp. 359–432. ISBN: 978-1-935704-06-5. DOI: 10.1007/978-1-935704-06-5_10.
- Barry, Roger G and Richard J Chorley (2009). *Atmosphere, Weather and Climate*. Routledge, p. 328. ISBN: 978-0-415-46569-4. DOI: doi:10.4324/9780203871027.
- Battán, Louis J. (1973). *Radar Observation of the Atmosphere*. University of Chicago Press.
- Birch, C. E., S. Webster, S. C. Peatman, D. J. Parker, A. J. Matthews, Y. Li, and M. E E Hassim (2016). “Scale interactions between the MJO and the western Maritime Continent”. In: *Journal of Climate* 29.7, pp. 2471–2492. ISSN: 08948755. DOI: 10.1175/JCLI-D-15-0557.1.
- Birch, Cathryn E., Malcolm J. Roberts, Luis Garcia-Carreras, Duncan Ackerley, Michael J. Reeder, Adrian P. Lock, and Reinhard Schiemann (2015). “Sea-breeze dynamics and convection initiation: The influence of convective parameterization in weather and climate model biases”. In: *Journal of Climate* 28.20, pp. 8093–8108. ISSN: 08948755. DOI: 10.1175/JCLI-D-14-00850.1. arXiv: arXiv:1011.1669v3.
- Bowman, Kenneth P., Amy B. Phillips, and Gerald R. North (2003). “Comparison of TRMM rainfall retrievals with rain gauge data from the TAO/TRITON buoy array”. In: *Geophysical Research Letters* 30.14, p. 1757. ISSN: 0094-8276. DOI: 10.1029/2003GL017552.
- Brier, G W and Joanne Simpson (1969). “Tropical cloudiness and rainfall related to pressure and tidal variations”. In: *Quarterly Journal of the Royal Meteorological Society* 95.403, pp. 120–147. ISSN: 1477-870X. DOI: 10.1002/qj.49709540309.

- Chan, C.L. and C.Y. Li (2001). “The East Asian Monsoon”. In: *East Asian Monsoon*. Ed. by C.P. Chang. World Scientific, pp. 54–102.
- Chang, C. P., P. a. Harr, and H-J. Chen (2005a). “Synoptic Disturbances over the Equatorial South China Sea and Western Maritime Continent during Boreal Winter”. In: *Monthly Weather Review* 133.3, pp. 489–503. ISSN: 0027-0644. DOI: 10.1175/MWR-2868.1.
- Chang, C. P., Z. Wang, and H. Hendon (2006). *The Asian Monsoon*. Ed. by B. Wang. Springer/Praxis Publishing Co., p. 78.
- Chang, C. P., Zhuo Wang, Jianhua Ju, and Tim Li (2004). “On the Relationship between Western Maritime Continent Monsoon Rainfall and ENSO during Northern Winter”. In: *Journal of CLimate* 17, pp. 665–672.
- Chang, C. P., Wang Zhuo, McBride John, and Liu Ching-Hwang (2005b). “Annual Cycle of Southeast Asia — Maritime Continent Rainfall and the Asymmetric”. In: *Journal of Climate* 18, pp. 287–301.
- Cheang, B. K. (1980). “Some aspects of winter monsoon and its characteristics in Malaysia”. In: *Malaysian Meteorological Department* 2.
- Chen, Shuyi S. and Robert A Houze (1997). “Diurnal variation and life-cycle of deep convective systems over the tropical Pacific warm pool”. In: *Quarterly Journal of Royal Meteorological Society* 123, pp. 357–388.
- Crook, N. Andrew (2001). “Understanding Hector: The Dynamics of Island Thunderstorms”. In: *Monthly Weather Review* 129.6, pp. 1550–1563. ISSN: 0027-0644. DOI: 10.1175/1520-0493(2001)129<1550:UHTDOI>2.0.CO;2.
- Dai, Aiguo (2001a). “Global Precipitation and Thunderstorm Frequencies . Part I : Seasonal and Interannual Variations”. In: *Journal of Climate* Dai 1999, pp. 1092–1111.
- (2001b). “Global Precipitation and Thunderstorm Frequencies . Part II : Diurnal Variations”. In: *Journal of Climate* 14, pp. 1112–1128.
- Dai, Aiguo, Filippo Giorgi, and Kevin E. Trenberth (1999). “Observed and model-simulated diurnal cycles of precipitation over the contiguous United States”. In: *Journal of Geophysical Research: Atmospheres* 104.D6, pp. 6377–6402. ISSN: 01480227. DOI: 10.1029/98JD02720.
- Davies, T., M. J. P. Cullen, a. J. Malcolm, M. H. Mawson, a. Staniforth, a. a. White, and N. Wood (2005). “A new dynamical core for the Met Office’s global and regional modelling of the atmosphere”. In: *Quarterly Journal of the Royal Meteorological Society* 131.608, pp. 1759–1782. ISSN: 00359009. DOI: 10.1256/qj.04.101.
- Dee, D. P. et al. (2011). “The ERA-Interim reanalysis: Configuration and performance of the data assimilation system”. In: *Quarterly Journal of the Royal Meteorological Society* 137.656, pp. 553–597. ISSN: 00359009. DOI: 10.1002/qj.828.

- Desa, M N and P R Rakhecha (1997). “Characteristics of short-duration extreme rainfalls in Selangor , Malaysia”. In: *Weather* 59.3, pp. 63–66.
- Fujita, Mikiko, Fujio Kimura, and Masanori Yoshizaki (2010). “Morning Precipitation Peak over the Strait of Malacca under a Calm Condition”. In: *Monthly Weather Review* 138.4, pp. 1474–1486. ISSN: 0027-0644. DOI: 10.1175/2009MWR3068.1.
- Furuzawa, Fumie a. and Kenji Nakamura (2005). “Differences of Rainfall Estimates over Land by Tropical Rainfall Measuring Mission (TRMM) Precipitation Radar (PR) and TRMM Microwave Imager (TMI)—Dependence on Storm Height”. In: *Journal of Applied Meteorology* 44.3, pp. 367–383. ISSN: 0894-8763. DOI: 10.1175/JAM-2200.1.
- Golding, B. W. (1993). “A Numerical Investigation of Tropical Island Thunderstorms.pdf”. In: *Monthly Weather Review* 121, p. 1417.
- Gray, William M. and Robert W. Jacobson (1977). “Diurnal Variation of Deep Cumulus Convection”. In: *Monthly Weather Review* 105, p. 1171.
- Gregory, D and P.R. Rowntree (1990). “A Mass Flux Convection Scheme with Representation of Cloud Ensemble Characteristics and Stability-Dependent Closure”. In: *Monthly Weather Review* 118, p. 1483.
- Hamada, Atsushi, Yuki Murayama, and Yukari N. Takayabu (2014). “Regional characteristics of extreme rainfall extracted from TRMM PR measurements”. In: *Journal of Climate* 27.21, pp. 8151–8169. ISSN: 08948755. DOI: 10.1175/JCLI-D-14-00107.1.
- Holloway, C. E., S. J. Woolnough, and G. M. S. Lister (2012). “Precipitation distributions for explicit versus parametrized convection in a large-domain high-resolution tropical case study”. In: *Quarterly Journal of the Royal Meteorological Society* 138.668, pp. 1692–1708. ISSN: 00359009. DOI: 10.1002/qj.1903.
- Houze, Robert A (2012). “Orographic Effects on Precipitating Clouds”. In: *Review of Geophysics* 2011, pp. 1–47. DOI: 10.1029/2011RG000365.1. INTRODUCTION.
- Huffman, George J., David T. Bolvin, Eric J. Nelkin, David B. Wolff, Robert F. Adler, Guojun Gu, Yang Hong, Kenneth P. Bowman, and Erich F. Stocker (2007). “The TRMM Multisatellite Precipitation Analysis (TMPA): Quasi-Global, Multiyear, Combined-Sensor Precipitation Estimates at Fine Scales”. In: *Journal of Hydrometeorology* 8.1, pp. 38–55. ISSN: 1525-755X. DOI: 10.1175/JHM560.1.
- Hung, Chih-Wen, Xiaodong Liu, and Michio Yanai (2004). “Symmetry and Asymmetry of the Asian and Australian Summer Monsoons”. In: *Journal of Climate*, pp. 2413–2426.
- Iida, Yasuhisa, Takuji Kubota, Toshio Iguchi, and Riko Oki (2010). “Evaluating sampling error in TRMM/PR rainfall products by the bootstrap method: Estimation of the sampling error and its application to a trend analysis”. In: *Journal*

- of Geophysical Research Atmospheres* 115.22, pp. 1–14. ISSN: 01480227. DOI: 10.1029/2010JD014257.
- Jamaludin, Suhaila, Mohd Deni Sayang, Wan Zawiyah Wan Zin, and Aziz Abdul Jemain (2010). “Trends in Peninsular Malaysia Rainfall Data During the Southwest Monsoon and Northeast Monsoon Seasons : 1975 – 2004”. In: *Sains Malaysiana* 39.4, pp. 533–542.
- Johnson, RH and Robert A Houze (1987). *Precipitating cloud systems of the Asian monsoon*.
- Johnson, Richard H. (2011). “Diurnal Cycle of Monsoon Convection”. In: *The Global Monsoon System: Research and Forecast*. Ed. by Chih-Pei Chang et al. 2nd. World Scientific Publishing Co., pp. 257–276.
- Johnson, Richard H., Paul E Ciesielski, and Jennifer A. Cotturone (2001). “Multi-scale Variability of the Atmospheric Mixed Layer over the Western Pacific Warm Pool”. In: *Journal of Atmospheric Sciences* 58, pp. 2729–2751.
- Joseph, B., B. C. Bhatt, T. Y. Koh, and S. Chen (2008). “Sea breeze simulation over the Malay Peninsula in an intermonsoon period”. In: *Journal of Geophysical Research* 113.D20, p. D20122. ISSN: 0148-0227. DOI: 10.1029/2008JD010319.
- Juneng, L, F T Tangang, and C J C Reason (2007). “Numerical case study of an extreme rainfall event during 9 – 11 December 2004 over the east coast of Peninsular Malaysia”. In: *Meteorology and Atmospheric Physics* 98, pp. 81–98. DOI: 10.1007/s00703-006-0236-1.
- Kamaruzaman, Mat, Mat Adam, and Subramaniam Moten (2012). “Rainfall Estimation from Radar Data”. In: *Malaysian Meteorological Department Publication* 6.
- Kraus, E. B. (1963). “The Diurnal Precipitation Change over the Sea”. In: *Journal of Atmospheric Sciences* 20, pp. 551–556.
- Lau, K M and H T Wu (2011). “Climatology and changes in tropical oceanic rainfall characteristics inferred from Tropical Rainfall Measuring Mission (TRMM) data (1998 – 2009)”. In: *Journal of Geophysical Research* 116, pp. 1–10. DOI: 10.1029/2011JD015827.
- Lau, Ka-Ming and Paul H Chan (1983). “Short-Term Climate Variability and Atmospheric Teleconnections from Satellite-Observed Outgoing Longwave Radiation. Part II- Lagged Correlations”. In: *Journal of the Atmospheric Sciences* 40, p. 2751.
- Lim, T.J. and A.A. Samah (2004). *Weather and Climate of Malaysia*. UM Press, p. 22.
- Lima, Maria Andrea and James W. Wilson (2008). “Convective Storm Initiation in a Moist Tropical Environment”. In: *Monthly Weather Review* 136.6, pp. 1847–1864. ISSN: 0027-0644. DOI: 10.1175/2007MWR2279.1.

- Love, Barnaby S., Adrian J. Matthews, and Grenville M. S. Lister (2011). “The Diurnal Cycle of Precipitation over the Maritime Continent in a High-Resolution Atmospheric Model”. In: *Quarterly Journal of the Royal Meteorological Society* 137.657, pp. 934–947. ISSN: 00359009. DOI: 10.1002/qj.809.
- Matsumoto, Jun and Takio Murakami (2000). “Annual changes of tropical convective activities as revealed from equatorially symmetric OLR data”. In: *Journal of the Meteorological Society of Japan* 78.5, pp. 543–561.
- (2002). “Seasonal Migration of Monsoons between the Northern and Southern Hemisphere as Revealed from Equatorially Symmetric and Asymmetric OLR Data.” In: *Journal of the Meteorological Society of Japan* 80.3, pp. 419–437. ISSN: 0026-1165. DOI: 10.2151/jmsj.80.419.
- MetMalaysia (2016a). *General Climate of Malaysia*.
- (2016b). *Monthly Weather*.
- Moten, Subramaniam, Fariza Yunus, Munirah Ariffin, Norazura Burham, Diong Jeong Yik, Mat Kamaruzaman Mat Adam, and Weng Sang Yip (2014). “Statistics of Northeast Monsoon Onset , Withdrawal and Cold Surges in Malaysia”. In: *Malaysian Meteorological Department*.
- Neale, Richard and Julia Slingo (2003). “The Maritime Continent and Its Role in the Global Climate : A GCM Study”. In: *Journal of Climate*, pp. 834–848.
- Nieuwolt, S (1986). “Diurnal Rainfall Variation in Malaya”. In: *Annals of the Association of American Geographers* 58.2, pp. 313–326.
- Nor, Mohd and P R Rakhecha (2008). “Analysis of a severe tropical urban storm in Kuala Lumpur , Malaysia”. In: *11th International Conference on Urban Drainage*, pp. 1–9.
- Oki, Taikan and Katumi Musiake (1994). “Seasonal Change of the Diurnal Cycle of Precipitation over Japan and Malaysia”. In: *Journal of Applied Meteorology* 33, p. 1445.
- Peatman, Simon C., Adrian J. Matthews, and David P. Stevens (2014). “Propagation of the Madden-Julian Oscillation through the Maritime Continent and scale interaction with the diurnal cycle of precipitation”. In: *Quarterly Journal of the Royal Meteorological Society* 140.680, pp. 814–825. ISSN: 00359009. DOI: 10.1002/qj.2161.
- Phang, Kun Liong and Noor Azam Shaari (2011). “A Study on the extreme daily rainfall cases in northwest peninsular malaysia”. In: *Malaysian Meteorological Department Publication* 6.
- Pope, V. D., M. L. Gallani, P. R. Rowntree, and R. a. Stratton (2000). “The impact of new physical parametrizations in the Hadley Centre climate model: HadAM3”. In: *Climate Dynamics* 16.2-3, pp. 123–146. ISSN: 0930-7575. DOI: 10.1007/s003820050009.

- Qian, Jian-Hua (2008). “Why Precipitation Is Mostly Concentrated over Islands in the Maritime Continent”. In: *Journal of the Atmospheric Sciences* 65.4, pp. 1428–1441. ISSN: 0022-4928. DOI: 10.1175/2007JAS2422.1.
- Ramage, C. S. (1968). “Role of a Tropical “ Maritime Continent ” in the Atmospheric Circulation”. In: *Monthly Weather Review* 96.June, pp. 365–370.
- Randall, D. A., Harshvardhan., and D. A. Dazlich (1991). “Diurnal Variability of the Hydrologic Cycle in a General Circulation Model”. In: *Journal of Atmospheric Sciences* 48, p. 40.
- Rodwell, M. J. and B. J. Hoskins (1996). “Monsoons and the dynamics of deserts”. In: *Quarterly Journal of the Royal Meteorological Society* 122, pp. 1385–1404.
- Roff, Gregory L. and Jun-Ichi Yano (2002). “Tropical convective variability in the CAPE phase space”. In: *Quarterly Journal of the Royal Meteorological Society* 128.585, pp. 2317–2333. ISSN: 1477870X. DOI: 10.1256/qj.01.138.
- Rutter, John (2009). “Variation in Weather Pattern on the ITCZ”. In: *Geofile Online*, pp. 2007–2010.
- Saito, K, T Keenan, G Holland, and Kamal Puri (2001). “Numerical Simulation of the Diurnal Evolution of Tropical Island Convection over the Maritime Continent”. In: *Monthly Weather Review* 129, pp. 378–400.
- Schiemann, R., M.-E. Demory, M. S. Mizielski, M. J. Roberts, L. C. Shaffrey, J. Strachan, and P. L. Vidale (2013). “The sensitivity of the tropical circulation and Maritime Continent precipitation to climate model resolution”. In: *Climate Dynamics* 42.9-10, pp. 2455–2468. ISSN: 0930-7575. DOI: 10.1007/s00382-013-1997-0.
- Sebastianelli, S., F. Russo, F. Napolitano, and L. Baldini (2010). “Comparison between radar and rain gauges data at different distances from radar and correlation existing between the rainfall values in the adjacent pixels”. In: *Hydrology and Earth System Sciences Discussions* 7.4, pp. 5171–5212. ISSN: 1812-2116. DOI: 10.5194/hessd-7-5171-2010.
- Semire, Folasade Abiola, Rosmiwati Mohd-Mokhtar, Widad Ismail, Norizah Mohamad, and J. S. Mandeep (2012). “Ground validation of space-borne satellite rainfall products in Malaysia”. In: *Advances in Space Research* 50.9, pp. 1241–1249. ISSN: 02731177. DOI: 10.1016/j.asr.2012.06.031.
- Sobel, Adam H. (2012). “Tropical Weather”. In: *Nature Education Knowledge* 3, pp. 1–8.
- Sow, Khai Shen, Liew Juneng, Fredolin T. Tangang, Abdul Ghapor Hussin, and Mastura Mahmud (2011). “Numerical simulation of a severe late afternoon thunderstorm over Peninsular Malaysia”. In: *Atmospheric Research* 99.2, pp. 248–262. ISSN: 01698095. DOI: 10.1016/j.atmosres.2010.10.014.
- Suhaila, Jamaludin and Abdul Aziz Jemain (2009). “Investigating the impacts of adjoining wet days on the distribution of daily rainfall amounts in Peninsular

- Malaysia". In: *Journal of Hydrology* 368.1-4, pp. 17–25. ISSN: 00221694. DOI: 10.1016/j.jhydro1.2009.01.022.
- Suhaila, Jamaludin, Abdul Aziz Jemain, Muhammad Fauzee Hamdan, and Wan Zawiah Wan Zin (2011). "Comparing rainfall patterns between regions in Peninsular Malaysia via a functional data analysis technique". In: *Journal of Hydrology* 411.3-4, pp. 197–206. ISSN: 00221694. DOI: 10.1016/j.jhydro1.2011.09.043.
- Tangang, Fredolin T. and Liew Juneng (2004). "Mechanisms of Malaysian Rainfall Anomalies". In: *Journal of Climate* 17.2003, pp. 3616–3622.
- Trier, S B (2003). "Convective Storms : Convective Initiation". In: *Encyclopedia of Atmospheric Sciences*. Ed. by James R. Holton. Oxford, pp. 560–570. ISBN: 978-0-12-227090-1.
- Varikoden, Hamza, B. Preethi, A.a. Samah, and C.a. Babu (2011). "Seasonal variation of rainfall characteristics in different intensity classes over Peninsular Malaysia". In: *Journal of Hydrology* 404.1-2, pp. 99–108. ISSN: 00221694. DOI: 10.1016/j.jhydro1.2011.04.021.
- Varikoden, Hamza, A.a. Samah, and C.a. Babu (2010). "Spatial and temporal characteristics of rain intensity in the peninsular Malaysia using TRMM rain rate". In: *Journal of Hydrology* 387.3-4, pp. 312–319. ISSN: 00221694. DOI: 10.1016/j.jhydro1.2010.04.023.
- Waliser, D. E. and C. Gautier (1993). *A satellite-derived climatology of the ITCZ*. DOI: 10.1175/1520-0442(1993)006<2162:ASDCOT>2.0.CO;2.
- Wallace, J.M. (1975). "Diurnal Variations in Precipitation and Thunderstorm Frequency over the Conterminous United States". In: *Monthly Weather Review* 103, p. 406.
- Wang, Bin (1994). "On the Annual Cycle in the Tropical Eastern Central Pacific". In: *Journal of Climate* 7, p. 1926.
- Wang, Zhuo and C-P. Chang (2008). "Mechanism of the Asymmetric Monsoon Transition as Simulated in an AGCM". In: *Journal of Climate* 21.8, pp. 1829–1836. ISSN: 0894-8755. DOI: 10.1175/2007JCLI1920.1.
- Webster, P J, V O Magafia, T N Palmer, J Shukla, R A Tomas, M Yanai, and T Yasunari (1998). "Monsoons : Processes , predictability , and the prospects for prediction". In: *Journal of Geophysical Research* 103, pp. 14451–14510.
- Weller, R. A. and S. P. Anderson (1996). *Surface meteorology and air-sea fluxes in the western equatorial pacific warm pool during the TOGA coupled ocean-atmosphere response experiment*. DOI: 10.1175/1520-0442(1996)009<1959:SMAASF>2.0.CO;2.
- Wheeler, Matthew C. and Harry H. Hendon (2004). "An All-Season Real-Time Multivariate MJO Index: Development of an Index for Monitoring and Prediction". In: *Monthly Weather Review* 132.8, pp. 1917–1932. ISSN: 0027-0644. DOI: 10.1175/1520-0493(2004)132<1917:AARMMI>2.0.CO;2.

- Yang, Gui Ying and Julia Slingo (2001). “The Diurnal Cycle in the Tropics”. In: *Monthly Weather Review* 1994, pp. 784–801.
- Yatagai, Akiyo, Osamu Arakawa, Kenji Kamiguchi, and Haruko Kawamoto (2009). “A 44-Year Daily Gridded Precipitation Dataset for Asia”. In: *SOLA* 5, pp. 3–6. DOI: 10.2151/sola.2009.
- Yatagai, Akiyo, Kenji Kamiguchi, Osamu Arakawa, Atsushi Hamada, Natsuko Yasutomi, and Akio Kitoh (2012). “APHRODITE: Constructing a Long-Term Daily Gridded Precipitation Dataset for Asia Based on a Dense Network of Rain Gauges”. In: *Bulletin of the American Meteorological Society* 93.9, pp. 1401–1415. ISSN: 0003-0007. DOI: 10.1175/BAMS-D-11-00122.1.
- Zhu, Min, Paul Connolly, Geraint Vaughan, Tom Choullarton, and Peter T. May (2012). “Numerical simulation of tropical island thunderstorms (Hectors) during the ACTIVE campaign”. In: *Meteorological Applications*, n/a–n/a. ISSN: 13504827. DOI: 10.1002/met.1295.